Characterization of changes in synaptic strength in the CA1 region of the hippocampus by the analysis of miniature synaptic currents.

by

Andrew William Baxter B.Sc (Hons) M.Sc

A thesis submitted for the degree of Doctor of Philosophy
at the University of Edinburgh

March 2005

Division of Neuroscience
School of Biomedical and Clinical Laboratory Sciences
College of Medicine and Veterinary Medicine
University of Edinburgh
Supervisor: Dr David J.A. Wyllie

Declaration of ownership

This submission is the result of my own endeavour. All help and advice, other than received from tutors, has been acknowledged. All primary and secondary sources of information have been properly attributed. Should this statement prove to be untrue, I recognise the right and duty of the Board of Examiners to recommend what action should be taken in line with the University's regulations on assessment contained in the postgraduate study handbook.

Signature _____

Date 1st June 2005

Abstract

A relatively small number of synapses are potentiated at individual CA1 neurones following conventional long-term potentiation (LTP) stimulating protocols. This makes it difficult to detect changes in the amplitudes of miniature excitatory post synaptic currents (mEPSCs) which can be used as a marker to provide evidence that changes in synaptic strength are mediated, in part, by alterations of synaptic AMPA receptors. Thus, to mimic the LTP-like postsynaptic calcium concentration change, that occurs following NMDA receptor activation, we have used a depolarizing voltage pulse (VP) stimulating protocol to increase intracellular calcium levels via L-type calcium channels. Characterization of VP stimulation was done by whole-cell patch-clamp recordings from CA1 pyramidal neurones in organotypic hippocampal slices. Culturing these slices maintains the hippocampal architecture, but results in an increase in the number of synaptic sites. The increase in synapse number, allows for the greater detection of mEPSCs allowing for the functional changes brought about by the VP stimulus to be better characterized. Following the VP stimulus there is a mean doubling of the amplitudes of the mEPSCs with a small non significant increase in mEPSC frequency. To assess whether the increase in amplitude of mEPSCs requires the insertion of AMPA receptors into postsynaptic sites we inhibited the actions of several proteins involved in intracellular membrane fusion events. In these experiments inhibitors were included in the patch-pipette to restrict their actions to the postsynaptic cell. We observed that both N-ethylmaleimide and botulinum toxin A inhibited the NSF dependent delivery of AMPA receptors to synapses, by blocking the induction of VP potentiation. The requirement for NSF was supported by a Pep2m blockade of the induction of VP potentiation. Pep2m, a peptide that blocks the NSF binding site on the C-terminus of the GluR2 AMPA receptor subunit also blocked VP potentiation, while a scrambled version of this peptide, Pep4c failed to block potentiation. Further experiments using Pep-AVKI characterized a second delivery system, dependent upon PDZ domains, and suggested the possible involvement of PICK-1 in VP potentiation. None of the peptides examined altered mean mEPSC amplitude (or frequency) in recordings where they were included in the patch-pipette but no voltage-pulses were applied. A final set of experiments were undertaken to determine the kinase regulation underlying the induction and maintenance of the potentiation of mEPSC amplitudes with the VP stimulus. Targeting phosphoinositide 3 kinase (PI-3 K) with both wortmannin and LY 294002 blocked the VP potentiation of mEPSC amplitudes, while LY 303511 an in active analogue of LY 294002 allowed potentiation of mEPSCs. In conclusion, it appears that VP potentiation shares common expression mechanisms with NMDA receptor-dependent LTP, and the VP protocol provides a valuable method for studying biochemical changes in individual neurones following changes in synaptic strength.

Table of contents

List of Figures

Acknowledgements

I would like to thank my supervisor, Dr. David Wyllie. Firstly, for taking the risk and allowing me to do a Ph.D in his lab, but more for all the help, guidance, and opportunities throughout my Ph.D. I believe that I have benefited immensely from my time at the University of Edinburgh and I am indebted to him for all his support.

I would also like to thank the BBSRC for there generous financial support for this project the over the last three years. Without this funding I would never be able to conduct this research and achieve my ambition.

Thanks must also be given to David's post-docs Dr Philip Chen and Dr Alex Johnston both for support and teaching in the Lab, but also for beer and the opportunity escape the rig and climb some magnificent Munros. Mr Darren Downing must also receive special mention for being a great friend, and for his continued heroic endeavour, with my work shy computer, rebuilding it at a moments notice on a weekly basis.

The other Ph.D students in the department for their support, friendship, and the general ridicule they have levelled at me over the course of my Ph.D. In addition I must thank the rest of the neuroscience department, for putting up with another Glaswegian in Edinburgh.

To my parents, thanks for understanding why I needed to do this, also for all the support and encouragement to get me through, for nodding your head at the appropriate moment, never saying more than once a month "when are you going to get a job".

Finally I must say thank you to Nicola Crawford, for being there for me, putting up with me ranting about mini's and electrophysiology, and for all the things you did and I never noticed.

Abbreviations

ABP	AMPA receptor binding protein
AC	Associated commissural pathway
AMPA	α-amino-3-hydroxy-5-methyl-isoxazole propionic acid
AMPAR	α-amino-3-hydroxy-5-methyl-isoxazole propionic acid receptor
APV	2-amino-5-phosphonopentanoic acid
BAPTA	1,2-bis(o-aminophenoxy)ethane *N,N,N,N*- tetraacetic acid
Botox	Botulinum toxin
Ca^{2+}	Calcium ions
CA1	*Cornu Ammonis* region 1
CA3	*Cornu Ammonis* region 1
CaMKII	Calcium/calmodulin-dependent protein kinase type II
cAMP	Cyclic adenosine monophosphate
CICR	Calcium induced calcium release
CNQX	6-cyano-7 nitroquinoxaline-2,3-dione
CREB	cAMP response element binding protein
DD	De-depression (LTP of previously LTD synapses)
DAG	Diacyl glycerol
DG	Dentate gyrus
DSI	Depolarisation-induced suppression of inhibition
EAAT	Excitatory amino acid transporter
EGTA	Ethyleneglycol-bis(β-aminoethylether)-*N,N*-tetraacetic acid
EPSC	Excitatory postsynaptic current
GABA	γ aminobutyric acid
GLAST	Glial glutamate and aspartate transporter
GLT	Glial glutamate transporter
GRIP1	Glutamate receptor interacting protein 1
GluR	Glutamate receptors (AMPA)

HBSS	Hanks balanced salt solution
HEPES	4-(2-hydroxyethyl)-1-piperazineethanesulfonic acid
IP3	Inositol trisphosphate
LEC	Lateral enterorhinal cortex
LPP	Lateral perforant pathway of hippocampus
LTD	Long term depression
LTP	Long term potentiation
MAGUK	Membrane-associated guanylate kinase homologs
MAP kinase	Mitogen-activated protein kinases
mEPSC	Miniature excitatory postsynaptic current
MEC	Medial enterorhinal cortex
MEM	Dulbecco's modified eagles medium
MF	Mossy fibre pathway of hippocampus
mGluR	Metabotropic glutamate receptor
mTOR	Mammalian target of rapamycin
MPP	Medial perforant pathway of hippocampus
NEM	N-ethylmaleimide
NMDA	N methyl D aspartate
NMDAR	N methyl D aspartate receptor
NSF	NEM sensitive fusion protein
PDK1	Phosphoinositide-dependent protein kinase-1
PDZ	Protein interaction binding domain
Pep1-TGL	Amino acid sequence targeted to TGL binding motif on GluR1
Pep2m	Amino acid sequence targeted to NSF binding motif on GluR2
Pep2m-AVKI	Amino acid sequence targeted to PICK1 binding motif on GluR2
Pep4c	Inactive form of Pep2m
PICK 1	Protein interacting with C kinase 1
PKA	Protein kinase A
PKB	Protein kinase B
PKC	Protein kinase C

PLC	Phospholipase C
PP	Perforant pathway of hippocampus
PPF	Paired pulse facilitation
PSD	Post synaptic density
PSD-95	Post synaptic density protein of 95 kDa
PTEN	Phosphatase and Tensin homolog deleted on chromosome Ten.
PTX	Picrotoxin
Ryr	Ryanodine
SAP-93	Synapse associated protein of 93 kDa
SAP-97	Synapse associated protein of 97 kDa
SC	Schaffer collateral pathway
SCC	Schaffer collateral commissural pathway
SH3	SRC tyrosine kinase binding region
SNAP-25	Soluble NEM adaptor protein of 25 kDa
SNARE	Soluble *N*-ethylmaleimide-sensitive factor-attachment protein receptor
Stargazin	Auxiliary protein for AMPA receptor trafficking
TTX	Tetrodotoxin
VAMP1	Vesicle-associated membrane protein 1 (synaptobrevin)
VDCC	Voltage dependent calcium channel
VP	Voltage-pulse
VPP	Voltage-pulse potentiation

Chapter One:

Introduction

1.1: Glutamate as a neurotransmitter

Glutamate is the primary excitatory neurotransmitter in the mammalian brain, utilized in approximately 60 % of all brain neurones. Glutamate is released into the synaptic cleft from vesicles when docked in the presynaptic terminal. This occurs in response to membrane depolarisation by a Ca^{2+} dependent mechanism which requires the activation of N and P/Q type voltage dependent Ca^{2+} channels (Birnbaumer et al., 1994) which are linked to SNARE complex dependent vesicle docking sites.

Release of neurotransmitter from the presynaptic membrane is tightly controlled by a range of pre-synaptic receptors, including cholinergic (nicotinic and muscarinic) receptors, γ-aminobutyric acid ($GABA_B$), adenosine (A1) receptor and the kappa opioid receptor (Meldrum, 1998, 2000). The glutamate concentration within the synaptic vesicle is a source of much debate and some groups have put it around 60 mM This debate is important as varying the concentration of synaptic glutamate released can have a modulatory effect on synaptic transmission and effectively the output from the cell. The second issue is whether the glutamate released in a single synaptic vesicle although a saturating concentration may not be sufficient for functional saturation of the receptors in the postsynaptic membrane (Mainen et al., 1999; Chen et al., 2001; Ishikawa et al., 2002). Therefore, synaptic activity may be sensitive to the number of quanta released by a burst of action potentials and to changes in the concentration profile of glutamate in the synaptic cleft.

Glutamate in the synaptic cleft is recycled via the excitatory amino acid transporters found both on neurones and glia cells. With glia uptake the glutamate is rapidly converted to glutamine and released back into the extracellular fluid, where upon it is reabsorbed into the presynaptic terminals and converted back to glutamate via the action of neuronal glutaminase.

Five types of glutamate transporters exist within the mammalian brain. Two are predominately expressed in the glia, the glial glutamate transporter (GLT) found mainly in the rat hippocampus and glial glutamate and aspartate transporter (GLAST) found mainly in the cerebellum (Lehre and Danbolt, 1998). Neurones possess the other three transporters classed as excitatory amino acid transporter called (EAAC in the rat and the human EAAT 1, 3, 5) (Seal and Amara, 1999). The mechanism of action of these transporters is dependent upon the Na^+/K^+ balance as the transporter uptakes one molecule of glutamate for the co transport of $3Na^+$ with $1H^+$ out of the cell and $1K^+$ into the cell (Levy et al., 1998). The rat neuronal transporter EAAC is highly expressed in the postsynaptic neural membranes (up to 15 times the density of the AMPA receptor); glutamate uptake by this transporter contributes to the termination of the

excitatory postsynaptic current and synaptic transmission. Such is the importance of this process, as free glutamate in the brain leads quickly to processes of cell death through excitotoxicity, that 2/3 of brain energy metabolism is related to reuptake and recycling of glutamate (Shulman et al., 2002).

The glutamate released from the synaptic vesicles, is known to act on four receptor types: α-amino-3-hydroxy-5-methyl-4-isoxazole propionic acid receptor (AMPAR), kainate receptors, *N*-methyl-D-aspartate receptors (NMDAR) and metabotropic receptors (mGluR) (Figure 1.1).

1.2: AMPA receptors

The fast components of a glutamatergic excitatory synaptic potential/current are mediated by AMPARs. These receptors require at least two molecules of agonist (glutamate) to be bound before the channel opens (Clements et al., 1998). There are four main subunits (GluR1-4, A-D) these range in size from 102 to 108 kDa and share 68-74% sequence identity at the protein level. These subunits are arranged as tetrameric complexes, comprising pairs of identical heteromeric dimers forming the functional AMPA receptor (Rosenmund et al., 1998). Typically in adult CA1 pyramidal cells the hetromeric expressions of the receptor are either paired dimers of GluR1/ GluR2 subunits or of GluR2/ GluR3 subunits (Wenthold et al., 1996; Collingridge et al., 2004). However, immature pyramidal cells and other brain regions will express the GluR4 subunit which combines with the GluR2 subunit to form an AMPA receptor (Zhu et al., 2000), but is lost in the adult CA1 pyramidal cell. The subunit composition of the AMPA receptor has a profound effect on the nature and the biophysical properties of the receptor. Homomeric assemblies of GluR1, 3 and 4 subunits have ionic permeability to sodium (Na^+) potassium (K^+) and calcium (Ca^{2+}), the inclusion of an edited GluR2 subunit in a heteromeric AMPA receptor confers the Ca^{2+} impermeability traditionally ascribed to the AMPA receptor.

The key features of the AMPA receptor subunit and its conformation during activation have been confirmed using 3D reconstruction (Nakagawa et al., 2005). An extracellular N terminus, comprising 400 amino acids, forms one half of the 'Venus fly trap' binding site for glutamate on the AMPA receptor. This N terminal domain is connected to the first of three transmembrane domains (M1) (Figure 1.2: The AMPA receptor). The second domain is not a membrane spanning domain but loops within the membrane and finishes on the intracellular side. A key feature of AMPA receptors found in CA1 pyramidal cells is conferred by the M2

loop of the GluR2 subunit; a single amino acid substitution at the 764 amino acid (Q/R site) confers Ca^{2+} impermeability. A small uncharged glutamine residue is replaced with a large positively charged arginine residue (Hume et al., 1991).

Furthermore, it was found that the arginine residue in the pore of the GluR2 was not encoded at the genomic level but was a result of RNA editing (Sommer et al., 1991). Control of the editing and effectively calcium permeability of the receptor is conferred by adenosine deaminase (ADAR2); conversion of inosine to adenosine within the CAG codon, (Codon switch CAG to CIG) which results in the switch from glutamine to arginine. Intron 11 in the GluR2 gene which is adjacent to the editing site was found to direct the editing process. Disruption of the editing process in mice causes severe brain injury and seizures, most probably due to excess calcium influx through activated AMPA receptors (Higuchi et al., 2000).

The second half of the glutamate binding pocket called S2 is formed by an extracellular loop between the M3 and M4 domains. A further feature of this loop is the 38 amino acid Flip/Flop cassette coded for by exons 14 and 15, alternative splicing of this cassette alters the kinetic properties of the desensitisation and deactivation of AMPA receptors. Flip containing receptors generally possess slower decay time than their flop containing counterparts. Flip being slow and flop inducing fast decays. The temporal distribution of these individual cassettes in AMPA receptors in the rat, shows that flip variants are widely expressed at birth and remain so as the animals mature. Flop variants have very low expression in the young (pre P8) and their expression is up regulated to a similar level as the flip variants in the adult (for a review see (Dingledine et al., 1999). The spatial distribution within the hippocampus varies as in CA3 pyramidal neurones flip versions dominate, whereas in neurones of the CA1 subfield flip/flop versions coexist (Sommer et al., 1990).

Another RNA edited feature of the AMPA receptor is the R/G splice variant. This mutation from arginine to glycine confers a unique property as the G forms recover from desensitisation more rapidly than those assembled from the unedited (R) form subunits. The expression of this editing shows temporal variations in the embryonic rat pup (E14) approximately 20 % of receptors show this editing, while in the adult (P21) there is approximately 70 % editing of this sequence (Lomeli et al., 1994).

The final part of the AMPA receptor is the intracellular carboxy terminal, usually referred to as the C domain. This comprises 50 – 100 amino acids and is important as the C terminus controls the interactions of the AMPA receptor subunits with membrane associated proteins in the postsynaptic membrane, which govern AMPA receptor trafficking and membrane

stability. Splice variants of the C terminal exist with the GluR2, Ca^{2+} impermeable AMPA receptor subunit (long and short C terminal) where only a small proportion of receptors existing in the long isoform (Kohler et al., 1994). This C terminal splice variance is also shown with the GluR4 usually expressed in the cerebellum (Gallo et al., 1992). Functional differences between the splice variants have not been reported, but the possibility exists that the different C terminals may interact with different intracellular proteins and may differently regulate this expression at active synapses (See Protein-Protein interaction section).

However, considerable diversity of AMPA subtypes can be achieved following alternative splicing and RNA editing. Information about the single channel conductance levels of synaptic channels is limited to estimates obtained from non stationary fluctuation analysis of synaptic currents (Smith et al., 2000) indicating that they show similar values to those obtained from studies of recombinant receptors in transfected cells or from channels isolated from patches excised from cell bodies in culture (Jonas and Monyer, 1999). What is striking is the fact that AMPARs display a multiplicity of unitary conductance levels (GluR1 Flip: 5, 14, 20 pS (Banke et al., 2000) GluR2 Flip: 7, 11, 18 pS). It remains to be seen to what extent changes in synaptic strength can be accounted for by alterations in this channel property (for example see (Benke et al., 1998). Additionally receptors containing GluR2 subunits have lower unitary conductances due to the presence of an arginine residue in the ion channel pore.

1.3: Kainate receptors.

Kainate receptors have been show to be widespread in the brain, and specifically found in the hippocampus (Huettner, 2003). Furthermore, their function has been linked with the induction of long term potentiation (LTP) at mossy fibre synapses in the CA3 region of the hippocampus (Harris and Cotman, 1986; Hirbec et al., 2003; Marchal and Mulle, 2004). An important finding as the expression of LTP in this region does not require the activation of the NMDA receptor, but maybe induced by the activation of both pre and postsynaptic kainate receptors.

Kainate receptors share 40% sequence identity with the AMPA receptor, but have a higher glutamate affinity [Ki = 290nM, Sommer et al.1992]. Their nomenclature is dependent upon their affinity for kainate, the low affinity kainate receptors are classed as GluR5-7 and have about 80 % sequence homology which defines them as a receptor family. The second group, the high affinity receptors (KA1-2) share a 69% inter-group homology, only 42 % sequence homology with the GluR5-7 group and only 35% sequence homology to the AMPA receptor

(Hollmann and Heinemann, 1994). As with AMPA receptors, kainate receptors display Q/R editing, which alters the single channel conductance of these receptors.

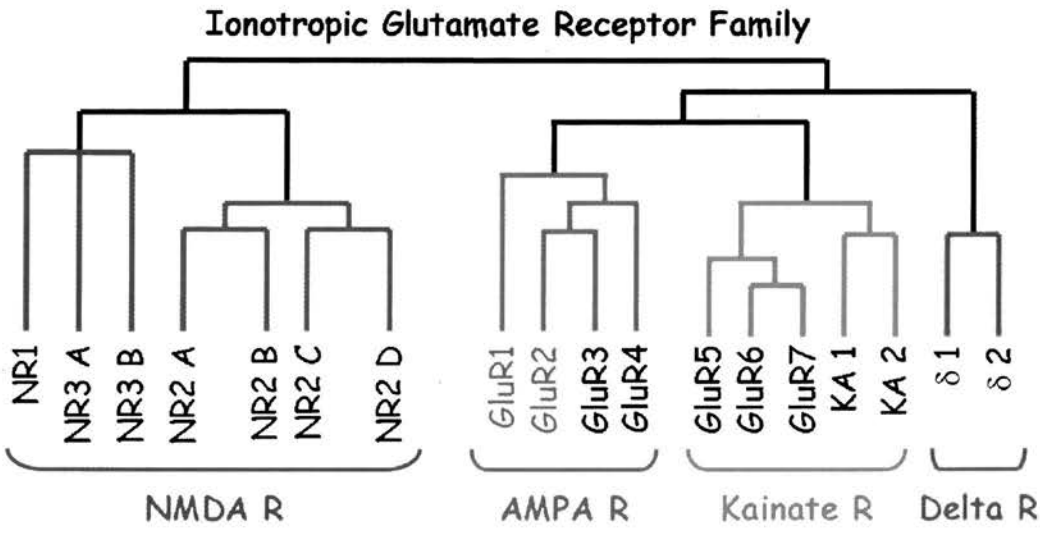

Figure 1.1: **Diversity of ionotropic glutamatergic receptors.** Ionotropic glutamate receptors include NMDA receptors which mediate the slow regulatory component of excitatory synaptic transmission, while AMPA/Kainate mediate the fast component of excitatory synaptic transmission; these later receptors display different functional and spatial characteristics. Delta subunits constitutes an orphan receptor sharing 30 % sequence homology with AMPA receptors

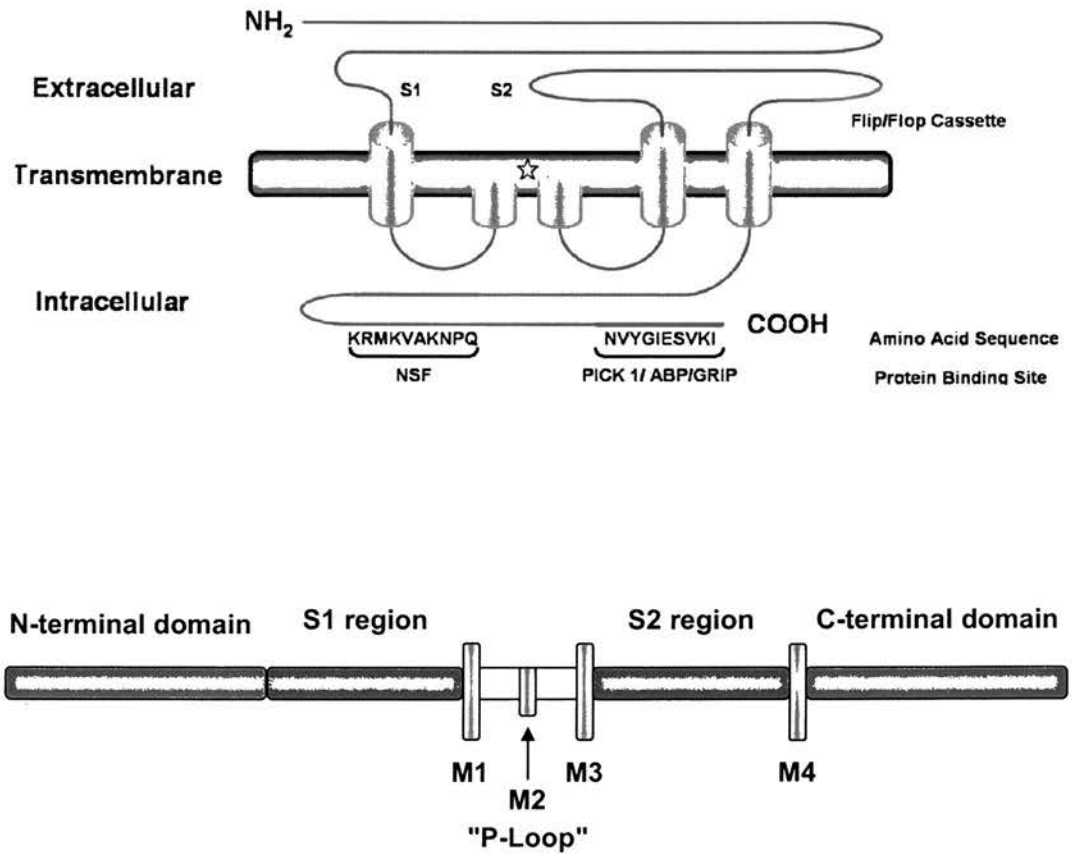

Figure 1.2: **The AMPA receptor.** Structure of a prototypical AMPA receptor subunit, the common transmembrane topology of all AMPA receptors is shown with the individual features taken from the GluR1 and GluR2 subunits. The glutamate binding site, the glutamine/arginine (Q/R) site, and the flip/flop cassette are common to all AMPA subunits. NSF and the PICK1 binding site are common to the GluR2 subunit.

(NSF) N-ethylmaleimide sensitive fusion protein, (PICK1) Protein interacting with C kinase 1, (ABP) AMPA receptor binding protein (GRIP1) Glutamate receptor interacting protein 1.

1.4: NMDA receptors.

The NMDA receptor, the third type of ionotropic glutamate receptor is highly permeable to Ca^{2+} ions. This receptor mediates the slow component of the glutamatergic synaptic current. Elucidation of the slow component was achieved by Collingridge et al. 1987, who blocked all $GABA_A$ receptor mediated inhibition, then depolarising the CA1 pyramidal cell to remove the magnesium block of the NMDA receptor increasing the NMDA receptor mediated current. Application of AP5, the prototypical NMDA receptor antagonist, blocked the NMDA mediated current, revealing the fast AMPA receptor mediated current, subtraction of these two currents revealed the slow decaying NMDA receptor dependent current.

These NMDA receptors show the lowest sequence homology between all glutamate receptors (25-30%). However, the receptor subunit grouping is somewhat more complex than that of the AMPA receptor. All NMDA receptor subunits have the same general structure as AMPA receptors, an extracellular N terminus, 3 transmembrane domains, a P loop and an intracellular C terminus, which are features of all ionotropic glutamate receptors.

These receptors are generally considered to be tetrameric in nature (Laube et al., 1998); consisting of heteromers of two NR1 subunits and two NR2 subunits. Although the identity of the NR2 subunits does not have to be the same, as NMDA receptors comprising 3 subunits (NR1 + NR2A + NR2C) have been expressed in *Xenopus laevis* oocytes (Chazot et al., 1994) and further, experimental immunoprecipitations from rat brain extracts have shown a receptor comprised of (NR1 + NR2A + NR2B) (Sheng et al., 1994).

Evidence from the literature supported an additional NMDA receptor subunit (Chatterton et al., 2002; Kemp and McKernan, 2002; Matsuda et al., 2003). A NR3 subunit, mRNA for this NR3 subunit is found to be highly expressed in motor neurons in the spinal cord, pons, and medulla, but not expressed in the cerebellum, although the expression of this mRNA is reduced by the second postnatal week (Sucher et al., 1996).

When co-expressed with the NR1 and NR2 subunits in cells (NR1/NR2A/NR3) these channels show a decrease in channel conductance and approximate 5 fold reduction in Ca^{2+} permeability when compared to the (NR1/NR2A) (Perez-Otano et al., 2001).

The NR1 subunit has two main functions the first is the binding the co-agonist glycine required for the activation of the receptor and the second is that the NR1 subunit is essential for the trafficking and insertion of the NMDA receptor into active synapses. A degree of diversity within the NR1 subunit is derived by the alternative splicing of three exons. The first of these (exon 5) is located near the amino (N) terminus, while the other two (exons 21 and 22) and

located towards the carboxy terminus of the protein. The NR2 subunits share about 30 % amino acid sequence identity with the NR1 subunit, and possess 4 principal subunits (A-D). All these subunits share 46-56 % amino acid sequence identity. The distribution of these subunits is controlled both temporally and spatially. Clements et al. (1991) determined the need for two glycine and two glutamate molecule to bind to the receptor to elicit full activation – which is consistent with the idea that this receptors are tetrameric in nature.

Another unique feature of NMDA receptors is that extracellular Mg^{2+} blocks these receptors by binding in the receptor channel at resting membrane potentials; this block is relieved by depolarisation of the membrane (i.e. it is voltage-dependent), allowing NMDA receptor to act as integrators of synaptic activity. The calcium conductance of the receptor is controlled by a specific extracellular region (C terminal to M3), unique to the NR1 subunit called DRPEER, which acts as a Ca^{2+} binding site and causes a constriction of the channel (Watanabe et al., 2002).

The spatial and temporal distribution for each subunit, has been characterised by *in situ* hybridisation studies for each subunit RNA. This has shown both periodic and regional expressional variation for the NR2 subunits. In the neonatal brain the greatest expression is for the NR2B and 2D subunits, but these receptors are replaced over the course of development with widespread expression of NR2A subunits, and specific expression of NR2C in the cerebellum.

The kinetic properties of NMDA receptors are dependent upon the subunit composition and these govern the decay time for the different receptor subtypes. Wyllie et al. (1998) showed there existed significant differences in the deactivation rates for diheteromeric NMDA receptors. For example, NR1/NR2A receptors deactivate in tens of milliseconds, while deactivation of NR1/NR2D receptors takes several seconds. The range of these deactivation times (τ_w) for each subunit gives a deactivation sequence of (NR2A (50 ms) < NR2C (300ms) = NR2B (280 ms) << NR2D (1.7 s) (Vicini et al., 1998). Indeed such differences in decay times have been used to infer subunit composition of native NMDA receptors (Misra et al., 2000). NMDARs containing NR2A or NR2B subunits (together with NR1) display a main single-channel conductance of around 50 pS and a sub conductance level of around 40 pS these receptors also have high sensitivity to blockade by Mg^{2+} ions (Monyer et al., 1994). NR1/NR2C and NR1/NR2D containing NMDA receptors exhibit lower conductance levels of approximately 35 pS and a sub-conductance level of about 17 pS (Stern et al., 1992; Wyllie et al., 1996) and have lower sensitivity to extracellular magnesium (Dingledine et al. 1999). It has been reported (Burnashev et al., 1995) that the Ca^{2+} permeability of the receptor is not affected by the composition of

which NMDA receptor subunit is present, as the fractional Ca^{2+} current varies between 8 and 14 %. Therefore, the differences in the sensitivity to external magnesium may account for the differences in calcium influx shown with activation of different NMDA receptors.

1.5: Metabotropic glutamate receptors

The metabotropic glutamate receptors (mGluR) are the final class of receptor which respond to the neurotransmitter glutamate. These receptors have a completely different structure and function, when compared to the AMPAR, as they have no transmembrane ion channel, but function through a series of 2^{nd} messenger molecules. mGluRs are seven transmembrane/domain, G-protein linked receptors. There are eight subtypes (mGluR1-8 with splice variants also occurring) which can be divided into 3 functional groups. mGluR group 1 receptors are coupled to phospholipase C (PLC) and mediate their effects via two well-characterized intracellular second messengers, inositol tris-phosphate (IP_3) and diacylglycerol (DAG). IP_3 usually acts to increase cytosolic Ca^{2+} by release from intracellular stores. DAG activates protein kinase C (PKC) and mediates its action via phosphorylation of various proteins. mGluR group 2 and group 3 are negatively coupled to adenylate cyclase which through generation of an intracellular second messenger cAMP (cyclic adenosine monophosphate) activates protein kinases and affects the function of various ion channels. These receptors have a vast diversity of locations as they are widespread through the brain and each group possesses a vast diversity of function. When located in the presynaptic terminal they modulate the vesicular release probability through actions on both N and L type Ca^{2+} channels (Fagni et al., 2000) at CA1 hippocampal synapses, and via modulation of potassium channels in the same locus. Application of the mGluR agonist ACPD, reduces the NMDA component of the EPSC with a similar potency to that of the AMPA component (Baskys and Malenka, 1991; Lovinger, 1991; Pacelli and Kelso, 1991). These papers highlight a presynaptic effect on vesicular release as the method for reduction of the EPSC, because if postsynaptically mediated; a different effect on each receptor EPSCs would be expected.

When located postsynaptically, the function and sites of actions of these receptors are vastly multiplied. Functional roles for mGluR receptors have been proposed in both NMDA receptor dependent and independent LTP. In CA1 hippocampal synapses, the expression is dependent upon the degree of depolarization of the postsynaptic cell. AP5 blocks ACPD induced LTP (Breakwell et al., 1996, 1998), but uncovered a second slow component, expression of which is dependent upon arachidonic acid and PKC activity.

Activation of postsynaptic mGluRs also directly modulates the function of AMPA receptors, inducing a reversible depression in the CA1 area in the presence of Mg^{2+}, a form of mGluR-sensitive LTD (Oliet et al., 1997). For review of mGluR receptors, see (Anwyl, 1999).

1.6: The Hippocampus and Synaptic Plasticity.

The role of the hippocampus in memory-related research starts with a Russian neurophysiologist and psychiatrist Dr Vladimir Bekhterev (1857-1927), who first noted a role of the hippocampus in memory around 1900, based on observations of a patient with profound memory disturbances. The importance of the hippocampus in memory was later characterized through the work of Dr Corkin with patient HM. At age 27 H.M had an 8 cm length of his medial temporal lode bilaterally excised, this included two thirds of the patient's hippocampus. This surgery was conducted as a cure for medically intractable epilepsy but left HM with partial retrograde amnesia, and extreme anterograde amnesia which confers an inability to encode new memories and remember events from a few years prior to the surgery (Corkin, 2002).

The hippocampal formation is comprised of two hippocampi one found in each hemisphere. Among mammals the hippocampi are bilateral curving sausage-shaped structures which cannot be seen from the brain surface as they lie lateral to the thalamus and medial to the temporal horns of the lateral ventricles. One end of each hippocampus borders the septum and is termed the septal pole; the opposite end extends anteriorly into the temporal lobe and is termed the temporal pole. The hippocampus and its neighboring cortical regions, the dentate gyrus, subiculum and entorhinal cortex, are collectively termed the 'hippocampal formation' (Amaral et al., 1990).

The anatomical structure of the hippocampal slice is well defined, the principal cell bodies of the two main regions form distinct curves around each other. The dentate granule cells form the smaller of the two curves and are the principal cells of the dentate gyrus (DG) and are estimated to number 1×10^6 cells (Boss et al., 1987). Granule cells density have been found to be at a 180:1 ratio, with the pyramidal basket cell (Seress and Pokorny, 1981).

The hippocampal pyramidal cells form a second curved layer, characterised by four general areas (CA1- CA4). The CA title refers to the Latin description *Cornu Ammonis* or Ammon's (ram's) horn, relating to the curved shape of the hippocampal structure, originally proposed by Lorente de Nó, 1934 (Nó, 1934). CA 2-3 region is thought to contain approximately 2.1×10^5 pyramidal cells and CA1 region 3.2×10^5 pyramidal cells, although species variability has been shown (Amaral et al., 1990; Amaral et al., 1995; Abe et al., 2004).

CA1 pyramidal cells tend to have dendritic homogeneity in total dendritic length (although number of principal dendrites may vary), despite differences in the number and distribution of dendritic branches. The excitatory synapses found in the CA1 pyramidal cells, are almost exclusively located on the dendritic spines (Andersen, 1990) with an estimated spine density of 2.5 - 3 per μm. This would give 25000-30000 spines per cell. It is thought that 100-300 synchronously active synapses are necessary for a CA1 neurone to discharge an action potential.

The trisynaptic pathway represents three main circuits, the first main input is to the dentate granule cells via the perforant pathway (PP), but this pathway also has direct projections to the CA1 and CA3 regions (Desmond et al., 1994; Pare and Llinas, 1995; Yeckel and Berger, 1995).

The next projection is from dentate granule cells to the proximal section of the apical dendrite of the CA3 pyramidal cells (*mossy fibre pathway*), with the distal section of the apical CA3 dendrite receiving a commissural projection. The CA3 pyramidal cells have three outputs; the first a commissural output projection through the fimbria, to the other hippocampi. The second projection is the "inward" commissural projection from the other hippocampi. The third projection of the CA3 pyramidal cell forms the third circuit of the trisynaptic pathway. This projection is from the CA3 to CA1 pyramidal cells through the stratum radiatum and called the *Shaffer collateral commissural pathway.* The last step of this pathway is the output axons of the CA1 pyramidal cells which project out to the entorhinal cortex via the subiculum.

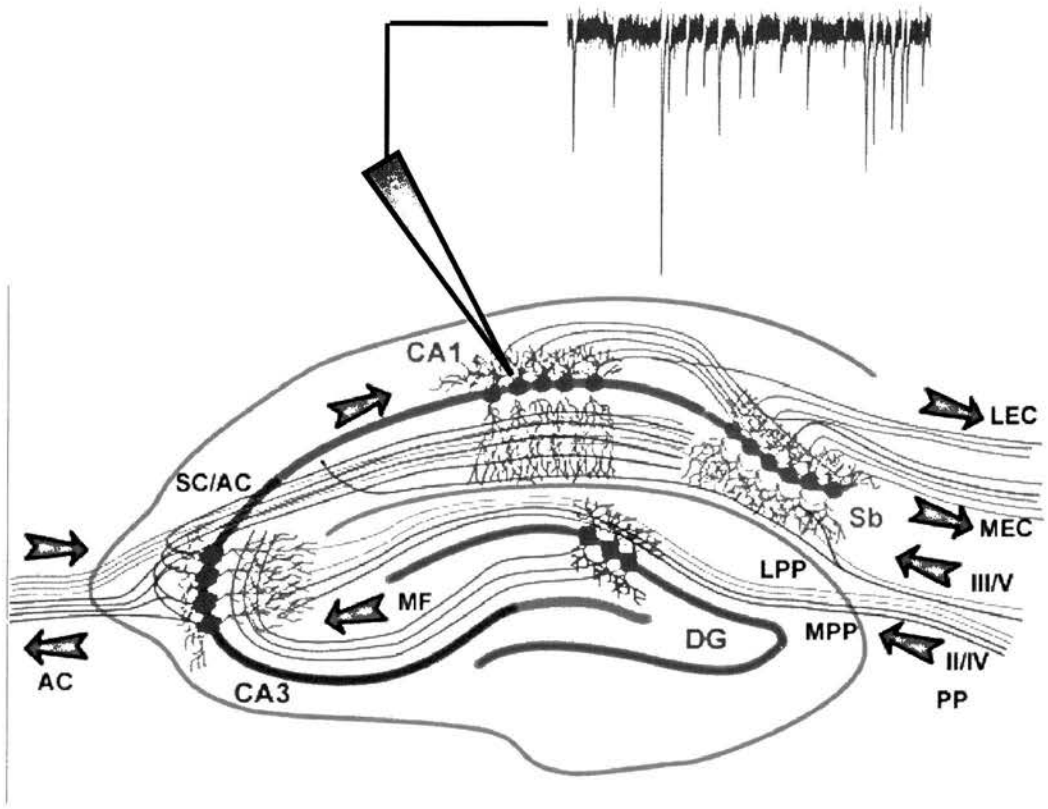

Figure 1.3: **Diagram of the tri-synaptic pathway of the rat hippocampus.** A figure representing the projections of the tri synaptic pathway, highlighting the input connections to the granule cells of the dentate gyrus (DG) via the perforant pathway (PP), and the subsequent projection to the pyramidal cells of the CA3 region is via mossy fibre pathway (MF). The third projection the one utilized in these experiments is the Schaffer collateral commissural pathway (SC/AC) from the CA3 pyramidal cells to the CA1 pyramidal cells. The output projection from the CA1 cell is to the entorhinal cortex (EC), via the subiculum (Sb) closing the pathway. Figure 1.3 adapted from www.bristol.ac.uk/fmvs/research/neurosciene.html. (L) lateral (M) medial.

Synaptic plasticity

The synaptic plasticity expressed by CA1 pyramidal cells of the trisynaptic pathway found in the hippocampus has been proposed as the mechanism by which processes of learning and memory can occur. Excitatory modifications to the strength of a synaptic signal can occur by six main mechanisms (see below); the balance between these effectors is what is termed synaptic plasticity.

Presynaptic mechanisms

1. Increasing the release probability of vesicles
2. Increasing the concentration of vesicular neurotransmitter.

Postsynaptic mechanisms

1. Increasing the number of receptors at the synapse
2. Increasing the conductance of receptors at the synapse
3. Increasing the open channel probability
4. Increasing the sensitivity of receptors at the synapse to agonists

Synaptic plasticity can be broken down into two main components, a process by which excitatory synaptic transmission can be increased (long term potentiation-LTP) and a complementary pathway by which synaptic transmission can be depressed (long term depression - LTD). Mechanisms of LTP have been most extensively studied in the hippocampus (2730 research papers on LTP and hippocampus from June 1979 to March 2005. LTP is usually generated by the pairing of a presynaptic stimulus with a depolarised post synaptic cell. The stimulus is applied to the Schaffer collateral commissural (SCC) axons; this presynaptic stimulus generates action potentials which bring about neurotransmitter release in a Ca^{2+} dependent mechanism. The SCC axons synapse with CA1 pyramidal cells and the released neurotransmitter acts on postsynaptic membrane bound receptors and generates a graded excitatory postsynaptic potential (EPSP), the strength of synaptic neurotransmission is defined by the amplitude of the EPSP. The typical stimulus to induce LTP is a high frequency burst typically (100 Hz) lasting for 1-3 seconds (called a tetanic stimulus). This stimulation usually induces an increase in the amplitude of the EPSP (between 50 – 100%), and the EPSC may stay at this potentiated level, as long as the slice is viable (2 - 8 hours).

LTD is the weakening process which is complementary to LTP. LTP occurs at synapses which have both presynaptic activity and a depolarised postsynaptic cell. LTD will occur with

either presynaptic activity or depolarised postsynaptic cell, but is still dependent upon an increase in postsynaptic calcium. In addition, if there is presynaptic activity and no postsynaptic depolarisation the synapse is still functionally weakened, termed homosynaptic LTD. The converse is also true, if the postsynaptic cell is active due to other sites of stimulation (neurones may have over 10,000 synapses) and there is no presynaptic activity then again the synapse will be weakened and this is termed heterosynaptic LTD (Oliet et al., 1997). The stimulation required to induce LTD is significantly different from that of LTP as it can require several minutes of stimulation at a low frequency (1-5 Hz). A significant difference in the stimulation period exists between LTP/LTD. The difference has been linked to a reduction in afferent innervation of these pyramidal cells, innervation which would normally occur in the intact brain, but are missing due to the slicing protocol. Application of a cholinergic agonist reduced the stimulus period to 20 ms to induce LTD (Abraham and Bear, 1996; Yang et al., 1999).

The cellular effects of LTD have been associated with a reduction in AMPA receptor number at the synapse, and the negative presynaptic modulation of transmitter release. Both of these phenomena can occur in the same cell and are dependent upon calcium influx but require different levels of stimulation. The higher order regulation of cell function, causing the switch between either form of plasticity been championed by Professor Mark Bear. Defined as metaplasticity it is described by the statement 'Metaplasticity has occurred if prior synaptic or cellular activity (or inactivity) leads to a persistent change in the direction or degree of synaptic plasticity elicited by a given pattern of synaptic activation' (Abraham and Bear, 1996). Basically this describes the state of weakly innervated cells. In that low levels of synaptic activity do not fully depolarise the cell and induce LTP, this low activity state maybe sufficient to prime the threshold for synaptic modifications making it easier to induce LTD.
In summary CA1 pyramidal cells display mechanisms, by which the ability to both strengthen and weaken the synaptic output of these cells are affected.

1.7: Functional cellular mechanisms for LTP

Historically the first experimental recording of long term potentiation comes from the laboratories of Per Andersen in Oslo Norway, with the first presentation of LTP by Terje Lømo (Lømo, 1966). However the most famous full account, regarded as the first publication of LTP, was published in 1973 by Tim Bliss and Terje Lømo (Bliss and Lomo, 1973).

The development of the now classical NMDA receptor-dependent LTP (Collingridge et al., 1983) occurs upon tetanic stimulation of Schaffer collateral/commissural fibres that synapse

on to CA1 pyramidal neurones in the hippocampus. Indeed pharmacological and genetic manipulations of NMDA receptor function can have profound effects on both LTP and spatial learning tasks (Martin et al., 2000; Martin and Morris, 2002).

Initially synaptic plasticity experiments focused on the induction mechanism for LTP, induced by brief repetitive stimulations of the excitatory Schaffer collateral pathway of the hippocampus. The induction was found to be dependent upon two key features, an increase in the postsynaptic calcium concentration and the activation of postsynaptic NMDA receptors the a source of the calcium increase (Collingridge et al., 1983).

In 1988, it was demonstrated that LTP in the CA1 region of the hippocampus required an increase in postsynaptic calcium concentration. This finding was elucidated by two groups, with Malenka et al. using the Ca^{2+} chelator Nitr-5 and Lynch et al. using EGTA. Both chelators were included in the internal recording solution in the glass electrode restricting the application to the postsynaptic cell. Through different mechanisms in the first case by Ca^{2+} flash photolysis (which generates a sudden increase in Ca^{2+} concentration) and in the second by chelation (which removes all of the Ca^{2+} present in the postsynaptic cell) these two papers indicated that a rise in the postsynaptic calcium concentration was essential to LTP induction in CA1 neurones.

Investigations by Collingridge (Collingridge et al., 1983), determined that postsynaptic Ca^{2+} enters the cell via three main routes. For the classical LTP-NMDA receptor-dependent mechanism in the CA1 pyramidal cell of the hippocampus, postsynaptic Ca^{2+} entry is through the NMDA receptor. The other pathways are somewhat controversial but rely upon entry through voltage gated calcium channels (Kapur et al., 1998; Morgan and Teyler, 1999; Matias et al., 2003; Woodside et al., 2004) and release from intracellular stores (Reyes and Stanton, 1996; Emptage et al., 1999; Nishiyama et al., 2000; Lauri et al., 2003; Kumar and Foster, 2004).

LTP induction is NMDA receptor-dependent, the increase in synaptic strength generated is mediated as an increase in the AMPA component of the EPSC (Andrasfalvy and Magee, 2004). This implies that this stimulating protocol has a distinct effect on AMPA receptor recruitment or modification, or is utilising a presynaptic mechanism, that facilitates an increase in pre-synaptic vesicle release. Postsynaptic mechanisms underlying this increase in the AMPA receptor mediated component are discussed in Protein-Protein interactions section 1.14.

1.8 Long Term Potentiation and Voltage-Pulse Potentiation

The conventional LTP stimulating protocol uses tetanic stimulation to relieve Mg^{2+} blockade of NMDAR, inducing a postsynaptic depolarisation with a corresponding increase in

postsynaptic Ca^{2+} dependent upon synaptic mechanisms involving NMDA receptors (Collingridge et al., 1983). Such a LTP stimulating protocol is likely to activate only a few hundreds of synapses impinging on the CA1 neurons. Such a protocol will potentiate too few of the total number of synaptic sites on the individual CA1 pyramidal neurone to resolve any alterations to miniature post synaptic current (mEPSC) amplitudes and frequencies before and alter LTP induction, in that any mEPSCs occurring at potentiated synapses would be lost in the background of small amplitude mEPSCs from other non-potentiated synapses.

Gustafsson and Wigstrom, (1990) suggested the need to depolarise the cells further than was done with LTP stimulation, to activate voltage operated Ca^{2+} channels. This approach was adopted by Kullmann et al. (1992), whose approach was to block the NMDA receptor using 2-amino-5-phosphonovaleric acid (AP5), and apply a series of depolarising pulses to the cell to activate voltage gated Ca^{2+} channels – this is referred to as voltage-pulse potentiation (VPP). The original induction protocol used in acute slices consisted of twenty, +100 mV depolarisations lasting 3 seconds in a two minute period. This protocol induces a global increase in Ca^{2+} in the postsynaptic cell, resulting from the activation of postsynaptic L-type voltage-gated calcium channels, either synaptic or at extra-synaptic sites. The small size and unique shapes of dendritic spines (site of synapses) lends itself well to the VPP stimulus, due to the small volume of the spine, a large postsynaptic calcium concentration can be obtained even after a small influx of calcium ions.

Experiments using the VPP stimulus in guinea-pig slices resulted in a transient increase in both the amplitude (2.5 fold) and frequency (1.6 fold) of mEPSCs (Wyllie et al., 1994). VPP was subsequently found to be dependent on kinase activity and intriguingly can be converted to a sustained potentiation if phosphatase inhibitors are present at the induction stage (Wyllie and Nicoll, 1994).

In this thesis I have looked solely at the AMPA receptor dependent component of this potentiation of synaptic output. To do this I used miniature excitatory postsynaptic currents (mEPSCs). Such miniature synaptic events were first described by Sir Bernard Katz in 1952 (Fatt and Katz, 1952) when recording from the frog neuromuscular junction. In these recordings he noted small depolarizations of the membrane potential which he first thought to be due to an artefact of the recording set-up. These were no artefact and for this and other work Katz was awarded the Nobel Prize in Physiology or Medicine in 1970.

Recording mEPSCs is an excellent way of looking at synaptic activity, as these small currents result from the spontaneous release of single glutamate containing vesicles and,

therefore act as a functional read out of the cell as they give an expression of both presynaptic (frequency changes) and postsynaptic (amplitude changes) functionality. Furthermore, since mEPSCs do not require the constant stimulation that (evoked) EPSC studies require these experiments are not hampered by the often overlooked phenomena of activity dependent synaptic silencing. This occurs when repetitive stimulation, required to generate EPSCs, acts on synapses with a weaker synaptic weight and functionally silences these synapses. This can be likened to LTD at the single synapse level (Xiao et al., 2004). The net result is an expression of a 'false' potentiation of EPSC amplitudes, false because of the selection of only larger amplitude events. This functional silencing is expressed as an increasing failure rate over the course of the experiment (a 'failure' is classed as each occurrence of an applied stimulus which fails to generate an EPSC).

mEPSC result from the spontaneous release of 'packets' of neurotransmitter, as Katz referred to them, from the presynaptic nerve terminal and give rise to a current from the activation of both AMPA and NMDA receptors. True mEPSCs are insensitive to the voltage-gated sodium channel blocker, tetrodotoxin. In the presence of tetrodotoxin (evoked) EPSC stimulation based experiments are impossible as generation of the presynaptic action potential cannot happen. The other advantageous features of mEPSC recordings over the EPSC stimulation experiments apart from the failure rate problems (expressed postsynaptically), is that EPSCs are also dependent on presynaptic properties of the cable conducting properties of the presynaptic (SCC) axons affecting the release probability i.e. failure of an action potential to be conducted. This is not a problem for mEPSC recording as release is spontaneous.

Glutamate release generates various types of EPSCs, either pure AMPA or kainate mEPSCs or mixed receptor type kainate/AMPA. Pure kainate mEPSCs are very rare and have a much slower rise and decay time, when compared to the pure AMPA mEPSC (Cossart et al., 2002). Since glutamatergic ionotropic receptors are believed to be co-localised at excitatory synapses (Bekkers and Stevens, 1995; Gomperts et al., 1998; Lissin et al., 1998; Gomperts et al., 2000) has increased the use of mEPSCs as a sensor for the changes applicable to a pre or postsynaptic mechanism/modification for plasticity.

There is, however, controversy that the majority of nascent glutamatergic synapses express both functional AMPA and NMDA receptors in the neonatal Wistar rat hippocampus (P0 - P8) (Groc et al., 2002). This is controversial, since there is physiological evidence during development, for certain synapses to contain only functional NMDA receptors, and lack the fast acting AMPA receptor. These synapses appear to be physiologically silent due to the NMDA

receptor being blocked by magnesium (Mg^{2+}) ions in a voltage-dependent manner. (Gasparini et al., 2000; Gomperts et al., 2000; Isaac, 2003). Therefore, these silent synapses are unable to respond to glutamate released from the presynaptic terminal. Silent synapse theory relates to that ability of functional AMPA receptors, to be quickly recruited into the postsynaptic membrane. Through the action of these new receptors the functional block is relieved and the synapse becomes active (Standley et al., 1995; Braithwaite et al., 2000; Isaac, 2003). One major argument against this silent synapses theory, is that 'spill over' (Diamond, 2002) from synapse to synapse could account for the sudden synaptic activity associated with silent synapses. Due to the approximate 100 fold difference in affinity for glutamate between AMPA and NMDA receptors (Gomperts et al., 1998), it is possible for glutamate to spill over from neighbouring synapses and selectively activate NMDA receptors in these synapses. Other possible mechanisms include incomplete uptake of glutamate, by transporter proteins on surrounding glial cells (Bergles and Jahr, 1997) resulting in a sufficient concentration to activate receptors in neighbouring synapses. Although immunohistochemical studies have provided evidence that synapses containing only NMDA receptor are present in some neurones (Liao et al., 1999). The possibility of glutamate spill over, occurring between the synapse can never be fully ruled out.

AMPA receptors can also move laterally within the plasma membrane during synaptic plasticity. Single particle tracking has shown that the GluR2 containing receptors rapidly alternate between highly mobile (6-12 $\mu m^2 s^{-1}$) and stationary ($< 0.05\ \mu m^2 s^{-1}$) states. Furthermore transition between these states is regulated by intracellular calcium (Borgdorff and Choquet, 2002). With AMPA receptor transport and insertion there has been shown a proportional increase in NMDA receptor number at synapses as well (Watt et al. 2004).

1.9 Why use organotypic hippocampal slices and what is the cellular purpose of mEPSCs?

In 1957 Henry McIlwain, showed that slices of hippocampal tissue retained their highly organized structure and circuitry and could be kept viable in an artificial experimental setting, enabling intracellular electrophysiological recording from CA1 pyramidal cells.

Gähwiler, (1981) first pioneered the application of cell culture techniques to nerve cells developing an artificial culture system, which produced viable nerve cells for experimentation. In 1981 this was further developed with the production of viable cultured acute hippocampal slices. (Gahwiler, 1984, 1988) (For review see Gähwiler et al. 1997).

Organotypic cultured hippocampal slices as described by (Stoppini et al., 1991), have the advantage, that their use allows better access these pyramidal cells, as through the culturing

process as the thickness of the tissue reduces to almost a monolayer, allowing for the characterization of cell network circuitry. Recordings from organotypic CA1 pyramidal cells have shown that these cells have very similar electrophysiological properties to CA1 pyramidal cells in traditional acute hippocampal slices, although the organotypic slices lack any development of synaptic connectivity and morphology which may be attributed from the normal behavior of these animals.

De Simoni et al. (2003) characterized the relationship between acute and organotypic slices. In this study acute slices prepared at postnatal day (P) 7, 14, 21 were found to be developmentally equivalent to organotypic slices cultured for 1, 2, 3 weeks in terms of synaptic transmission and dendritic morphology. Furthermore, the development of dendritic length and primary branching as well as spine density and the proportions off spine types were also similar in both preparations and at equivalent ages. The only significant difference was the frequency of glutamatergic (not GABAergic) miniature postsynaptic currents (mEPSCs) in the organotypic slice, which showed a four fold increase. This significant increase in event frequency was attributed to an increase in the complexity of higher order dendritic branching in these organotypic slices.

This higher event frequency is beneficial for this study as a large number of synaptic events, will be advantageous in this study as it will allow better resolution of any change in mEPSC amplitudes or frequencies.

Katz suggested that the miniature end plate potentials (mEPPs) recorded at the neuromuscular junction could summate to an action potential. Per Andersen (1990) later found that only 100-300 synchronously active excitatory synapses seem necessary to make the cell discharge.

To date the functionality of the mEPSC has been described by two diverging principles; the first from McKinney & Gähwiler who investigated the changes in dendritic spine size/shape as an enduring structural correlate for synaptic plasticity (McKinney et al., 1999b; McKinney et al., 1999a). Structural changes in dendritic spine size and shape are associated with LTP (Edwards, 1995). Hence, spine size and shape influence the electrical transfer of synaptic currents and the intracellular Ca^{2+} concentration transients generated in spines thereby modifying synaptic integration and plasticity. What was shown by McKinney et al., (1999b) was that a low mEPSCs frequency and subsequent AMPA receptor activation was sufficient to maintain dendritic spine structure, useful for maintaining the architecture of quiescent cells in the brain.

The second functional property shown by the laboratories of Erin Schuman, highlighted that the spontaneous activity of the mEPSC acutely regulated dendritic protein synthesis. Blocking action potentials with TTX caused a reduction in protein synthesis, while blockade of both action potentials and mEPSCs resulted in an increase in dendritic protein synthesis. The functional consequence is the possibility of local translational regulation on a rapid scale which may define use dependent change in synaptic strength and hence modify synaptic plasticity (Sutton et al., 2004).

1.10: Organisation of the postsynaptic density

The postsynaptic compartment, found at the spine head, represents the site of the synapse and hence the site of excitatory cell to cell signalling. At the spine head, there exists a specialisation called the postsynaptic density (PSD), which acts as a scaffold to hang the effectors of synaptic activity upon, thereby stabilising these effectors in the postsynaptic membrane.

The PSD comprises a disk like structure 30 - 40 nm thick and a few 100 nm long, the PSD is found at postsynaptic sites directly apposed to the active zones in the presynaptic terminal. The PSDs are also subject to activity dependent remodelling as activating stimuli induce changes in spine shape and volume the PSD must also be able to change to continue synaptic action.

There are five main components of postsynaptic density:

1. Cytoskeletal proteins, such as actin and tubulin (Brown, 1999; Krupp et al., 1999; Braithwaite et al., 2000; Chen et al., 2004), which are required to support the architecture of the spine projection.
2. Cell adhesion molecules required for the binding of new components to the postsynaptic density.
3. Receptors involved in excitatory signal transduction are held in the PSD.
4. Signal transduction proteins, including the calcium binding protein calmodulin (CaM); serine/threonine protein kinases such as the calcium/calmodulin dependent kinase II (CaMKII) and cAMP dependent kinase (PKA). These proteins conduct the signal from the postsynaptic desity to the cell, and also interact directly with postsynaptic receptors modifying their function and facilitating LTP.

5. Scaffolding proteins, these proteins have the largest diversity of function; they act to cluster receptors (of different types) at activated synapses. These facilitate the targeting of newly synthesised receptors to specific membrane domains, which cause the membrane immobilization necessary for the function of the receptor by anchoring to cytoskeleton. Scaffolding proteins effect coupling of the receptor to down-stream signalling molecules, which is necessary for the long term potentiation of excitatory synaptic activity.

1.11: Protein-Protein interactions governing AMPA receptor transport to synapses

Both AMPA receptors (Liu and Cull-Candy, 2000; Borgdorff and Choquet, 2002) and NMDA receptors (Tovar and Westbrook, 2002) have been shown to be highly dynamic, in that receptors can be rapidly interchanged between the synapse and the various intracellular receptor stores.

This dynamic transport of receptors suggests that a rapid incorporation of the receptor into synapses is a possible mechanism for development of the potentiated EPSC amplitude shown with LTP. With this rapid incorporation of new receptors there exists the further phenomena, the generation of silent and nascent synapses and the synaptic effects of the subsequent removal of receptors by endocytosis (Carroll et al., 2001). Such cycling of receptors may provide a method for the rapid alteration in synaptic strength seen with some forms of synaptic plasticity.

This transport of AMPA receptors is thought by many groups to be dependent upon activity of the neuron, as chronic NMDA receptor blockade experiments show rapid AMPA receptor synaptic delivery (AMPAifcation) (Zhu and Malinow, 2002). Thus this suggests a possible activity-dependent mechanism underlying the relief of the NMDA receptor Mg^{2+} block and therefore synaptic plasticity. Moreover Washbourne et al (2002) have indicated that there is a distinct difference in the recruitment interval for NMDA and AMPA receptors, strengthening the silent synapse theory. They suggest that vesicles of NMDA receptors move to synapses faster than the AMPA subunits are recruited to the same synapse. Therefore the NMDA receptors are already in situ waiting to be activated when the AMPA receptors arrive, effectively generating a functional but silent synapse, with a further proportional delayed increase in NMDA receptor number following AMPA receptor transport (Watt et al. 2004).

Silent synapse theory, describes any synapse which has *in situ* NMDA receptors but lacks AMPA receptors, they are physiologically silent or deaf due to Mg^{2+} block of the NMDA receptor at resting membrane potentials. This theory is further complicated by synapses

displaying degrees of silence depending upon a pre/postsynaptic locus for activation. Postsynaptically silent/deaf synapses are unable to detect glutamate release and do not conduct due to the lack of AMPA receptors. Presynaptic silent synapses do not conduct because the release probability is close to zero (mute synapse) or there is a small degree of receptor activation (whispering synapse) due to the temporal profile of glutamate in the cleft. This idea of low cleft concentration for glutamate was proposed by Kullmann (Kullmann, 2003), as a mechanism of synaptic spill-over to neighbouring synapses, which brings about their activation (Kullmann, 1994; Kullmann et al., 1996; Kullmann and Asztely, 1998).

As shown with NMDA receptors the trafficking of receptors to membrane sites is dependent upon interactions with various membrane associated proteins, from the literature there appears to be three well defined protein complexes with bring about the insertion of AMPA receptors into active membrane. Trafficking properties of these complexes NSF related protein complexes, the PDZ domain related proteins (PICK1/GRIP/ABP) and stargazin/PSD-95 a modification of the NMDA receptor delivery mechanism.

1.12: NSF protein

Initially N-ethylmaleimide sensitive fusion (NSF) protein was characterised as an ATPase with diverse cellular actions, but primarily involved in the docking and fusion of presynaptic vesicles facilitating transmitter release (Patel and Latterich, 1998; Finley et al., 2002). This protein was found to exist independently as NSF and act as a chaperone for the SNARE complex proteins (soluble NSF attachment protein receptor) which include SNAP 25 (soluble N-ethylmaleimide adaptor protein of 25 kDa) and VAMP1 (vesicle associated membrane protein also called synaptobervin). Through various interactions these proteins in the presynaptic terminal facilitate the association of vesicle and the presynaptic membrane to allow neurotransmission, and for the subsequent removal of the vesicle from the docking site (Littlejohn et al 2001; for review see Chen and Scheller, 2001; Ziv and Garner, 2004).

Functional NSF shows a wide tissue distribution and is abundant in the hippocampus (Hong et al., 1994), the protein presynaptically exists as a hexamer, and only in this oligomeric form does it exert any functional action on SNARE complexes. NSF has 3 domains an N domain which is essential for function and a D1 domain which requires ATP binding and hydrolysis for the SNARE complex disassembly reaction to occur and ATP binding but not further hydrolysis by the D2 subunit is necessary for hexamer formation.

However these proteins were later identified in the postsynaptic membrane (Walsh and Kuruc, 1992), an unusual finding as this part of the synapse typically receives the presynaptic signal, and so has no vesicles with neurotransmitter.

Postsynaptically NSF was found to associate with the GluR2 AMPA receptor subunit and modify its activity dependent insertion into the postsynaptic membrane as pharmacological blockade of NSF with NEM inhibited the induction of LTP (Lledo et al., 1998). Association of NSF and other glutamate receptor subunits proved ellusive, as NSF is only weakly associated with the GluR3 subunit and does not bind to the GluR1 or GluR4 AMPA receptor subunits, or the kainate GluR6 and finally does not associate with the NR1 subunit of the NMDA receptor (Nishimune et al., 1998), but is involved in the transport of nicotinic acetylcholine receptors. (Liu et al., 2005).

The reduction of the LTP potentiated AMPA component of the EPSC, by the application of NSF blocking drugs has two possible mechanisms of action. The first is that NSF is required for the surface expression of AMPA receptors and blockade of this interaction inhibits this expression (Nishimune et al., 1998; Osten et al., 1998; Song et al., 1998; Luthi et al., 1999; Noel et al., 1999; Osten and Ziff, 1999; Banke et al., 2000). The second mechanism is that NSF acts as a stabiliser of membrane integrated AMPA receptors. This limits exocytosis and insertion of new receptors into these synapses (Braithwaite et al., 2002).

Multiple mechanisms exist for the delivery of new receptors to active synapses. In the GluR2 knockout mouse, AMPA receptors are still present at CA1 synapses, and AMPA-receptor mediated EPSCs are reduced by 50 % compared to wild type litter mates (Jia et al., 1996).

1.13: PDZ scaffolding protein dependent transport of AMPA receptors

PDZ domains are small 90 amino acid long binding domains, which have the sole function of tethering the carboxy terminal on one protein to another; by this mechanism they form large protein complexes which facilitate activity-dependent synaptic plasticity. PSD95/Synapse associated protein (SAP)-93 is a well characterised scaffolding protein (Lim et al., 2003; Lin et al., 2004; Romorini et al., 2004), which is part of the membrane associated guanylate kinase-like (MAGUK) family. The PSD 95 protein has 3 PDZ binding domains, a SH3 (Src homology 3 domain) domain which will facilitate an interaction with kainate receptors, and a guanylate kinase- like (GK) domain (Figure 1.4).

These proteins have been shown to be principally responsible for the delivery of NMDA receptors to active synapses (Lin et al., 2004); via the interactions of a C-terminal amino acid sequence (ESDV or ESEV) on the NMDA NR2 (A-D) subunits and the PDZ domains of PSD 95/SAP 90.

PSD 95 does not directly bind or facilitate the transport of AMPA receptors to synapses. However, PSD 95 when associated with stargazing, another membrane associated adaptor protein, and has been shown to facilitate the transportation of AMPA receptors to synapses (Chen et al., 2000; Schnell et al., 2002; Dakoji et al., 2003{Rumbaugh, 2003 #438; Rumbaugh et al., 2003; Vandenberghe et al., 2005); for review of PSD see Kim and Sheng, 2004. This PSD95/stargazin interaction is regulated by phosphorylation of Stargazin, as in the phosphorylated state stargazin is prevented from binding to PSD95 (Chetkovich et al., 2002; Choi et al., 2002).

Only SAP 97 acts to directly transport AMPA receptors to the synapse, unlike NSF transportation of the GluR2 AMPA subunit, SAP 97 interacts with the GluR1 subunit (Leonard et al., 1998; Rumbaugh et al., 2003).

Three types of PDZ domain containing AMPA receptor specific scaffolding proteins have been classified: protein interacting with C kinase 1 (PICK1), glutamate receptor interacting protein (GRIP), and AMPA receptor binding protein. Within the literature there is much debate over the functional actions of these scaffolding proteins in CA1 LTP. PICK 1 structurally is the simplest of the PDZ containing AMPA receptor scaffolding proteins, as it contains only one PDZ domain and a coiled coil domain which allows dimerism of this protein (See Figure 1.4 and Figure 1.5).

This scaffolding protein displays a high degree of promiscuity as interactions with mGluRs and kainate receptors have also been shown, and inhibition experiments have shown effects on kainate mediate synaptic transmission (Hirbec et al., 2003).

PICK 1 via an interaction with protein kinase C (PKC) has been shown to regulate an increase in AMPA receptor surface expression in a population of CA1 pyramidal neurones (Banke et al., 2000; Chung et al., 2000; Daw et al., 2000; Perez et al., 2001; Hirbec et al., 2003; Terashima et al., 2004). However there is also a proposed role for PICK 1, with internalisation of AMPA receptors in LTD in CA1 neurones (Kim et al., 2001). Differences may be accounted for by the phosphorylation state of the AMPA receptor. Phosphorylation of Ser 880 in the C terminus of GluR2 by PKC prevents the interaction with GRIP/ABP but not with PICK1, this suggests that phosphorylation might selectively displace AMPA receptors from GRIP in favour

of PICK 1. This phosphorylation is well characterised in cerebellar LTD, and has been shown with hippocampal LTD (Perez et al., 2001). In summary, evidence can be proposed for an action of PICK1 in both pathways. Therefore it is logical to believe that PICK 1 regulates both insertion and internalisation of AMPA receptors.

1.14: GRIP/ABP

GRIP and ABP represent large multi PDZ AMPA receptor binding proteins, these proteins contain 7 PDZ domains in comparison to the singular PDZ domain found with PICK1. These proteins are expressed throughout the brain, and at the cellular level are found both on excitatory and inhibitory neurons, suggesting a vast diversity of action (Wyszynski et al., 1999).

Two variants of GRIP exist (1 and 2). Although homologous proteins of 130 kDa they display different temporal patterning during embryonic development. GRIP1 is highly expressed at a point pre AMPA receptor expression, while GRIP2 is expressed later and parallels the cellular expression of AMPA receptors. A further protein ABP is regarded as a splice variant of GRIP2. These proteins are almost identical, bar the expectation that ABP lacks a 7^{th} PDZ domain. (Srivastava and Ziff, 1999; Braithwaite et al., 2002)

GRIP is also capable of forming dimers through an interaction between the PDZ 6 domains of 2 monomers (Im et al., 2003). The binding of AMPA receptors to GRIP occurs through PDZ 5 but requires interaction from PDZ 4 to stabilise the binding (Dong et al., 1999; Feng et al., 2003); AMPA receptor interactions occur at three PDZ domains (3,5,6) (Srivastava et al., 1998; Srivastava and Ziff, 1999).

1.15: AMPA PDZ protein regulation of LTP and LTD

Under basal synaptic transmission, PDZ interactions with the C terminus of GluR2/ GluR3 regulate the insertion and retrieval of receptors from the synapse. The idea is that GRIP/ABP proteins regulate the sorting and delivery of AMPA receptors to active synapses, while PICK1 controls the binding and stability of these receptors in membranes (Dong et al., 1999). Induction of LTP activates PKC and subsequently phosphorylation of the GluR2 receptor subunit at serine 880; this promotes dissociation of receptors from a rapidly releasable pool (PICK1 and GRIP/ABP bound synaptically located receptors) allowing for receptor insertion.

The opposite is also applicable during LTD experiments where receptors which have undergone activity-dependent internalisation may bind to multi-protein complexes of GRIP/ABP

which would anchor these receptors to the sub-synaptic domain preventing their reinsertion (Chung et al., 2000) and acting as a functional store.

De-depression experiments (Heynen et al., 2000; Lee et al., 2000; Bear, 2003), which show LTP in cells which have previously expressed LTD, display this functional plasticity where AMPA receptors dissociate from PICK1 or GRIP/ABP and PKC phosphorylation at serine 880 prevents rebinding to GRIP/ABP (Chung et al., 2000) and allows insertion of these unbound receptors.

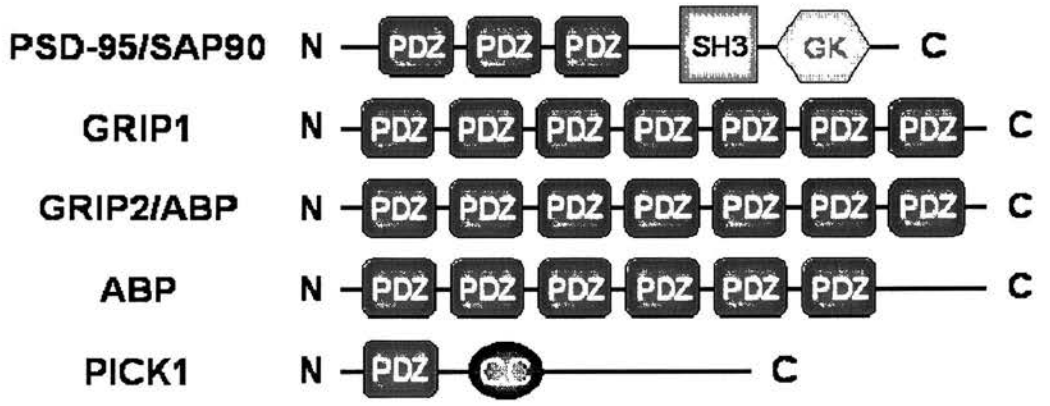

Figure 1.4: **Structural domains of PDZ containing proteins which interact with glutamate receptors.** SAP90/ PSD95 are principal scaffolding protein for NMDA receptor insertion into active synapses. PSD 95 comprises 3 PDZ domains, one SH3 domain through which kainate receptors can bind, and a guanylate kinase binding domain which is used to attach to the postsynaptic cytoskeletal matrix. GRIP 1/2 and the splice variant ABP all contain simple PDZ binding domains which facilitate AMPA receptor incorporation into synapses. PICK1 another AMPA receptor scaffolding protein which has a function linked with GRIP/ABP complexes contains only 1 PDZ binding domain and a coiled coil domain (CC).

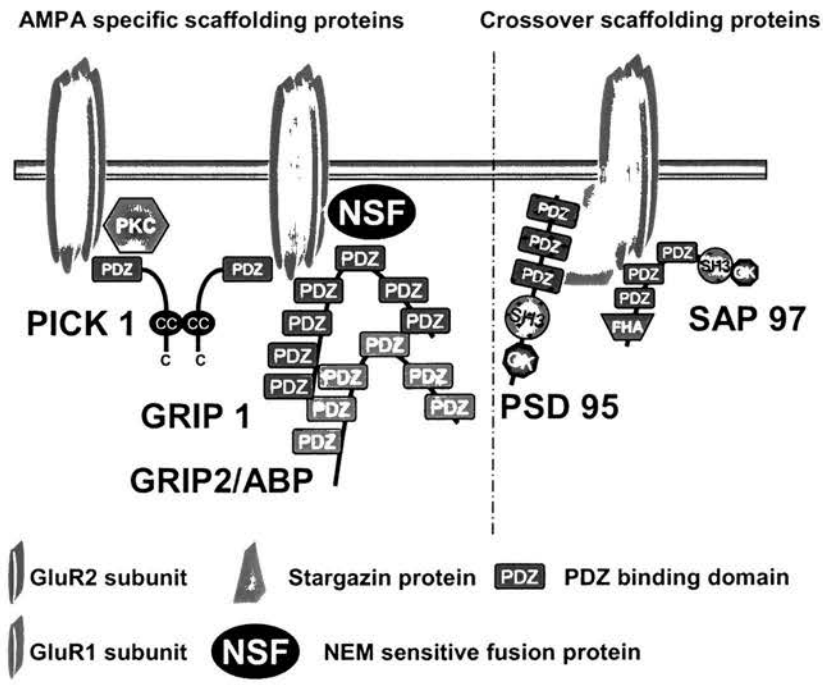

Figure 1.5: **Scaffolding proteins controlling AMPA receptor insertion.** AMPA receptor specific scaffolding proteins used for the insertion for new receptors include PICK1, GRIP1 and the splice variant GRIP2/ABP. This transport of receptors is mediated via an interaction with the GluR2 subunit. Furthermore, AMPA receptors can also be transported via the traditional NMDA receptor transport machinery, in the case of PSD 95 this transport is dependent upon the auxiliary protein Stargazin for the transport of the GluR2 receptor subunit. SAP 97 governs the transport of the GluR1 subunits. The multiple transport mechanisms for AMPA receptors when compared to the NMDA receptor could reflect the diversity and speed of novel AMPA receptor function.

1.16: Protein kinase regulation

For LTP based synaptic plasticity the diversity of higher order regulation at the protein kinase level is staggering. Within neurones there exists over 2,000 protein kinases and over 1000 protein phostphatases estimated from the human genome (Hunter, 1995). These kinases regulate all cell function including synaptic plasticity and cell homeostasis through interactions with cellular substrates and most importantly diverse interactions with other protein kinases. In order to facilitate an effect, kinases must be located close to their substrate, and an example of this is the interaction between A-kinase anchoring proteins (AKAP- For review see Colledge and Scott, 1999) and protein kinase A (PKA), which brings about the synaptic insertion of GluR1 containing AMPA receptors in a SAP97 dependent delivery mechanism (Colledge et al., 2000). Another well characterised protein kinase regarded as the molecular switch for LTP and memory storage, via both the transmission and activation of AMPA and NMDA receptors, is calcium/calmodulin-dependent protein kinase II (CaMKII) (Ghetti and Heinemann, 2000; Bayer et al., 2001; Lisman et al., 2002; Poncer et al., 2002; Machaca, 2003). CaMKII was found to be essential for the induction of LTP, as it holds the NMDA receptor in an open conformation for longer and facilitates AMPA receptor trafficking (Liao et al., 2001; Lisman and Zhabotinsky, 2001). As well as directly phosphorylating a serine 831 residue of the GluR1 subunit altering the conductance level, pushing the receptor to higher conductance levels (Benke et al., 1998; Lisman et al., 2002).

Membrane bound lipids, are substrates for many kinases, these lipids have a diversity of function. Not only are they utilised for the structural stability of the spine; they are used in receptor stimulated signalling. Well characterised membrane lipid family known to be involved in cell signalling are the inositol phospholipids. The classical mechanism for the hydrolysis of phosphatidylinositol (4,5) bisphosphate (PtdIns $(4,5)P_2$) is mediated by phospholipase C (PLC) to produce inositol (1,4,5) trisphosphate (Ins $(1,4,5)P_3$) which acts at various sites to bring about an increase in intracellular calcium. This breakdown also produces diacylglycerol (DAG), which activates serine/threonine kinases such as protein kinase C (PKC).

However, ($PtdIns(4,5)P_2$) acts as a substrate that has a wide diversity of effectors. Through a second metabolic pathway, phosphoinositide 3 kinase (PI3K) phosphorylates the 3'-OH position of the inositol ring of phospholipids and produces PtdIns(3)P, $PtdIns(3,4)P_2$, and $PtdIns(3,4,5)P_3$ all second messenger phospholipids with a diverse cellular functions. In mammalian cells PI3 kinases have multiple isoforms, but are divided up into three groups (Class 1,2,3). Class 1 PI3 kinases, typically have a p110 catalytic subunit of which 4 isoforms exist (α,

β, γ, and δ) and a p85 adaptor subunit, for review see Rameh and Cantley, 1999. The principal mechanism of action is that the p85 domain regulates an interaction with serine/theronine kinases in the cell membrane. This interaction brings the p110 domain into functional proximity with its main substrate, PtdIns (4,5) P_2 and generates PtdIns (3,4,5) P_3 thereby facilitating cell signalling. Class 2 PI3 kinases are bigger than Class1, but show 45 % homology, and show binding to PKC isoforms. Their cellular actions are not well characterised. Class 3 PI3 kinase appears to be a yeast isoform.

Scientific interest in PI3 kinases stems from cancer research, due to the finding that PTEN (Phosphate and TENsin homologue deleted on chromosome TEN) manages the degradation of PtdIns (3,4,5) P_3 (Cantley and Neel, 1999). Mutation or loss of the (PTEN) tumour suppressor gene has been found in many human tumours including breast and prostate cancers (Li et al., 1997; Steck et al., 1997) and at high frequency in endometrial tumours (Bonneau and Longy, 2000). Mice homozygous for target embryonic deletions of the PTEN gene, die during embryonic development (between 6 and 9 days), while heterozygous mice develop normally, but are prone to a wide range of tumour types (Dahia, 2000; Leslie and Downes, 2002). Cells which lack PTEN have elevated levels of PtdIns (3,4) P_2 and PtdIns (3,4,5) P_3 and exhibit constitutive activation of PI3 kinase signalling pathways mediated via PKA/AKT (Cantley and Neel, 1999; Cantrell, 2001) and Rac/Rho GTPases (Liliental et al., 2000). Due to the functional crossover with PLC, and the knowledge that PLC products mediate cellular trafficking mechanisms, the role of phosphoinositide 3 kinase (PI3 kinases) in excitatory synaptic transmission was highlighted when PI3 kinase was shown to be required in the glycine induced LTP of mEPSCs in cultured hippocampal neurones (Sanna et al., 2002; Man et al., 2003).

The mechanism for receptor trafficking and functional modification at the synaptic membrane requires interactions with other cellular protein kinases (See Figure 1.6). PKB has been shown to mediate the action of PI3 K. PtdIns(3,4)P_2 and PtdIns(3,4,5)P_3 bind to a PH domain of PKB recruiting the kinase to the plasma membrane. Furthermore the activation of PI3 K is sufficient in turn to mediate the activation of PKB (Datta et al., 1996). PKB shares sequence homology with PKA and PKC. Its activation regulates cell survival through *Bad* and can induce protein synthesis through mTOR. The activation of PKB also governs inter kinase interactions as PKB will activate Raf and subsequently MAP kinase signalling pathway which acts directly on AMPA and NMDA receptors. Within the PKB signalling pathway, a feed back

loop exists via phosphoinositide-dependent protein kinase-1 (PDK1) and activates PKC (Chou et al., 1998) for review see Chou et al.,1998;Vanhaesebroeck and Alessi 2000; Cantrell, 2000). In summary, the kinase regulation of cellular processes is a vast highly complex inter-regulating system. PI3 kinase has been shown to be important in the regulation of LTP in pyramidal cells although the mechanism has never been fully described (Hisatsune et al., 1999; Cantrell, 2001; Man et al., 2003; Huang et al., 2004).

1.17: The present study

My thesis work examined three areas which affect the potentiation of mEPSC amplitudes, mediated by increases in post synaptic calcium. In chapter three I will discuss the mechanisms for the induction of voltage pulse potentiation. Included in this is the dependency of the potentiation on various receptor subtypes. Furthermore I will examine the requirement for a post synaptic rise in intracellular calcium and possible sources of this calcium.

In chapter four I will look at intracellular postsynaptic docking proteins and their interactions with different AMPA receptor subunits as mechanisms for bringing about the voltage-pulse induced potentiation of mEPSC amplitudes. Chapter five will look at the kinase regulation of voltage-pulse potentiation and highlights one kinase upon which the induction and maintenance of voltage-pulse potentiation is dependent.

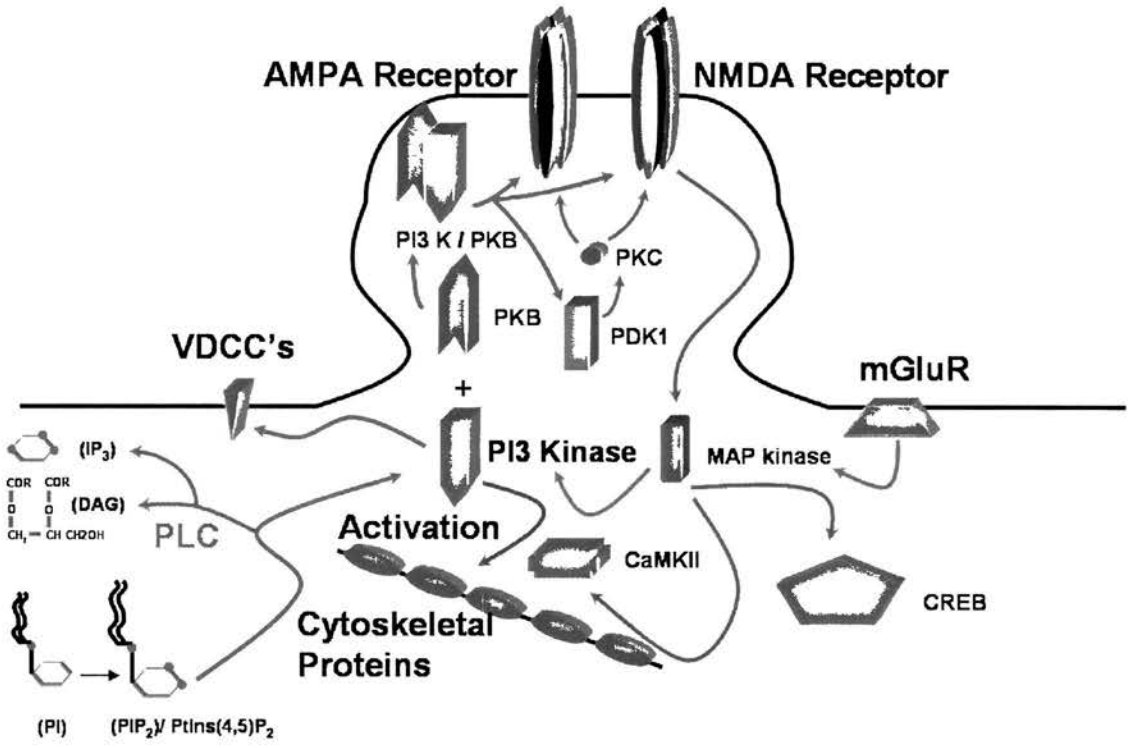

Figure 1.6: **PI3 Kinase interactions at the synapse**: PI3 kinases have a vast diversity of function they interact with PKB (Bondeva et al., 1998; Cantrell, 2001) and effect AMPA receptor trafficking (Sanna et al., 2002; Man et al., 2003), further mediate upstream signalling via PDK1 to PKC (Chou et al., 1998) with cytoskeletal proteins (Ma et al., 1998; Ditlevsen et al., 2003) and higher order kinases (Bondeva et al., 1998; Du and Montminy, 1998; Vanhaesebroeck and Alessi, 2000; Perkinton et al., 2002; Wang et al., 2003) and receptors. (Steinberg, 2001; Rong et al., 2003).

Chapter Two:

Materials and Methods

2.1: Experimental animals

Animals used in these studies were male Wistar rat pups aged between post natal day 7 and 11 (P7-P11) all pups used weighed between 20-30 grams, with the breeding stock being obtained from the supplier, (Charles River). The breeding adults were maintained on a 12 hour light/12 hour dark cycle and given food and water *ad libitum.*

2.2: Preparation of acute slices for organotypic slice culture

Organotypic slice cultures used in this research were an extension of the traditional acute slice preparation (Edwards et al 1989; Gibb & Edwards 1994). Acute slices were prepared from juvenile male Wistar rats (P7-P11). The animals were decapitated using surgical shears (Solingen 92008. Germany), the skin and fur layer was removed, using surgical scissors (FST 14003-12. Germany) to reveal the skull cap. The initial incision made with flexing surgical scissors (FST 15372-62. Germany) at the foramen magnum and the mid line of the skull cap sectioned; additional incisions were made at 45° angle at the front portion of skull cap junction, and rostral incisions (again 45°) at the cerebellum hindbrain junction of the skull cap.

Following incisions the skull cap was pealed back using curved surgical forceps (FST 11003-12. Germany) to reveal the underlying brain. The brain was then levered out from the skull plate, starting in the forebrain domain, using a curved surgical spatula (FST10093-13. Germany). The brain was then immersed in an ice cold artificial cerebrospinal fluid (aCSF, Figure: 2.4). This cutting aCSF is continually gassed with 95% O_2/ 5% CO_2 (BOC gas, UK).

The brain was then placed on an ice cold sectioning table for dissection (See Figure 2.1) The cerebellum was removed at the hind brain junction and discarded (cut 1.), the forebrain was also removed to form a block of brain tissue (2.). The brain was then hemi-sectioned along the mid line (5.) and the base of the brain removed to form a smooth fixing surface (3. & 4.).

The tissue blocks containing each hippocampi were then mounted, using an cyanoacrylate based glue, against a 5% agar block, in a purpose-made cutting chamber (See Figure 2.1b). The cutting chamber is then mounted onto a Vibratome 1000 Plus tissue slicer (Campden Instruments, Loughborough UK) and slices cut at 250 μm using Valet auto strop blades (World Precision Instruments, Inc). The tissue blocks when being sliced were submerged in an ice cold slush aCSF solution gassed with 95% O_2/ 5% CO_2 (BOC gas. UK).

Cut slices were transferred to a 60mm Petri dish (Sterilin. UK Bs611), containing ice cold, gassed cutting Ringer in a slush solution. The hippocampus was then dissected out using

10a scalpel blade (Swann Morton Ltd) or a dissecting micro knife (FST 10055-12 Germany) and a flat spatula (FST 10094-13 Germany). Dissected hippocampi were then transferred to the organotypic culture system.

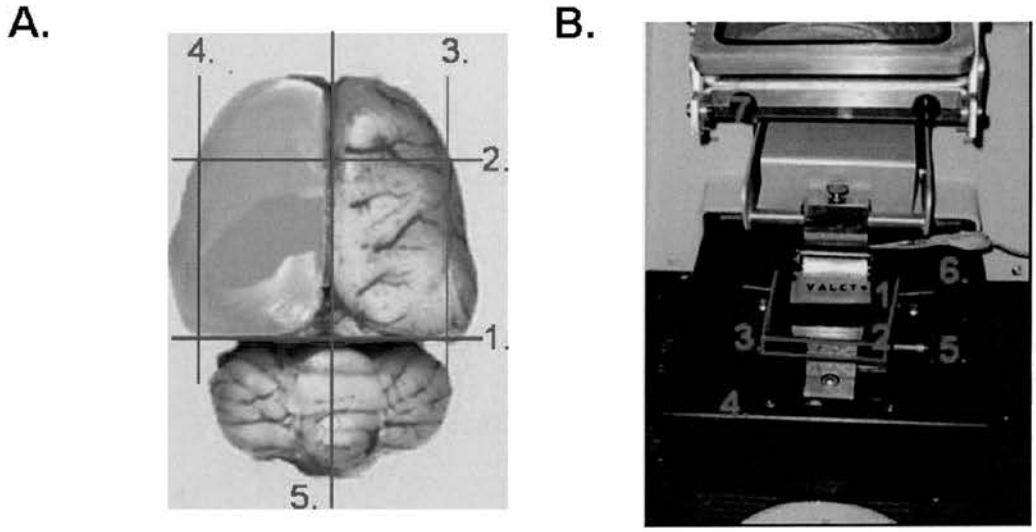

Figure 2.1: **Sectioning procedure for removal of the hippocampus.** Firstly, the forebrain and the cerebellum were removed (Cut 1. & 2.). The brain was then sectioned along the midline creating two blocks (Cut 5.). Then the blocks were smoothed (Cut3. & 4.) to allow for mounting in the holding chamber, with this as the basal surface.

(B.) **Vibratome tissue slicing chamber**. This picture shows the mounting chamber for the production of acute slices. Commencing with the Valet microtome blade (1.) progress though the brain blocks, which were mounted against a 5% agar block (2.). (3.) Indicating the outline of the tissue holder which is filled with ice cold slush solution when preparing slices. This small holding chamber is then mounted in a larger ice filled for slicing (4.). (5.) Represents the chamber clamp (6.) the air perfusion system, (7.) optics.

2.3 Culture system for organotypic slices.

Organotypic slices were prepared according to a slightly modified method described by Stoppini et al (1991). Each culture system comprises one 35 mm petri dish (Nunclon^{Tm}: Cat no: 153066) with a 0.4 μm Millipore cell culture insert (PICMORG50). The insert was immersed with 1 ml of organotypic cell culture media (See 2.6a). These petri dishes were then placed in a Galaxy R CO_2 incubator (Scientific Laboratory Suppliers (SLS) and incubated at 37°C in 95% air 5% CO_2 for 20 minutes.

After incubation period, under sterile conditions in a Class 2 flow cabinet (uniMAT Class 2 Microbiological Safety Cabinet), the hippocampi were transferred to the Millipore cell culture inserts, using two purpose made glass tools (see preparation of glass ware). The hippocampi were lifted from the ice cold gassed aCSF solution in a drop of solution and placed onto the cell culture insert. The second action was to use a fine fire polished glass suction pipette to remove excess solution encasing the hippocampi, leaving only the hippocampi on the insert membrane. Two to three hippocampi were placed per petri dish.

The organotypic cell culture media was replaced three times per week, (De Simoni et al., 2003). This method involves the removal of the residual media using a Gilson 1000μl manual pipette, with a 1000μl filter pipette tip (Rainir). Fresh pre-incubated (20 minutes at 37°C) organotypic cell culture media (500μl) was then added to the petri dish between dish wall and filter housing, not directly to the filter membrane. The organotypic slices were kept in the incubator at 37°C 95% air / 5% CO_2 for seven days before being used for recording.

2.4: Preparation of experimental glass ware

2.4a: Transfer pipette for organotypic slice culture

The preparation of the glass (Volac: ref D812) for the transfer pipette, involved the removal of the pipette nozzle at the base of the shank. This was achieved using a diamond knife and snapping the glass. This rough end was then fire polished to a smooth edge, ensuring a reduced aperture, so application of a small volume of aCSF containing a single suspended hippocampal slice, to the cell culture insert was possible. These glass pipettes were pre-made and stored in 100% ethanol (Fisher scientific Ltd. UK), and used once per culture set, to minimise cross contamination.

2.4b: Angled suction pipette for organotypic slice culture

The angled suction pipette was fabricated from Volac glass (ref D812). The aperture of the pipette was reduced using the ethanol burner, and an approximate 35 degree bend put in the glass approximately 2.5 cm from the tip of the pipette. Again, these pipettes were pre-made, single use and stored in 100% ethanol (Fisher scientific Ltd. UK).

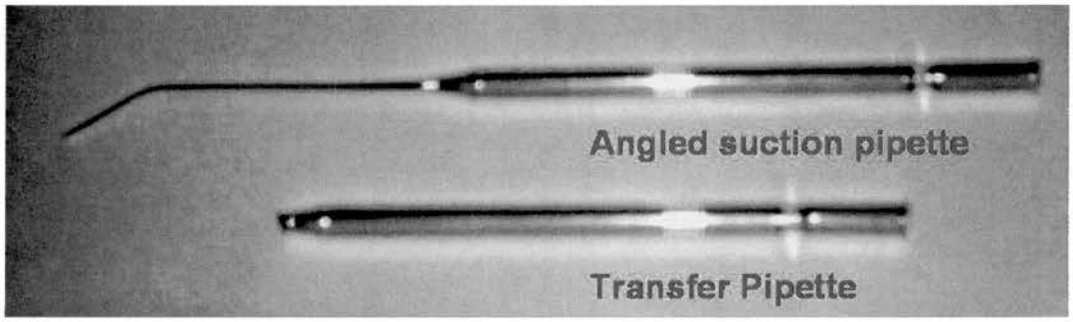

Figure 2.2: **Suction pipettes for slice transfer**: Glass pipettes used to transfer acute slices to the filter membranes for culturing. Using the transfer pipette only a small volume of culturing medium is transferred to the filter membrane, this is then easily removed using the small aperture angled suction pipette.

2.5: Preparation of recording electrodes.

Glass electrodes for whole-cell patch electrodes were made from a thick walled borosilicate glass (Harvard Apparatus, GC150F-7.5) with glass dimensions of 1.5mm O.D x 0.86mm I.D and containing a filament. The glass was mounted onto a Flaming Brown Micropipette Puller (Model 97; Sutter instruments Co. USA) and pulled with respect to the ramp value of the glass, into a patch electrode. The pulled shank of patch electrodes were further treated with heat cured Sylgard 184 (Dow Corning GmbH. USA), in order to reduce the noise level of the recording. The electrode tips were then fire polished using a Narishige – Microforge (MF-830. Japan) to the required resistance; between 5 and 10 MΩ for patch electrophysiology.

2.6: Organotypic cell culture and electrophysiological recording solutions

2.6a: Organotypic culture media

Preparation of this solution requires the sterile filtering of a series of solutions, including MEM (Eagle's) solution, Hank's balanced salt solution (HBSS) and Horse Serum (Figure 2.3) all of which were accurately measured and dispensed using Sterilin 25ml pipettes (40125). This final mixture was filtered using a Nalgene Filter Unit (218795-2) with a 50 mm membrane diameter and a 0.2μm pore size and was stored at 4°C

Figure 2.3: Components of organotypic cell culture media

Organotypic cell culture media	Volume	Catalogue Number
MEM (Eagle) + 25mM HEPES, with Earles Salt solution without L-Glutamine	100 mls	23360-026
Hank's Balanced Salts (HBSS)	50 mls	24020-091
Horse Serum - Heat Inactivated	50mls	26050-088
Penicillin/ Streptomycin (5000/5000)	1ml	15140-122
L-Glutamine x100 (200mM)	0.5mls	25030-032

2.6b: Slice cutting solution

This solution composition as described in Misra et al. (2000), has a low calcium and high magnesium concentration to protect the cells of the organotypic slice, from excitatory cell death produced by NMDA receptor activation due to an increase in free glutamate because of the slicing process. This solution was made to 1000 mls in volume, pH adjusted to 7.4 and the osmolarity ranged between 300-310 mOsm. This solution was continually gassed with 95% O_2/ 5% CO_2 (See table: Cutting and external recording solutions).

2.6c: External recording solution

This solution from Wyllie & Nicoll (1994) has the calcium/ magnesium concentration reversed, in order to promote mEPSC generation. This solution contains tetrodotoxin (300 nM) and picrotoxin (50 μM) to block the effects of excitatory voltage gated sodium channel dependent action potentials, and inhibitory GABA receptors dependent currents. Again this solution was made to 1000 mls in volume, pH adjusted to 7.4 and osmolarity of between 300-310 mOsm. This solution was continually gassed with 95% O_2/ 5% CO_2. This external solution was applied at a flow rate of 4 mls per minute, and at room temperature (22-25°C). This solution was modified by the inclusion of various drug components (See Figure: 2.4).

Figure 2.4: Components of external recording solution

Solution Components	Slice Cutting Solution (mM)	External recording Solution (mM)	Source	Reference Number	Molecular Weight
Sodium Chloride (NaCl)	125	119	Fisher Chemicals. UK	s/3160/60	58.44
Sodium Hydrogen Carbonate ($NaHCO_3$)	26	26.2	Fisher Chemicals. UK	s/4240/53	84.01
Glucose	25	25	Fisher Chemicals. UK	g/0500/53	180.16
Potassium Chloride (KCl)	2.5	2.5	Fisher Chemicals. UK	p/4280/53	74.56
Sodium dihydrogen orthophosphate dihydrate (NaH_2PO_4)	1.25	1	Fisher Chemicals. UK	s/3760/53	156.01
Calcium Chloride ($CaCl_2$	1	4	BDH - Anala R	190464K	110.98
Magnesium Chloride	4		Fluka	378/041	95.21
Magnesium Sulphate (Mg_2SO_4)		1.3	Fisher Chemicals. UK	m/1050/53	246.48

Figure 2.4a: Toxin components of external recording solution.

Solution Components	Slice Cutting Solution (mM)	External recording Solution (mM)	Source	Reference Number	Molecular Weight
Tetrodotoxin		300 nM	Tocris Cookson Ltd	1069	319.27
Picrotoxin		50μM	Tocris Cookson Ltd	1128	602.00

Figure 2.5: Experimental inhibitors used

Drug/toxin	Concentration	Source	Reference: number	Molecular weight
CNQX	20 μM	Tocris	1045	303.14
D-AP5	30μM	Tocris	0106	197.13
Nifedipine	10 μM	Sigma Aldrich	N 7634	346.3
Thapsigargin	10 μM	Tocris	1138	650.75
Ryanodine	10 μM	Sigma Aldrich	R 6017	494.6
LY 294002	5 μM	Sigma Aldrich	L-9908	343.81
LY 303511	5 μM	Sigma Aldrich	L-2786	379.3
Wortmannin	100 nM	Sigma Aldrich	W 1628	428.4

CNQX: 6- Cyano-7-nitroquinoxaline-2,3- dione

D-AP5: 2-Amino-5-phosphonopentanoic acid

Figure 2.6 Structure of inhibitors

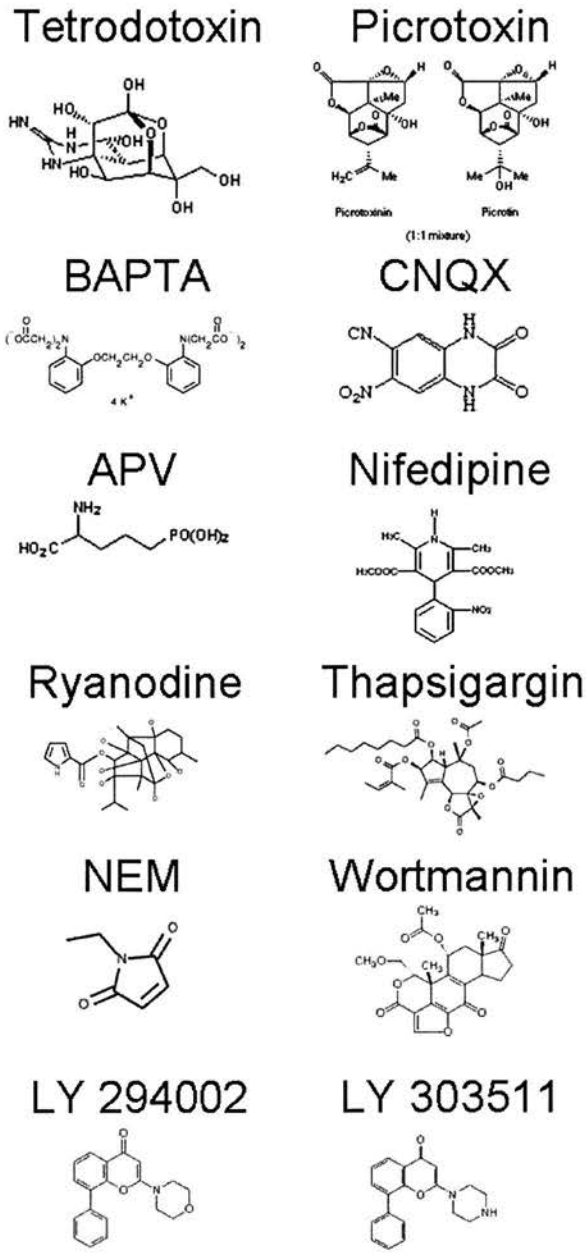

(NEM) N-ethylmaleimide (BAPTA) 1,2-bis(o-aminophenoxy) ethane *N,N,N,N*- tetraacetic acid (CNQX) 6-cyano-7 nitroquinoxaline-2,3-dione (APV) 2-amino-5-phosphonopentanoic acid.

2.7: Pipette recording solution,

The internal recording solution, used was an ATP-based regenerating solution found in Wyllie & Nicoll (1994). They found that the use of this regenerating internal solution increased the time period through which mEPSC could be recorded, secondly that its use increased the ability to induce VPP (90% of cells). The use of the regenerating solution, did not affect the amplitude of the kinetics mEPSC recorded (See Figure 2.7).

This solution was then further modified by the inclusion of various drugs/toxins (Figure 2.8). Through inclusion in the internal solution, the application of these drugs was compartmentalised to the postsynaptic cell, therefore these drugs will only affecting postsynaptic internal signalling events. Furthermore in the following table (Figure 2.9) shows the amino acid composition for all peptides used. All internal solutions used in these experiments were pH to 7.4 and had an osmolarity of between 280 –295 mOsm determined in all cases by a freezing point osmometer (Advanced osmometer: Model 3D3, Advanced Instruments Inc).

Figure 2.7: Pipette solution composition

Solution Component	Concentration (mM)	Source	Reference Number	Molecular Weight
Cesium Gluconate	105	Sigma-aldrich	G-1139	346.41
Cesium Chloride	17.5	Anala Biochemical	10067	168.36
Cesium HEPES	10	Sigma- Aldrich	H3375	238.3
EGTA	0.2	Fluka	03778	380.35
Sodium Chloride (NaCl)	8	Fisher Chemicals. UK	s/3160/60	58.44
Mg-ATP	2	Sigma- Aldrich	A-9187	507.2
Na_2- ATP	2	Sigma- Aldrich	A-7699	551.1
Na_3-GTP	0.3	Fluka	51123	589.13
Phosphocreatine	20	Sigma- Aldrich	P-7936	255.1
Creatine Phosphokinase	50U/ml	Sigma- Aldrich	C-3755	

Figure 2.8: Inhibitors added to internal solutions

Internal toxin/drug	Concentration	Source	Reference Number	Molecular Weight
N-ethylmaleimide (NEM)	5 mM	Sigma- Aldrich	02460	125.13
Botulinum Toxin A (BoTox)	10 ng/ml	Sigma- Aldrich	B8776	
Pep2m	50 μM	Tocris Cookson	1595	1173.44
Pep4c	50 μM	Tocris Cookson	1596	1146.42
Pep2m-AVKI	50 μM	Tocris Cookson	1600	1268.47
Pep-TGL	50 μM	Tocris Cookson	1601	990.14

Final Botulinum Toxin A is made up from a stock solution of 1mg/ml.

Figure 2.9: Peptide inhibitor amino acid composition.

Peptide	AA1	AA2	AA3	AA4	AA5	AA6	AA7	AA8	AA9	AA10	AA11
Pep2m	Lys	Arg	Met	Lys	Val	Ala	Lys	Asn	Ala	Gln	
Pep4c	Lys	Arg	Met	Lys	Val	Ala	Lys	Ser	Ala	Gln	
Pep2m-AVKI	Tyr	Asn	Val	Tyr	Gly	Ile	Glu	Ala	Val	Lys	Ile
Pep1-TGL	Ser	Ser	Gly	Met	Pro	Leu	Gly	Ala	Thr	Gly	Leu

Peptide reference. Ala: Alanine. Lys: Lysine. Met: Methionine. Val: Valine. Asn: Asparagine. Gly: Glycine. Pro: Proline. Ile: Isoleucine. Leu: Leucine. Tyr: Tyrosine. Ser: Serine.

2.8: Electrophysiology

All recordings were conducted in a purpose built Faraday cage (Technical Manufacturing Corporation (TMC) with the recording equipment mounted on a pressurised air table (TMC. Micro-g Vibration isolation system), to reduce the ambient noise and vibration which is a major problem with this experimental technique. Organotypic hippocampal slices were first visualised using 4x optic lens (Olympus. Japan Plan 4 x /0.10 ∞/-) then a higher magnification lens using Normanski optics to visualise the cells (Acroplan. Carl Zeiss Germany water immersion 40x /0.98w Ph2 ∞/-). All imaging was done using an Axioskop FS microscope (Carl Zeiss. Germany), mounted on a Gibraltar platforms X-Y stage. Whole-cell patch-clamp recordings were then made from visualised CA1 pyramidal cells. The backfilled borosilicate glass patch electrodes were mounted on a head stage (Axon instruments; CV4 head stage) which was fixed to a micromanipulator (Sutter instrument company, MP-285) in order to allow the movement of the electrode, which was aligned to the microscope by mounting on a Gibraltar static table (Gibraltar Platforms, Burleigh). After breakthrough from the cell-attached configuration to the whole-cell configuration, the pyramidal neurons were clamped at -80mV by an Axopatch 1D amplifier. (See Figure 2.10 for recording rig set up).

Perfusion of the organotypic slices was achieved by gravity feed system at a rate of 4 mls / min into a holding chamber with a volume of approximately 2 mls. Suction occurs at a similar rate to allowing for a circulation of the recording solution in the holding chamber at almost a constant volume.

The general recording parameters used to determine suitable cells, included any CA1 pyramidal cell with a holding current under -100 pA, when voltage clamped at -80 mV. In addition these cells must further have a series resistance less than 20 MΩ and this series resistance must not vary by more than 15 % of the original value during the entire recording period which was typically 30-40 minutes.

2.9: Stimulating protocol.

The voltage pulse stimulating protocol, described by Wyllie and Nicoll (1994), involves a depolarising voltage step of +100 mV (typically from the holding potential of -80 mV to +20 mV). Each pulse lasted for three seconds with an interpulse interval of three seconds. Within this experimental paradigm, 10 pulses were applied to each neurone in whole-cell voltage-clamp. The generation of the +100 mV pulse was done via the Gate setting on the Axopatch 1D. The

signal generation for the timing of these pulses is programmed and executed through a Master 8, (Intracel. Eight channel programme pulse generator).

2.10: Filtering of miniature synaptic currents

The whole-cell currents recorded were visualised on an oscilloscope (Teckronix TDS210) and recorded on computer hard disk via an interface board using, WinEDR 6.1 data capture software by Dr John Dempster, Department of Physiology, and Pharmacology, University of Strathclyde (http://innovol.sibs.strath.ac.uk/physpharm/ses.html). All mEPSC viewed were initially sampled at 20 kHz on to DAT tape (120 min) for storage, using a SONY digital tape recorder (DTR-1205). mEPSCs were then analysed off line; currents were replayed from the tape with a 2 kHz filter using an 8^{th} order low pass bessel filter (University College London), then digitized at 10 kHz with the WinEDR capture software. This .EDR file was then converted with a utility function to an .ABF file (ABF utility. Minianalysis, Synaptosoft) and transferred to a DVD for long term storage.

2.11: Selection and analysis of miniature synaptic currents

.ABF was the file format which allows for the digitised mEPSC trace to be analysed with Mini analysis software (Justin Lee. http://www.synaptosoft.com/MiniAnalysis/). This software employs a semi automated detection procedure. mEPSCs were detected by eye and displayed using an event threshold of 3 pA. The rejection protocol focused on the initial parameters of the data derived by mini analysis: any mEPSC with a time to rise greater than 5 ms was discarded (Figure 2.11).

mEPSCs were further analysed for peak amplitude, rise and decay time constants (single decay exponential) using a template fit algorithm written in the Synaptosoft mini analysis software. Selection parameters for the mEPSCs were not as stringent as those used by Smith et al., (2003) for two main reasons. Firstly they discarded any event with a rise time constant over 400 μs as these mEPSCs did not arise from local sites. I did not adopt this approach since theoretically VP potentiation produces a global potentiation of mEPSC amplitudes from events all over the patched pyramidal cell. The Smith-Magee selection would restrict VP potentiation to local sites thereby restricting the global effect of VP phenomena.

The second reason is possible dendritic filtering of mEPSCs, if filtering occurs with distal mEPSC then the rise and decay times will be significantly slower than those events arising at local synapses, and these events would be excluded from the study. Although dendritic filter

shaping of the mEPSCs occurs, this phenomenon is counterbalanced by the idea that the further away from the soma the site of activation is, the greater the synaptic conductance of the synapses found there producing bigger events (Magee and Cook, 2000).

2.12: Protocol for graphing and statistical analysis

The total data produced from each recording is further analysed using Microsoft® Excel 2003. The first step with data analysis was to calculate the average amplitude for the control period, the standard deviation, and standard error of the mean. Early in this study, substantial variability in the base line average values for amplitude, frequency, and total current output of each individual cell was noted. To account for this variability each data point in the pre and post manipulation period, was normalised against the control average. Therefore, each event is represented by its relationship to the control average. Events were then grouped into 30 second bins, and an average taken. These average values were then graphed using Microcal ™ Origin ® Version 6. Data when appropriate will be presented as mean ± S.E.M. Graphical representation of mean data traces for mEPSC amplitude, frequency were shown by scatter plots with error bars. Further plots including cumulative probability and amplitude histograms, were used as they display any small differences in mEPSC amplitudes following either VP stimulation or inhibitor application. Representations of typical mEPSCs were a mean average of 100 events from each representative experimental period shown for comparison.

All statistical analysis was conducted using Sigma Stat version3, the statistical significance between data groups was determined using the Mann/ Whitney U test. Due to the data originating from spontaneous release of vesicles, these events indicate a non-parametic alignment (skewed distribution) further shown by a failure to pass a normality test that indicates a normally distributed data set typical of a Gaussian distribution.

Amplitudes of VP potentiated mEPSCs display a rightward shift, from the skewed distribution of the control events, highlighting a large probability of large amplitude events. Testing the shift in mEPSC amplitudes distribution was conducted using the Kolmogorov - Smirnov test, to evaluate changes in the distribution of potentiated and non-potentiated event histograms.

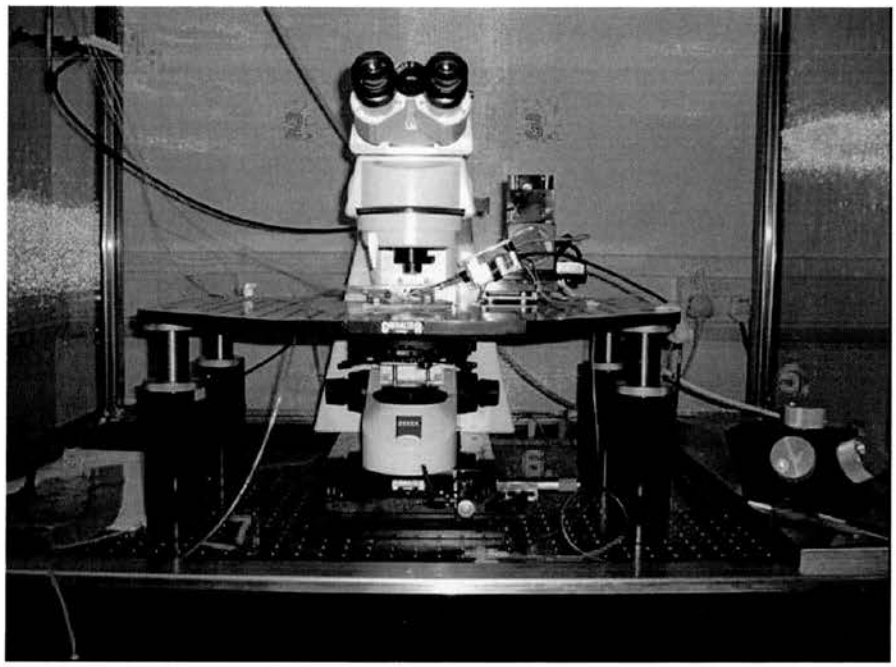

Figure 2.10: **Setup of electrophysiology recording rig**: The recording apparatus is mounted on a pressurised air table (7.) contained within a faraday cage, used to reduce both vibrational and electrical noise. A gravity feed system (1.) is used to perfuse the slice cultures, when placed in a holding chamber attached to a static Gibraltar table (4.). A Zeiss Axioskop microscope (2.) was used to view the cells in the culture system, movement of the microscope was controlled via a Gibraltar micromanipulator table (6.). Movement of the recording electrode (3.) was controlled using a Sutter micromanipulator (5.). Finally, a copper mesh shield (8.) was placed in front of the recording electrodes again to reduce noise.

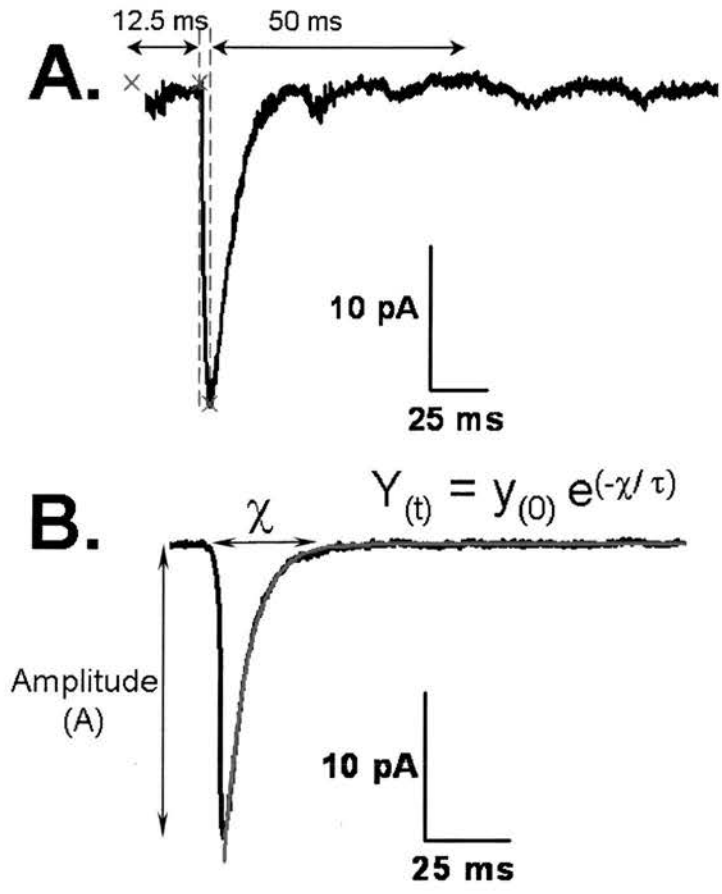

Figure 2.11: **Selection criteria for mEPSCs**: The amplitude of any mEPSC was calculated from analysis of the previous 12.5 ms to find the base line value and then calculate the peak amplitude of the mEPSC. Rejection of the mEPSC events occurred if the initial time to rise (period indicated between two dotted lines) was greater than 5 ms, further indicated is the time period selected in which the mEPSC must decay back to baseline. (B.) mEPSC with single exponential decay fit, showing expression used to characterise this decay. (χ) time decay to baseline (A) amplitude (τ) decay time constant.

Chapter Three:

Characterisation of the voltage-pulse potentiation of mEPSC amplitudes

3.1: Summary

This chapter describes experiments that evaluated rat organotypic slices for electrophysiological recording and characterises the voltage-pulse stimulating protocol as a system to understand the mechanisms of LTP-like plasticity in the CA1 region of the hippocampus.

3.2: Spontaneous event recording

The first set of experiments, were conducted to characterise typical spontaneous whole-cell currents from patch-clamped CA1 pyramidal cells, in which three current types are typically observed. The first of these are large spontaneous unclamped currents (Fig 3.1) which result from action potentials in these pyramidal cells and I will refer to these as "action currents". The second are very large currents, which result from the loss of all GABAergic inhibition, and are seen in the presence of PTX. The third are TTX insensitive currents called miniature postsynaptic currents. These small currents can be either excitatory i.e. miniature excitatory post synaptic currents (mEPSCs) or inhibitory (mIPSCs).

To resolve a neuronal form of what Sir Bernard Katz (1950) described as spontaneous miniature end plate potentials (mEPPs), voltage-clamped whole-cell current recordings were made from CA1 pyramidal cells in organotypic hippocampal slices which were incubated with both picrotoxin (PTX: 50 μM) and tetrodotoxin (TTX: 300 nM). Miniature excitatory postsynaptic currents (mEPSCs), are events which are insensitive to tetrodotoxin, and therefore arise from the release of single packets of neurotransmitter released from the presynaptic nerve terminal, acting on membrane bound postsynaptic receptors. In the case of CA1 pyramidal cells previous investigators have shown that under these conditions AMPA receptors mediate the resulting synaptic currents and recordings of mEPSCs will give a direct measure of AMPA receptor function in CA1 pyramidal cells.

3.3: Spontaneous events

These initial recordings were conducted to ensure that the organotypic slices had remained a viable preparation through the culturing process. In the absence of TTX, whole-cell spontaneous currents (Figure 3.1a) display a fast rising phase and decay phase. Andrásfalvy & Magee (2004) indicate that these spontaneous events are the result of action potentials from the pyramidal cells when the cell is held in voltage clamp (Figure 3.1a). When switching to current clamp in the same cell at a more depolarised membrane potential (-40mV) the action potentials are evident (Figure 3.1b). Analysis of 50 spontaneous events, show a mean event with a large amplitude (Figure 3.2: 368.1 ± 26.7 pA).

Application of picrotoxin (Figure 3.1c) to the whole-cell patch clamped CA1 pyramidal cell inhibits both the $GABA_A$ receptors (Davies and Collingridge, 1996) and therefore the inhibitory GABAergic currents from interneurones synapsing onto the pyramidal cell. The physiological consequence of the loss of GABAergic inhibition are spontaneous events which have large amplitudes and slow decay phases. The mean analysis of 50 events shows a doubling of the amplitude of the spontaneous events (934.2 ± 14.1 pA). The purpose was to characterize the effects of the loss of GABAergic component on these spontaneous events, the explanation is drawn from the Nernst equation, which describes the membrane reversal potential of chloride (or any ion) as a relationship between the cytosolic and extra cellular chloride concentrations.

$$E_{Cl} = \frac{RT}{FZ_{Cl}} \ln \frac{Cl_o^-}{Cl_i^-}$$

Nernst Equation determinants: E_{Cl} = equilibrium potential for Cl^-, R = gas constant, T = absolute temperature, F = Faraday constant. Z_{Cl} = valence of Cl^- (-1) $[Cl_o^-]$ = Cl^- concentration outside the cell $[Cl_i^-]$ = Cl^- concentration inside the cell.

In these experiments, the internal/ external Cl^- concentrations were 25 mM and 140 mM respectively. This represents an equilibrium potential of about – 40 mV. As we employ a voltage clamp of -80mV, these GABAergic currents are inward in nature acting to return the cell potential from this voltage clamped level of -80 mV back towards the reversal potential at -40 mV.

The viability of the cells is compromised with this loss of inhibition, therefore the next experimental step was application of TTX which has a well characterized action (Mosher, 1986). When used in the peripheral nerves in the neuromuscular junction preparation, the application of TTX blocks action potential-dependent presynaptic vesicle release, by inhibition of axonal transmission of nerve impulses as the toxin inhibits the opening of sodium channels (Na^+) at the Nodes of Ranvier. When applied to this system TTX has two actions, the first is the blockade of the neuronal action potential, and the second is the inhibition of inhibitory GABAergic interneurones. The net result of applying both toxins is that all action potential evoked synaptic transmission is blocked and only spontaneously released vesicles, as Katz described as single packets of neurotransmitter remain, acting on the postsynaptic receptors generating the miniature excitatory postsynaptic currents (Figure 3.1d.e).

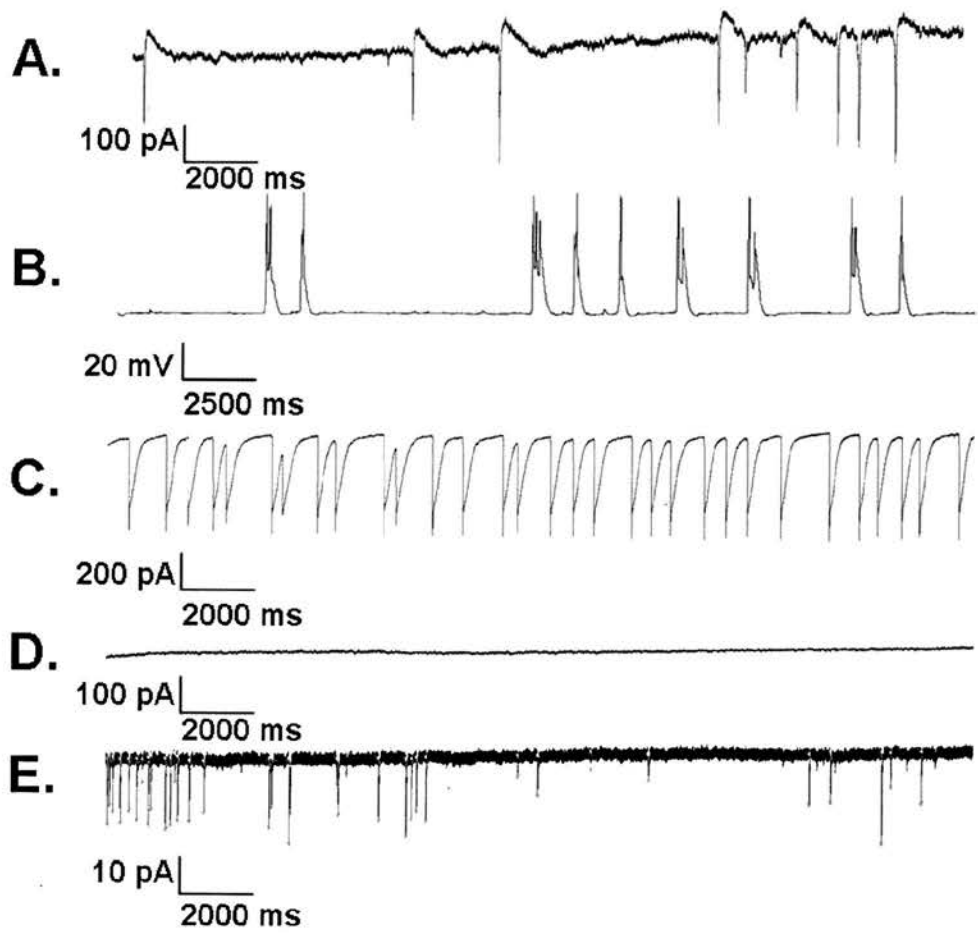

Figure 3.1A: **Whole-cell voltage-clamped spontaneous events**. Trace of spontaneous events from whole-cell patched CA1 pyramidal cell at -80 mV. Figure (B.) **Whole-cell current clamped action potentials.** When in current clamp action potentials underlie the spontaneous events. (C.): **Application of Picrotoxin (50 μM).** PTX removes all GABAergic inhibition and increases EPSC activity. (D.) **Application of Tetrodotoxin.** The application of TTX 300 nM abolishes all visible currents. (E.): **TTX insensitive events.** Increasing the gain function from 5 mV/pA to 50 mV/pA allows for the visualisation of mEPSC events.

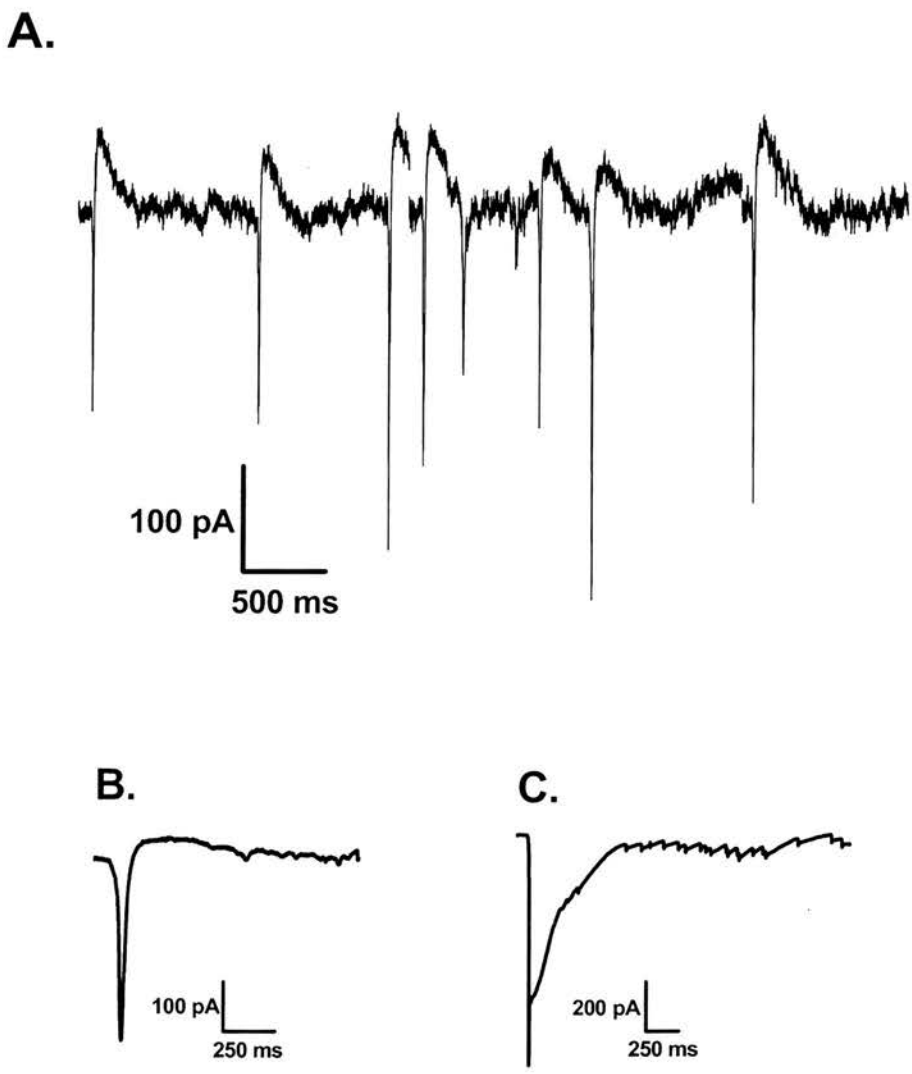

Figure 3.2: **Examples of single spontaneous events.** (A.) Typical spontaneous events, likely to be the result of an unclamped action potential: (B.) Mean spontaneous event trace, the average of 50 spontaneous events (C.) mean trace of PTX insensitive events, highlighting larger slower events following the loss of GABAergic inhibition.

3.4: mEPSC recording.

After resolution of mEPSCs from the hippocampal CA1 pyramidal cells, characterisation of stable baseline recordings were conducted to evaluate the typical characteristics of mEPSCs in the rat organotypic hippocampal slice. In this thesis changes in mEPSC amplitudes were used as an indirect measure of AMPA receptor insertion and any functional alteration of these receptors in active synapses.

Eight experimental recordings from individual cells were taken and analysed for changes in mEPSC amplitude over the time course of the experiment (Figure 3.3A). Recordings indicated no significant difference in mEPSC amplitudes across the 30 minute time period, the mean amplitude of these mEPSC was 20.6 ± 1.7 pA (n = 8), with a range of mean amplitudes from 15.4 ± 2.0 to 27.2 ± 2.4 pA. What was obvious from these initial recordings was the degree of variability of the mean amplitude and frequencies of the mEPSCs between cells. Therefore, all data are normalised with respect to the mean control mEPSC value (Section 2.11).

Analysis of a typical single cell recording with a mean mEPSC amplitude of 21.3 ± 0.3 pA and showed the same trend as the grouped amplitude time course again with no significant deviation from the normalised value. The stable mEPSC amplitude baseline indicates that this system has either a stable surface expression of AMPA receptors or if turnover of the AMPA receptors is facilitating this stability then the population of receptors being removed is almost identical to the population being inserted, or a change in mEPSC amplitude would be evident.

Figure 3.3B shows a scatter plot of the amplitudes of control mEPSCs and highlights the degree of variability of mEPSC amplitudes which contribute to the mean mEPSC amplitude value at each time point. This difference is not unusual, but reflects the fact that the total output from each individual cell, will differ due to the factors which underlie mEPSC events. Factors which generally underlie mEPSC event amplitude include the dependency upon receptor number at the active synapse, the sensitivity of these receptors to neurotransmitter. Presynaptic effectors include changes in detection rate due to the low probability of vesicle release, in combination with the concentration of L-glutamate contained within these vesicles. Silent synapse activation, which is a postsynaptic expression of a frequency change, must also be considered.

Further analysis of the single cell recording gives the cumulative probability plot (Figure 3.3C); this graph indicates the probability of events having a specific amplitude. What is indicated is that the 50 % probability for this cell is about 15 pA and the 80 % probability is 20 pA. This data is reinforced with the amplitude event histogram which

indicated a typical leftward skewed distribution and features that the majority of events will be found in the range from 15 to 20 pA. Any change in mEPSC amplitude caused by stimulus or by ligand application can be easily shown with sort of analysis.

Figure 3.4A, shows a typical control mEPSCs Raster plot, all events are about 25 pA in amplitude and display the spontaneous nature of these events, showing no distinct temporal pattern. Analysis of 500 mEPSCs from a control recording indicates events with mean amplitude of 19.7 ± 0.4 pA, this average event has a typical rise time of 1.2 ± 0.1 ms and a single exponential fit of the decay phase shows a τ decay of 16.7 ± 0.2 ms.

Frequency changes with the mEPSC have traditionally been linked to presynaptic mechanisms for LTP, with the proviso of a postsynaptic mechanism for frequency change. In these experiments, the mean control frequency was 1.5 ± 0.3 Hz with a range of 0.5 Hz to 2.3 Hz. Over the time course, this control frequency reduced to 1.2 ± 0.3 by 20 minutes (Figure 3.5A).

This reduction in mEPSC frequency, but not mEPSC amplitude is indicative of the dialysation of the cell cytoplasm, as whole-cell patch configuration allows the internal solution direct access to the cells cytoplasm, allowing for a reduction in the cellular components necessary for cell function. This finding limits the maximum recording period for each experimental series to approximately 30 minutes.

Due to this change in mEPSC frequency, the total current produced by the cell for each time bin is a measure of cell function, as a means of drawing any comparison between changes in mEPSC amplitudes and frequencies. The mean current output for these cells 1.2 ± 0.2 nA, with a range from 0.7 ± 0.1 nA to 2.6 nA ± 0.1 nA (Figure 3.5B). Total current output for these cells across the time course mirrors the frequency change, as by 20 minutes the mEPSC current produced had reduced to 0.9 ± 0.25 nA.

All recorded events were compared for factor dependence of the mEPSC, by rating the r^2 value of each determining factor against the event amplitude (rise time, decay time). The amplitude of any event was shown to be independent of both the time to rise and the time to decay period (Figure 3.6).

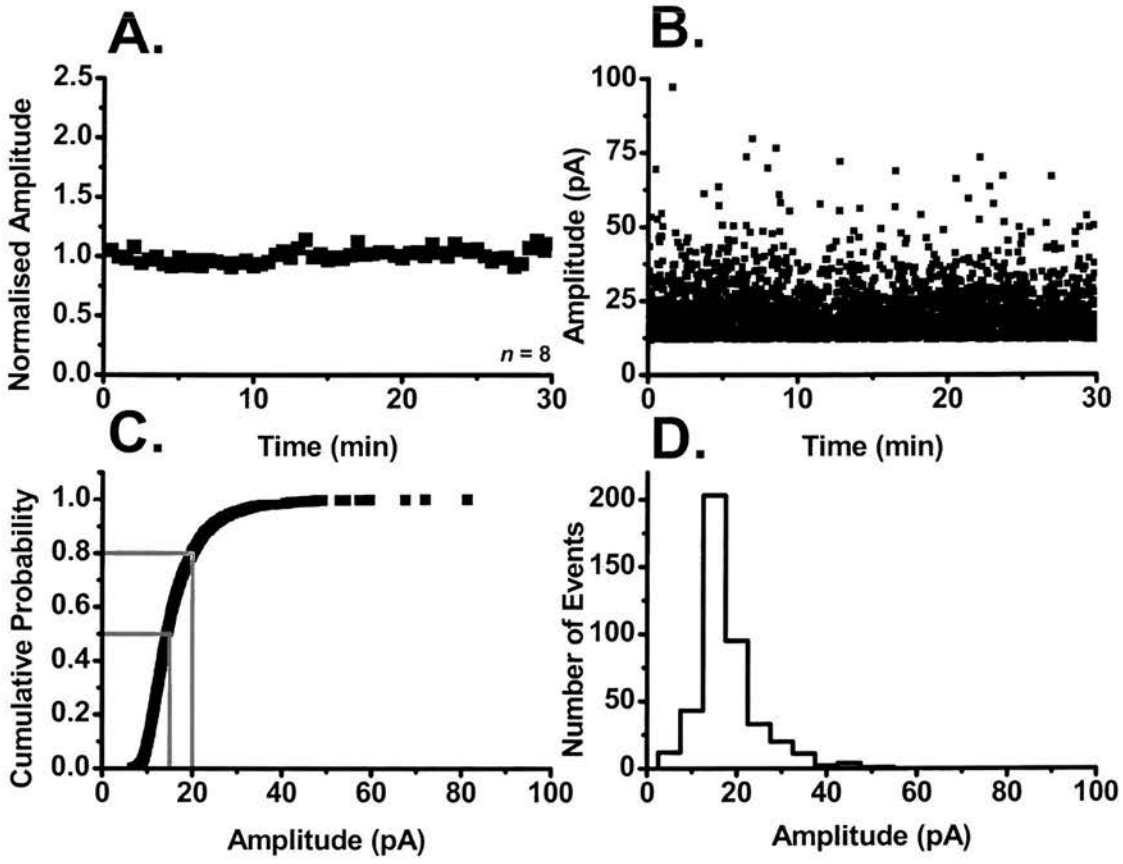

Figure 3.3A: **Time course for control mEPSCs amplitudes.** Over the 30 minute time period there is no significant deviation from the mean amplitude of 20.55 ± 1.67 pA. (B.) **Amplitude scatter plot**. Scatter of mEPSC amplitudes across the thirty minute period. (C.) **Cumulative Probability.** Typical left ward skewed distribution showing a low probability of large amplitude events. (D.) **Amplitude histogram.** Again, a left ward skewed distribution, showing a predominance of small amplitude events

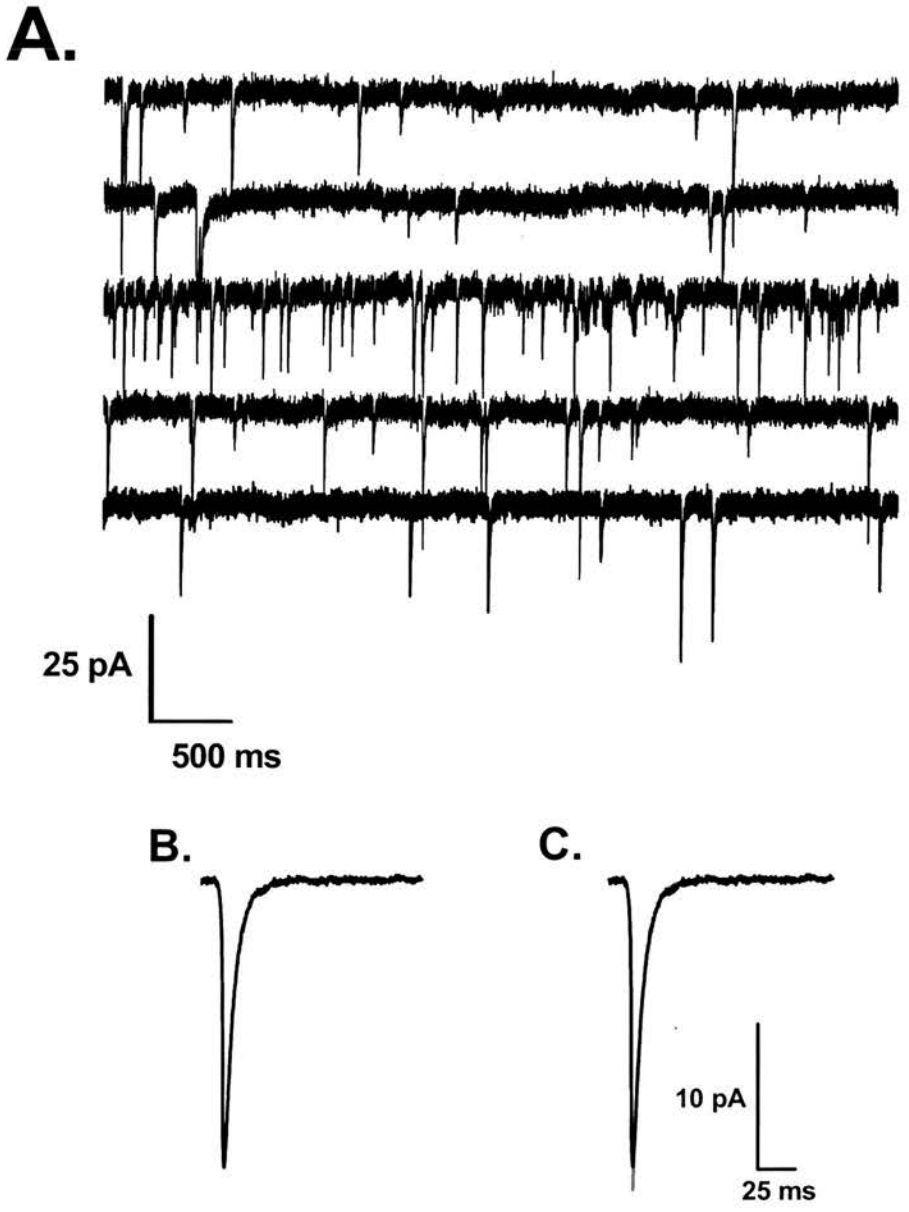

3.4A: **Raster plot for control mEPSCs.** This figure highlights the differences in mEPSC frequency, and small changes in mEPSC amplitude, which occur over the 30 minute time period. (B.) **Typical averaged control mEPSC**, from analysis of 100 mEPSCs shows low amplitude and a fast rise and decay time (C.) Control averaged mEPSC with exponential decay fit (in red).

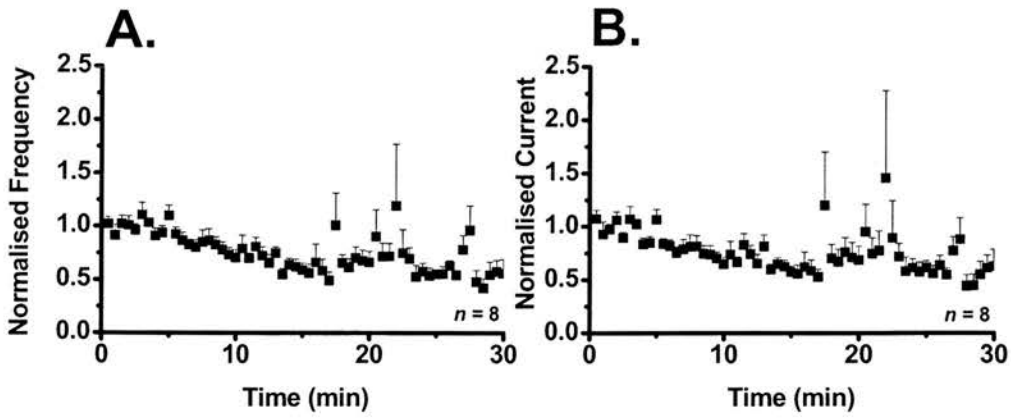

Figure 3.5A : **Time course for control mEPSCs frequency.** A small reduction in event frequency occurs over the experimental time course. (B.) **Time course for control mEPSC total current**. The current output of the cell parallels the reduction shown with frequency.

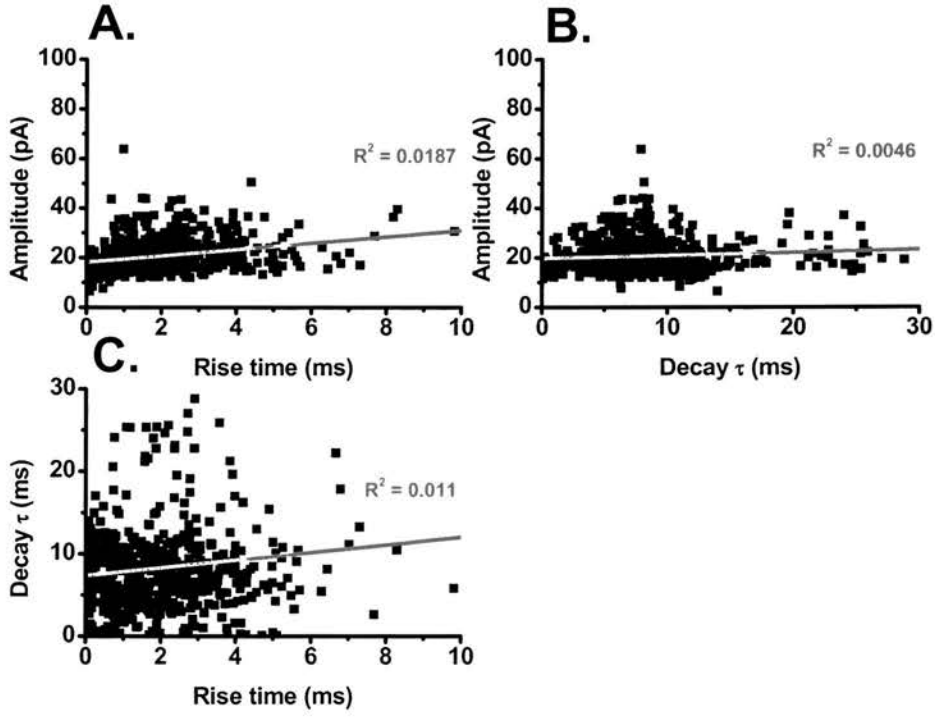

Figure 3.6A: **Amplitude-rise time correlates.** No correlation is shown between the rise time and amplitude of mEPSC events. (B.) **mEPSC amplitude τ decay correlates.** R^2 values indicate little correlation between the mEPSC amplitudes and decay τ. (C.) **mEPSC rise time decay τ correlates.** No correlation is shown between the rise time and decay τ of mEPSC events.

3.5: Voltage pulse potentiation

Long term potentiation of excitatory synaptic transmission between the synapses of the CA3 and CA1 pyramidal cells via the Schaffer Collateral/Commissural (SCC) fibers, is a long debated and researched area as well as being a well known model for certain forms of learning and memory. Conventional stimulating protocols require activation of SCC fibers, to induce the most commonly studied form of LTP. LTP is known to be dependent upon a rise in the postsynaptic calcium concentration and dependent upon NMDA receptor activation in the CA1 pyramidal cell. These trigger cellular events which activate intracellular protein cascades, and enhance the transmitted signal.

Early LTP is an enhancement of synaptic efficacy mediated by AMPA receptor synaptic transmission, as changes in receptor number, distribution, and function in the spines of these cells are mechanisms by which the functional increase in synaptic strength in LTP can be explained. Here we use a modified version of the voltage-pulse stimulating protocol, first used by Kullmann et al (1994), and then later adopted by Wyllie & Nicoll (1994). The later research showed transient but significant increases in mEPSC amplitude (2.5 fold), which could be converted into a sustained potentiation by the addition of phosphatase inhibitors, a second finding which accompanies the amplitude change is a non significant increase in mEPSC event frequency. This work was conducted on CA1 pyramidal cells in acute guinea pig slices, not the traditional rat brain slices. The stimulating protocol revolves around a series of depolarizing voltage pulses; a +100mV step which lasts for 3 seconds at a frequency of 0.2 Hz, applied for a duration of 120 seconds. Use of organotypic slices required a modification of the stimulating protocol due to the thinner slice. The parameters of this stimulating protocol were reduced to a +100mV depolarizing step lasting 3 seconds with a 3 second interval, and applied for only 60 seconds. The main outcome of this protocol is the generation of a sustainable potentiation of mEPSC amplitudes, with no significant increase in event frequency, when compared to the control period.

3.6: Application of voltage pulse potentiation to mEPSCs

Whole-cell voltage clamp were used to examine the potentiation of miniature excitatory whole-cell postsynaptic currents (mEPSC) in CA1 pyramidal cells by the voltage pulse technique. The potential of the VP stimulating technique for dissection of postsynaptic function is immense. A traditional LTP stimulation protocol requires a stimulating electrode placed distally in the stratum radiatum to stimulate the Schaffer collateral commissural (SCC) pathway. Stimulating through this electrode requires a high presynaptic release of vesicles from a few synapses and modification of the postsynaptic membrane. If the voltage

pulse protocol was applied in this manner, then conceivably only a small proportion of the total number of synapse available would be stimulated. Any observable change in mEPSC amplitudes brought about by modification of the postsynaptic membrane at these synapses, could be lost due to combination with small non potentiated mEPSC events being generated elsewhere in the pyramidal cell, and would not result in an observable potentiation of mEPSC amplitudes. Switching the site of stimulation to the whole-cell voltage clamped pyramidal cell, firstly removes the need for the stimulating electrode, so after the VPs only the specific output of the cell was recorded. The second advantage is by stimulating through the recording electrode, it is possible to induce a global calcium change through the cell, and potentiate a far greater proportion of the total number of synapses present. The experimental protocol for VP potentiation (Figure 3.8A) consists of recording a whole-cell current for a 5 minute period, then applying the depolarizing voltage pulse stimulus as described in methods section. This resulted in a reliable sustainable potentiation of mEPSC amplitudes, (control 22.1 ± 0.9 pA: VP 46.1 ± 0.1 pA. n = 60) for the 35 minute time period (Figure 3.7A). A characteristic of the VP potentiation protocol are spontaneous inward currents which further investigation (shown later 3.8A) were shown to be found mediated by L-type voltage dependent Ca^{2+} channels.

Figure 3.7B shows typical mEPSC traces from the control period and from around the peak of the voltage pulse potentiation. Analysis of 50 events from both the control and VP potentiated period (Figure 3.8B) indicated an increase the amplitude of the average mEPSC event with VP stimulation (control 21.2 ± 0.1 pA: VP 45.2 ± 0.1 pA). VP has little detectable effect on the mEPSC rise time (control 1.4 ± 0.1 ms: VP 1.4 ± 0.1 ms) or mEPSC decay times (control 11.9 ± 0.1 ms: VP 12.6 ± 0.1 ms).

With this increase in mEPSC amplitudes, there is a corresponding non significant transient increase in mEPSC frequency (control 1.6 ± 0.2: VP 1.9 ± 0.2 Hz. n = 60), prior to the potentiation there appears to be a depolarisation-induced suppression of inhibition (DSI), gained from a postsynaptically released endocannabinoid regulating presynaptic function. This potentiated frequency then decays to 0.9 ± 0.1 Hz by 30 minutes (Figure 3.9A).

Due to the degree of fluctuation with both the amplitude and frequency of mEPSCs, the total current output of the cell will give a true reflection to the degree of potentiation as it is dependent upon both factors. This shows a significant but transient (20 min) increase in the total current generated by the pyramidal cells (control 1.2 ± 0.1 nA; VP 3.1 ± 0.6 nA. n = 60), while thirty minutes post VP potentiation the total current output returned to 1.3 ± 0.1 nA (Figure 3.9B).

The single cell VP potentiation shows the same trend of mEPSC amplitude potentiation, confirmed with the amplitude scatter plot, where potentiated mEPSCs show a far greater range of amplitudes than is shown with the control mEPSCs. Investigation of mEPSC amplitude probability showed a trend for the control mEPSC to have a high probability of smaller amplitude events (80% probability equals 21.2 pA), while the 80 % probability for the VP potentiated mEPSC equals 81.17 pA equivalent to a 3.8 fold change in mEPSC amplitude (Figure 3.10.C). This change in amplitude probability is further described, by a significant shift (KSV $p < 0.01$) in the amplitude distribution following VP stimulation. The distribution trend for the control mEPSCs is a leftward skew, following stimulation the events shift rightward toward a more bell shaped distribution. This distributional shift indicates a higher occurrence of large amplitude mEPSCs in the potentiated period (Figure 3.10.D).

The amplitudes and time course of the mEPSCs recorded may be subject to distortion by dendritic filtering (Ulrich and Luscher, 1993; Pare et al., 1997; Smith et al., 2003). The extent of filtering may depend on pyramidal cell structure, the distance from the soma to the synapse at which the signal is generated, and the time course of the event. Although the cable properties of the CA1 cells may influence the shape of the mEPSCs recorded, it is unlikely that this accounts entirely for the range of mEPSC amplitudes observed. Both control and potentiated mEPSCs showed little correlation between the rise time and the decay time constant or amplitude for individual events. Furthermore there was only poor correlation between the decay and amplitude of mEPSCs. This data suggest that the variation in mEPSC amplitudes cannot be explained by dendritic filtering of events generated at dendritic sites (Figure 3.11).

The mechanisms by which this potentiation of mEPSC amplitudes maybe achieved are by alterations in the conductance of the receptors present in the synapses as shown by (Benke et al., 1998) or via the insertion of new AMPA receptors into active synapses. This process of receptor insertion requires postsynaptic membrane fusion events and is the focus of the next chapter.

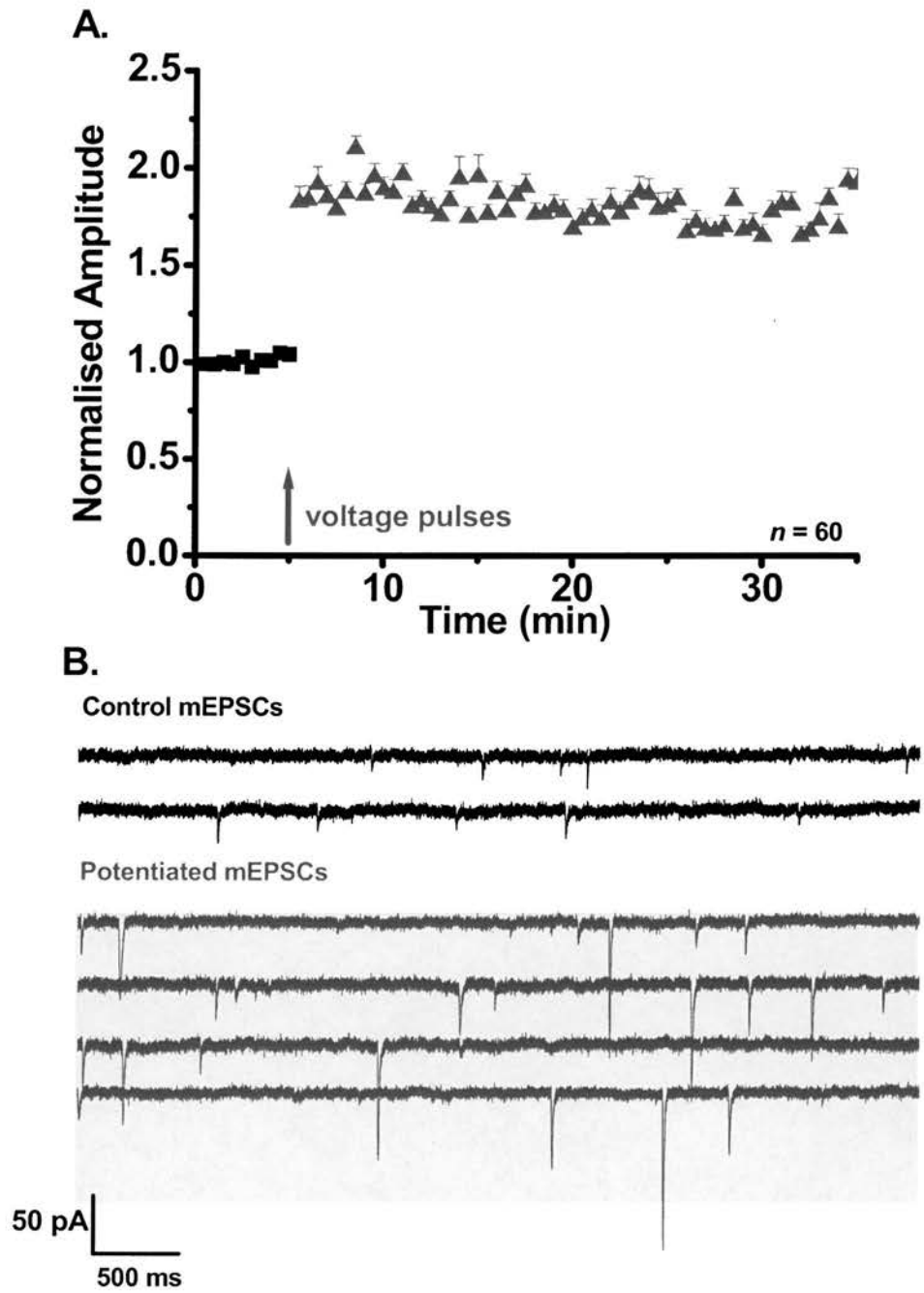

Figure 3.7A: **Voltage pulse potentiation of mEPSC amplitudes.** Application of the voltage pulses induces a significant increase in mEPSC amplitude over the 35 minute time course. (B.) **Raster plot for control and potentiated mEPSCs.** Following potentiation there is an obvious increase in mEPSC amplitudes.

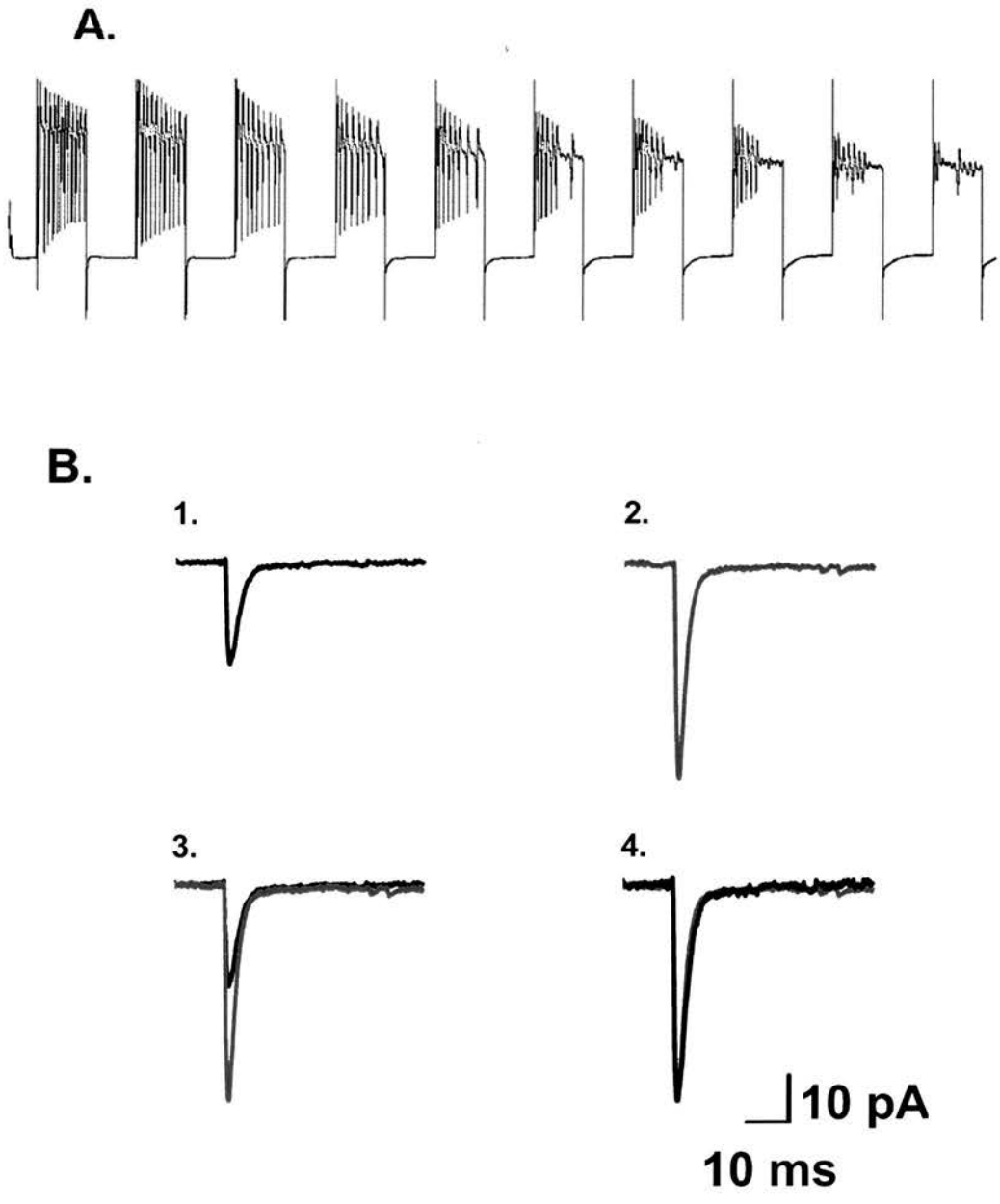

Figure 3.8A: **Voltage Pulses**. This picture highlights typical inward currents shown with VP stimulation. (B.) **mEPSC overlay** analysis of 100 mEPSCs from the control period (1.) and the VP potentiated (2.) period show a significant increase when overlaid (3.) with little change in rise or decay times when mEPSC are scaled (4).

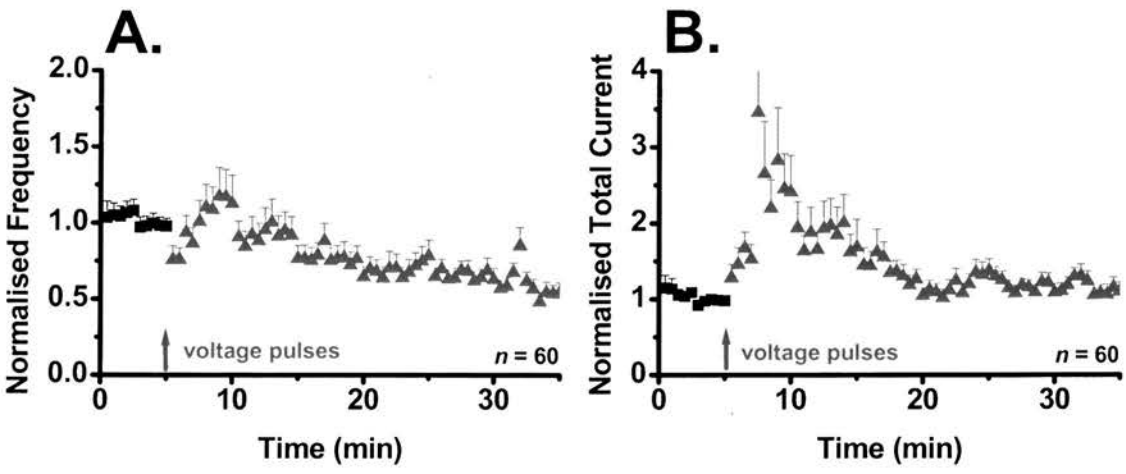

Figure 3.9 **Voltage pulse potentiation of mEPSC frequency.** A small transient potentiation of mEPSC frequency occurs following stimulation. (B.) **Voltage pulse potentiation of total mEPSC current.** A significant but transient potentiation of the current output of the cell was shown following VP stimulation.

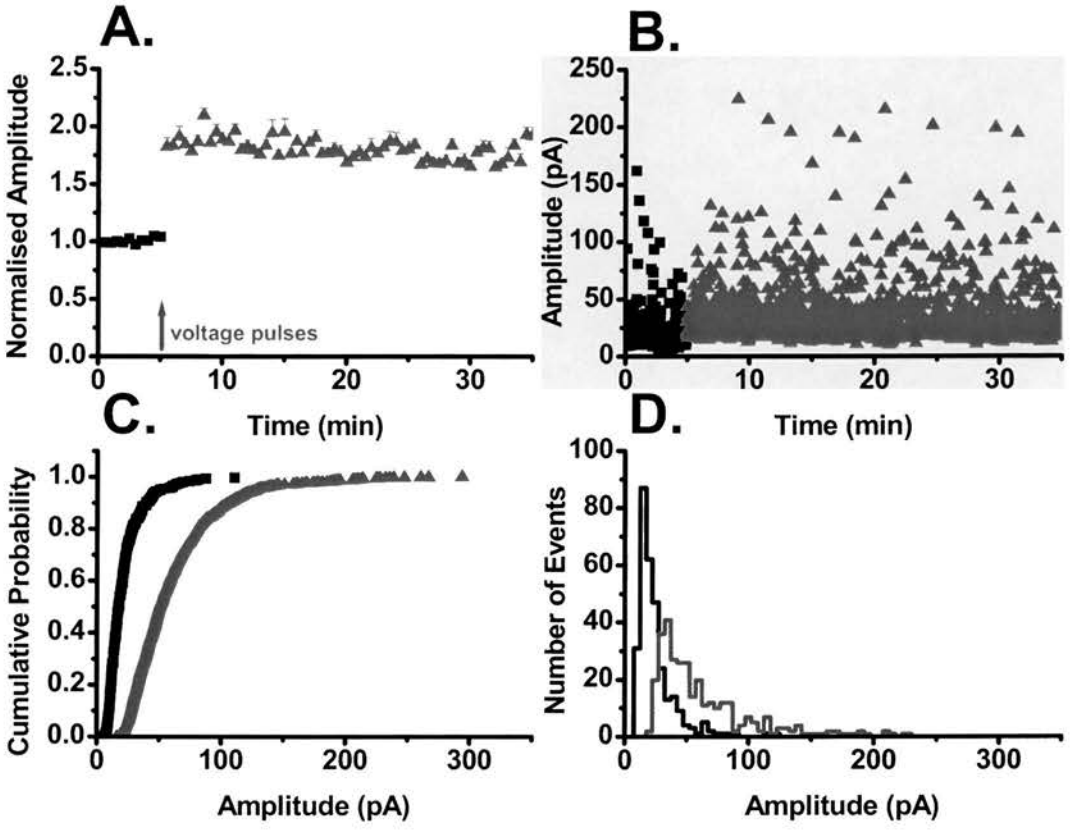

Figure 3.10. **Typical single cell mEPSC amplitude potentiation.** (A.) Following VP stimulation there is a sustainable potentiation (2 fold) of the mEPSC amplitudes. (B.) **mEPSC amplitude scatter plot** highlighting the raw increase in mEPSC amplitudes. (C.) **Cumulative probability plot**, following VP stimulation there is a significant increase in the probability of large amplitude mEPSC, when compared with control. (D.) **Amplitude histogram of mEPSCs**, the rightward shift for the VP mEPSCs suggests bigger mEPSCs following the stimulus.

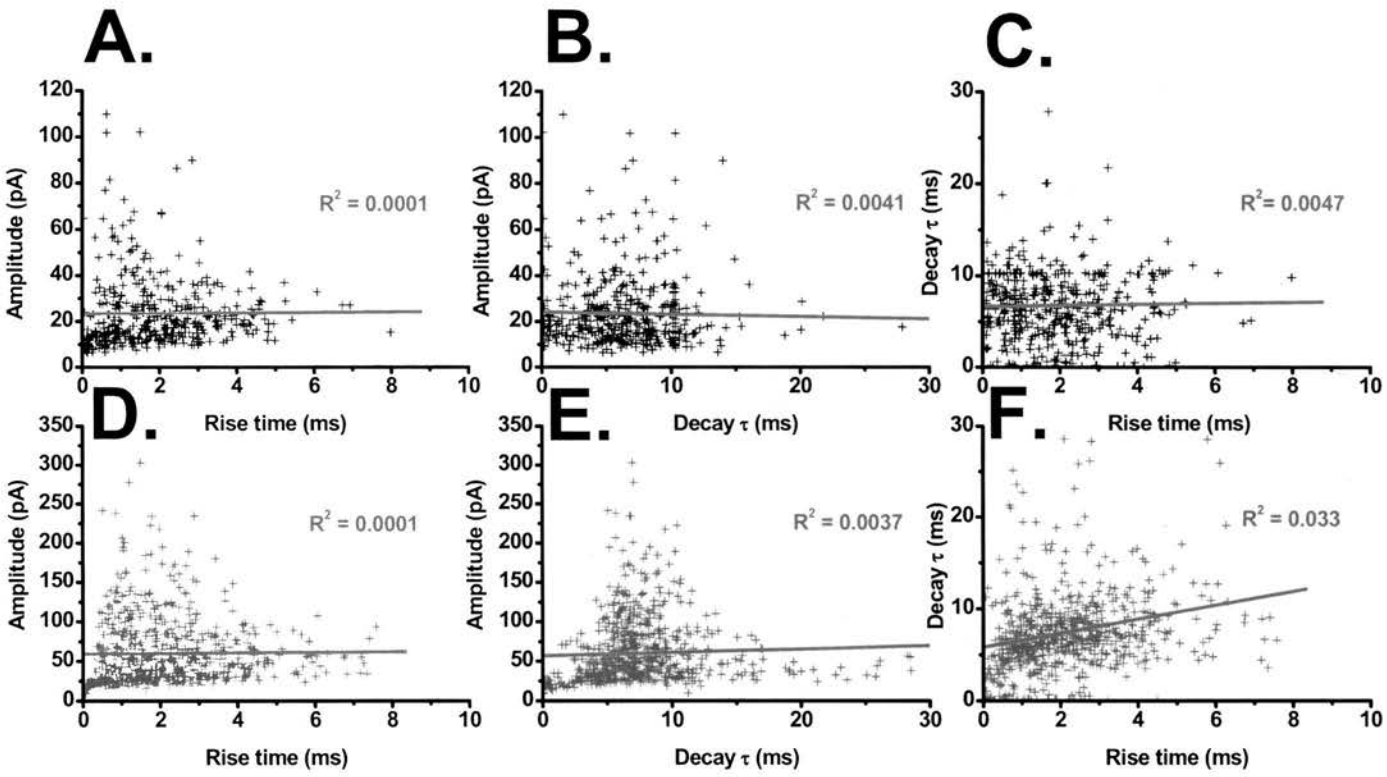

Figure 3.11: **mEPSC events display no correlation between rise and decay times.** Amplitudes of control mEPSCs show no correlation between rise time of the event (A. $R^2 = 0.0001$) or τ decay time (B. $R^2 = 0.0041$) and no correlation between rise and decay τ (C. $R^2 = 0.0047$). Following VP potentiation no correlations are evident between these parameters.

3.7: VP potentiation- some interesting observations

The reliability of this stimulating protocol was the next question addressed. Analysis of the average degree of potentiation for the 5 minute period following the stimulus, showed the main potentiation levels to be between 75 and 100 % above the control amplitude, with the skew of the distribution favoring greater degrees of potentiation. Choquet & Triller., (2003), published the idea that synapses must have a maximum level for receptor insertion, over which the synapse cannot accept more receptors and hence there must be a limit on the amplitude potentiation of the mEPSC. Although the cumulative probability data (Figure 3.10 C) suggests that this is not the case due to the largest events of the VP potentiation period being much bigger than the largest event of the control period. The idea that the degree of mEPSC potentiation could be dependent upon the mean amplitude of the control mEPSC, as a reflection of the receptor number at the synapse is important (Figure 3.12B). When this correlation of postsynaptic function, the mean amplitude of the control period against the percentage potentiation form five minutes post VP potentiation, was plotted it was shown that no relationship exists ($R^2 = 0.0126$). The idea that the degree of potentiation achievable is dependent upon initial frequency was also investigated. The mean control frequency was plotted against the percentage potentiation, again no correlation was found (Figure 3.12.C $R^2= 0.0006$). There was also no correlation between the mean amplitude and frequency showing complete independence of the VP potentiation. In summary, the degree of VP potentiation of mEPSCs achieved is not dependent upon the initial mean amplitude of the events or on the frequency of these events.

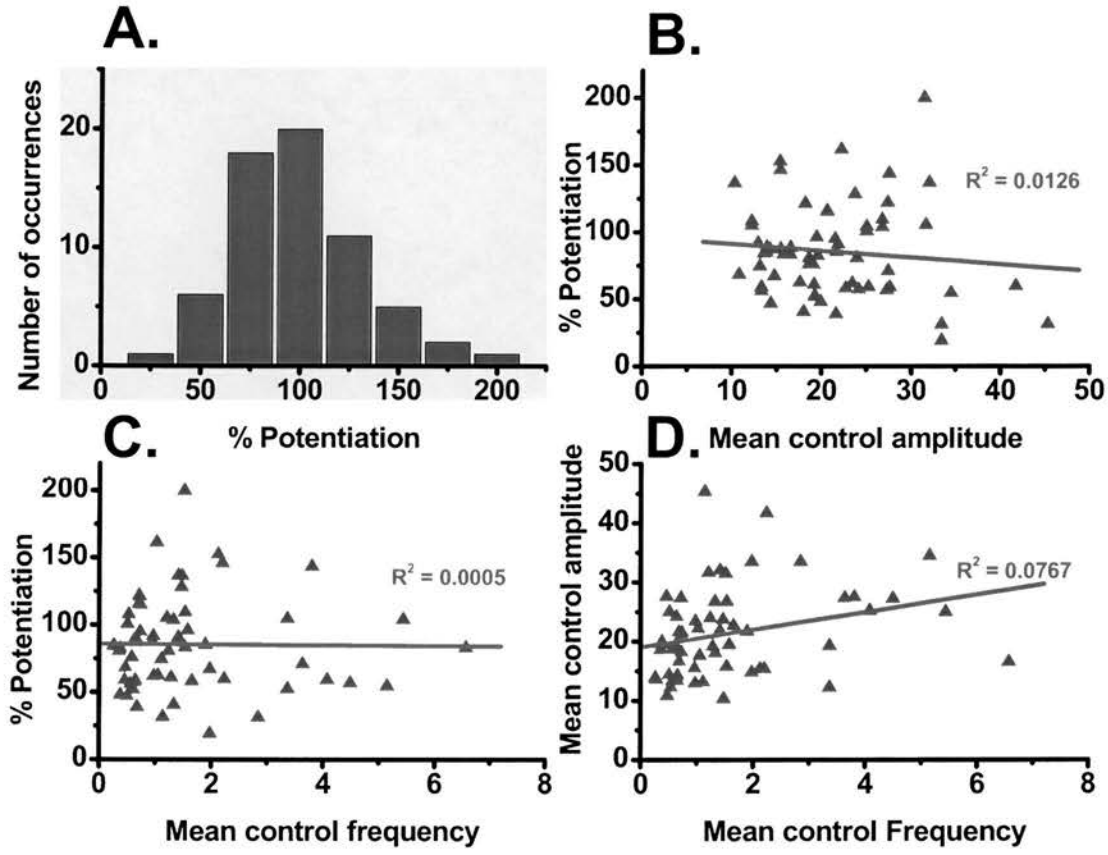

Figure 3.12A: **Spread of potentiation.** This histogram indicated that the VP stimulation resulted normally in a 100 % potentiation of the mEPSC amplitudes, with the trend to larger degrees of potentiation with this stimulus. (B.) **Correlation between degree of potentiation and mean amplitude.** The mean amplitude of the control mEPSCs are not a factor in the size of the potentiation gained from the stimulus. (C.) **Potentiation frequency correlations.** The mean control mEPSC frequency is not a determinant of the degree of potentiation elicited by the VP stimulus. (D.) **Amplitude, frequency correlations.** There is no correlation between mean control amplitudes and frequencies of the mEPSCs.

3.8: Long lasting VP potentiation of mEPSC amplitudes

In previous experiments the VP stimulus induced a sustainable potentiation of mEPSC amplitudes, but the time course in terms of LTP experimentation is short. Increasing the experimental time course showed a reduction in the potentiated mEPSC amplitudes. The difference between in the long term sustainability of VP potentiation and NMDA receptor dependent LTP, may in fact be the activation of the NMDA receptor. Long time period recordings in the organotypic slice preparation are technically difficult, due to mechanistic problems of holding a cell in the whole-cell configuration, and the viability of thin slices in a submerged chamber decreases over time. In a series of experiments VP potentiation was recorded over a long time course of 45-50 minutes (Figure 3.13A: control 24.3 ± 2.5 pA: VP 53.1 ± 1.8 pA: late VP (45 min): 37.1 ± 1.5 pA. $n = 10$).

With the potentiation of mEPSC amplitudes there is a corresponding decease in event frequency (Figure 3.13B: control 1.6 ± 0.5 Hz: VP 1.2 ± 0.2 Hz: VP 45 min 0.7 ± 0.1 Hz) over the same time course. Current output for the same time course as above shown an initial potentiation of the total current output, as the time period increases the degree of potentiation reduces (Figure 3.13C: control 1.3 ± 0.35 nA: VP 2.2 ± 0.4 nA : VP 45 min 1.0 ± 0.3 nA). Analysis of 100 events from equivalent time periods highlighted above show mean amplitudes of (control 20.5 ± 1.9 pA: VP 53.6 ± 1.2 pA: Late VP 30.9± 0.6 pA). Rise time data for the three time periods shows no significant change. (control 2.1 ± 0.3 ms: VP 2.1 ± 0.2 ms: late VP 2.0 ± 0.3 ms). The decay time constant show a small non significant variation (control 13.7 ± 1.4 ms: VP 15.7 ± 1.6 ms: late VP 16.7 ± 1.7 ms) (Figure 3.14).

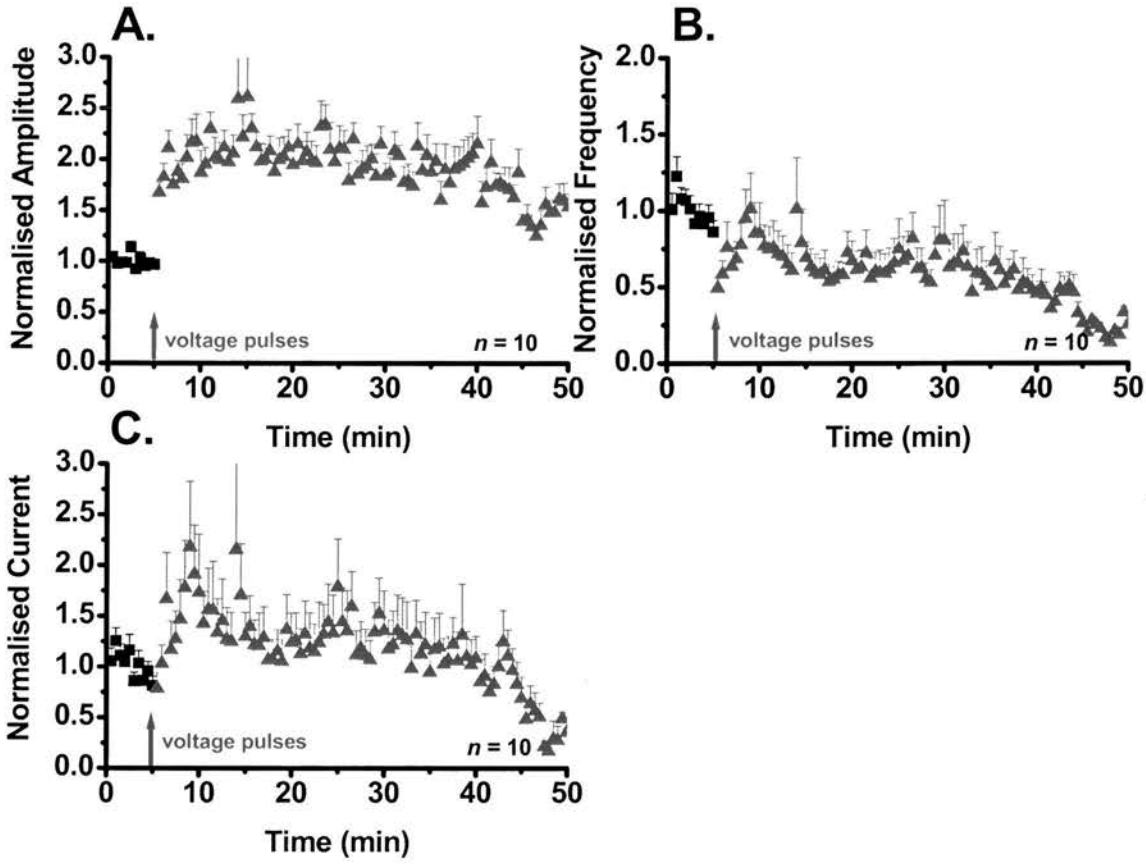

Figure 3.13 **Late phase VP potentiation**. (A.) The amplitude time course shows typical potentiation over the first thirty minutes of the experiment, and then the mean amplitude decreases over the last 20 minutes. (B.) The mEPSC frequency shows a prominent DSI current, and continues to decline over the experimental time course (C.) the total current produced potentates following the VP stimulus, but then displays a similar parallel reduction displayed with the frequency time course.

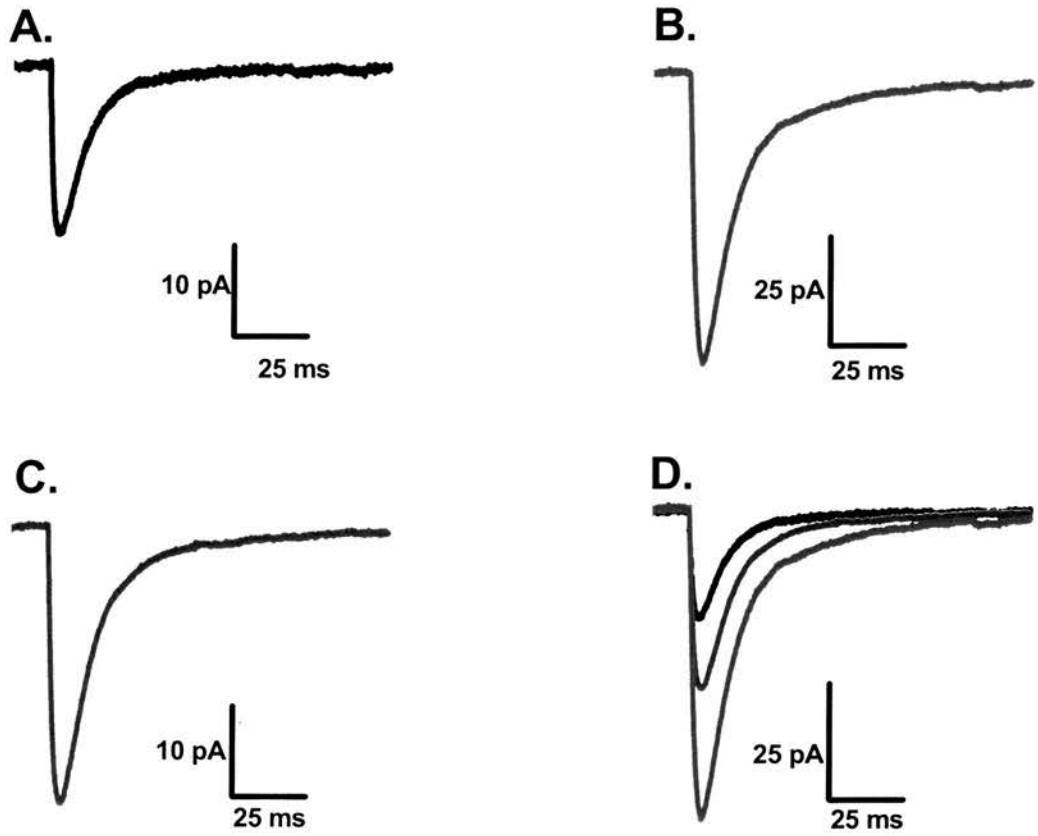

Figure 3.14: **mEPSC overlays for late VP potentiation.** Analysis of 100 mEPSCs from the control period (A.) and the VP potentiated (5-10 min) (B.) and late VP period (40-45) (C.) show a significant increase when overlaid (D.) with the late VP mEPSC having a smaller amplitude than the VP potentiated period.

3.9: Pharmacological characterization of voltage pulse potentiation

Application of the voltage pulses induces sustainable potentiation of the mEPSC, but in this system it is still unproven as to what factors contribute to this potentiation. Therefore, receptor antagonists for the AMPA receptor, and NMDA receptor were used to determine the receptor requirement for this potentiation of mEPSC amplitudes.

3.10: Receptors required for mEPSCs

mEPSCs have long been known to be generated by the activation of AMPA receptors in the postsynaptic membrane. Therefore, it was important to determine if these receptors are responsible for mediating VP potentiation. In these experiment, control recording were made and a significant potentiation of the mEPSC amplitude induced, (Figure 3.15: control 13.0 ± 0.2 pA; VP 24.1 ± 1.6 pA n = 3). At the peak of the potentiation, 5 minutes after the induction of VP stimulus, the AMPA receptor antagonist 6-cyano-7-nitroquinoxaline-2, 3-dione (CNQX 20 μM) was bath applied. As expected the application of this AMPA receptor antagonist quickly abolished all mEPSC events.

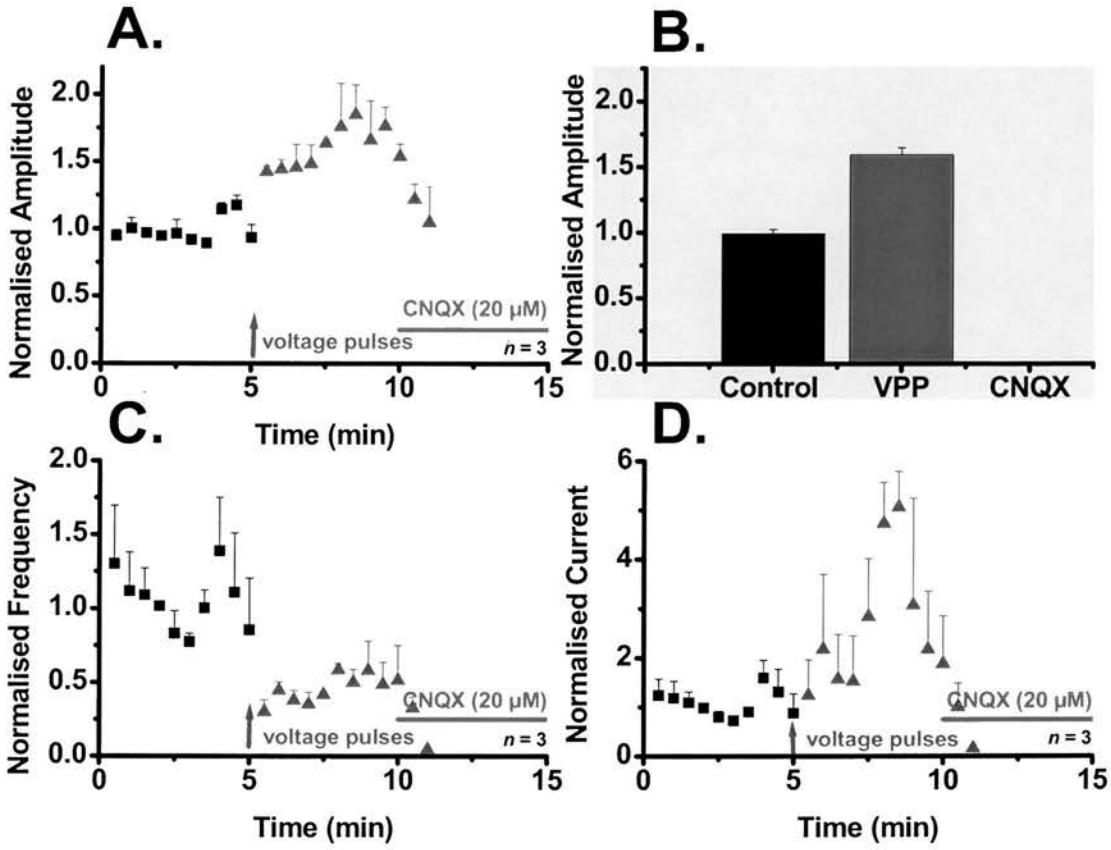

Figure 3.15: **CNQX blocks VP potentiation of mEPSC amplitudes.** (A.) following potentiation of mEPSC amplitude, CNQX (20 μM) was bath applied and this blocked all mEPSC events. (B.) Histogram representing loss of potentiation with CNQX application. (C.) Corresponding reduction in mEPSC frequency (D.) potentiation of mEPSC currents was abolished with CNQX application.

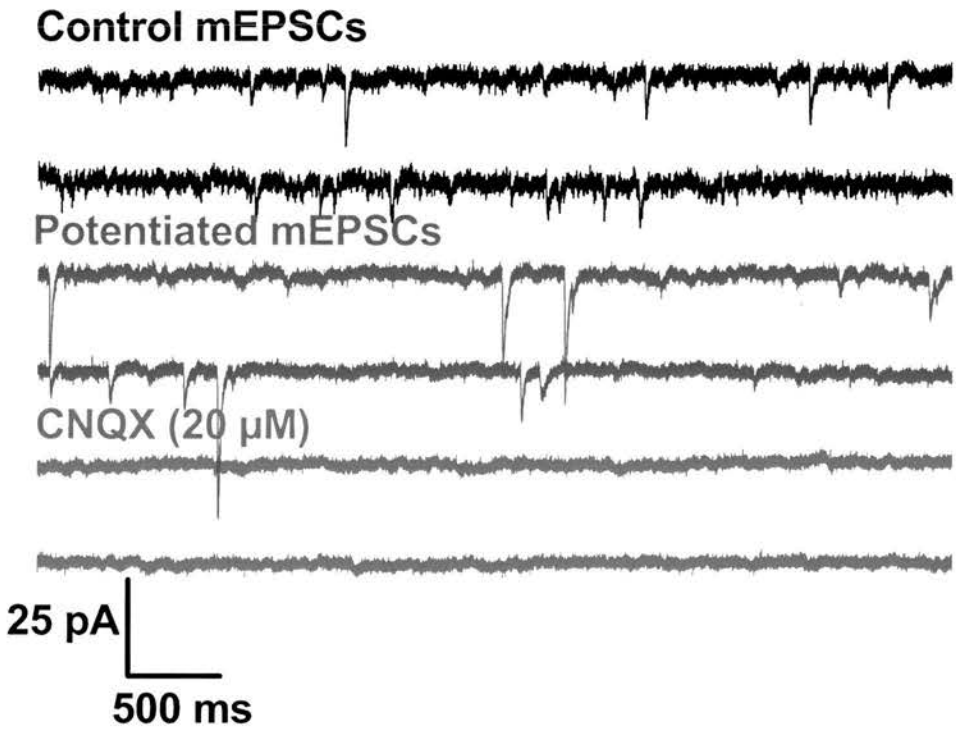

Figure 3.16: **mEPSC raster plot for mEPSCs with CNQX (20 µM)**. Control mEPSC are typically 15 pA, application of the VP stimulus induces a significant potentiation of mEPSC amplitudes, while application of CNQX (20 µM) abolishes all events.

3.11: Is Voltage Pulse potentiation dependent upon NMDA receptor activation?

If the mEPSC event potentiation induced by the voltage pulse stimulus, was to be consistent with traditional LTP, there would have to be a dependency upon the activation of the NMDA receptors present in the synapses to generate the increase in mEPSC amplitudes. In these experiments, 2-amino-5-phosphonovaleric acid (APV 30 μM) the prototypical NMDA receptor antagonist was bath applied, to inhibit the action of this receptor, and to further characterize any background effect on mEPSCs.

These experiments characterize the effects of NMDA receptor blockade on the control mEPSC, in a series of three experiments no significant change in the amplitude of the mEPSCs was shown after the bath application of the APV (30 μM) (Figure 3.17A: control 23.4 ± 1.9 pA: APV 24.3 ± 1.9 pA. $n = 3$). A typical scatter plot shows little difference in the distribution of mEPSC amplitudes for both control and APV mEPSC. The cumulative probability plot for both control and APV treated mEPSCs overlap indicating little difference between control and APV treated events. Analysis of events in the control period (5 min) and treated period (5 min) show firstly a leftward skewed distribution for both groups.

Raster plots from both control and APV treated periods show events of similar amplitude (Figure 3.18A). Analysis of 100 mEPSC events from both control and APV treated mEPSCs show an average mEPSC amplitude of 21.4 ± 0.3 pA: APV 21.3 ± 0.4 pA respectively. These average mEPSCs have a rise time of control 1.7 ± 0.5 ms: APV 1.6 ± 0.7 ms respectively, and have a τ decay time of 16.0 ± 0.9 ms and (APV) 17.2 ± 0.8 ms.

The time course of mEPSC frequencies does change, but the reduction shown is similar to that shown with both the control mEPSC and the VP potentiation frequency recordings (Figure 3.19A: control 1.5 ± 0.6 Hz: APV 1.4 ± 0.3 Hz. $n = 3$). The total current generated in these experiments shows a reduction in current output after the application of APV (Figure 3.19B: control 0.9 ± 0.3: APV 0.8 ± 0.1 nA. $n = 3$).

In summary the application of APV was used as a check of the functionality of the NMDA receptors in these cells. The experimental set up precludes activation of these receptors, as the combination of voltage clamping the cells at -80 mV and the inclusion of 1.3 mM $MgSO_4$ would inhibit the NMDA receptor, and mEPSCs recorded would not be expected to express a NMDA component.

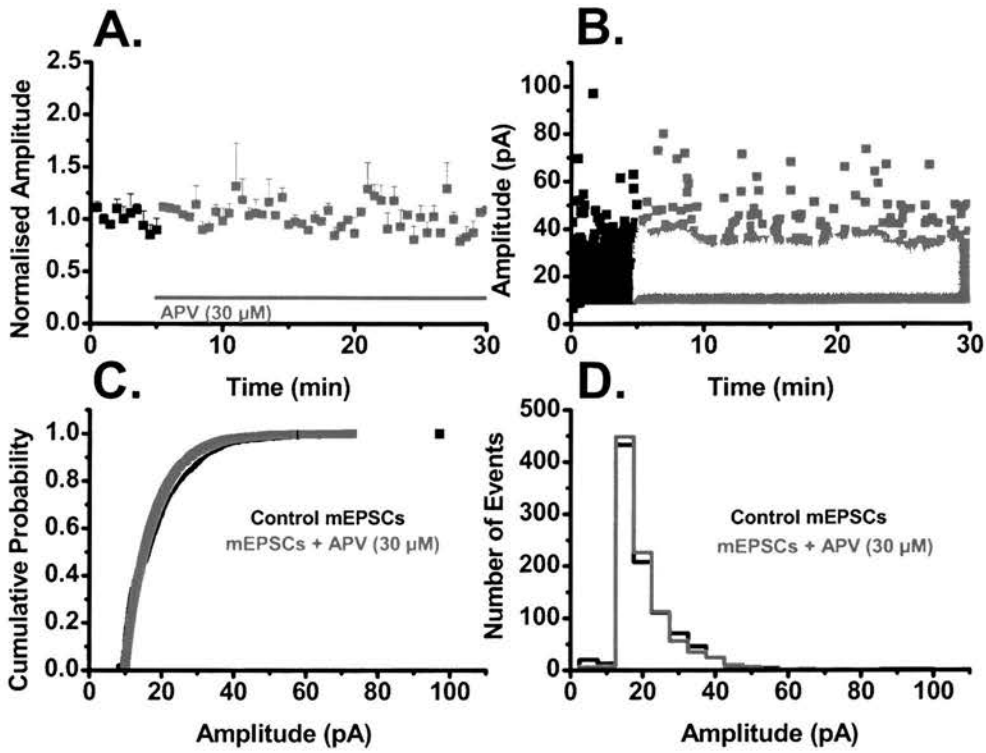

Figure 3.17: **Control and APV (30 µM) mEPSCs.** (A.) Application of APV has no significant effect on mEPSC amplitudes (B.) Scatter plot shows similar amplitude distributions for both control and APV treated mEPSCs (C.) Cumulative probability plot shows no difference between control and APV treated mEPSCs (D.) Analysis of event in the control period (5 min) and treated period (5 min) show a leftward skewed distribution for both groups, with no difference in the distribution of the histogram

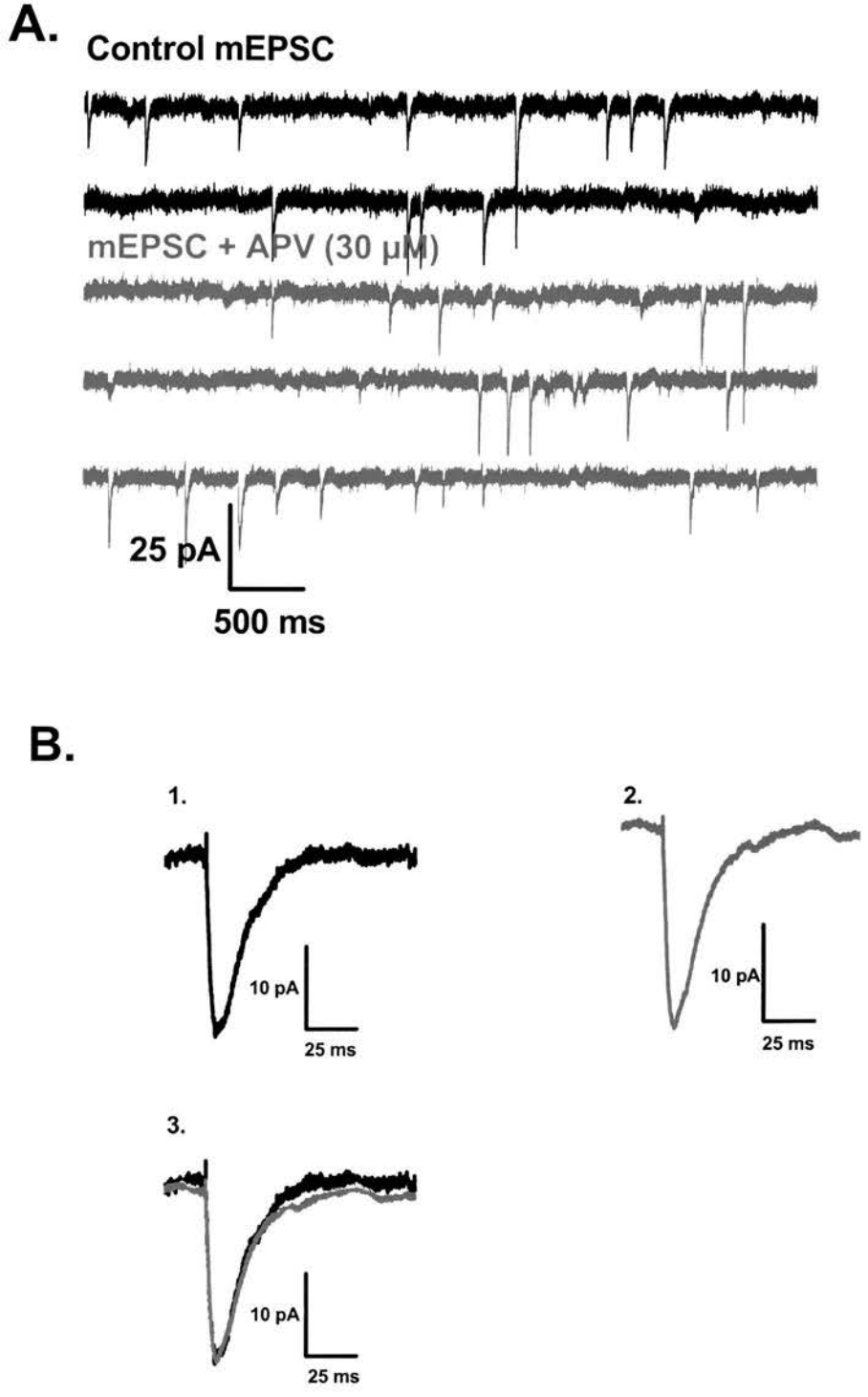

Figure 3.18: **Raster and overlay plots for control and APV treated mEPSCs**. (A.) Raster plot show mEPSCs with similar amplitudes for both control and APV treated mEPSCs. (B.) analysis of 100 mEPSCs from the control period (1.) and the APV treated period (2.) show no significant increase when overlaid (3.) with little change in rise or decay times.

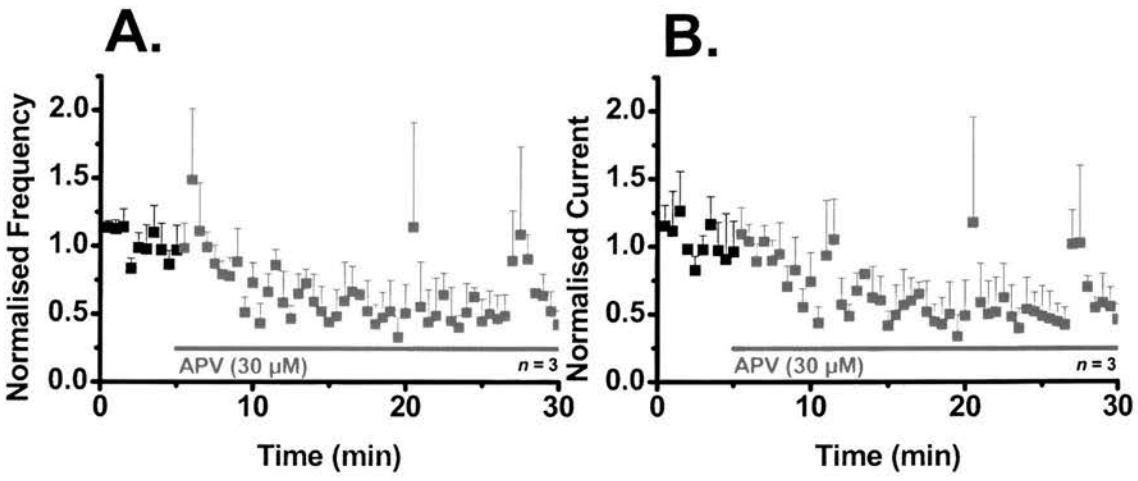

Figure 3.19: **mEPSC frequency and current with APV.** Application of APV (30 μM) shows the same trend of reducing mEPSC frequency shown with control recordings. (MacDermott et al., 1999) suggested a role for presynaptic NMDA receptors facilitating vesicular release, but if this was a factor then frequency would reduce to zero. (B.) The total mEPSC current output shows the expected reduction paralleling the reducing mEPSC frequency.

3.12 Does inhibition of the NMDA receptor affect the induction of VP potentiation?

Inhibition of the NMDA receptor has no effect on the control amplitudes of mEPSC, indicating that synaptic AMPA receptors are stable and that turnover of new AMPA receptors in non potentiated cells is at a low level. As previously suggested mEPSC amplitude potentiation, could be mediated by insertion of new patches of AMPA receptors. If VP potentiation is expressed using similar mechanisms as traditional LTP, then this receptor insertion will be dependent upon the activation of the NMDA receptor.

After stable control recording in the presence of APV (30 μM), the voltage pulse stimulus was applied and a significant mEPSC amplitude potentiation was shown (Figure 3.20A: control 26.7 ± 4.9 pA; VP 53.1 ± 5.6 pA $n = 5$). Figure 3.20B indicates Raster plot of typical control and potentiated mEPSCs, both event types were treated with the NMDA receptor antagonist APV.

Frequency time course for this experiment, again shows no significant decrease following the VP stimulus (Figure 3.21A: control 1.5 ± 0.3 Hz; VP 1.47 ± 1.6 Hz), but mEPSC frequency was shown to reduce across the time course of the experiment. Total current output for this experiment as expected potentiates following the VP stimulus, (Figure 3.21B: control 1.3 ± 0.5 nA; VP 2.1 ± 0.4 nA).

Single cell event data show the same trends as shown in the grouped data; with amplitude increase, post stimulation (Figure 3.22A) the corresponding single cell scatter plot shows a large distribution of mEPSC events following VP stimulation (Figure 3.22B). Cumulative probability diagram shows clear differences between the control and VP protestation data, the 50 % probabilities are 17.1 pA and 27.9 pA. 80 % probabilities for this single cell represent are 27.7 pA and 45.3 pA respectively, clear difference between these values (Figure 3.22C). The amplitude index shows significant differences between the control recording and VP potentiated data, (KSV $p<0.05$) both results indicate that after VP stimulation there is an increased likelihood of larger amplitude events (Figure 3.22D).

Analysis of 100 mEPSC events from the APV treated control and VP potentiated periods, showed a 96 % potentiation of mEPSC amplitudes (17.8 ± 0.4 pA: APV 35.0 ± 0.4 pA). The rise time for these two classes of events was not significantly different (1.7 ± 0.3 ms: APV 1.7 ± 0.2 ms). τ Decay times again fitted with a single exponential differ by 10.5 % (16.9 ± 1.9 ms: APV 18.6 ± 1.2 ms), but when a scaled control mEPSC is compared to the VP potentiated mEPSC little difference is evident between the two types of event (Figure 2.21C).

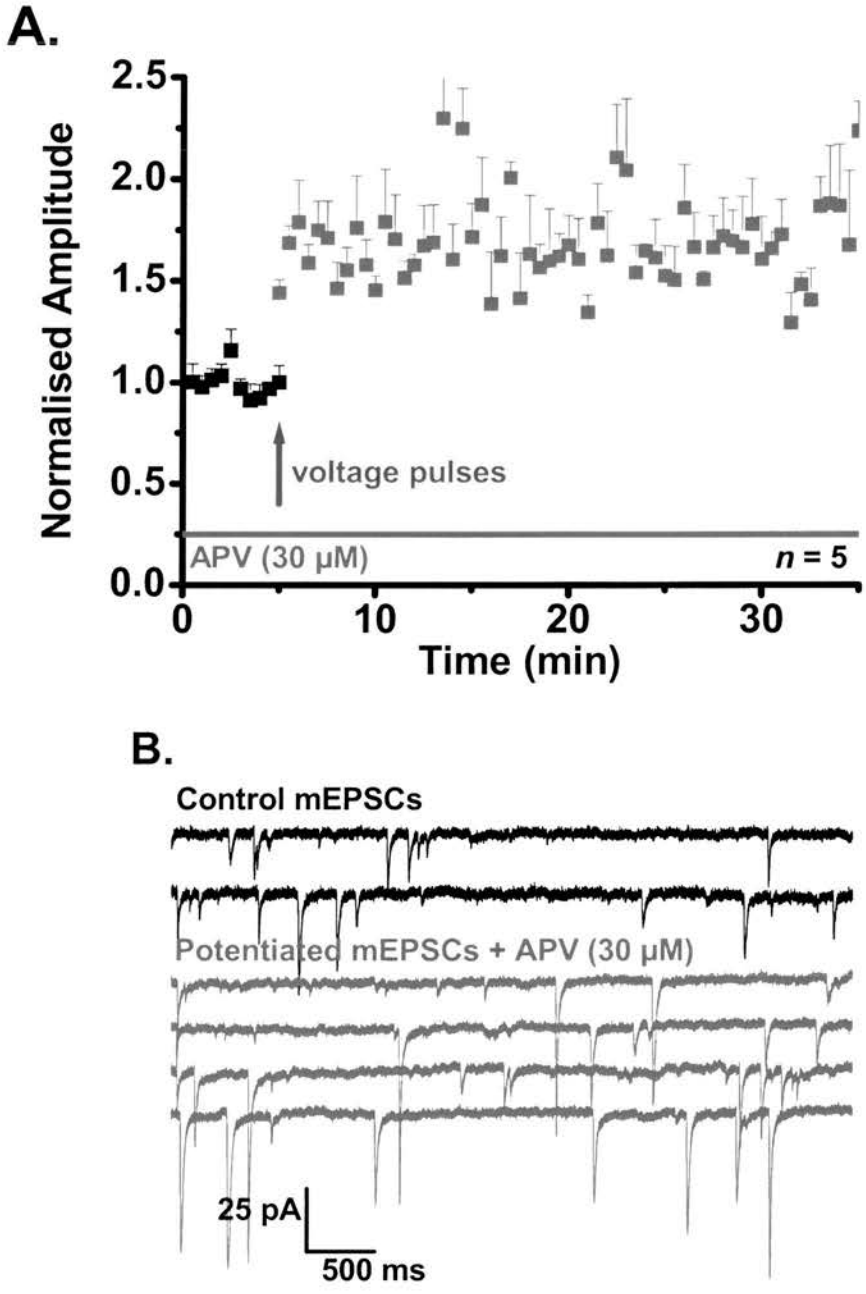

Figure 3.20. **VP potentiation of mEPSC amplitudes is independent of NMDA receptor activation.** (A.) A significant potentiation of mEPSC amplitudes was generated following stimulation and with APV in the bath solution. (B.) Raster plot for both control and potentiated APV mEPSCs

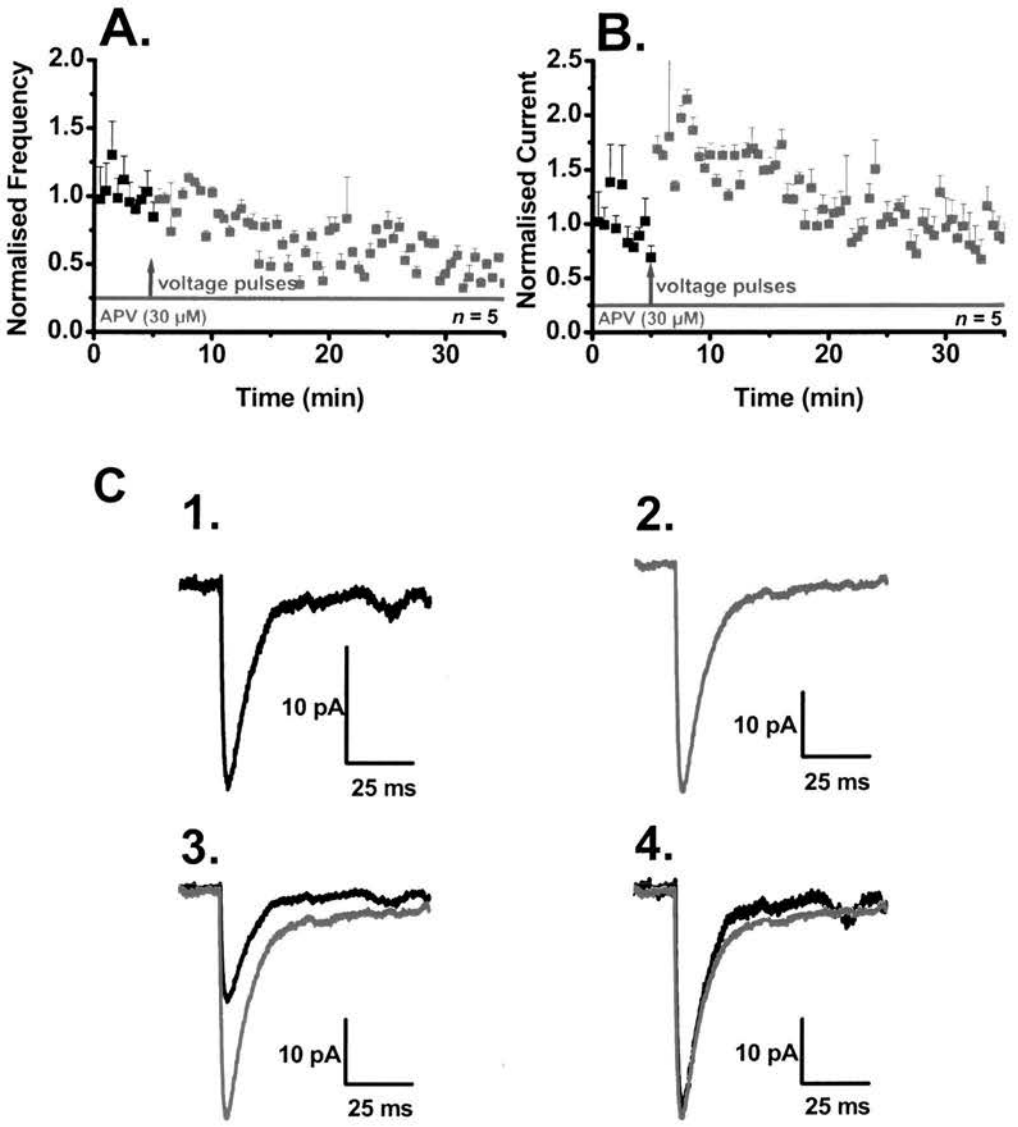

Figure 3.21: **VP stimulated mEPSCs frequency and currents with APV:** Following the VP stimulation in the presence of the prototypical NMDA receptor antagonist 30 μM APV there is no potentiation of either mEPSC frequency, (A.), but mEPSC currents potentate as a factor of the increase in mEPSC amplitudes (B.). **mEPSC overlays for control and APV potentiated mEPSCs.** (C) Analysis of 100 mEPSCs from the control period (A.) and the APV treated period (B.) show a significant increase when overlaid (C.) with little change in rise or decay times when mEPSC are scaled (D.)

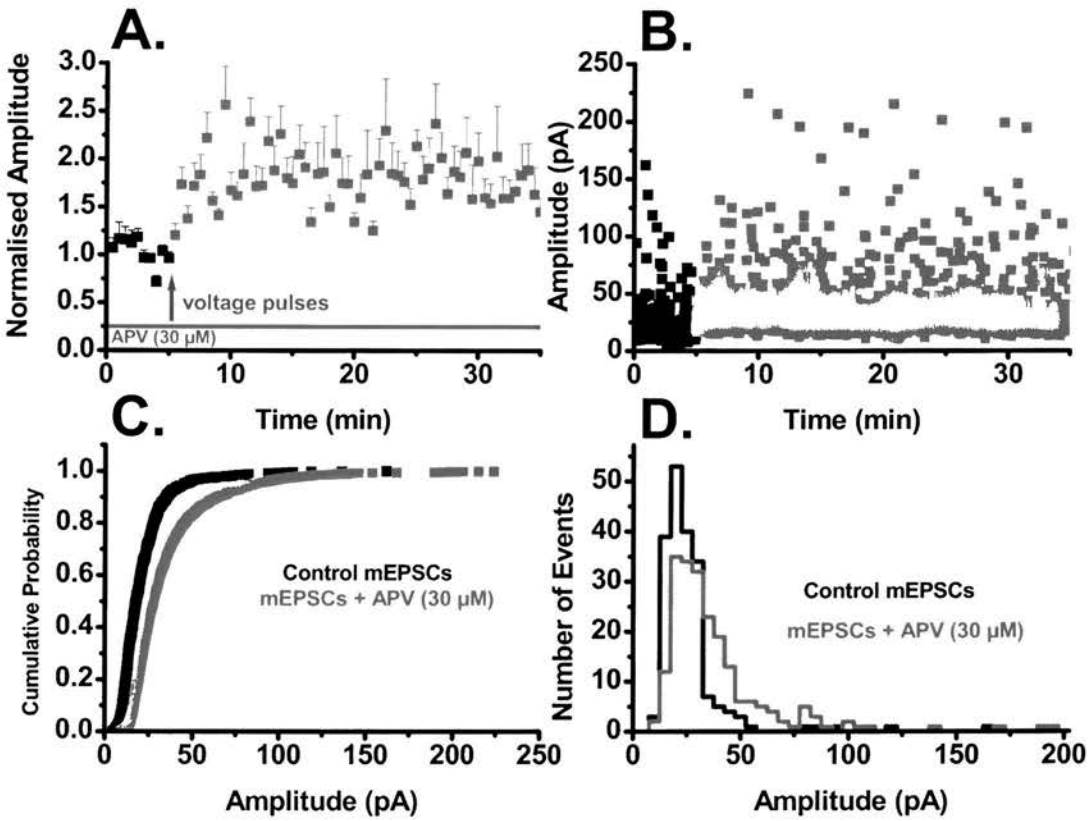

Figure 3.22 **Properties of APV treated mEPSCs.** A single cell amplitude time course shows typical potentiation of the mEPSC amplitudes. (B.) The scatter plot of the raw data for this single cell trace shows an increase in the amplitude distribution as expected if potentiation was occurring reinforces this. (C.) The cumulative probability shifts rightwards indicating a higher probability for larger amplitude mEPSCs. (D.) Amplitude histogram indicating a control leftward skewed distribution which shifts rightwards following potentiation.

3.13: Is the APV functioning?

To test the viability of the APV recordings evoked excitatory postsynaptic currents were recorded at depolarized potentials, at a holding potential of +50 mV to reveal the NMDA component of these EPSCs (Figure 3.23A).

Recording of mEPSCs were similarly made at + 50 mV, at this holding potential these events have a large NMDA receptor mediated component in the decay phase of the event, due to the release of the physiological Mg^{2+} ion blockade of this receptor (about a + 25 mV holding potential). When APV is applied, there is a significantly reduction in the decay time for the mEPSC events. This figure is a qualitative representation, since the control mEPSC will be a mixed group of pure AMPA mEPSC and the AMPA/NMDA mEPSC, therefore the average decay time will be affected by the faster AMPA mEPSC. mEPSCs from both control and APV treated time periods are shown in a Raster plot 3.23B.

Therefore, Figure 3.24 indicated the differences between an obviously selected NMDA component mEPSC and an AMPA mEPSC. Clearly, there is a significant difference in the decay time, the reason that this phase does not return to the zero level, is due to the positive potential.

The voltage pulse stimulation protocol, highlights another small problem. This is that the voltage step from -80 mV to + 20 mV may remove the voltage sensitive magnesium block of the NMDA receptor, and this sudden transient activation of this receptor is all that is required for the mEPSC amplitude potentiation shown. Evoked EPSC at stepped positive holding potentials from 0 mV to + 40 mV, highlighted the removal of the magnesium block on the NMDA receptor at the + 20 mV trace. At a holding potential; of + 20 mV a small 20.5 pA current is evident. The possible contribution of this small current to VP potentiation is not known, but the clear result from these experiments is that VP potentiation of mEPSC amplitudes is still possible in the presence of APV.

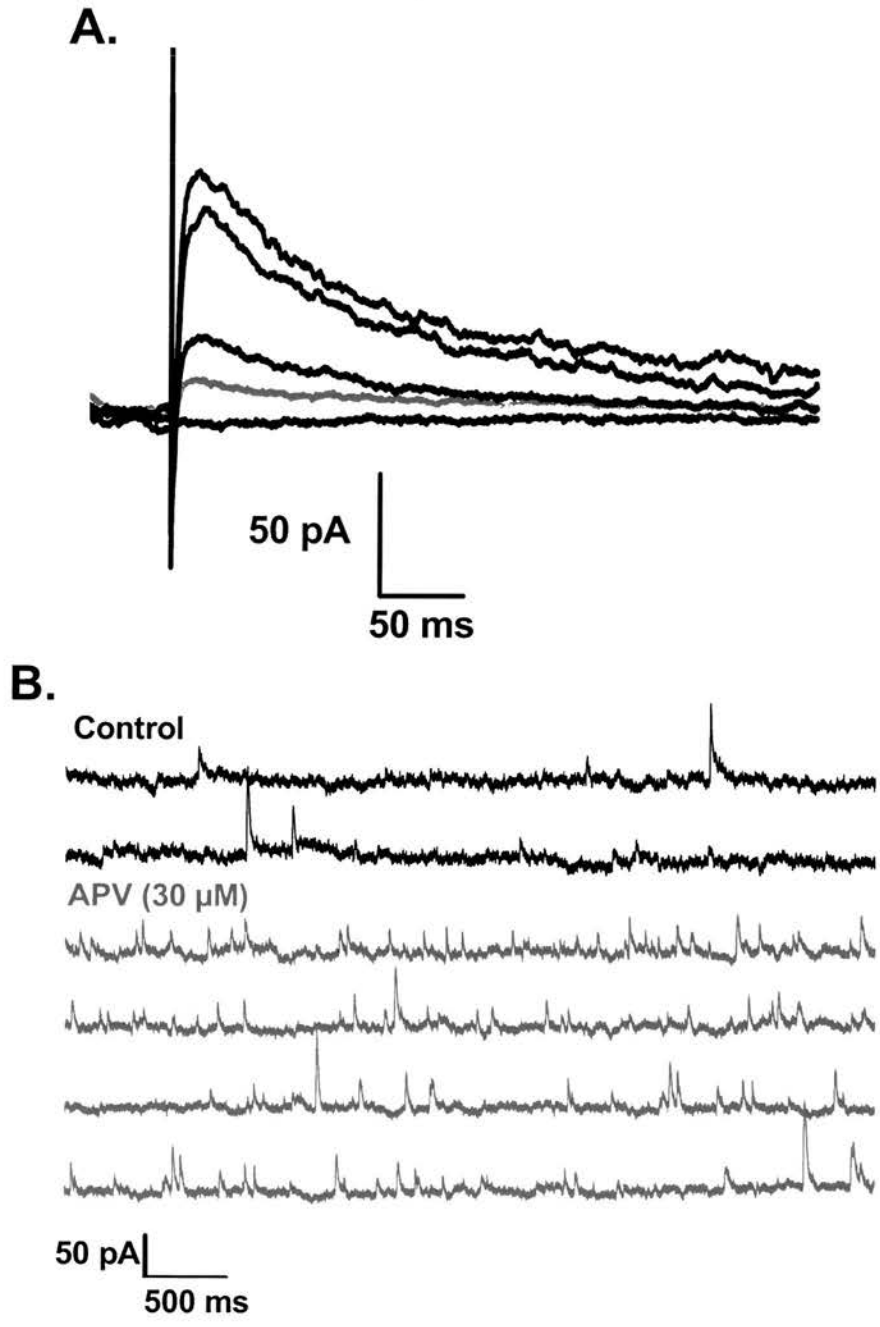

Figure 3.23: **NMDA receptor dependent currents** (A.) evoked EPSCs recorded at a positive holding potentials (+10 mV increments) showing relief of magnesium block of the NMDA receptor. (B.) **Raster plot of mEPSCs at positive holding potentials.** mEPSC with large NMDA components which are blocked by APV (30 µM)

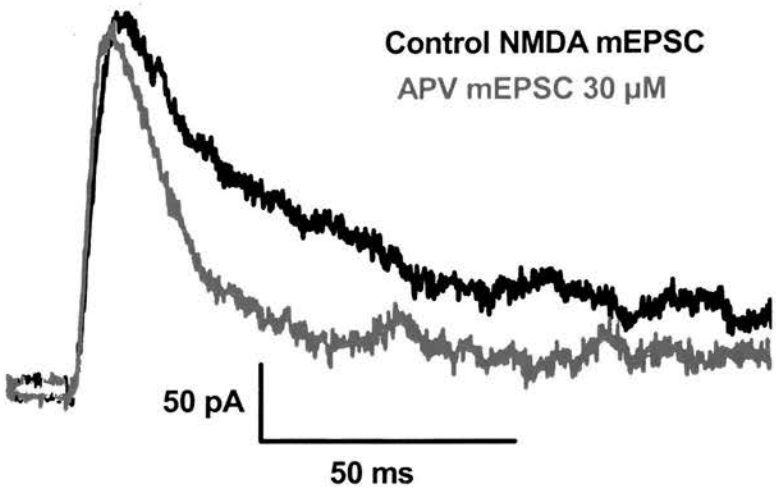

Figure 3.24: **The NMDA receptor component of the mEPSC.** mEPSC recorded at positive holding potentials (+ 50 mV) show large slow NMDA components in the decay phase of the mEPSC (Black trace). This slow decay phase significantly reduced with the application of APV (30 µM)

3.14: Calcium source and homeostasis

With NMDA receptor mediated LTP, there has to be, as Malenka & Bear (2004) defined, a contributing mediating factor that when not present, LTP simply cannot be generated. This trigger, the influx of calcium has long been the focus of rigorous debate in the LTP field; whether it is calcium flow through the NMDA receptor or simply the increase in postsynaptic calcium concentration which is essential for LTP induction. The next set of experimental defines a requirement for an increase in postsynaptic calcium, and then identifies both an internal and external source for calcium is required.

In this series of experiments, the calcium chelator BAPTA (10 mM) was included in the recording pipette; this effectively compartmentalizes the application of this drug to the internal compartment of the cell, effectively removing any presynaptic effect. Application of this chelator by this method, blocks the potentiation of mEPSC amplitudes (Figure 3.25: control 18.8 ± 2.4 pA: VP 17.8 ± 0.6 pA. n = 3), while interleaved controls show typical potentiation. (control 23.3 ± 4.0 pA: VP 43.1 ± 3.0 pA. n = 2). Raster plot (Figure 3.26C)

shows typical mEPSCs from both control and the BAPTA treated VP stimulated time periods.

This result signifies that the mechanism for VP potentiation is clearly dependent upon an increase in the postsynaptic calcium concentration. However, the trend of event amplitude time course is interesting as the control period is stable, but after VP stimulation, there is not the characteristic amplitude potentiation. The mean amplitude of the events in the control period with BAPTA are smaller than typical control mEPSC amplitude values; over the time period of the experiment after the potentiation stimulus the amplitude increases towards the amplitude for the non potentiated control values. mEPSC frequency does not potentiate with the application of BAPTA (10 mM) (0.7 ± 0.1 Hz: VP 0.6 ± 0.1 Hz. n = 3) which also applies to the frequency of the interleaved control mEPSCs (0.6 ± 0.1 Hz: VP 0.6 ± 0.1 Hz. n = 2). The total current produced by the mEPSC events over the time course is sensitive to BAPTA, as potentiation was blocked (0.4 ± 0.1 nA: VP 0.3 ± 0.1 nA. n = 3) while interleaved control recordings show an increase in current (0.4 ± 0.1 nA: VP 0.6 ± 0.1 nA. n = 2) (Figures 3.26 A + B). Figure 3.27 shows a single cell recording for VP potentiation with BAPTA (10 mM), following VP stimulation there is no obvious potentiation of mEPSC amplitude, the amplitude scatter plot does appear to have an increase in distribution, due to random large amplitude events. The cumulative probability for all events in both time periods overlaps indicating little change in amplitude probability, similarly the amplitude histograms overlap and indicate no rightward distribution shifts following VP stimulation.

Analysis of 100 mEPSCs from each of the three time periods show no significant difference in amplitude between the BAPTA treated control mEPSCs and potentiated mEPSC (control 17.9 ± 1.6 pA: BAPTA 18.2 ± 1.4 pA) while VP potentiated mEPSCs from an interleaved control recording show a typical potentiated mEPSC amplitude (VP 46.1 ± 2.1 pA). Analysis of the rise time data show no difference between the control mEPSCs and potentiated mEPSC with BAPTA (2.7 ± 0.1 ms: BAPTA 2.7 ± 0.1 ms), while the interleaved control average rise time was not significantly increased (2.8 ± 0.5 ms). Decay times when fitted with a single exponential again show little difference between the BAPTA control mEPSCs and potentiated mEPSC (13.6 ± 0.3 ms: BAPTA 14.2 ± 0.5 ms).

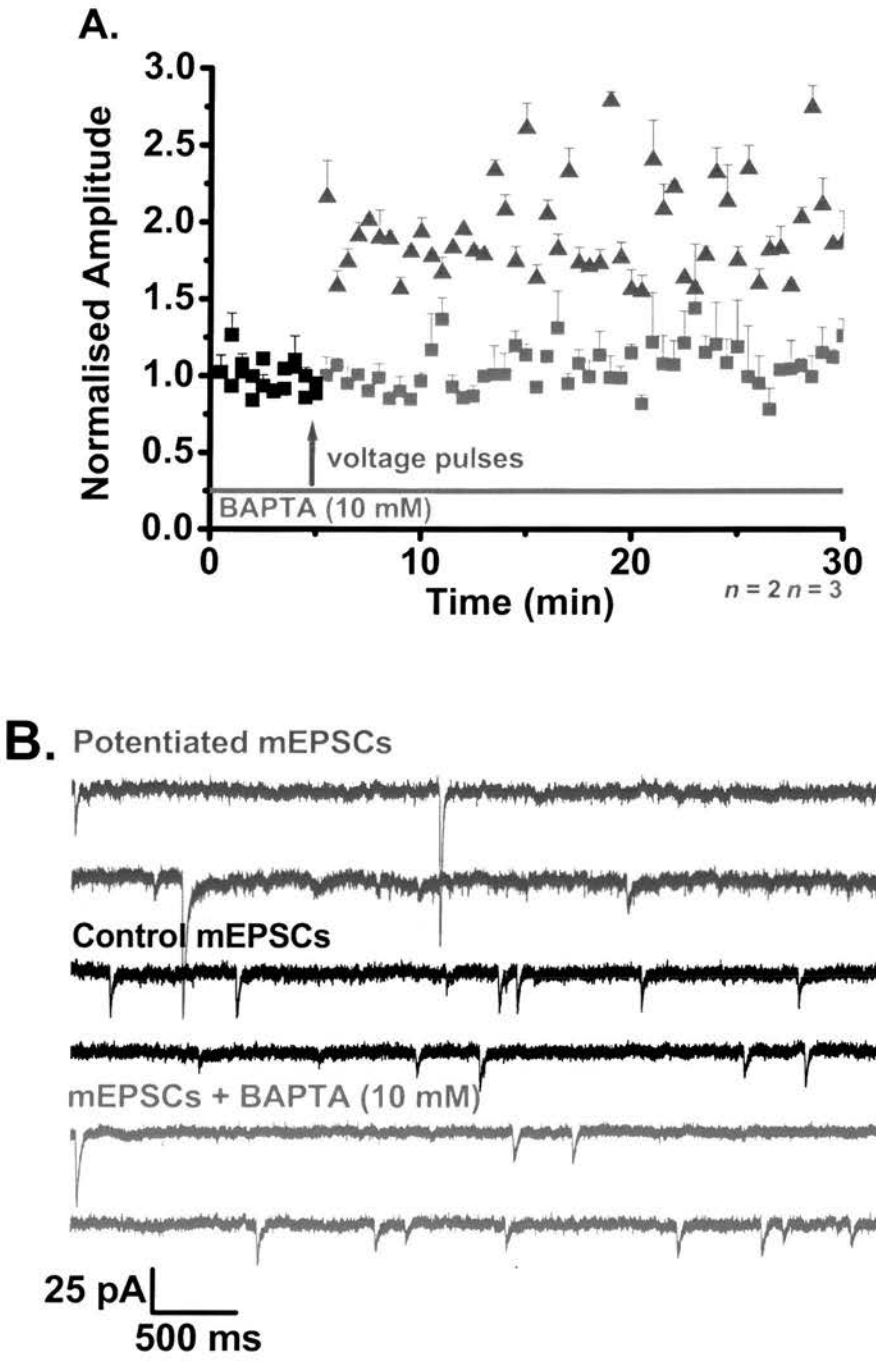

Figure 3.25: **BAPTA blocks VP potentiation of mEPSC amplitudes.** (A.) The pipette inclusion of BAPTA (10 mM) inhibited the voltage pulse potentiation of mEPSC amplitudes. (B.) Raster plot of mEPSCs from control, BAPTA and the interleaved periods.

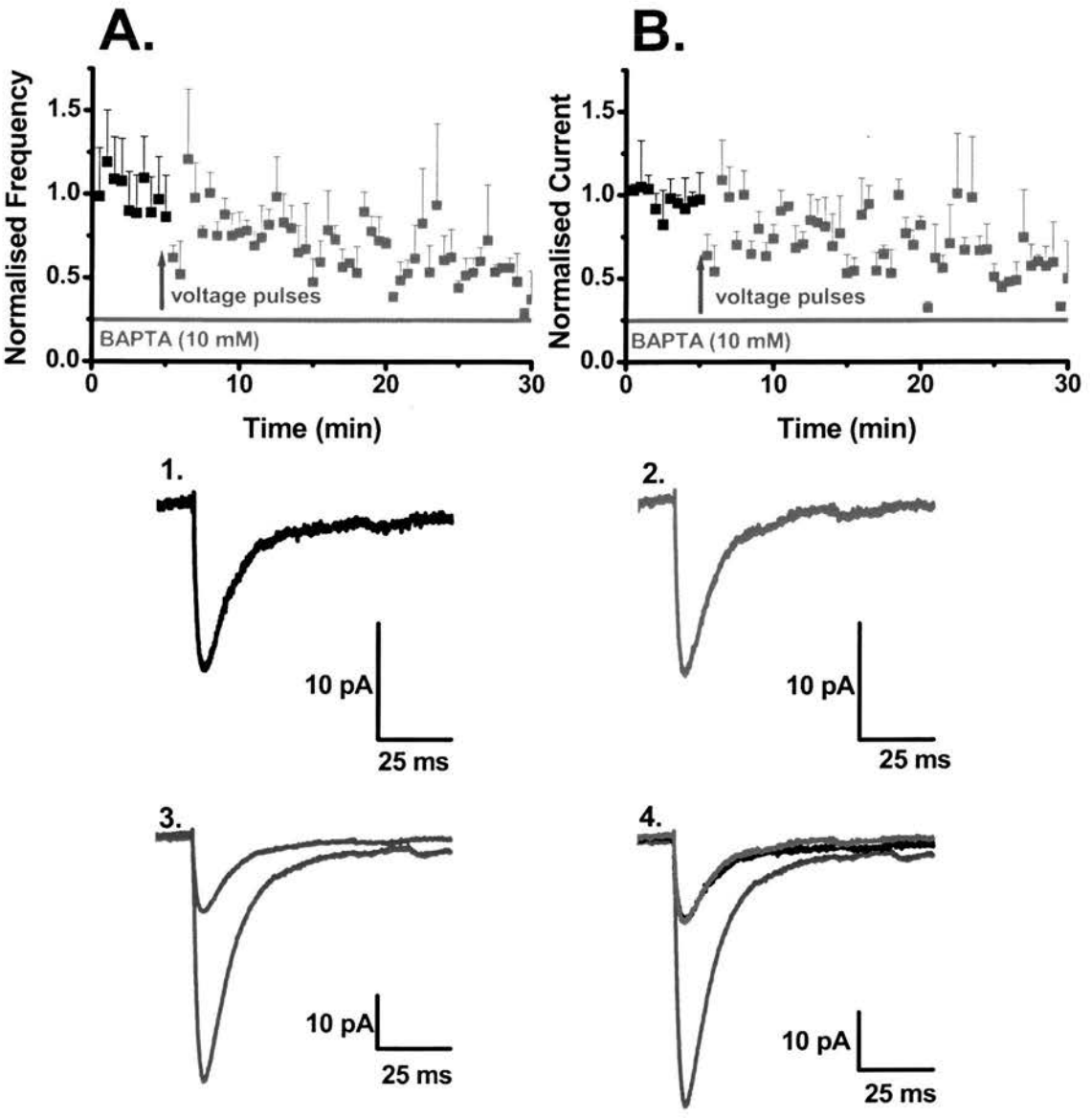

Figure 3.26 **Potentiation of mEPSC frequency and current was blocked by BAPTA.** Following the VP stimulation in the presence of the calcium ion chelator BAPTA (10 mM) there was no significant potentiation of either mEPSC frequency, (A.) or total current (B.). **mEPSC overlays for BATPA treated and potentiated mEPSCs (C.)** Analysis of 100 mEPSCs from the BAPTA treated control period (1.) VP potentiated period with BAPTA (2.). Interleaved control overlays highlight the degree of amplitude potentiation shown with the VP stimulus (3.) Control and BAPTA mEPSC show no significant difference when overlaid with little change in rise or decay times when mEPSC are scaled (4.)

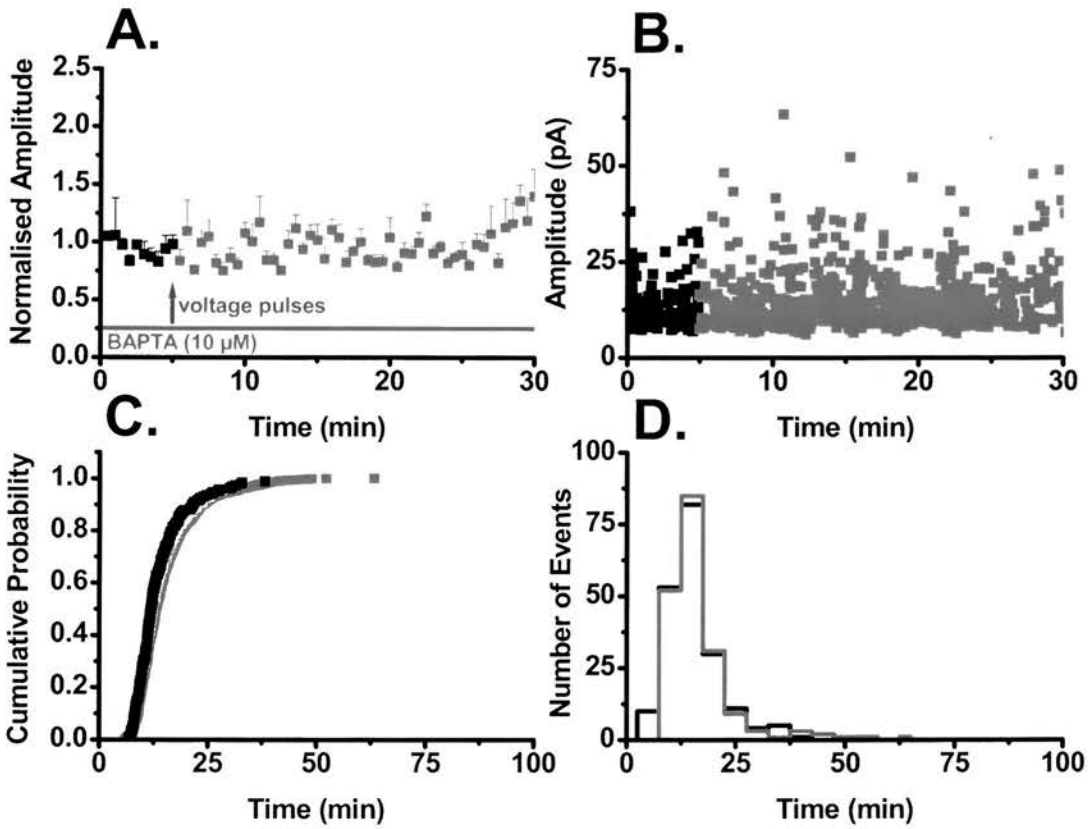

Figure 3.27: **Properties of BAPTA treated mEPSCs.** The pipette application of BAPTA blocks the VP potentiation of mEPSCs amplitudes. (B.) The scatter plot of the raw data for this single cell trace shows no significant increase in the amplitude distribution. (C.) The cumulative probability plots overlap showing no potentiation of mEPSC amplitudes after stimulation. (D.) Amplitude histogram for both the control and BAPTA treated mEPSCs display a leftward skewed distribution.

3.15: Source of the postsynaptic calcium rise

As with NMDA receptor LTP the importance of a calcium increase has been confirmed. However the mechanism through which this increase results in potentiation needs to be addressed. From previous experiments, I have demonstrated that activation of NMDA receptors are not required for this form of synaptic efficacy enhancement. From the original work by Kullmann et al (1992) and Wyllie & Nicoll (1994), the increase in postsynaptic calcium was thought to be supplied via the large conductance voltage sensitive L-type Ca^{2+} channel. To validate this hypothesis, in the rat organotypic system used here, the slices were incubated in nifedipine (10 μM). This application of nifedipine has no significant effect on the baseline amplitude of the mEPSCs when the same time periods as analyzed for VP potentiation were considered (Figure 3.28A: control 28.1 ± 1.3 pA: nifedipine 27.1 ± 1.8 pA (n = 3). mEPSC frequencies showed no significant potentiation (control 0.9 ± 0.11 Hz: nifedipine 1.0 ± 0.1 Hz. n = 3) (Figure 3.29A). Similarly, the total current output data showed that nifedipine blocked this potentiation (control 0.8 ± 0.1 Hz: nifedipine 0.9 ± 0.1 Hz. n = 3) (Figure 3.29B), but these reducing trends are similar to the general reduction shown with normalized mEPSC amplitudes through the whole time course. An amplitude scatter plot for this experiment shows no major differences in mEPSC amplitude distribution, cumulative probability plots, and amplitude histograms overlay highlighting no major differences in mEPSC amplitudes between the two experimental sections.

Typical mEPSCs from both control and nifedipine treated sections are shown in Figure 3.29C. Analysis of 100 mEPSC from both the control and nifedipine treated time periods shows average mEPSCs with similar mean amplitude (control 23.5 ± 0.4 pA: nifedipine 23.7 ± 0.5 pA). Rise time values for the control and nifedipine mEPSC are not significantly different (control 2.3 ± 0.2 ms: nifedipine 2.4 ± 0.1ms). Decay times for the control and nifedipine show little difference (control 13.0 ± 2.4 ms: nifedipine 13.3 ± 0.5 ms).

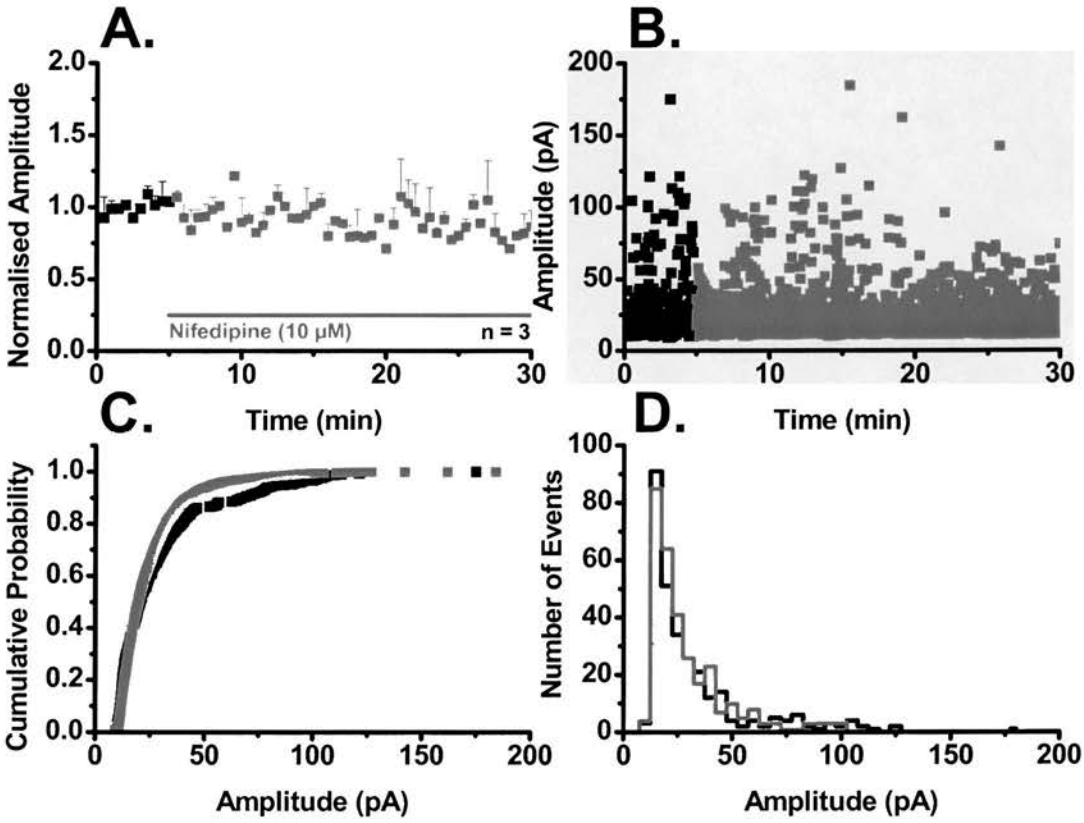

Figure 3.28: **Properties of nifedipine treated mEPSCs.** (A.) Nifedipine has no significant effect on the baseline amplitude of the mEPSC. (B.) Analysis of the scatter plot distribution shows, a small degree of amplitude variance in the first 20 minutes following application of nifedipine. (C.) The cumulative probability plot for the most part overlay and shows only a small degree of variance over the 85 % probability point. (D.) This is further substantiated with the amplitude histogram which shows a leftward skewed distribution for both groups

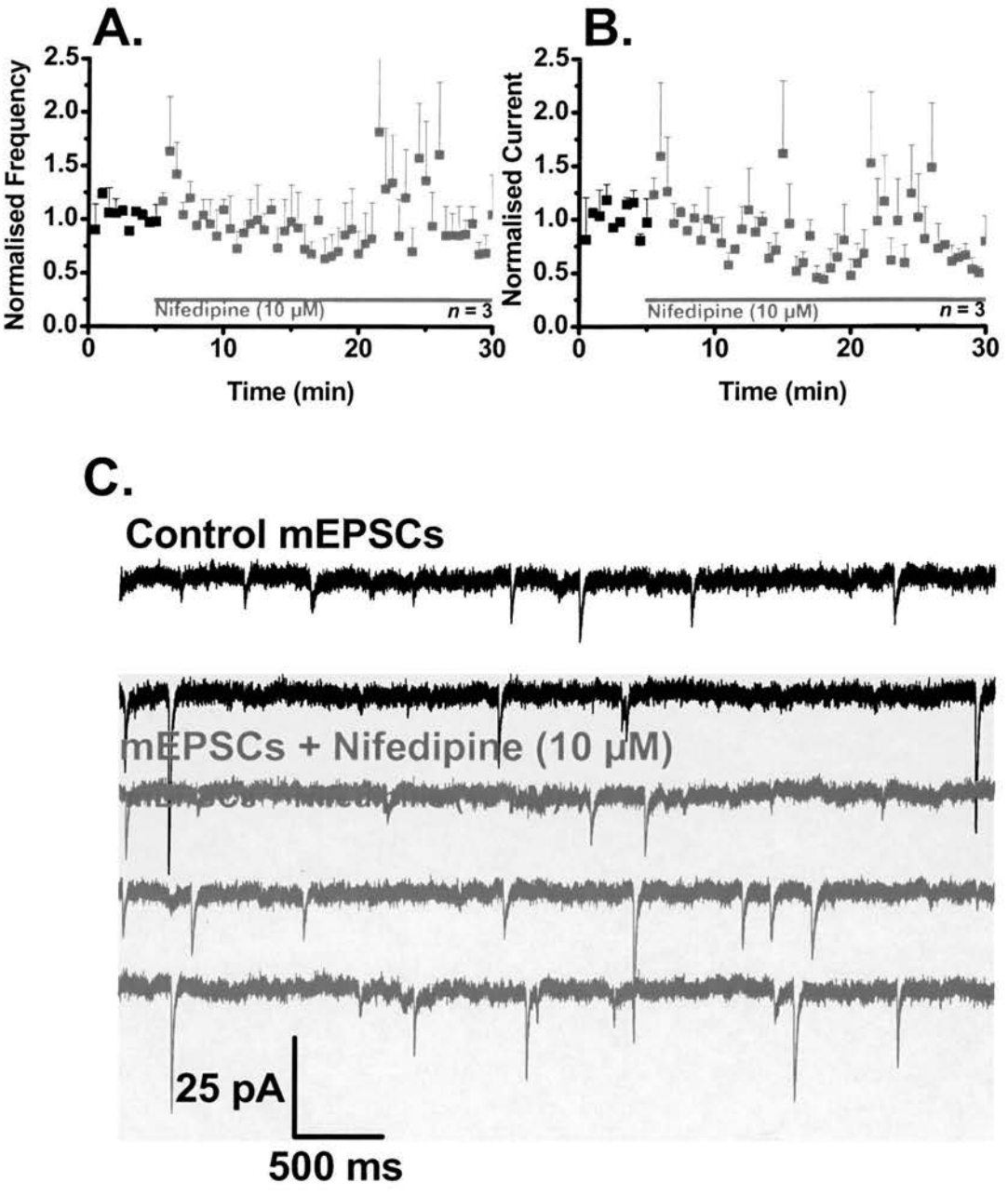

Figure 3.29: **Properties of nifedipine treated mEPSCs. (con't).** (A.) application of nifedipine induces no significant potentiation of either mEPSC frequency, (A.) or total current (B.) (C.) Raster plot showing typical mEPSC from both control and nifedipine time periods.

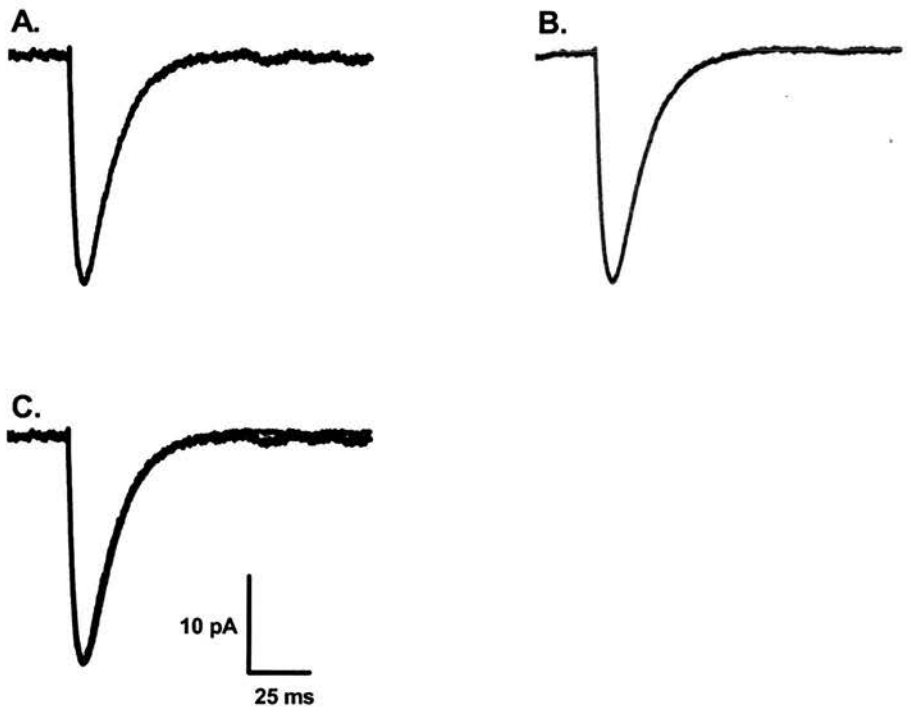

Figure 3.30: **mEPSC overlays for control and nifedipine treated mEPSCs.** Analysis of 100 mEPSCs from the control period (A.) and the nifedipine treated period (B.) show no significant change when overlaid, with little change in rise or decay times of the mEPSC

3.16: Inhibition of VP potentiation by nifedipine

Non VP stimulated mEPSCs, are resistant to the effects of nifedipine. This result taken with the results from the chelation of the intracellular calcium, leads to the idea that the increase in mEPSC amplitudes are dependent upon some intracellular calcium activated cascade which may govern AMPA receptor movement to active synapses in these cells. Control nifedipine experiments have shown that the population of receptors present in the synapses is relatively stable in both number (amplitude) and their ability to be activated (frequency). Therefore, if VP potentiation involves similar postsynaptic mechanisms known to be important for receptor trafficking in NMDA receptor LTP experiments, inhibition of the source of the postsynaptic calcium increase should block VP potentiation of mEPSC amplitudes.

The application of this L-type calcium channel inhibitor blocked the induction of voltage pulse potentiation of mEPSC amplitudes (Figure 3.31A: control 27.4 ± 3.6 pA: nifedipine 25.0 ± 1.7 pA. n = 4), while interleaved control recordings showed typical potentiation of mEPSC amplitudes.

The time course profile for potentiated mEPSC frequency when nifedipine was applied is interesting, as it does not display the typical rundown profile shown in other experiments. Here the frequency drops and remains relatively stable (Figure 3.32A: control 1.8 ± 0.6 Hz: nifedipine 1.2 ± 0.8 Hz. n = 4). This profile is also shown with mEPSC current output (Figure 3.32B: control 1.6 ± 0.6 nA: Nifedipine 1.1 ± 0.1 nA. n = 4).

Figures 3.32B & C, highlight the loss of the depolarization induced L-type voltage gated channel currents, shown with the application of the voltage-pulses.

Comparison of the kinetics of 100 mEPSCs from each point of the experiment, show similar mEPSC amplitudes values for both control and nifedipine mEPSCs are 22.1 ± 0.3 pA and 23.5 ± 0.1 pA respectively (Figure 3.34), while interleaved control mEPSC potentiated amplitude is 45.7 ± 0.1pA. Overlay plot of each mEPSC type shows similar rise time (control 1.5± 0.1ms: nifedipine 1.4 ± 0.1ms) and τ decay values (control 10.4 ± 0.1ms: nifedipine 10.8 ± 0.1ms) for control and nifedipine mEPSCs. Interleaved control data shows the typical potentiation of mEPSC amplitudes and potentiated mEPSCs have rise and decay times values of 1.6 ± 0.7 ms and 10.9 ± 0.1 ms respectively.

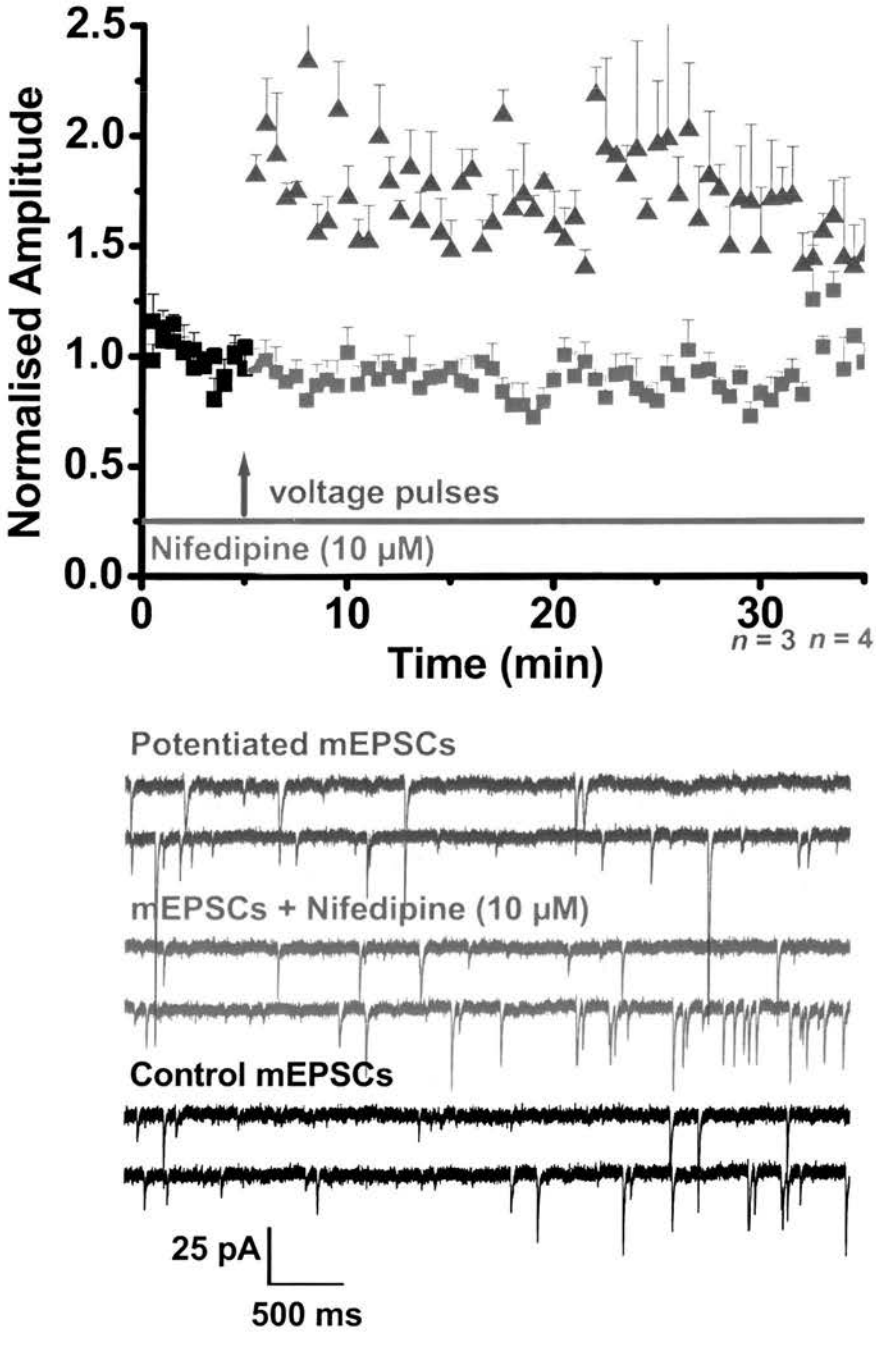

Figure 3.31: **Nifedipine blocks VP potentiation of mEPSC amplitudes.** (A.) Potentiation of mEPSC amplitudes is blocked by pipette application of nifedipine (10 µM). (B.) Raster plot of mEPSCs from control, nifedipine and the interleaved periods.

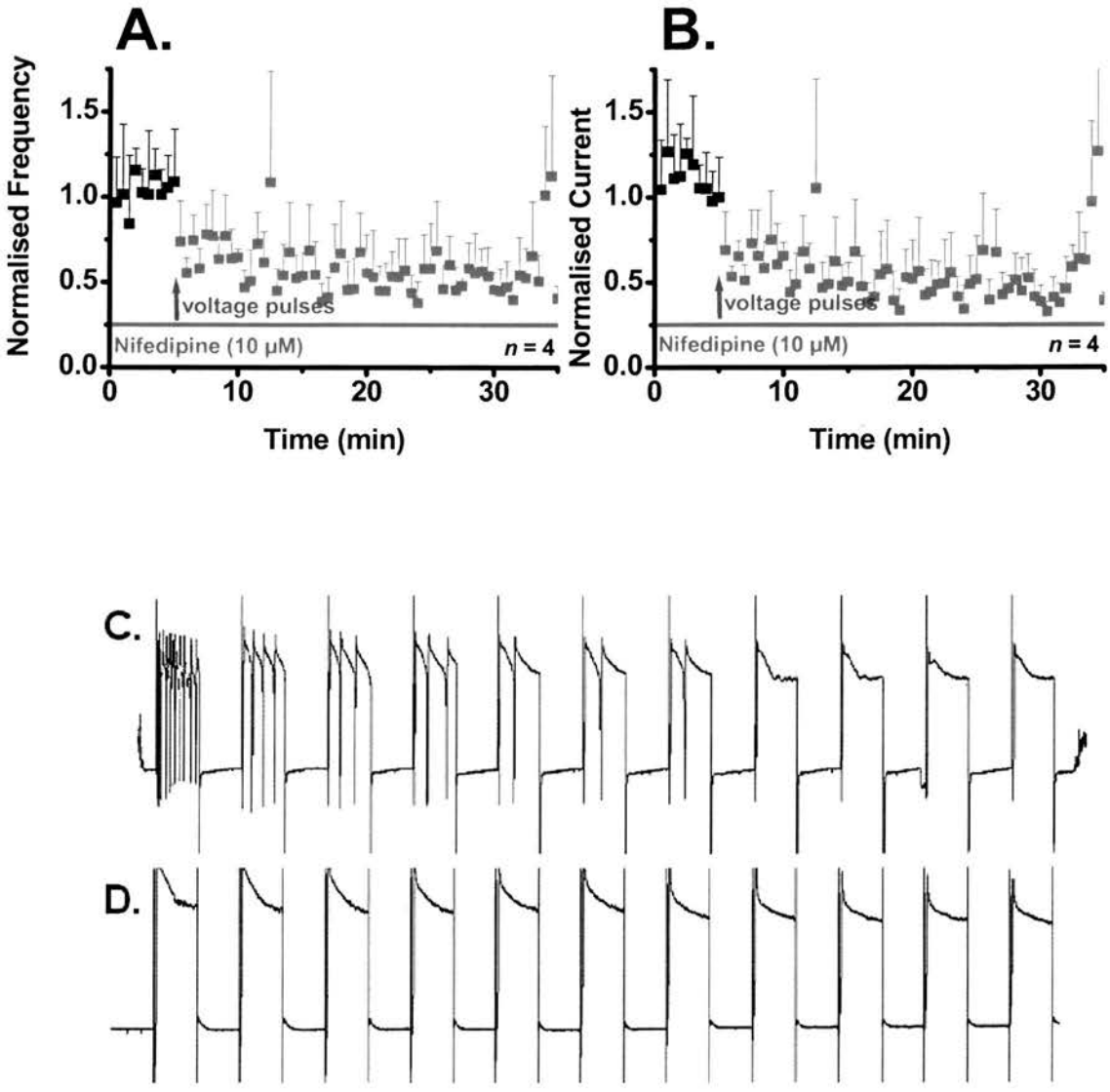

Figure 3.32: **Frequency and currents of mEPSCs treated with nifedipine.** Following the VP stimulation in the presence of the L-type Ca^{2+} channel blocker nifedipine there was no significant potentiation of either mEPSC frequency, (A.) or total current (B.). Furthermore, the characteristic inward currents shown with VP stimulation (C.) are absent when the stimulation protocol was applied in the presence of nifedipine.

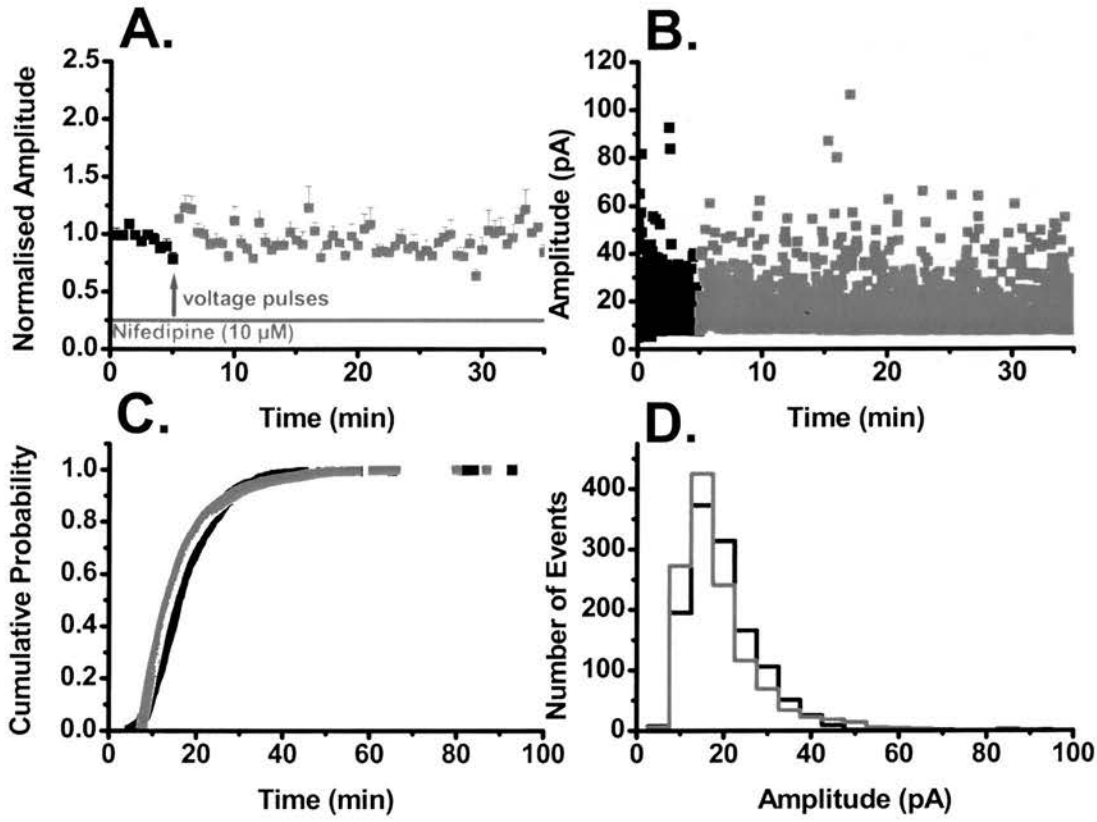

Figure 3.33 **Properties of nifedipine treated mEPSCs (con't).** A single cell amplitude time course shows block of the potentiation of the mEPSC amplitudes by nifedipine. (B.) The scatter plot of the raw data for this single cell trace shows little variance in the range of amplitudes following VP stimulation (C.) The cumulative probability plots overlap showing little change in amplitude probability. (D.) Amplitude histogram for both control and nifedipine treated VP stimulated mEPSC show a leftward skewed distribution indicating small amplitude events.

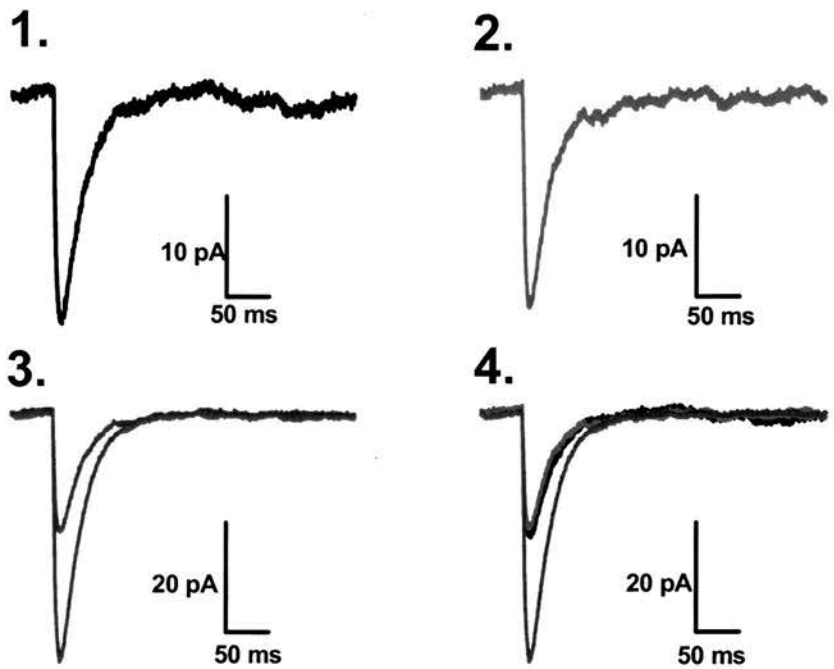

Figure 3.34: **mEPSC overlays for nifedipine treated and potentiated mEPSCs.** Analysis of 100 mEPSCs from the nifedipine treated control period (1.) VP potentiated period with nifedipine (2.) show no significant differences when these events are overlaid (4.). Interleaved control overlays highlight the degree of amplitude potentiation shown with the VP stimulus (3.)

3.17: Intracellular sources of calcium

The calcium concentration in the pyramidal cell is typically 100 nM (Syntichati & Tavernarakis., 2003). However, the actual increase in concentration of calcium ions required to initiate LTP like plasticity in CA1 pyramidal cells is still unknown. From the previous experiment, I have determined that the increase in postsynaptic calcium supplied via the L-type Ca^{2+} channel is required to induce the potentiation of mEPSC amplitudes shown with VP potentiation, but is it sufficient to induce the potentiation.

To investigate this phenomenon further the slices were incubated again for approximately 10 minutes prior to control recordings with both ryanodine (10 μM) and thapsigargin (10μM). These drugs act by inhibiting the internal calcium store. Ryanodine inhibits the intracellular ryanodine receptor and control the calcium-activated-calcium-release current (CACR current) and thapsigargin inhibits Ca^{2+} dependent responses via the sarco- and endoplasmic reticulum (SERCA) type ATPases (Davidson and Varhol, 1995) which controls the specific release and uptake of the calcium. With combined application this internal calcium current in inhibited.

The application of thapsigargin and ryanodine block the induction of voltage pulse potentiation of mEPSC amplitude (Figure 3.35: control 21.2 ± 1.2 pA: thap/ryr 21.4 ± 1.5 pA. $n = 6$). mEPSC frequencies show a non significant increase of 11.1 percent (control 0.6 ± 0.1 Hz: thap/ryr 0.72 ± 0.7 ± 0.2 Hz. $n = 6$), this increase is transient and is followed by a typical reduction in mEPSC frequencies to around 0.5 Hz . The current output for these cells show a transient non-significant potentiation of 8.5 % (control 0.8 ± 0.1 nA: thap/ryr 0.9 ± 0.2 nA. $n = 6$). Interleaved control data show a significant potentiation of mEPSC amplitude (control 19.3 ± 2.5 pA: VP 34.5 ± 1.5 pA. $n = 3$). mEPSC frequencies showed a non significant transient potentiation (control 1.3 ± 0.4 Hz: VP 1.8 ± 0.8 Hz. $n = 3$). Similarly, after VP stimulation a transient non significant potentiation of the total current produced by the cell was shown (control 0.7 ± 0.8 nA: VP 1.4 ± 0.8 nA).

Analysis of 100 mEPSCs from each time period show no significant difference between mean the amplitude values for thapsigargin and ryanodine treated mEPSCs, and the VP potentiated thapsigargin and ryanodine treated mEPSCs (control 20.59 ±0.31 pA: thap/ryr 19.35 ± 0.4 pA). The rise time correlates for these mEPSC again show no significant differences (control 1.98 ± 0.33 ms: thap/ryr 2.01 ± 0.42 ms). Decay time values again fitted to a single exponential, show no significant difference between thapsigargin and ryanodine treated mEPSCs, and the VP stimulated thapsigargin and ryanodine treated mEPSCs (control 14.9 ± 3.2 ms: thap/ryr 12.6 ± 2.1 ms). The interleaved control data give a

mean potentiated amplitude of 45.6 ± 0.6 pA with a rise and decay time constant values of 2.5 ± 0.3 ms and 26.4 ± 4.6 ms respectively.

These experiments suggest that the calcium supplied from the external source via the calcium channel, is insufficient to induce the VP potentiation. There is a dependency upon calcium from the internal store to facilitate the VP potentiation of mEPSC amplitudes. In conclusion, these three experiments have demonstrated that calcium is the major mediator as suggested by Malenka & Bear (2004), this is a pathway convergence with traditional NMDA receptor dependent LTP. However in this system, the trigger for all potentiation is calcium influx via the L-type, but this is not sufficient to induce VP potentiation, the calcium influx must in turn activate the internal calcium currents (CRAC), to produce the sustainable short term potentiation shown here.

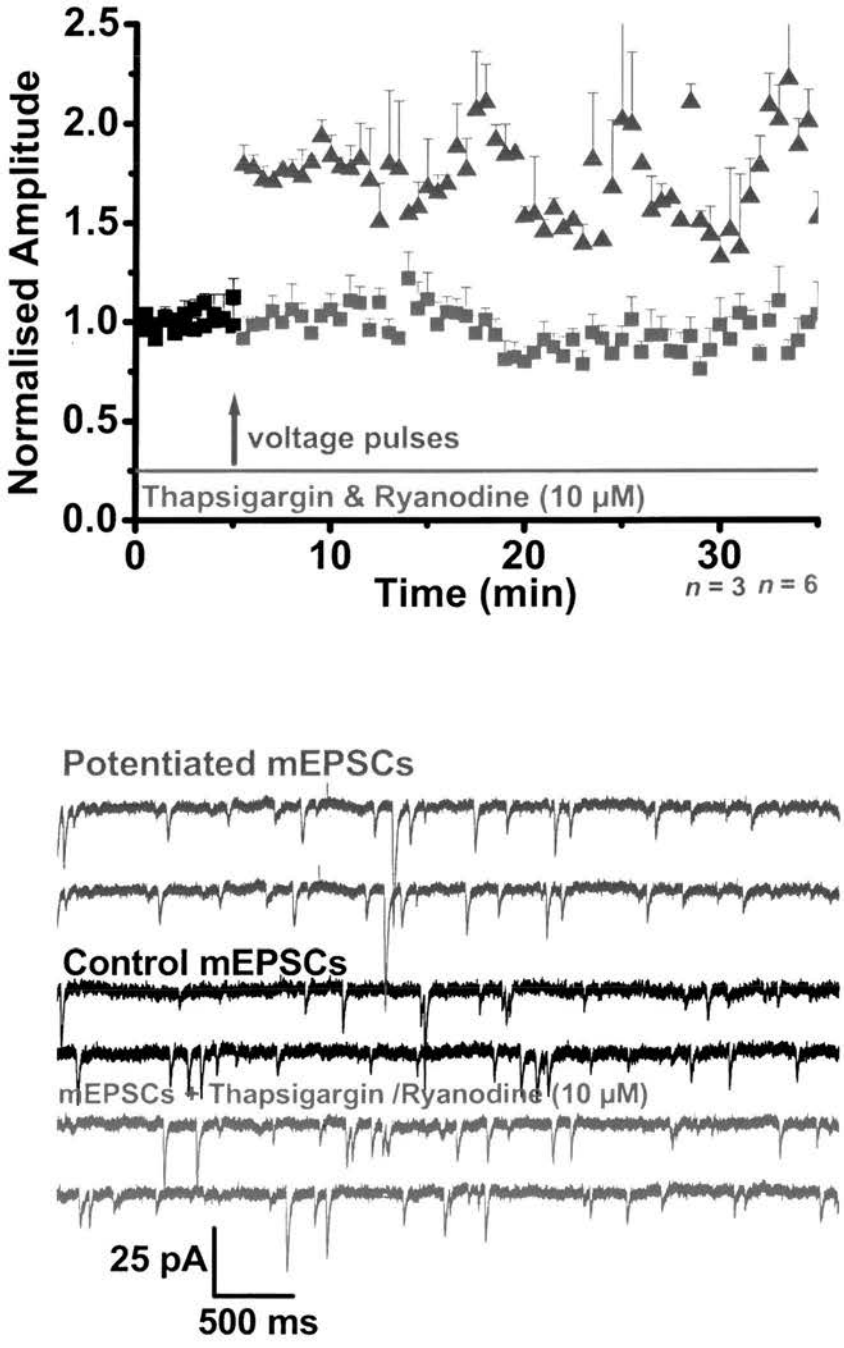

Figure 3.35: **Thapsigargin and ryanodine block the VP potentiation of mEPSC amplitudes.** (A.) Potentiation of mEPSC amplitudes is blocked by inhibiting the internal calcium stores with the application of thapsigargin and ryanodine (10 µM), while interleaved control recordings showed typical potentiation of mEPSC amplitudes (B.) Raster plot showing typical mEPSCs from each time period.

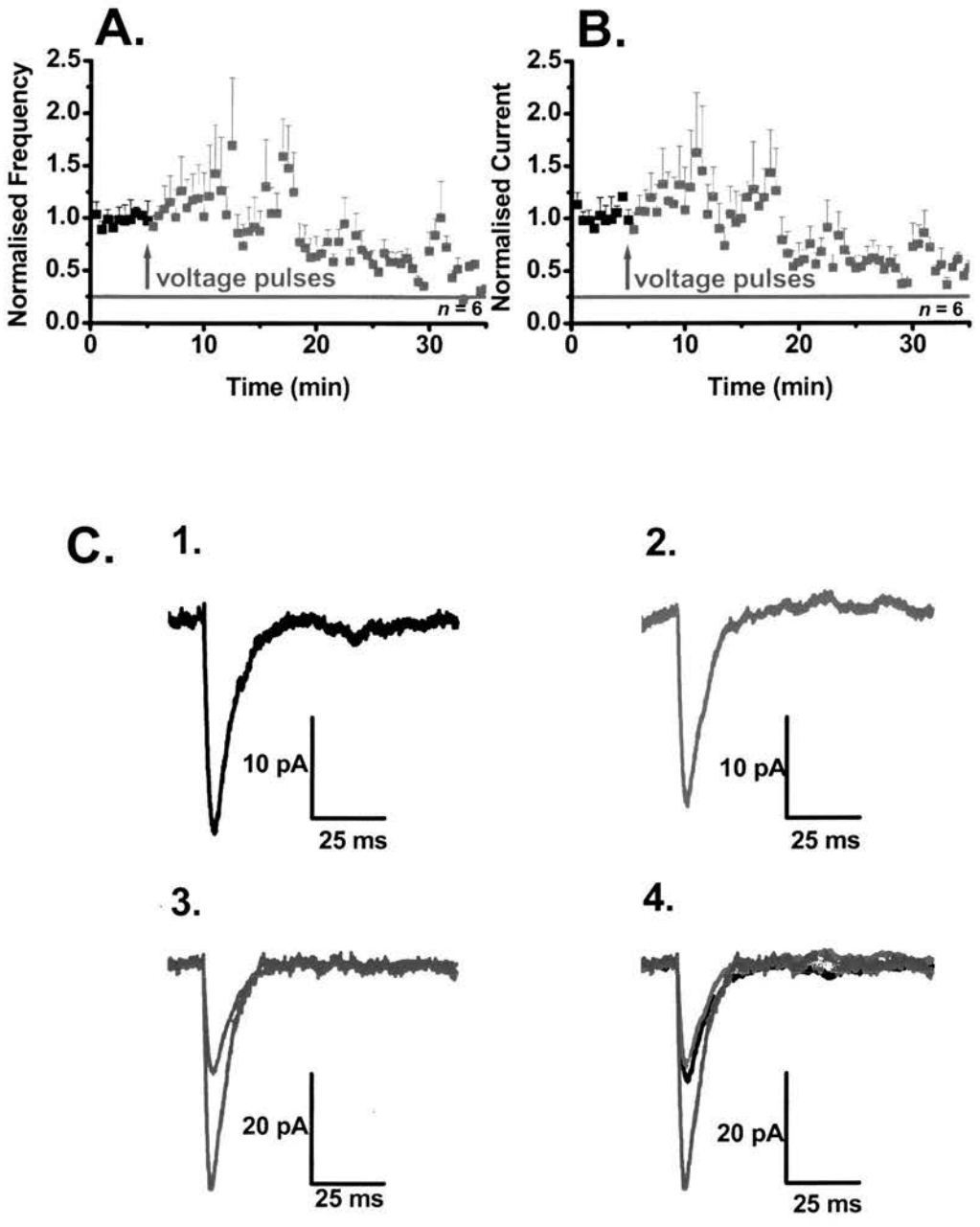

Figure 3.36: **Properties of thapsigargin and ryanodine treated mEPSCs.** Following the VP stimulation in the presence of the internal calcium store blockers there was no significant potentiation of either mEPSC frequency, (A.) or total current (B.). (C.). **Overlays thapsigargin and ryanodine treated mEPSCs.** Analysis of 100 mEPSCs from the control period (1.) and the VP stimulated thapsigargin and ryanodine treated period (2.) show no significant change in mEPSC amplitude when events are overlaid (4.) mEPSCs from the interleaved control recording show typical potentiation of mEPSC amplitudes(3.).

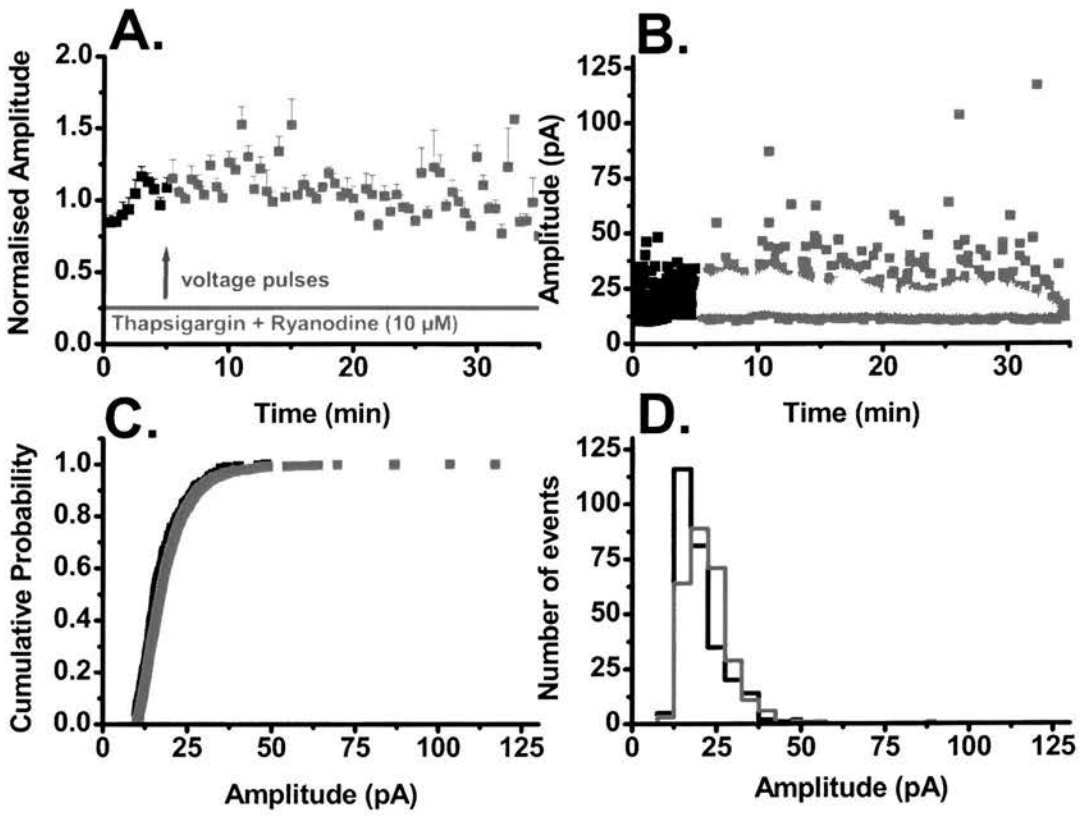

Figure 3.37: **Properties of thapsigargin and ryanodine treated mEPSCs (con't).** A single cell amplitude time course shows block of the potentiation of the mEPSC amplitudes by thapsigargin and ryanodine. (B.) The scatter plot of the raw data for this single cell trace shows little variance in the range of amplitudes following VP stimulation (C.) The cumulative probability plots overlap showing little change in amplitude probability. (D.) Amplitude histogram for both control and nifedipine treated VP stimulated mEPSC show a leftward skewed distribution indicating small amplitude events

3.18: Control mEPSC recordings

The initial whole-cell recording experiments were conducted to characterise the viability and responsiveness of the organotypic cell culture system. From the whole-cell patch-clamped pyramidal cell I determined the characteristic properties of synaptic current in these cells. The changes in cell physiology found with the application of TTX and PTX, are well characterised in acute slice systems and with this information, I could further identify identical changes in cellular physiology with the application of these toxins to cells within the organotypic slice culture.

In the presence of TTX and PTX the conditions permitted the isolation and recording of spontaneous mEPSCs. In the first instance, the experimental premise investigated was that whole-cell patching did not affect the viability of the cell. Whole-cell patching causes the cell contents to be dialysed with the 'internal' solution contained within the patch-pipette. If this was to reduce the responsiveness of the cell to the spontaneously released vesicles of glutamate then one might anticipate seeing a reduction in the frequency of events detected. Indeed, in these experiments mEPSC frequency does reduce across the time course from 1.6 ± 0.3 Hz to 1.2 ± 0.3 Hz, but still at this end point there are still more than 1 mEPSC every second. As one of the hypotheses being tested is the concept that alteration in postsynaptic responsiveness is a result of the postsynaptic insertion of AMPA receptors this frequency was sufficient to generate a suitable number of mEPSCs and to observe subsequently changes in mEPSC amplitudes – the quintessential marker of postsynaptic function. In terms of postsynaptic response, this experiment displays stable normalised amplitudes across the time period of the experiment. In terms of AMPA receptor mechanics at the synaptic level, a stable mean amplitude relates to two possible states. The first is a balanced cycling of receptors, those being inserted are balance by loss of receptors, possibly at the single synapse or perhaps regulated throughout the entire cell, an idea confirmed by Ehlers (Ehlers, 2000), who also proposed dual fast and slow mechanisms for the insertion of AMPA receptors. One further point about AMPA receptor trafficking and number of receptors at the synapse shows great variability. Nusser et al (1998), has shown through quantitative immunogold labelling that the number of receptors at CA3/CA1 synapses can vary between 3 and 140 AMPA receptors per synapse. Here the idea is that loss of AMPA receptor and silencing at one specific synaptic site, may preferentially strengthen other synapses which have a higher function weight than the one being silenced, thereby maintain the total synaptic signal, in fact the basis for a cell wide integrated system. An alternative explanation is

that there is no baseline receptor cycling and the receptors are stable in the membrane, and just activated.

The literature on mEPSC function and baseline activity has shown baseline turnover of AMPA receptors and that this is a highly dynamic but regulated system. Therefore the underlying factors must be that these mEPSCs result from the stable cycling of comparable numbers of receptors into and out of synapses, so timescale of this turnover is the important factor, and unfortunately there is no way to address this in the current system (see further work for the address to this problem). The third consideration for this is the reduction in mEPSC frequency (and excluding a presynaptic locus), occurs when one considers the receptor recycling process and the possibility of activity dependent synaptic silencing. Thus this would give a postsynaptic locus for this frequency change, as if the total number of synapses being activated were to reduce due to silencing then the frequency of mEPSCs would reduces as we are effectively generating 'deaf' (i.e. a postsynaptic silent synapse) and whispering (i.e. presynaptic release occurs but there is no postsynaptic response) synapses. Therefore, this failure of detection would represent a post synaptic locus for a decrease in mEPSC frequency.

3.19: Comparison of mEPSCs recorded in this study with other studies of mEPSCs

Moving away from the dynamics of AMPA receptor cycling, the properties of the mEPSCs recorded here are no different to those recorded from rat CA1 pyramidal cell from other groups, matching not only in the amplitudes of the events, but the rise and decay time constant for these events as well. The only minor difference is that the mEPSC frequency (1.57 ± 0.23 Hz) from this present study is comparable but slightly higher than other groups 1.34 ± 0.24 Hz (Tyler and Pozzo-Miller, 2001) and 1.44 ± 0.33 Hz (McKinney et al., 1999). Event frequencies from all control recordings across the three years of experimenting have shown consistent control frequencies and the range of control mEPSC frequencies is similar throughout every experiment.

The original study of voltage-pulse potentiation of mEPSCs (Wyllie et al., 1994) shows the biggest difference in mEPSC amplitudes, although kinetically these events are very similar. The mEPSC mean amplitude reported in the study of Wyllie et al (1994) was 7 pA, while the mean control mEPSC in this study was nearer to 21 pA a 3 fold difference. Such a difference could results from differences in species (rat vs guinea-pig) age of animal or different degrees of innervation. For example, guinea-pigs are known to have greater levels of corticosteroids in brain tissue, when compared to rats and such differences may contribute to differences in mean mEPSC amplitudes. Nonetheless my studies indicated that prior to the application of the

voltage-pulse stimulation protocol there is a low probability of observing events with large amplitudes.

3.20: Voltage-pulse potentiation

The mechanistic theory behind voltage-pulse potentiation revolves around a global potentiation of many synapses in the postsynaptic cell. To discuss the functionality of this stimulus one must consider the conventional NMDA receptor dependent LTP induction protocol. In such a setup responses are evoked by a stimulating electrode placed within the Shaffer collateral commissural fibres, which deliver a preset stimulus pattern, with EPSCs being generated following every stimulus (assuming that the stimulus being used is sufficiently large). This leads to two separate but increasingly interlinking problems which are firstly a failure rate change at individual release sites, meaning that no EPSCs are generated by the presynaptic stimulus, for example as a result of the action potential not being conducted. Secondly, due to a postsynaptic alternation proposed by (Xiao et al., 2004) where failure rate changes are linked to a physiological silencing of postsynaptic weakly weighted synapses in preference for the more strongly weighted synapses, with the silencing effector being the actual stimulus used to generate the EPSC. This can be likened to synaptic LTD, where repetitive low frequency stimulation retards active synapses. The result of these two factors are an increase in the failure rate, a well known effect of field LTP recording and a constantly large potentiated EPSC, due to the loss of the weak signal from the weakly innervated synapses.

In my experimental set up using voltage clamped whole-cell patched CA1 pyramidal cell, cable properties, failure rate, or functional silencing are not problems as all mEPSCs are the result of spontaneously released vesicles of glutamate. Cable properties conducting an action potential to facilitate release of presynaptic vesicles do not apply as this is blocked by application of TTX. Failure rate changes similarly do not apply as again there is only a single stimulus paradigm applied, all mEPSCs are spontaneous and do not require the patterned stimulus required to evoke EPSCs. Similarly this single stimulating paradigm negates the functional silencing problems associated with EPSC recording. In all this makes for a superior experimental setup to look at the short term effects of receptor trafficking following stimulation.

The application of depolarising voltage pulses is thought to bring about a global synaptic potentiation, by activating voltage-gated calcium channels resulting in the potentiation of many more synaptic sites than could be activated by the presynaptic stimulus applied with LTP. The result of the application of depolarising voltage pulses stimulus is interesting in the first point as this study compared to the earlier Wyllie and Nicoll studies, shows that there is sustained potentiation of mEPSC amplitudes and a small transient potentiation of mEPSC

frequency. Overall the effect is to cause a very large, but transient potentiation of the total current produced following voltage-pulse stimulation. With the proposed mechanism for this amplitude potentiation being brought about through a synergistic combination of effects including a change in the conductance of the receptors already present at the synapse, and through the insertion of new AMPA receptors into active synaptic membranes

However, there are some significant differences in the nature of the amplitude potentiation, as previous studies indicated voltage-pulse induced potentiation is transient in nature, but can be converted to a sustainable form in the presence of phosphatase inhibitors (Wyllie and Nicoll, 1994). In my studies voltage-pulse-induced potentiation in organotypic slices is sustained and a doubling of the mean mEPSC amplitude has been recorded for up to an hour.

Differences also exist in the degree of stimulus, in that their stimulus consisted of a three second depolarising step, with a two second latency, which lasted for a total of 2 minutes, resulting in the application of 24 depolarising pulses. This stimulus when applied to the organotypic slices was obviously too strong as I observed concentric rings of degraded tissue originating from the site of the recording electrode, with an accompanying loss of the recording. Reducing the total stimulating period to 1 minute and increasing the latency by one second while keeping the duration constant, resulted in a stimulus suitable to bring about the potentiation of mEPSC amplitudes.

This form of organotypic voltage-pulse potentiation is very interesting as all the analysis carried out indicates the simple conclusion that following the stimulus there is a sustainable potentiation of mEPSC amplitudes and that this potentiation is the result of a possible increase in the number of AMPA receptors at these synapses. Thus following the voltage pulses there is a greater probability of large amplitude mEPSCs being recorded than there was prior to the stimulus. Furthermore, the largest potentiated mEPSC amplitude far exceeds the largest amplitude event from the control period. The second feature I observed was that the increased mEPSC amplitudes appear to be stable, allowing this potentiation protocol to permit the identification of factors responsible for the possible insertion of new AMPA receptors into synapses.

3.21: mEPSC frequency changes and the DSI current.

Further observations include a phenomenon which results in the transient suppression of mEPSC frequency following the voltage-pulse stimulus, possibly mediated by retrograde signalling (Fitzsimonds and Poo, 1998) or via a depolarisation-induced suppression of inhibition (DSI) (Wilson et al., 2001)[see figure 3.9A]. This is a retrograde signalling pathway which

regulates the vesicular release probability; the DSI pathway is initiated by calcium influx through postsynaptic voltage dependent calcium channels. This increase in postsynaptic calcium regulates the release of endocannabinoids possibly anandamide or 2 arachidonylgycerol (Piomelli et al., 1998; Ameri, 1999). These diffuse retrogradely to activate presynaptic G protein coupled receptors (presumably CB1) which in turn negatively modulate the N type ($Ca_V2.2$) voltage-dependent calcium channels (VDCC) found at the presynaptic terminal and suppress the release of vesicles of neurotransmitter (Hajos et al., 2000; Hoffman and Lupica, 2000). To date investigation of the DSI current has focused on its induction at GABAergic synapses, Wilson et al 2001, but endocannabinoids have been found to regulate glutamatergic synaptic transmission during LTP (Misner and Sullivan, 1999; Sullivan, 2000; Robbe et al., 2001). This presynaptic regulation introduces another interesting possibility by which mEPSC frequency potentiation following the DSI is mediated. So far all frequency change is thought to be mediated via presynaptic vesicular release. But in this system the reversal of the DSI suppression (from depressed to potentiated level) by a purely presynaptic mechanism would require a large increase in the release of synaptic vesicles, effectively an extra 267 vesicles on top of the 1.6 vesicles per second (control frequency 1.6 ± 0.1 Hz) for the period of the frequency potentiation. I feel that the vesicular release probability in this system is too low due to the inhibition by TTX, to be able to facilitate this change; therefore a change in the postsynaptic detection rate is more probable and indicates the activation of previously silent synapses. Furthermore activation of silent synapses has been suggested as a mechanism of postsynaptic expression for LTP in CA1 pyramidal cells.

This idea of a postsynaptic expression mechanism is further supported by the data. If an increase in the number of vesicles being released at synapses was to occur then one would expect a significant change in the rise time of the mEPSCs, and secondly if two vesicles were released from the synapse one would expect a significant increase in the number of double mEPSCs (two events overlapping), both of which do not occur. If this increase in frequency was to occur by a presynaptic mechanism then both vesicles must be released at exactly the same time to have equal diffusion and activation characteristics as not to cause a double. Again this is unlikely; it is far more likely that two vesicles would be released with a fractional delay between release, and this delay underlies the shudder in the rise time or the increase in the number of doubles. mEPSC doubles are very rare events, even in the highest frequency recordings, so the possibility of a presynaptic locus facilitating the frequency change is even more remote.

Nicoll and Malenka, (1999) investigated presynaptic expression mechanisms for LTP, using a paired pulse facilitation (PPF) recording paradigm, which is generally agreed to be a

method of studying any change in presynaptic release probability. In these experiments application of 4-AP saturated the vesicular release probability. With this maximised release probability no change in the PPF ratio occurred when they increase the number of activated synapses by increasing the stimulus strength (Kauer et al., 1988; Nicoll and Malenka, 1995). This finding indicates that LTP cannot be mediate by a simple change in presynaptic function, but requires a post synaptic mechanism for expression.

3.22: Maximising potentiation

Another interesting observation from the voltage-pulse study concerns limits to the degree of potentiation achievable as (Choquet and Triller, 2003) proposed a limit for the number of AMPA receptors found in a normally active synapse to be between 1 and 50 receptors. This was later found to be greatly underestimated as (Nusser et al., 1998) using quantitative immunogold labelling put the count between 3 and 140 receptors. It is thought that space at the spine head limits the number of receptors which could possibly be inserted into the synapse. To a degree I feel that this is true as there are space limitation due to the volume of the spine head, but in comparison between the volume of an AMPA receptor and the volume of the synapse it would be anticipated that the synapse volume must outweigh by many fold the number of AMPA receptors which can be inserted. This might suggest that a large number of receptors can be inserted and overload, in terms of space, is unlikely to be achieved. Clearly in such a complex system this insertion has to have limiting functional regulation. Choquet's premise about limitation would indicate that the number of AMPA receptors contributing to the amplitude of the mean mEPSCs would regulate the total degree of potentiation achievable by that cell. An example would be that cells with small mean amplitudes would be able to generate a large degree of potentiation simple due to the fact that they have more space at the synapse, to incorporate more AMPA receptors. This is further flawed by the fact that the volume of pyramidal spines have been shown to increase with the activation of AMPA receptors, but shrink with the application of NMDA (McKinney et al., 1999; Luthi et al., 2001). However, analysis of the mean amplitude (reflective of number of AMPA receptors at the synapse) plotted against the degree of potentiation I found no correlation. Thus, it would appear that mean amplitude does not govern the degree of potentiation achievable.

This theory about limits to the degree of potentiation was also checked against the presynaptic locus for potentiation, again no correlate was found between the control mEPSCs frequency and the degree of potentiation, and the same is also true when mean and frequency are compared directly.

One interesting characterising experiment which was not done due to the experimental difficulty is the comparison with late phase NMDA receptor-dependent LTP. In these experiments field recordings are made and an applied stimulus recorded, this set up enables the study of the longer term potentiation, due to there being no experimental washout of the cell, because in field recording configuration the CA1 pyramidal cells are not patched. A comparison of late phase LTP potentiation with voltage-pulse potentiation would be interesting as it would provide evidence for the function of the NMDA receptor in potentiation. But, impracticable using our experimental setup, due to as the requirements for the stimulus (whole-cell patched CA1 pyramidal cell to deliver global postsynaptic potentiation) preclude the ability of it to work. When the voltage-pulse stimulus is applied presynaptically as in the traditional LTP set up, too few synapses are stimulated and no change in mEPSC signal can be detected.

3.23: Characterisation of voltage-pulse potentiation of mEPSC amplitudes

The initial characterisation experiments with the prototypical AMPA receptor antagonist CNQX did not throw up any unexpected results as mEPSCs have long been known to be mediated by AMPA receptors (Alford et al., 1993). Following the voltage-pulse stimulus all potentiated mEPSCs were blocked by the application of CNQX thereby reinforcing the belief that voltage-pulse potentiation is mediated by the AMPA receptor.

A more significant result is gained from the blockade of the NMDA receptor with APV. As the two central dogmas surrounding potentiation of a LTP nature in the CA1 pyramidal cells has been, firstly a requirement for an increase in postsynaptic calcium and the second that this calcium increase and the mechanisms of signal potentiation are as a result of the activation of NMDA receptors (Matias et al., 2003).

The experimental premise which I'm trying to introduce is that activation of the NMDA receptor may not be the critical component for the development of synaptic potentiation rather that it is the increase in postsynaptic calcium which is the critical step and the source is not the fundamentally important point. In the experiments shown previously, after determining no significant effect of APV application on the baseline amplitudes of the mEPSCs and a functional back check of the antagonist potency in this system, application of functional APV did not inhibit the induction of voltage-pulse potentiation. This finding, although never before shown with voltage-pulse potentiation in the rat organotypic slice, has been shown in the guinea-pig slices (Wyllie et al. 1994).

Therefore characterisation of the postsynaptic calcium component within mEPSC amplitude potentiation was the next important step in this line of investigation; inclusion of the calcium chelator (BAPTA 10 mM). Application via the pipette solution restricted its application to the

postsynaptic cell only ruling out a significant presynaptic component. Inclusion of this chelator blocked the potentiation of mEPSC amplitudes, while interleaved control recording, interspersed between each drug application to ensure that potentiation of mEPSC amplitude could be achieved on each experimental day showed typical potentiation of mEPSC amplitudes. This finding confirms the first dogma of LTP potentiation, the requirement for postsynaptic calcium increases.

The mechanisms by which the postsynaptic calcium concentration increase comes about was investigated by identifying two effectors of changes in intracellular calcium levels – voltage-dependent Ca^{2+} channels and release from an internal source of calcium. Calcium from an external source must have a mechanism through which transport to the internal cytosol is achieved. I used a depolarising voltage pulse with a voltage step of sufficient range to bring about the activation of the postsynaptic L-type voltage gated calcium channel, and that this channel has been identified as having a role in the induction of various forms of LTP (Morgan and Teyler, 1999; Yasuda et al., 2003; Woodside et al., 2004).

L-type Ca^{2+} channels ($Ca_V1._{1-4}$) have been found in all types of excitable cells, four main subtypes exist and are divided into both high ($Ca_V1.1$ & $Ca_V1.2$) and low ($Ca_V1.3$ & $Ca_V1.4$) thresholds for activation. With different activation profiles being fast activating for the low threshold and slow activating for the high threshold, but all L-type Ca^{2+} channels have a large single channel conductances (Lipscombe et al., 2004). Location of the subtypes varies $Ca_V1.1$ are primarily found in skeletal muscle mediating muscle excitation–contraction coupling. $Ca_V1.2$ and $Ca_V1.3$ are found in neuronal cell bodies and dendrites and are utilised for the integration of signal transduction, and $Ca_V1.4$ are located primarily within the retina.

Other calcium channels types are also located in the presynaptic terminal, these channels act to facilitate calcium dependent vesicle release, these types of calcium channel include the P-Q type ($Ca_V2.1$), N type ($Ca_V2.2$), R type ($Ca_V2.3$) and the T type ($Ca_V3.1$). It is a mistake to assume that these receptor are only located presynaptically. They are also found distributed across the cell bodies and dendrites of neurones; the only spatial restriction applies to the L-type channels as these are not found at the presynaptic terminal.

The unique spatial features and kinetic properties of the L-type channel make it an excellent target through which the effects of voltage-pulse potentiation may be mediated. Therefore I used nifedipine, an L-type calcium channel antagonist, to block the rise in intracellular calcium following the application of voltage-pulses. Application of nifedipine blocked voltage-pulse potentiation of mEPSC amplitudes, as well as the inward calcium currents observed during the application of the depolarising pulses. This finding confirms a role

for this channel in mediating the initial calcium change which facilitates the voltage-pulse potentiation of mEPSC amplitudes.

I next addressed whether this calcium influx through the L-type calcium channel was sufficient for the induction of voltage-pulse potentiation or if was merely a trigger in the signalling cascade? To address this question I used a combination of drugs which target the internal calcium store. The endoplasmic reticulum (ER) and non ER associated calcium containing organelles (CCOs)(Korkotian and Segal, 1997, 1998) constitute large and centrally important internal sources of calcium, for various neuronal signalling processes (Mattson et al., 2000). Release of ER calcium is controlled by two receptors the ryanodine receptor (RyR) and the inositol 1,4,5 trisphosphate receptor (IP_3R). RyRs are activated by increases in cytosolic Ca^{2+} and are therefore responsible for the phenomenon of Ca^{2+} induced Ca^{2+} release (CICR) (Zucchi and Ronca-Testoni, 1997). IP_3Rs are activated by IP_3 generated via metabotropic receptors linked to phospholipase C (PLC) although these receptors show modulation in response to increasing cytosolic calcium (Simpson et al., 1995). In CA1 RyRs are present throughout the neurone, including the dendritic spines and shafts, whereas the IP_3Rs are predominantly located in the dendritic shafts (Sharp et al. 1993). Inhibition of these receptors with application of ryanodine or depletion of ER Ca^{2+} stores by inhibition of the Ca^{2+} ATPase pump with thapsigargin has been shown to inhibit the induction of LTP (Harvey and Collingridge, 1992; Paschen et al., 1996; Treiman et al., 1998).

However a conflicting result does exist for the IP_3R as analysis knockout' mice revealed facilitation of LTP induced by very weak stimulation (Fujii et al., 2000). In a series of experiments the application of thapsigargin and ryanodine blocked the induction of voltage-pulse potentiation of mEPSCs amplitudes. In these experiments inward voltage-activated calcium channel currents were still evident upon the voltage-pulse stimulus indicating the presence of still functional L-type calcium channels. Thus to conclude the activation of L type calcium channels is essential but not sufficient for the induction of voltage-pulse potentiation, as this phenomenon requires release of calcium from the internal store.

This concludes the initial characterization of the properties of mEPSCs in CA1 pyramidal neurones in organotypic slice cultures. In the next results chapter I will describe a series of experiments that test directly the hypothesis that the potentiation induced by this protocol arises from the insertion of AMPA receptors into the postsynaptic membrane.

Chapter Four:

Voltage-pulse potentiation is dependent upon postsynaptic membrane fusion events

In the previous chapter, the focus was the characterisation of a sustainable potentiation of mEPSC amplitudes. This potentiation is thought to be expressed by either change in the conductance of receptors already in the synapses, or through insertion of patches of new AMPA receptors into membranes. The possible insertion of receptors can only be brought about by postsynaptic membrane fusion events, between AMPA receptors and PSD scaffolding proteins. These interactions will be the focus of this chapter.

4.1: Inhibition of the NSF domain

The first protein isolated and found to be a crucial factor in membrane fusion events, such as synaptic vesicle fusion to the pre-synaptic membrane during neurotransmission, was the NSF protein. Protein complexes containing NSF are collectively referred to as SNAREs or the SNARE complex (soluble NSF-attachment protein (SNAP) receptors; where NSF is N-ethylmaleimide sensitive fusion protein.

These NSF containing complexes have been associated with induction of LTP (Lledo et al., 1998) and receptor trafficking through an association with the GluR2 receptor (Nishimune et al., 1998). These protein complexes represent the first target tested for the dependence of mEPSC amplitude potentiation on membrane fusion events.

In the first series of experiment the broad spectrum NSF inhibitor NEM (N- ethylmaleimide) was included into the patch pipette; this inclusion causes a functional compartmentalisation of this inhibitor, limiting it only to the postsynaptic cell. If bath applied then NEM would have a presynaptic effect inhibiting all release of glutamate vesicles.

The grouped control data for the NEM treated mEPSCs show no significant deviations in the normalised amplitudes of these mEPSCs across the time course of the experiment (Figure 4.1). Giving a mean amplitude of 24.1 ± 0.4 pA (n = 3) with a range of 23.3 ± 0.2 pA to 24.9 ± 0.3 pA. The frequency of mEPSCs with NEM indicates a mean control frequency of 1.9 ± 0.1 Hz (n = 3) with a range of 1.7 ± 0.2 Hz to 2.0 ± 0.1 Hz. Over the time course of this experiment the frequency of the mEPSCs reduces, by 25 minutes time point the frequency was 1.0 ± 0.1 Hz. This finding that mEPSCs still spontaneously occur in the presence of the membrane fusion inhibitor, even at the 30 minute time period is important, as NEM may display a small degree of membrane permeability and therefore would interfere with presynaptic release.

As expected the current output across the experimental time period parallels the reduction in the frequency of mEPSCs. The control current value was 1.2 ± 0.1 nA with a range

of 1.1 ± 0.1 nA to 1.6 ± 0.2 nA and this shows a similar reduction across the experimental time course, by the 25 minute time point the current was 0.5 ± 0.1 nA.

Analysis of 100 mEPSC from both periods, indicate little difference in the mean amplitudes of the events control and NEM are 21.3 ± 0.2 pA and 23.1 ± 0.5 pA respectively. Rise times for these events again show no statistically significant difference, control equally 0.9 ± 0.1 ms and NEM mEPSC rise time was 1.0 ± 0.3. The decay time constant for both these events are similar to control equals 10.2 ± 1.9 ms and NEM 11.0 ± 1.5 ms.

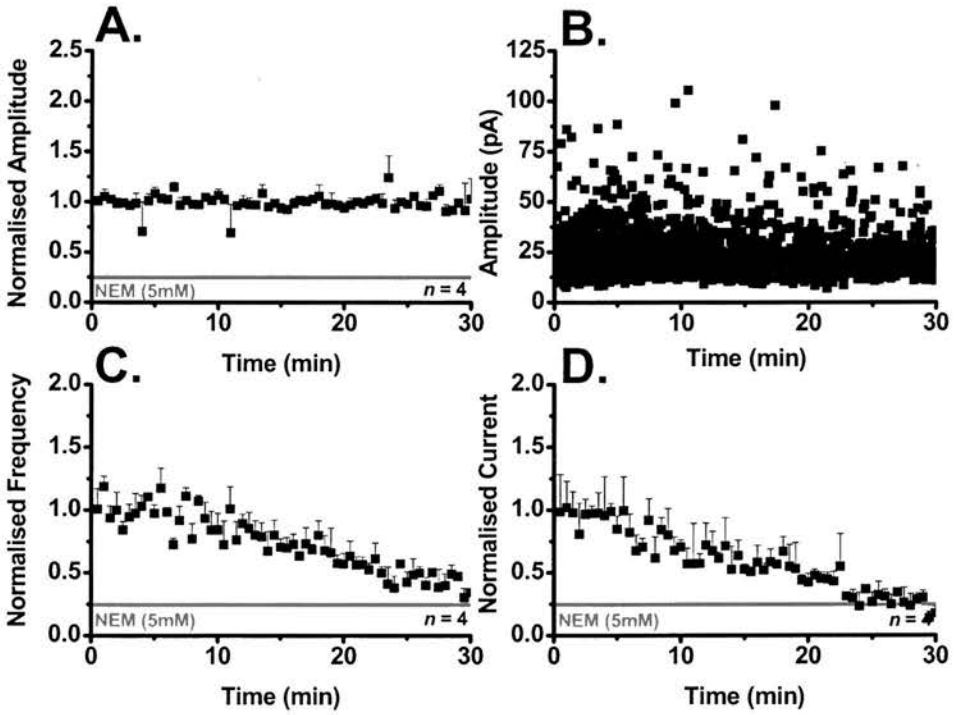

Figure 4.1: **NEM does not affect non potentiated mEPSC amplitudes**. (A.) Control recording show no change in mEPSC amplitude with application of NEM (5mM). (B.) The distribution of mEPSC amplitudes does not increase with application of NEM. (C.) The frequency of mEPSC events decreases across the experimental time period. This reduction is mirrored by the total current produced by the mEPSCs (D.).

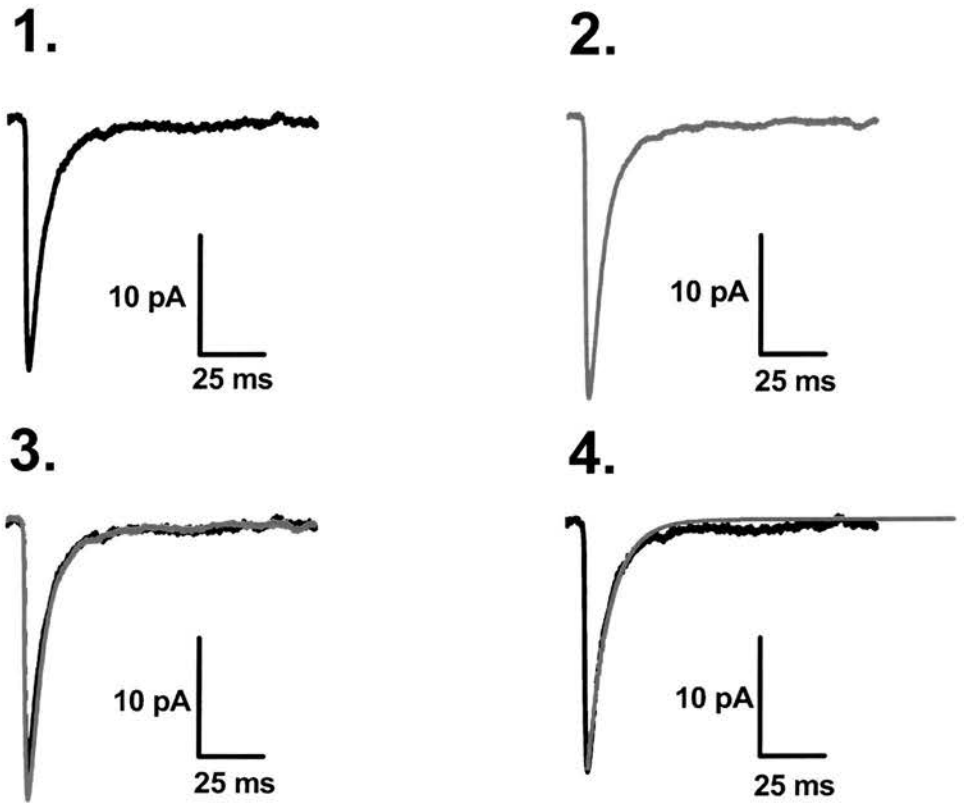

Figure 4.2: **Control and NEM treated mEPSCs.** Analysis of 100 mEPSCs from the control period shows a mEPSCs which typically have mean amplitudes of about 20 pA (1.). Application of the NSF peptide inhibitor has NEM (5 mM) has no significant effect on the amplitude of the mEPSC (2.). When these mean events are overlaid, there is little obvious difference in the rise or decay phase of these mEPSCs (3.). Fitting control mEPSC with a single exponential indicates the goodness of fit for the τ decay constant.

4.2: Inhibition of VP potentiation by the postsynaptic application of NEM

The application of NEM is known to inhibit membrane fusion events in the presynaptic nerve terminal, effectively silencing vesicle release. When application of this toxin is compartmentalised to the postsynaptic cell, NEM was found to have no significant effect on the baseline control amplitudes of the mEPSCs. Using the hypothesis I tested whether VP potentiation utilises postsynaptic membrane fusion events to bring about an increase in AMPA receptor number at active synapses.

Previous studies utilizing an NMDA receptor dependent LTP stimulating protocol have shown a relationship between NSF protein and the GluR2 AMPA receptor. The aim of these experiments is to investigate these mechanisms through which AMPA receptors maybe trafficked to the active synapses. NEM by action is a crude broad spectrum NSF inhibitor. Therefore in this experiment the application of NEM should block all NSF, SNAP-25 and SNARE complexes.

The results show that the induction of the VP potentiation of mEPSC amplitudes was inhibited by NEM (Figure 4.3: control 21.5 ± 1.5 pA: NEM 20.6 ± 0.9 pA. $n = 6$). The range of mean mEPSC amplitudes was 15.8 ± 0.6 pA to 25.2 ± 0.1 pA. Interleaved control recordings of normal VP potentiation show a 95% increase in the mean mEPSC amplitude after VP stimulation (control 19.6 ± 1.3 pA: VP 38.5 ± 2.2 pA. $n = 6$). mEPSC raster plots from each time period indicating little obvious change between the control NEM mEPSCs and the VP stimulated NEM mEPSC, while the amplitudes of the interleaved control VP potentiated mEPSCs are significantly increased (Figure 4.3 B).

The amplitude time course for the single cell VP potentiation experiment with NEM shows no significant deviation from the normalised amplitude value following the VP stimulus across the time period of the experiment, the mean amplitude was 21.8 ± 0.06 pA. Plotting all mEPSC amplitudes in both the control and NEM groups show a cumulative probability plot that overlaps, the 50 % probability of 21.4 pA, and an 80 % probability of 23.5 pA. This indicates little difference in the mEPSC amplitude between the two groups, this result was further backed up by a mEPSC amplitude histogram of the mEPSC from the control and NEM groups over the same time period, and this histogram shows no significant difference between the two groups (KS > 0.05. Figure 4.4C).

In the previous chapter it was shown that VP potentiation protocol causes a transient not significant potentiation of mEPSC frequency lasting only 5 minutes. The application of NEM

blocks this transient the potentiation of mEPSC frequency (Control: 1.4 ± 0.3 Hz: NEM 1.2 ± 0.1 Hz), with a range of recordings from 0.5 ± 0.1 Hz to 2.5 ± 0.2 Hz. These data further show a similar trend as the control NEM mEPSC recordings, a gradual reduction in mEPSC frequency by the 20-25 minute time period (Figure 4.5A). The interleaved control frequency shows a similar reducing trend from 1.1 ± 0.2 Hz to the VP potentiated mEPSC frequency of 0.9 ± 0.2 Hz.

VP potentiation protocol shows at its peak a larger than 3 fold increase in the total current after VP stimulation (Figure 3.9 B). The application of NEM blocks the VP potentiation of the total current produced by these cells (control 1.7 ± 0.2 nA: NEM 1.4 ± 0.2 nA). The range of mean current recordings was 0.6 ± 0.1 nA to 5.1 ± 0.1 nA (Figure 4.5B). The interleaved control recordings show an increase in the total current produced after the application of VP stimulus (Control 1.0 ± 0.5 nA: VP 1.7 ± 0.6 nA).

This is further highlighted by mEPSC overlays, 100 mEPSCs from each time period were analysed, control NEM mEPSC and VP stimulated NEM mEPSC had no significant difference in mEPSC amplitudes, rise or decay times. The interleaved control VP potentiated mEPSC shows a mean amplitude of 43.9 ± 0.2 pA, again with similar rise and decay time constant characteristics 1.037 ± 0.1 ms and 11.1 ± 0.9 ms respectively (Figure 4.5C).

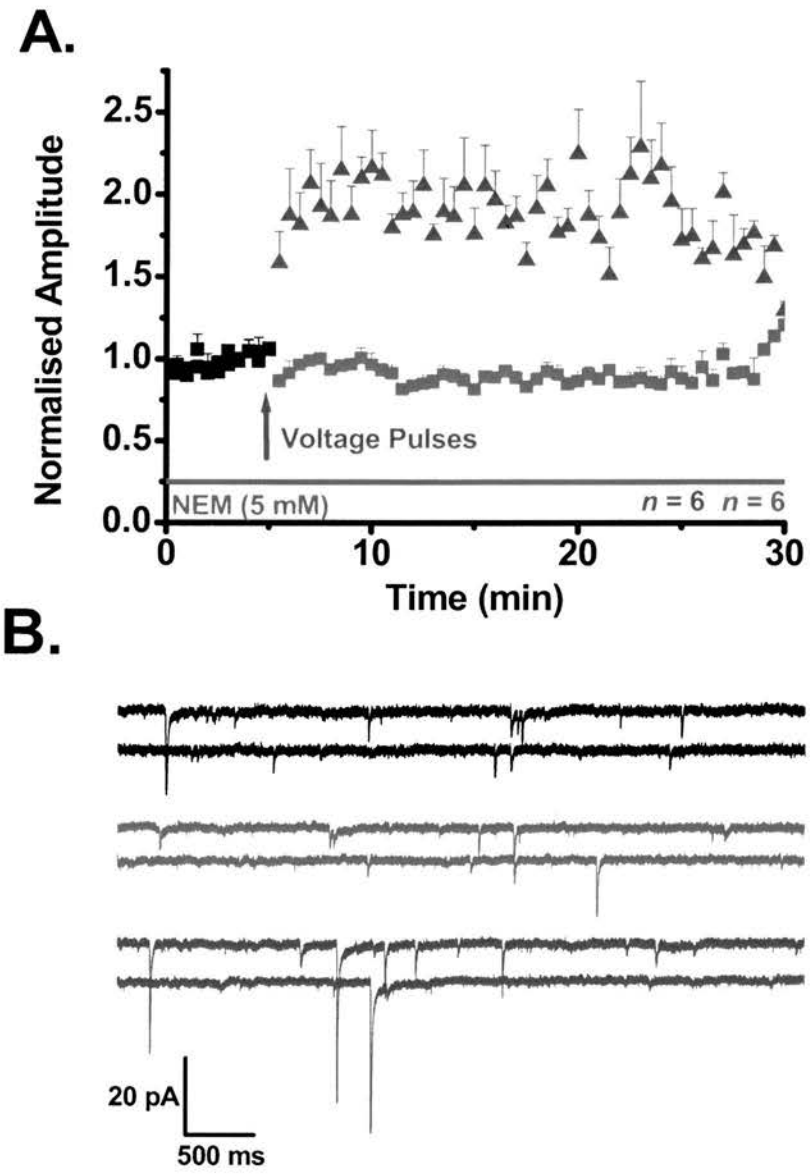

Figure 4.3: **Blockade of VP potentiation of mEPSC amplitudes by NEM.** (A.) The induction of VP potentiation of mEPSC amplitudes is blocked by NEM (5 mM). (B.) **Raster plot of the blockade of VP potentiation by NEM**. Corresponding traces for the control NEM mEPSC (**Black**) VP stimulated mEPSC with NEM (**Red**) and VP potentiated mEPSCs (**Blue**).

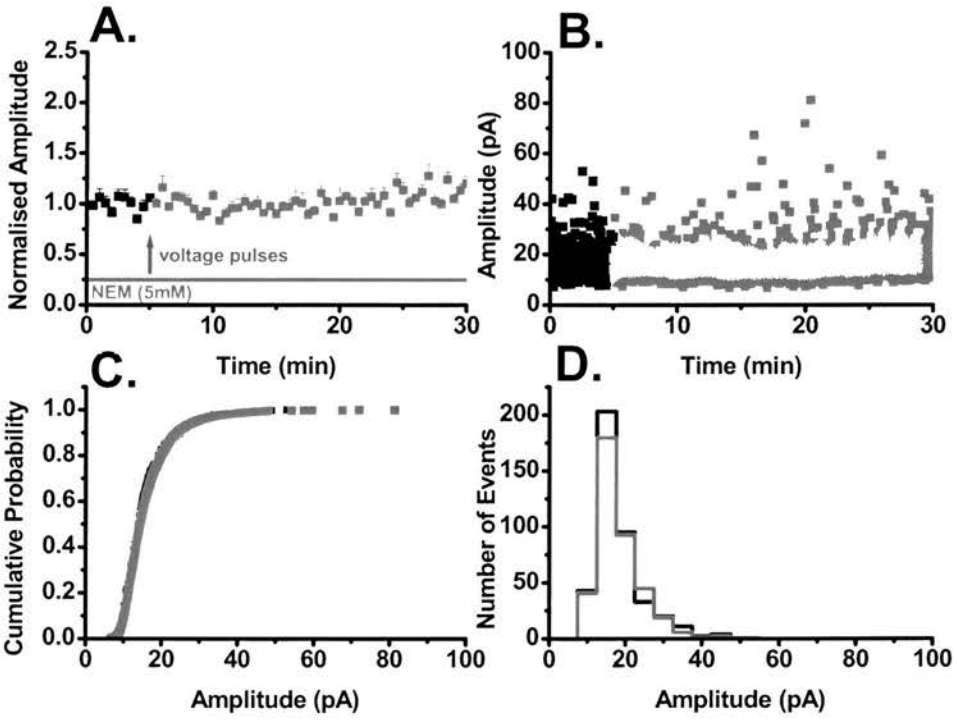

Figure 4.4: **Blockade of VP potentiation of mEPSC amplitudes by NEM (con't).** (A.) A single cell amplitude time course showing blockade of VP potentiation by the application of NEM. (B.) Corresponding scatter plot of mEPSC amplitudes, showing no increase in event distribution. (C.) Cumulative probability plots for both control and VP stimulated NEM treated mEPSCs overlap, indicating no increases in mEPSC amplitudes following stimulation. (D.) Amplitude histograms for control and NEM mEPSC over the same time period (5 min) show no significant change in event distribution.

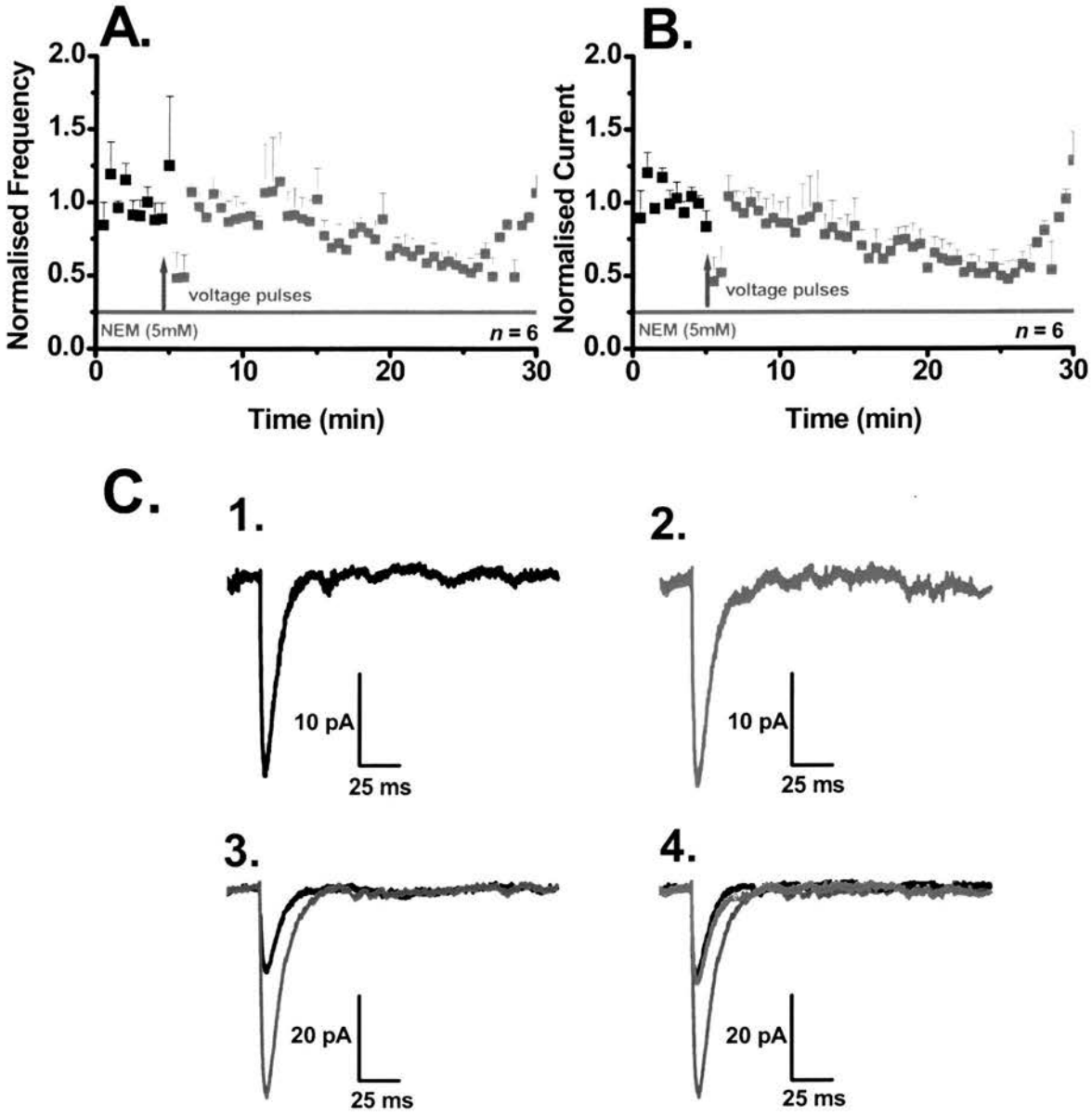

Figure 4.5: **Further characterization of NEM block of VP potentiation.** Pipette inclusion of NEM blocked the VP potentiation of mEPSC frequency (A.) and currents (B.) **mEPSC overlays for NEM** (C.) Analysis of 100 mEPSCs from the control period (1.) and the NEM treated period (2.) show no significant change in rise or decay times when overlaid (4.) mEPSCs from interleaved recording have significantly larger amplitudes following stimulation (3.).

4.3: Inhibition of SNAP 25 blocks VP potentiation of mEPSC amplitudes.

Botulinum neurotoxin is produced by the anaerobic bacterium *Clostridium Botulinum.* It is an extremely poisonous biological substance; infection in people can occur by two methods, the infection through bacterial spore growth and toxin release in intestinal enteric infectious botulism or from the ingestion of the toxin from a contaminated food source (food borne botulism). The mechanism of action at the neuromuscular junction is well understood and acts via a blockade of acetylcholine vesicle release and hence neurotransmission. What is interesting is that nerve terminals do not degenerate, but the blockade of neurotransmitter release is irreversible. Function can be recovered by the sprouting of nerve terminals and the formation of new synaptic contacts.

In this series of experiments, the unique properties of Botulinum toxin A (Botox) will be used to probe postsynaptic membrane fusion events governing AMPA receptor delivery to synapses. The properties which will be exploited are the specific inhibition of the SNAP-25 protein, (Synaptosome associated protein of 25-kD molecular weight). In the presynaptic nerve terminal SNAP-25 has a fascinating spectrum of action. Characterisation of this protein's function from homozygous knock out animal against heterozygous litter mates, have shown normal embryonic development, but animals are slightly smaller, they show no obvious signs of neurodegeneration up to birth although some neuromuscular junctions are weakly developed (Meunier et al., 2003). Electrophysiological studies at the neuromuscular junction have indicated a hierarchy of function for the SNAP/ SNARE proteins as SNAP-25 knockouts have shown that spontaneous vesicle fusion is not dependent upon the SNAP-25 protein, and that blockade of these events is achieved through linking with the SNARE complex. Furthermore mEPSCs were still reported, despite complete lack of evoked synaptic transmission in these animals at the same neuromuscular junction; this finding indicates that SNAP-25 is a crucial component of the machinery that mediates evoked fusion.

In the postsynaptic cell, the application of Botox should inhibit the actions of SNAP-25, interacting with vesicular SNARE proteins which facilitate patches of membrane (possibly vesicular) containing new AMPA receptors into active synapses.

The positive control for this experiment, was done the laboratories of Dr Richard Ribchester at the University of Edinburgh was successful inhibition of peripheral nerve innervation of the neuromuscular junction in the Wlds mouse, was achieved with the same Botox sample and at the same concentration.

In this series of experiments Botox was included in the pipette solution again compartmentalising its application to the postsynaptic cell. The application of Botox blocked the induction of VP potentiation of mEPSC amplitudes (control 21.3 ± 2.9 pA: Botox 21.4 ± 1.4 pA. n = 7), while interleaved control recordings showed typical significant potentiation of mEPSC amplitudes (control: 23.0 ± 3.6 pA: VP 48.0 ± 3.2 pA. n = 5) (Figure 4.7). Raster Plots from each time period show little difference between the control Botox mEPSCs and VP stimulated mEPSCs, while interleaved control VP stimulated mEPSCs show a significant potentiation of mEPSC amplitudes (Figure 4.6B). The single cell mEPSC amplitude distribution shows a control mean amplitude of 27.6 ± 1.3 pA, cumulative probability plot for this Botox treated cell shows control and VP stimulated mEPSCs which overlap, indicating an equal probability of mEPSCs with similar amplitude, effectively application of Botox blocks the VP potentiation of mEPSC amplitude (Figure 4.7C). A result further supported by an amplitude histogram (Figure 4.7D) which shows no significant difference between both groups (KSG > 0.05).

Frequency of the mEPSCs with Botox show a gradual reduction after application of the VP stimulus (control 1.6 ± 0.3 Hz: Botox 1.3 ± 0.2 Hz). This decrease in event frequency is paralleled by the interleaved control frequency which similarly reduces (Control 1.2 ± 0.2 Hz: VP 0.7 ± 0.2 Hz).

As expected the interleaved VP recordings show a typical transient potentiation of mEPSC current (Control 0.8 ± 0.2 nA: VP 3.5 ± 1.4 nA), while application of Botox blocked the current potentiation produced by the VP stimulus (Control 1.1 ± 0.3 nA: 0.7 ± 0.1 nA).

Analysis of 100 mEPSCs from each time period show little difference in mEPSC amplitude for the control Botox treated and VP stimulated mEPSC (Control 24.8 ± 0.1 pA: VP 24.0 ± 0.2 pA) or with rise (Control 1.9 ± 0.1 ms: VP 1.8 ± 0.1 ms) and decay time constant (Control 9.6 ± 1.5: VP 9.9 ± 1.0 ms). The interleaved control VP potentiated mEPSCs mean amplitude was significantly increased 44.6 ± 0.97 pA with rise and decay time constant of 2.0 ± 0.1 ms and 10.5 ± 1.9 ms respectively (Figure 4.8 C).

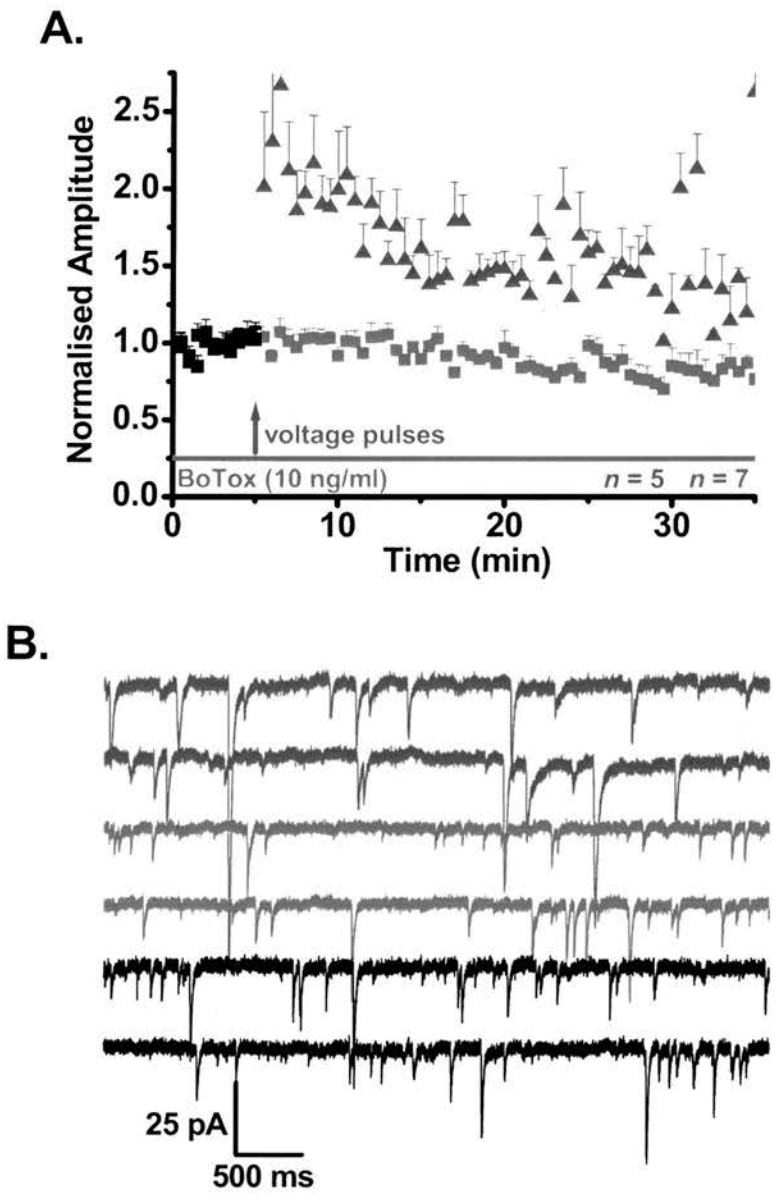

Figure 4.6: **Blockade of VP potentiation of mEPSC amplitudes by Botox.** (A.) The induction of VP potentiation of mEPSC amplitudes is blocked by Botox (10ng/ml). (B.) **Raster plot of the blockade of VP potentiation by Botox**. Corresponding traces for the control Botox mEPSCs (**Black**) VP stimulated mEPSC with Botox (**Red**) and VP potentiated mEPSCs from interleaved control recordings (**Blue**).

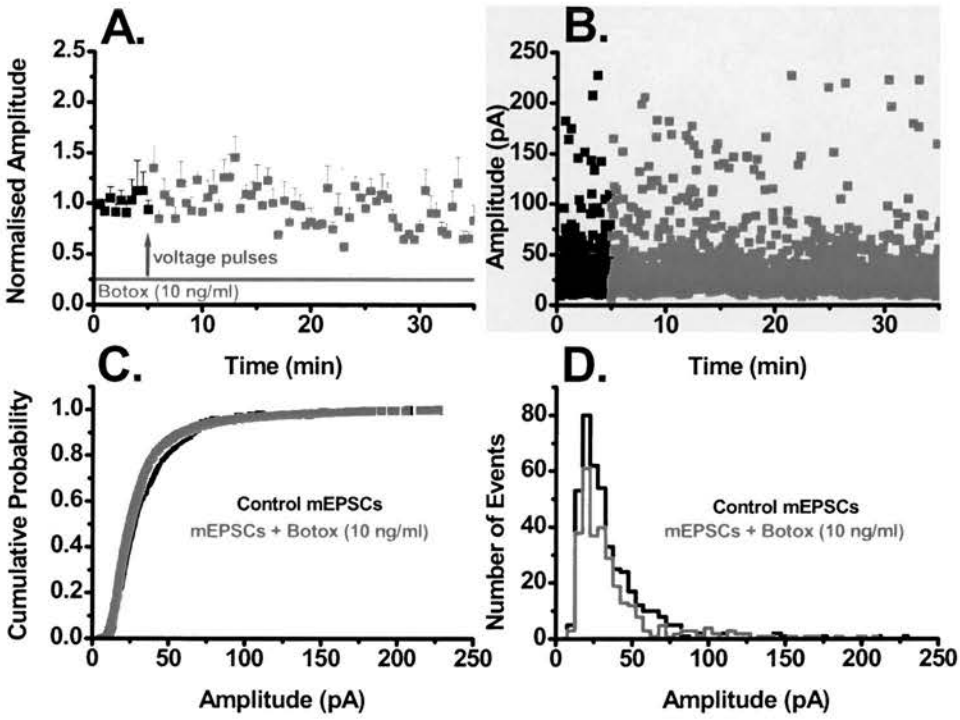

Figure 4.7: **Blockade of VP potentiation of mEPSC amplitudes by Botox (con't).** (A.) A single cell amplitude time course showing blockade of VP potentiation by the Pipette inclusion of Botox. (B.) Corresponding scatter plot of mEPSC amplitudes, showing no increase in event distribution. (C.) Cumulative probability plots for both control and VP stimulated Botox treated mEPSCs overlap, indicating no increases in mEPSC amplitudes following stimulation. (D.) Amplitude histograms for control and Botox mEPSC over the same time period (5 min) show no significant change in event distribution.

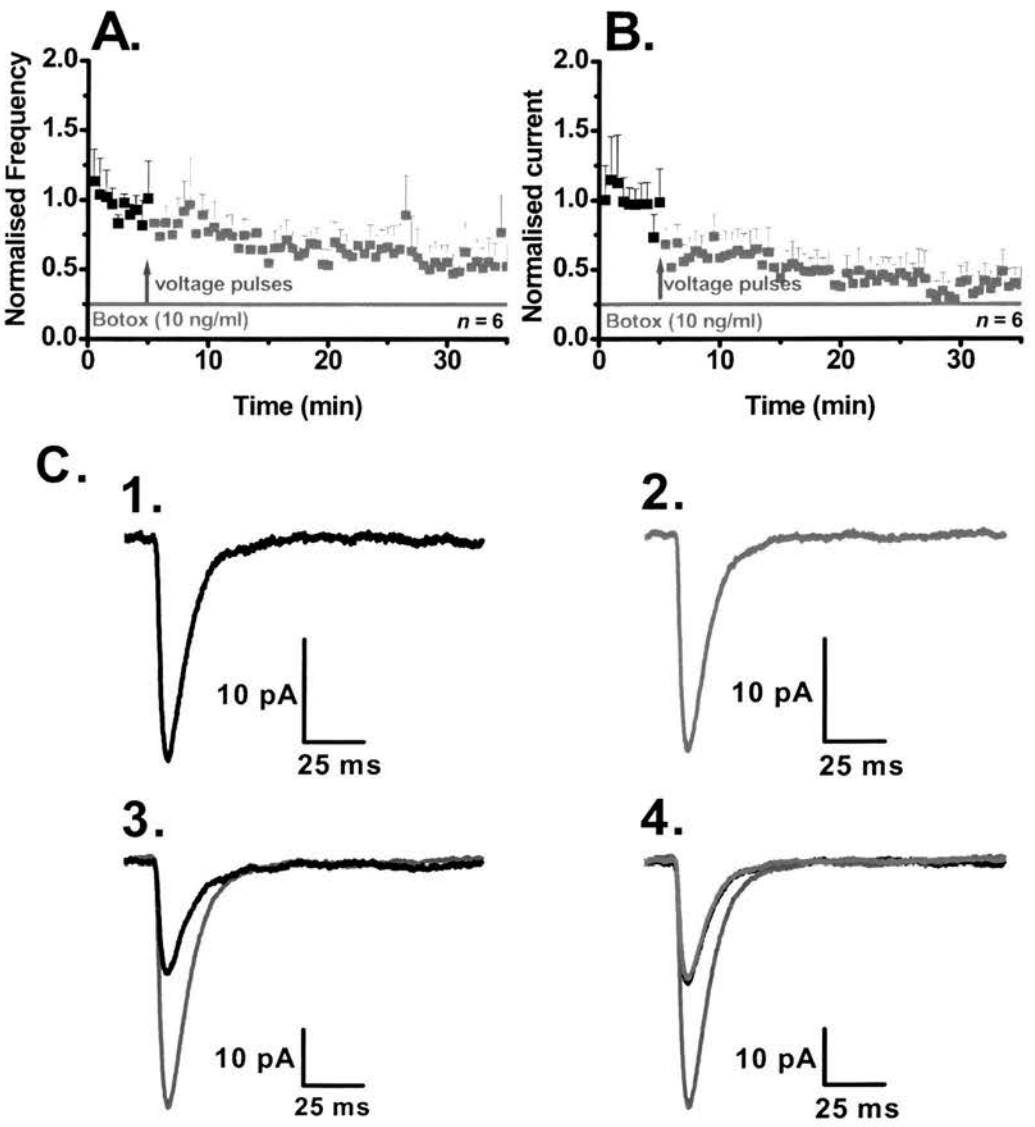

Figure 4.8: **Further characterization of the Botox block of VP potentiation.** Pipette inclusion of Botox blocked the VP potentiation of mEPSC frequency (A.) and currents (B.) **mEPSC overlays for Botox** (C.) Analysis of 100 mEPSCs from the control period (1.) and the **NEM** treated period (2.) show no significant change in rise or decay times when overlaid (4.) mEPSCs from interleaved recording have significantly larger amplitudes following VP stimulation (3.).

4.4 Specific inhibition of postsynaptic membrane fusion events.

So far this investigation of postsynaptic membrane fusion events has focused on the blockade of NSF peptide related complexes associated with the postsynaptic membrane. Although data from both the NEM and Botox experiments are encouraging, an approach with greater specificity was employed to investigate this phenomenon. Again with a postsynaptic compartmentalisation a specific peptide targeted to the NSF binding motif on the GluR2 AMPA receptor was applied to the CA1 pyramidal cells. This approach guarantees a greater degree of specificity; unlike the NEM experiment this peptide will leave the action of the NSF proteins intact, as it affects the receptor. Furthermore Pep2m has no metabolic activity unlike Botox with the catabolism of the SNAP-25 protein, and membrane permeability issues are removed.

The application of Pep2m (Lys-Arg-Met-Lys-Val-Ala-Lys-Asn-Ala-Gln) to control cells had no significant effect on the mean amplitude of the mEPSCs (Figure 4.9A: Control 25.1 ± 2.3 pA: Pep2m 29.5 ± 3.3 pA: 20-25 minutes 22.4 ± 2.0 pA. $n = 4$).

The frequency of mEPSCs with inclusion of Pep2m reduces from the control value of 1.3 ± 0.2 Hz to 0.9 ± 0.1 Hz by the 25th minute, this decrease in mEPSC frequency is previously shown in control studies, without peptide inclusion. As expected the total current parallels the reduction in mEPSC frequency from a control value of 1.1 ± 0.2 to by the 25th minute 0.5 ± 0.2 nA. Analysis of all the mEPSC events recorded from the 0-5 minute period with Pep2m (50 μM), generated a mEPSC with mean amplitude of 25.1 ± 1.0 pA. This averaged event indicated a rise time of 1.7 ± 0.1 ms and a τ decay time of 21.1 ± 0.9 ms both of these values are larger than expected for mEPSCs of this amplitude (Figure 4.10). When compared to an average of mEPSCs from the 10-15 minute period no significant difference was found between the rise and decay time for these events.

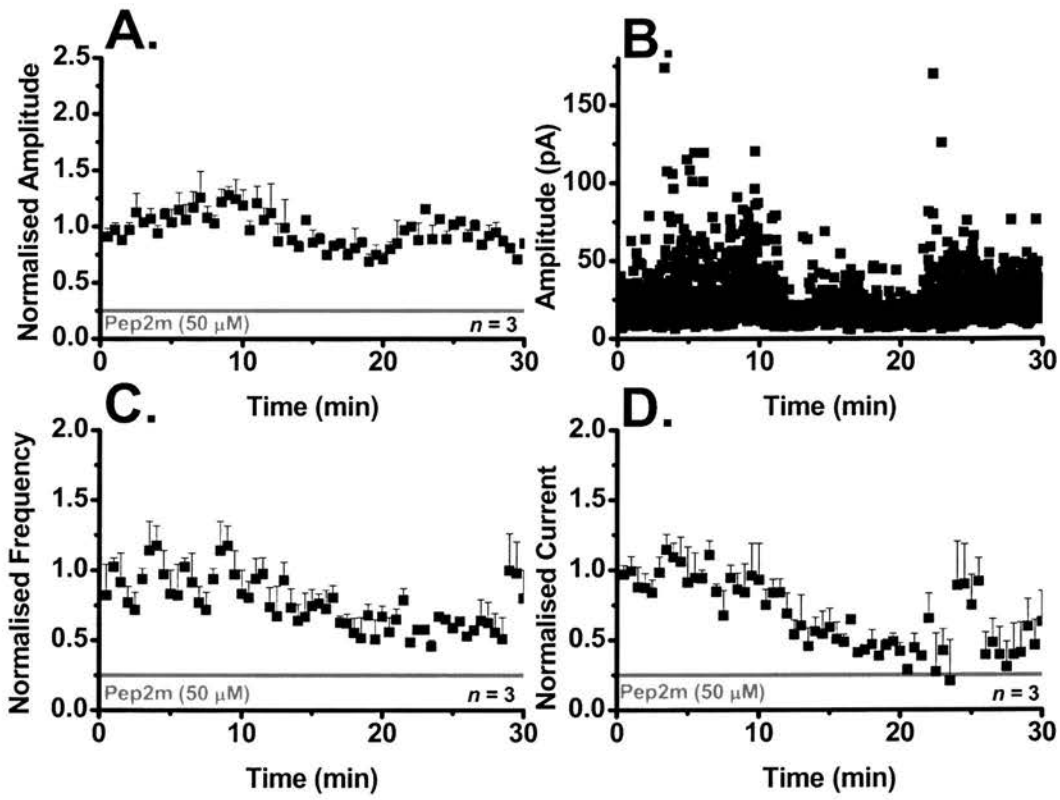

Figure 4.9: **Pep2m does not affect non potentiated mEPSC amplitudes.** (A.) Control recording show no significant change in mEPSC amplitude with application of Pep2m (50 μM). (B.) The distribution of mEPSC amplitudes does not increase with application of Pep2m. Application of Pep2m reduces mEPSC frequency (A.) and the total current produced by the mEPSCs

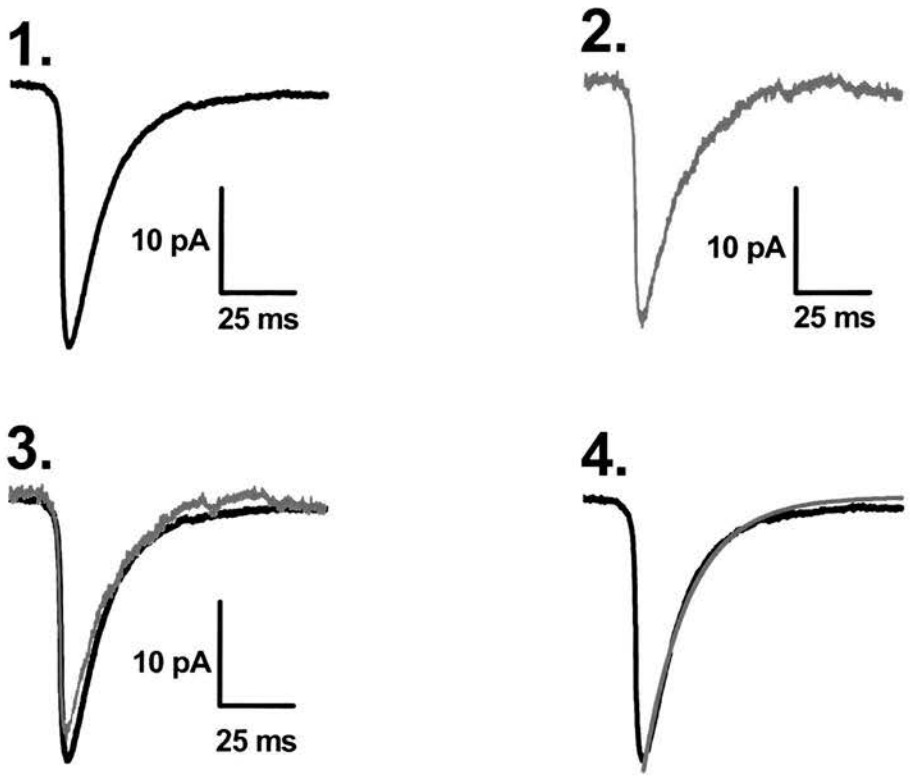

Figure 4.10: **Control Pep2m treated mEPSCs.** Analysis of 100 mEPSCs from the 0-5 minute period shows a mEPSCs which typically have mean amplitudes of about 25 pA (1.). Infusion of the AMPA receptor GluR2 NSF binding site inhibitor Pep2m has no significant effect on the amplitude of the mEPSC (2.). When these mean events are overlaid, there is a 2 pA difference in the mean amplitude, while the rise or decay phase of these mEPSCs are similar (3.). Fitting control mEPSC with a single exponential indicates the goodness of fit for the decay time constant.

4.5: Pep2m inhibits the VP potentiation of mEPSC amplitudes.

The previous experiments demonstrated a requirement of functional NSF protein complexes to facilitate the VP potentiation of mEPSC amplitude. In these experiments we again target the NSF peptide by use a peptide Pep2m (Lys-Arg-Met-Lys-Val-Ala-Lys-Asn-Ala-Gln) which specifically targets the NSF binding motif on the GluR2 AMPA receptor, and was found to have no significant effect on the amplitude of non VP stimulated mEPSCs. This amplitude measure is an indirect measure of AMPA receptor number in the synapses. If the amplitudes of mEPSCs increase as with VP stimulation, it is possible that insertion of new receptors into the postsynaptic membrane has occurred.

In this series of experiments Pep2m was included in the internal solution, restricting the peptide to the postsynaptic cell. After VP stimulation a small non significant transient potentiation of mEPSC amplitudes lasting for 2 minutes was observed (Figure 4.11A: Control 22.8 ± 1.6: VP Pep2m 24.8 ± 2.1 pA. n = 8). Interleaved recordings were conducted with Pep4c (50 μM). Pep4c is the control peptide for Pep2m, which has a single amino acid residue of the Pep2m protein changed (position 8, asparagine to serine) This change render a non-functional peptide sequence, application of VPs to the Pep4c containing cells induces a significant sustained potentiation of mEPSC amplitudes (Figure 4.13C: Control 22.5 ± 1.3 pA: VP Pep4c 47.0 ± 2.1 pA. n = 4). A full review of the Pep4c peptide can be found in the next section (Section 4.6).

Figure 4.13B, highlights typical mEPSCs from each of the Pep2m time periods, control mEPSCs display a tight amplitude distribution, with few large amplitude mEPSCs, following stimulation there is a small increase in these larger amplitude events. For comparison Pep4c mEPSCs following VP stimulation as shown, the degree of potentiation is evident as Pep4c mEPSCs display significantly larger amplitudes.

The single cell amplitude time course with the Pep2m highlights this transient potentiation to a fuller extent. VP stimulation brings about a non significant transient 25% potentiation of mEPSC amplitudes lasting for 2 minutes (Control 17.5 ± 0.4 pA: VP Pep2m 21.8 ± 3.7 pA). The scatter plot of mEPSC amplitudes shows no significant spread of mEPSC amplitude following VP potentiation, in combination with the overlapping cumulative probability and amplitude histogram; indicate that the application of Pep2m blocks the potentiation of mEPSC amplitudes.

The mEPSC frequency plots show a decrease in event frequency from the control value of 1.0 ± 0.3 Hz to 0.8 ± 0.1 Hz by the 25th minute. In previous experiments the VP stimulating protocol, induced a 3 fold increase in the current produced by the potentiated mEPSCs. The inclusion Pep2m, blocked the VP potentiation of mEPSC currents (Control 0.7 ± 0.2 nA: VP Pep2m 0.9 ± 0.3 nA. $n = 8$).

Analysis of 100 mEPSCs from each time period, indicate for the Pep2m exposed mEPSCs mean amplitude of 19.7 ± 0.4 pA with a rise time and decay time constant of 1.9 ± 0.2ms and 19.3 ± 1.5 ms. The VP stimulated mEPSCs with Pep2m taken from the peak of the transient potentiation, display a small increase in mean amplitude (20.1 ± 0.2 pA) the rise and τ decay times for these events are similar to the control mEPSC values (1.8 ± 0.3 ms and 19.57 ± 1.5 ms respectively). The data from both control Pep2m and VP stimulated groups show similar rise and τ decay times, but the parameters of these mEPSC are slower than typical mEPSC rise and decay times. The mean Pep4c mEPSC displayed had mean amplitude of 45.2 ± 0.4 pA with comparable rise (2.1 ± 0.2 ms) and τ decay times (22.8 ± 2.1 ms). The Pep4c data is discussed in the next section.

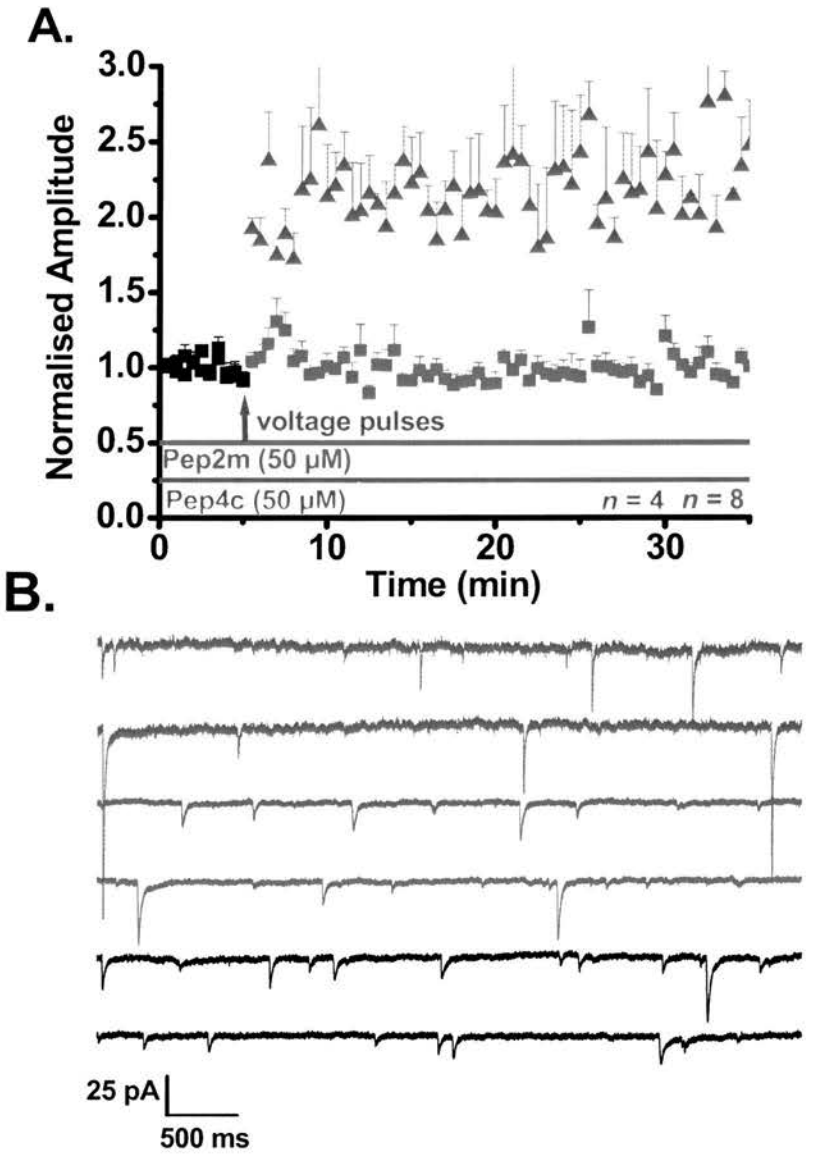

Figure 4.11: **VP potentiation of mEPSC amplitudes was blocked by Pep2m.** Pep2m blocks the potentiation of mEPSC amplitude, while Pep4c does not. Figure 4.10: **Raster plot of mEPSC events.** Control mEPSCs (**Black**) VP stimulated mEPSCs with Pep2m (**Red**) and VP potentiated mEPSCs with Pep4c (**Purple**).

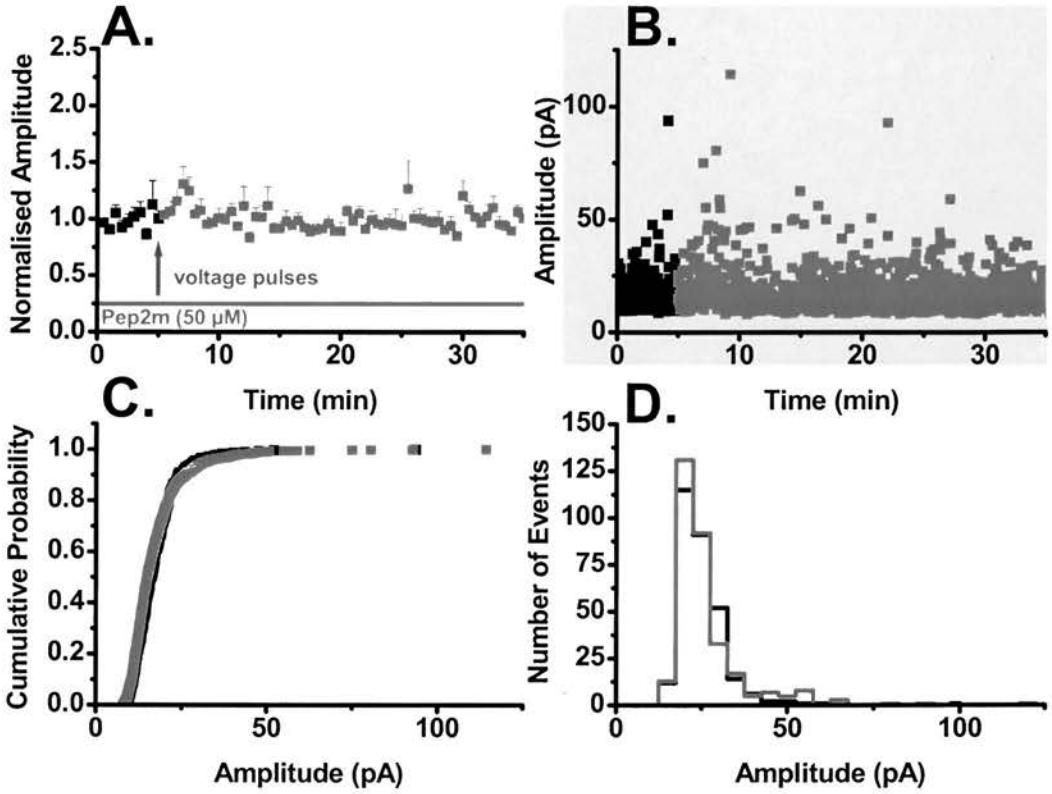

Figure 4.12: **VP potentiation of mEPSC amplitudes was blocked by Pep2m (con't).** (A.) A single cell amplitude time course showing blockade of VP potentiation by the pipette inclusion of Pep2m. (B.) Corresponding scatter plot of mEPSC amplitudes, showing no increase in event distribution. (C.) Cumulative probability plots for both control and VP stimulated Pep2m treated mEPSCs overlap, indicating no increases in mEPSC amplitudes following stimulation. (D.) Amplitude histograms for control and Pep2m mEPSC over the same time period (5 min) show no significant change in event distribution.

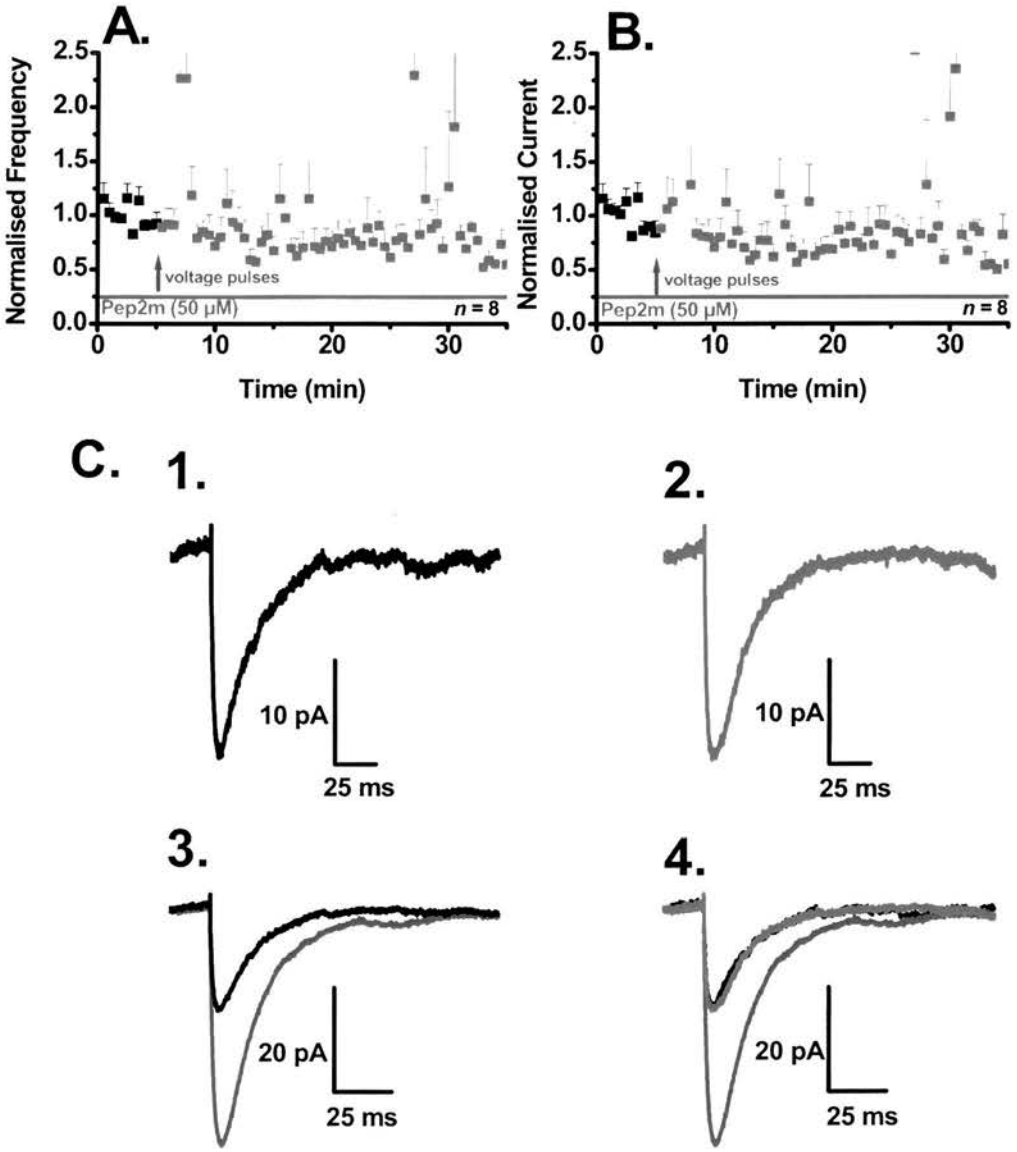

Figure 4.13: **Further characterization of Pep2m block of VP potentiation.** Pipette inclusion of Pep2m blocked the VP potentiation of mEPSC frequency (A.) and currents (B.) **mEPSC overlays for Pep2m** (C.) Analysis of 100 mEPSCs from the control period (1.) and the Pep2m treated period (2.) show no significant change in rise or decay times when overlaid (4.) mEPSCs from interleaved Pep4c recording have significantly larger amplitudes following VP stimulation (3.).

4.6: The characterization of the inactive peptide Pep4c

The approach of using specific peptide sequences allows for effective characterization experiments, due to the ability to swap the amino acids in the peptide sequence. In this series control non potentiated mEPSC recordings were done with Pep4c (50 μM) to characterize any possible effect on mEPSC amplitudes and frequencies.

Inclusion of Pep4c (Lys-Arg-Met-Lys-Val-Ala-Lys-Ser-Ala-Gln) the inactive control analogue of Pep2m has no significant effect on the amplitudes of the mEPSC across the time course of the experiment (Figure 4.16: Control 25.8 ± 3.4 pA: Pep4c 23.1 ± 2.0 pA. n = 3). The frequency of the mEPSC with Pep4c transiently increases across the time course, (Figure 4.16 C: Control 0.9 ± 0.1: Pep4c 1.2 ± 0.3 Hz. n = 3). This increase in mEPSC frequency as expected causes an increase in the normalized total current plot (Figure 4.17 D: Control: 1.0 ± 0.2 nA to 1.1 ± 0.1 nA. n = 3).

Analysis of 100 control mEPSCs renders an event with a mean amplitude of 24.6 ± 0.2 pA, with a rise and decay time of 1.4 ± 0.1 ms and 13.5 ± 0.8 respectively. Analysis of the 100 events from the Pep4c period, indicate a non stimulated mEPSC with a mean amplitude of 22.0 ± 0.3 pA with a rise time and decay time constant of 1.2 ± 0.2 ms and 14.0 ± 1.0 ms respectively.

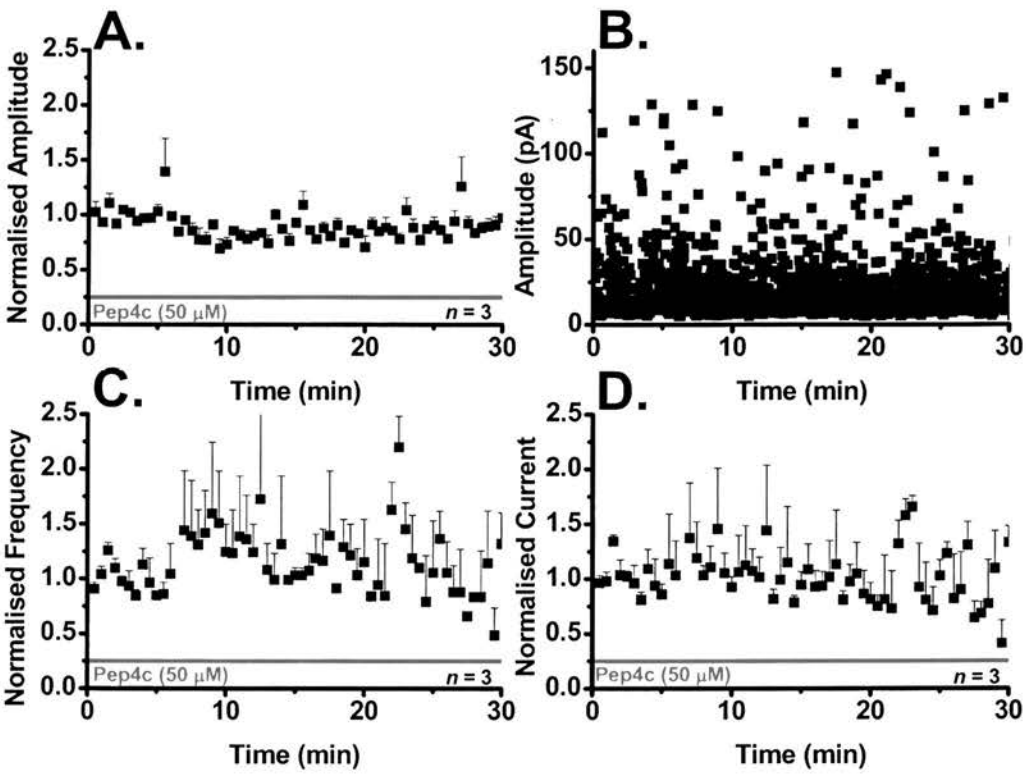

Figure 4.14: **Pep4c does not affect non potentiated mEPSC amplitudes.** (A.) Control recording show no significant change in mEPSC amplitude with application of Pep4c (50 μM). (B.) The distribution of mEPSC amplitudes does not increase with inclusion of Pep4c, mEPSC have an 80% amplitude probability of 26.3 pA. (C.) Inclusion of Pep4C causes a transient potentiation of mEPSC frequency (D.) and the total current produced by the mEPSCs.

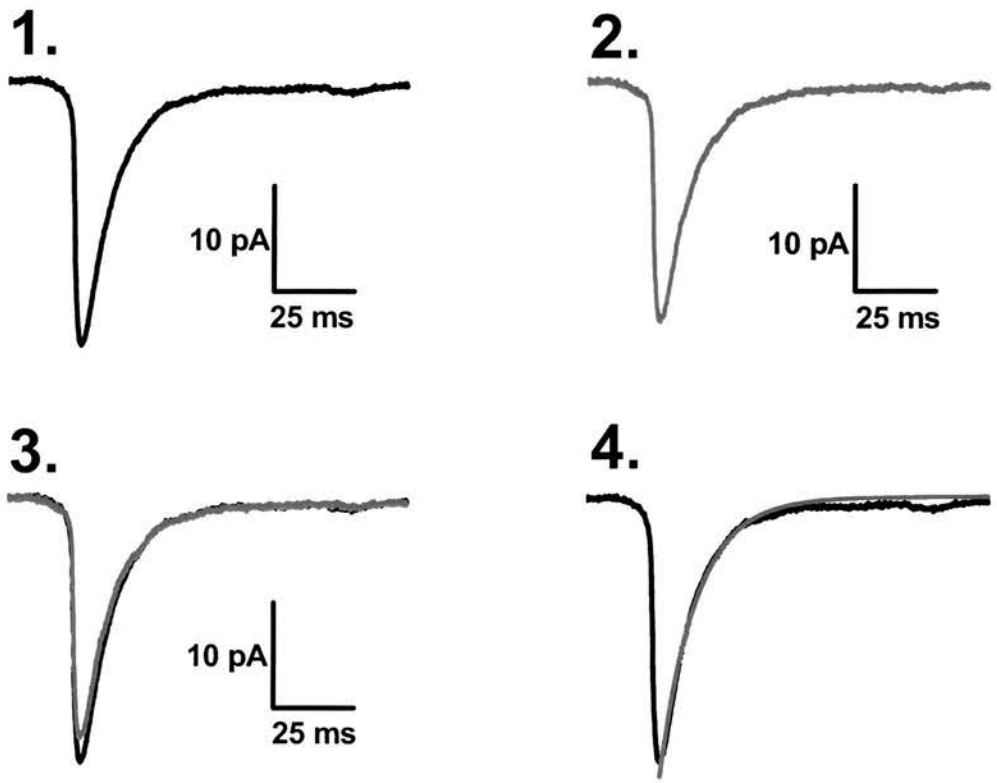

Figure 4.15: **Control Pep4c treated mEPSCs.** Analysis of 100 mEPSCs from the control period shows a mEPSCs which typically have mean amplitudes of about 25 pA (1.). Inclusion of the inactive NSF binding site inhibitor Pep4c has no significant effect on the amplitude of the mEPSC (2.). When these mean events are overlaid, there is a 1 pA difference in the mean amplitude, while the rise or decay phase of these mEPSCs are similar (3.). Fitting control mEPSC with a single exponential indicates the goodness of fit for the decay time constant.

4.7: Point mutations within the Pep2m peptide allow VP potentiation of mEPSC amplitudes.

As mentioned previously Pep4c is the non functional version of the Pep2m peptide which selectively inhibits the NSF binding site on the GluR2 AMPA receptor. This peptide is made from a single amino acid swap, asparagine to serine at the eighth position (out of total 10 amino acids) on this peptide. The effect of this mutation had some interesting effects on the control frequency and current recordings, in that these recordings had a lower mean frequency and current than the typical mEPSC frequency and current, but increases or ran up to a level which was consistent with previous experimental findings.

The effect of this non functional peptide Pep4c (50 μM) on the VP potentiation of mEPSC amplitudes, is as expected after stimulation there was a significant sustained increase in the mean mEPSC amplitude (Figure 4.16A: 22.5 ± 1.3 pA: VP Pep4c 47.0 ± 2.1 pA. n = 4). These large mEPSCs at the peak of the potentiation are shown in Figure 4.16B, with control Pep4c mEPSCs for comparison.

The cumulative probability plots for the mEPSCs from both Pep4c control and VP stimulated periods show a clear difference, indicating a higher probability of the VP stimulated mEPSC to be a large amplitude event. Similarly a histogram of Pep4c mEPSC amplitudes from both time periods shows a clear rightward shift following the VP stimulus, this right ward shift is indicative of mEPSC with larger amplitudes.

As mentioned earlier the mEPSC frequencies with Pep4c for the control recordings are below the typical frequency for mEPSCs. This finding is carried through in this experiment, where VP stimulation induces a transient potentiation of mEPSC frequency (Figure 4.18A: 0.6 ± 0.1 Hz: VP Pep4c 1.0 ± 0.1 Hz). VP potentiated frequency of these mEPSC is not significantly different from the control mEPSC frequency.

Previous experiments have shown a three fold potentiation of total mEPSC current with VP potentiation, the application of Pep4c does not inhibit the potentiation of the mEPSC currents (Control 0.3 ± 0.1 nA: VP Pep4c 0.7 ± 0.1 nA).

The kinetics of 100 analysed mEPSC for each time period show little significant difference, this is further true of the 100 largest mEPSC recorded, as Pep4c treated VP stimulated recording yielded some of the biggest events recorded in any of the experiments presented. Control mEPSC has mean amplitude of 23.4 ± 0.8 pA with a rise time and decay time constant of 1.5 ± 0.2 ms and decay time constant of 17.9 ± 2.2 ms respectively. The VP

Pep4c mEPSCs have mean amplitude of 49.9 ± 0.9 pA with rise and τ decay times of 1.4 ± 0.3 ms and 15.1 ± 1.1 ms respectively. The analysis of the 100 largest events gave a mean VP Pep4c mEPSC of 150.9 ± 2.7 pA with rise time and decay time constant of 1.2 ± 0.1 ms and 16.7 ± 0.6 ms respectively.

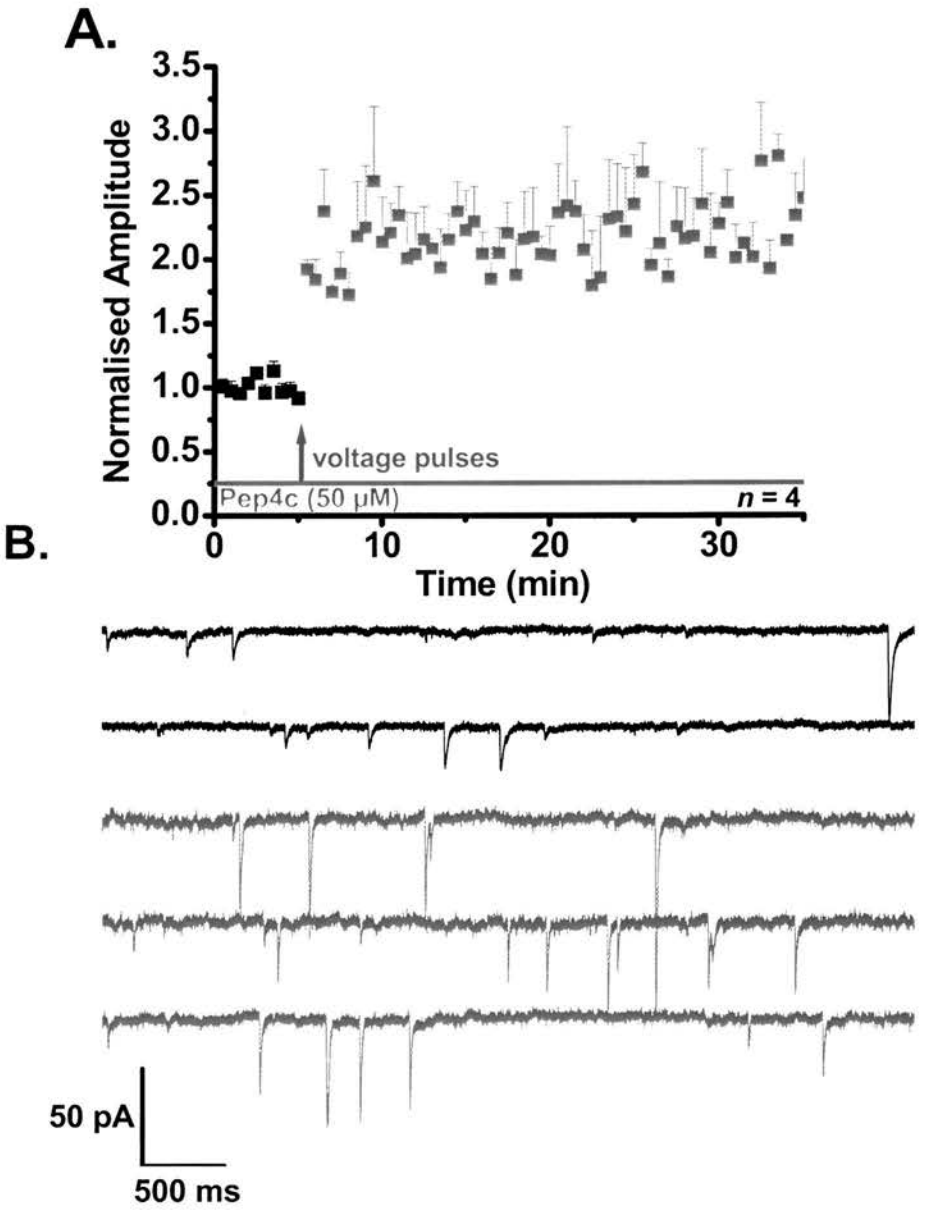

Figure 4.16: **VP potentiation of mEPSC amplitudes occurs with application of Pep4c.** (A.) pipette inclusion of Pep4c does not inhibit VP potentiation of mEPSC amplitudes (B.) **Raster plot of mEPSC events.** Control mEPSCs (**Black**) VP stimulated mEPSCs with Pep4c (**Purple**).

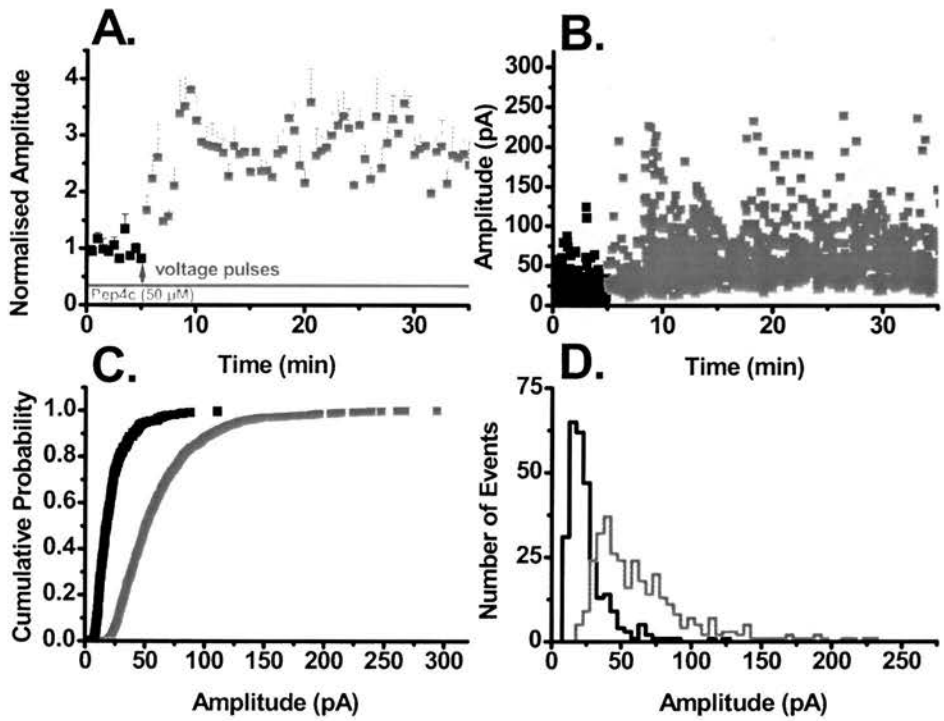

Figure 4.17: **Pep4c does not block VP potentiation of mEPSC amplitudes**. (A.) Single cell recording shows a significant potentiation of mEPSC amplitudes following VP stimulation with Pep4c (50 μM). (B.) The distribution of mEPSC amplitudes increase with application of Pep4c following the VP pulses. (C.) Cumulative probability plots do not overlap indicating mEPSC amplitude potentiation via the VP stimulus (D.) Amplitude histograms for control and Pep4c (5 min following application) show a significant right ward shift in the amplitude distribution of the mEPSCs following VP stimulation.

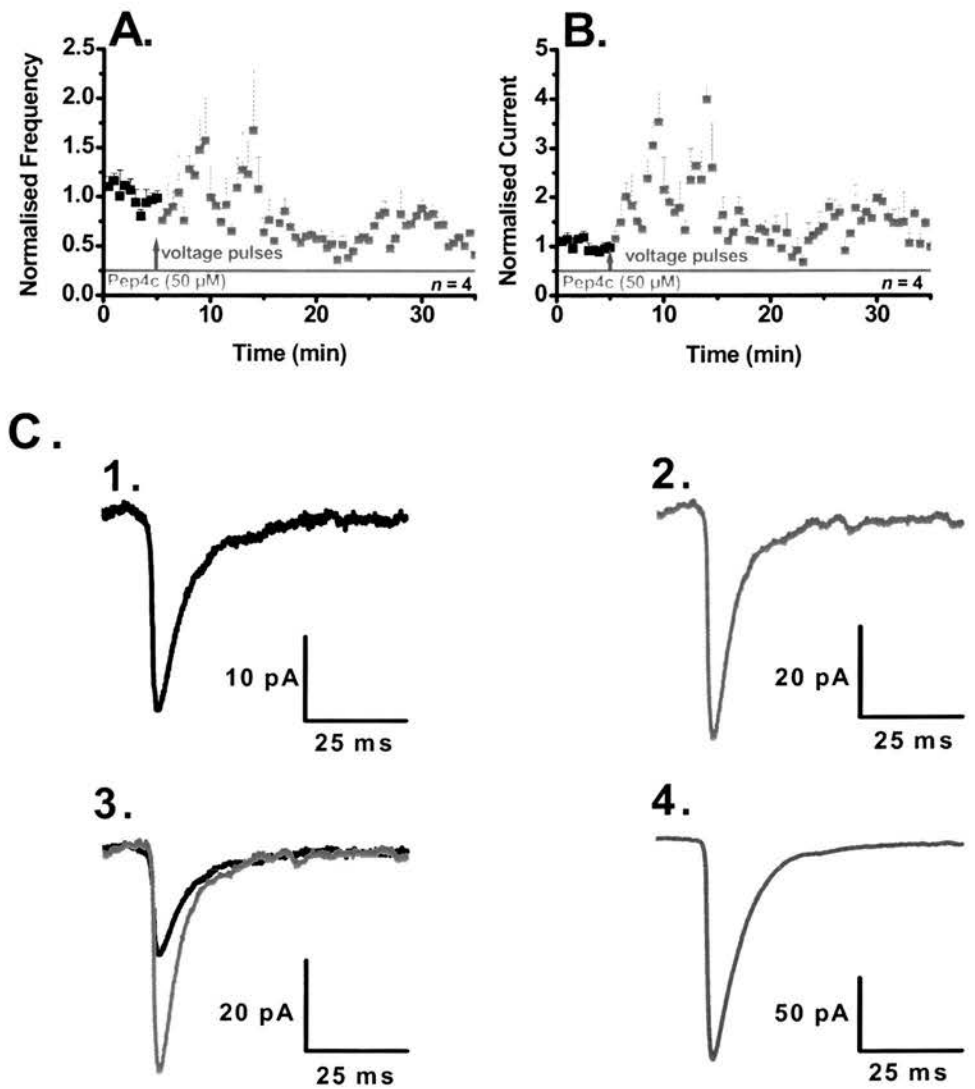

Figure 4.18: **Further characterization of Pep4c.** (A.) Pipette inclusion of Pep4c, allowed for the transient potentiation of mEPSC frequency following VP stimulation (B.) The total current produced by the mEPSCs showed significant but transient potentiation following VP stimulus. (C.) Analysis of 100 mEPSCs from the control period (1.) and the Pep4c treated period (2.) show significant amplitude potentiation, with little change in rise or decay times when overlaid (4.) 100 of the largest mEPSCs from interleaved Pep4c recording (3.).

4.8: Effects of PICK 1 inhibition on mEPSC amplitudes.

Synaptic membrane expression and composition of AMPA receptors has been shown to be dependent upon the action of PICK1 (protein interacting with C-kinase-1) (Terashima et al., 2004). As discussed previously PICK1 interacts with GRIP (glutamate receptor interacting protein) and ABF (AMPA receptor binding protein to facilitate this trafficking but the mechanisms and functional consequence is still unclear. In this experimental study, it was important to characterise the action of Pep2m-AVKI (50 μM) on properties of the mEPSCs. Pep2m-AVKI (Tyr-Asn-Val-Tyr-Gly-Lle-Gln-Ala-Val-Lys-Lle) is a peptide directed against the PICK1/ AMPA receptor binding motif, which should inhibit the ability of AMPA receptors to be functionally inserted into active synapses.

In this series of experiments, the application of Pep2m-AVKI (50 μM) was via the patch pipette, again restricting the application of this peptide to the postsynaptic compartment. This application had no significant effect on the amplitudes of non VP stimulated mEPSCs (Figure 4.19A: Control 19.3 ± 0.7 pA: Pep2m-AVKI 20.0 ± 3.6 pA. $n = 3$).

The scatter plot of all events recorded shows a tight distribution of smaller amplitude events with the occasional lager amplitude mEPSC, there appears no obvious difference between the two groups. mEPSC frequencies show a non significant transient increase (Figure 4.19B: Control 1.5 ± 0.4: Pep2m-AVKI: 1.6 ± 0.2 Hz), and reduce to half of the control frequency by 15 minutes. The current time course for these mEPSCs is nearly stable for the first twenty minutes, with only small non significant deviations from the normalised value (Control 1.3 ± 0.5 nA: Pep2m-AVKI 1.4 ± 0.2 nA). At twenty minutes there is a large deviation in the mEPSC current plot; this was caused by the single cell burst activity and results in a current value of 2.6 ± 2.0 nA,

Analysis of 100 control Pep2m-AVKI mEPSC indicates little difference in the kinetic parameters of theses events when compared to other control mEPSC from other peptide experiments, the mean mEPSC has an amplitude of 21.7 ± 0.7 pA and displays rise and τ decay times of 2.0 ± 0.1 ms and 11.1 ± 1.0 ms respectively (Figure 4.20). Analysis of 100 mEPSCs from the Pep2m-AVKI period indicate a mEPSC with a mean amplitude of 22.0 ± 1.0 pA and displays rise time and decay time constant of 1.9 ± 0.2 ms and 12.5 ± 0.9 ms respectively.

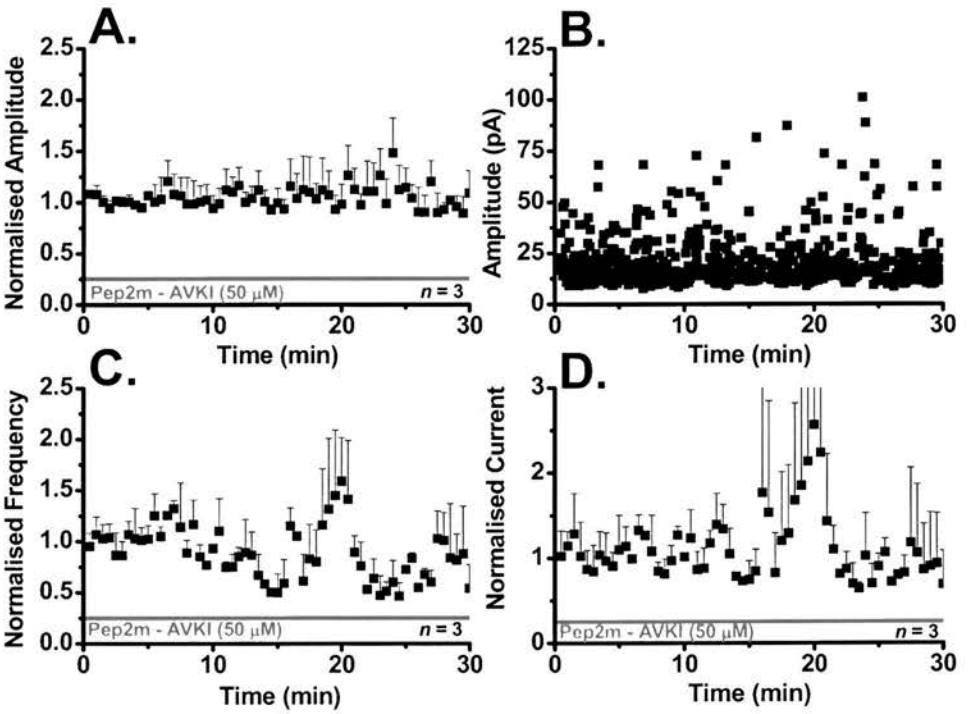

Figure 4.19: **Pep2m-AVKI does not affect non potentiated mEPSC amplitudes**. (A.) Control recording show no significant change in mEPSC amplitude with application of Pep2m-AVKI (50 μM). (B.) The distribution of mEPSC amplitudes does not increase with application of Pep2m-AVKI. (C.) mEPSC frequency reduces with the inclusion of Pep2m-AVKI across the experimental time course. (D.) Inclusion of Pep2m-AVKI has no significant effect on non VP stimulated mEPSCs.

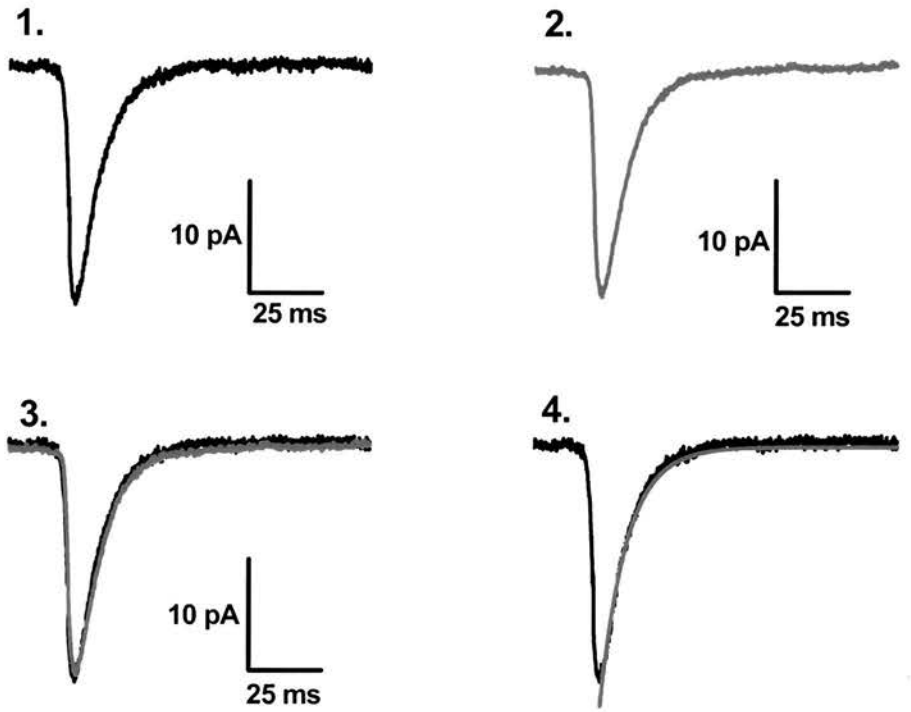

Figure 4.20: **Control Pep2m-AVKI treated mEPSCs.** Analysis of 100 mEPSCs from the 0-5 minute period shows a mEPSCs which typically have mean amplitudes of about 20 pA (1.). Inclusion of the PICKI binding site inhibitor Pep2m-AVKI has no significant effect on the baseline amplitude of the mEPSC (2.). Overlaid events from 0-5 minute and 10-15 minute periods show little difference in the mean amplitude, and rise or decay phase of these mEPSCs are similar (3.). Fitting control mEPSC with a single exponential indicates the goodness of fit for the decay time constant (4.).

4.9: PICK-ing out membrane fusion events underlying mEPSC amplitude potentiation.

In the previous experiment the application of PICK1 binding site inhibitor Pep2m-AVKI has no significant effect on the non VP stimulated mEPSC amplitudes. Pep2m-AVKI (Tyr-Asn-Val-Tyr-Gly-Lle-Gln-Ala-Val-Lys.Lle) peptide sequence is directed against the PICK1/ AMPA receptor binding motif, which should inhibit the ability of AMPA receptors to be functionally inserted into active synapses. In this experimental series the Pep2m-AVKI peptide was applied via the patch pipette. After the application of voltage pulses there is a transient non significant potentiation of mEPSC amplitudes, which retains this elevated level across the time course of the experiment (Figure 4.21A: control 20.0 ± 1.3 pA: VP Pep2m-AVKI 22.8 ± 2.3 pA. n = 8). Interleaved control recordings show a significant potentiation of mEPSC amplitudes after VP stimulation (control 20.4 ± 0.2 pA: VP 40.5 ± 0.2 pA. n = 3). This is highlighted with the Raster plots for this experiment (Figure 4.21 B), which clearly show VP potentiated mEPSCs from the peak of the potentiation which are larger than the control mEPSCs.

The mEPSC frequency time course shows no significant change after the VP stimulus in the presence of Pep2m-AVKI (control 0.6 ± 0.1 Hz: VP Pep2m-AVKI 0.6 ± 0.1 Hz:), but reduces over the rest of the experimental time course. The frequency of mEPSCs from the interleaved control recordings show the typical non significant transient potentiation (Control 0.7 ± 0.1 Hz: VP 1.5 ± 0.4 Hz). VP potentiation of mEPSC currents as with mEPSC amplitudes is blocked by the application of Pep2m-AVKI (control 0.7 ± 0.1 nA: VP Pep2m-AVKI 0.4 ± 0.1 nA), while interleaved control recordings show a 1.5 fold potentiation of mEPSC currents (0.4 ± 0.1 nA : VP 1.9 ± 0.7 nA).

In this single cell experiment the postsynaptic restriction of this peptide, blocked the VP potentiation of mEPSC amplitudes (Figure 4.22A: Control 20.8 ± 0.9pA: VP Pep2m-AVKI 20.2 ± 2.4 pA). This blockade of potentiation is again shown by a lack of change in the distribution of the mEPSC amplitudes. The cumulative probability plots (Figure 4.22 C) for the mEPSC amplitudes in this experiment overlap, highlighting little effect of the VP stimulation in promoting an increase in AMPA receptor number at the synapse. This lack of potentiation highlighted with the histogram of mEPSC amplitudes, which has a clear rightward skew, indicating a high probability of small amplitude mEPSC, in both the Pep2m-AVKI control and the VP stimulated time periods (Figure 4.22 D).

Analysis of 100 mEPSCs from both of the time periods, show little change in the mean amplitudes or kinetic behaviour of these events. Control mean mEPSC was 22.8 ± 0.3 pA with a rise and τ decay time of 2.0 ± 0.3 pA respectively, while the VP Pep2m-AVKI mEPSC had similar values with a mean amplitude of 20.2 ± 0.1 pA and rise and τ decay time of 1.9 ± 0.3 ms and 25.2 ± 2.7 ms respectively. Analysis of 100 mEPSC from the VP potentiated interleaved control show a mEPSC with a mean amplitude of 77.2 ± 2.6 pA with rise time and decay time constant of 2.5 ± 0.1 ms and 28.3 ± 2.2 ms.

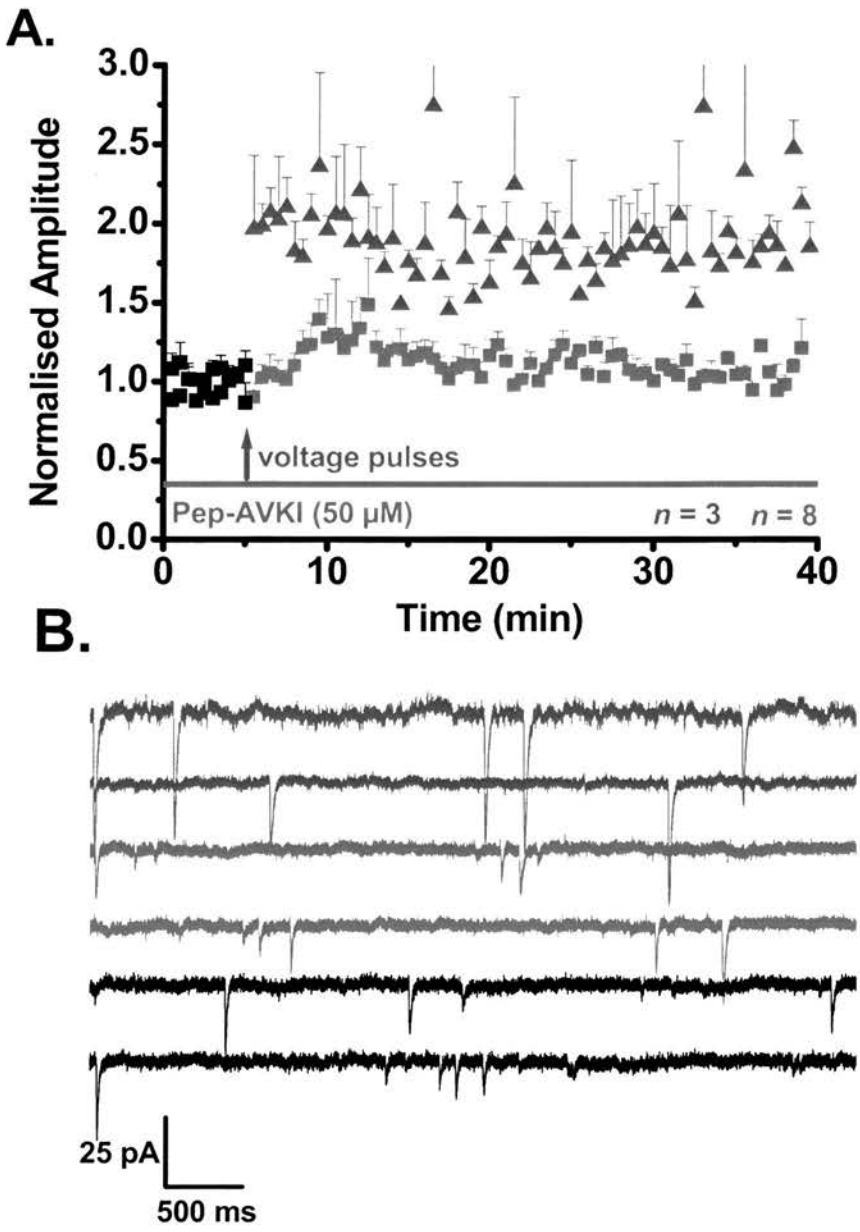

Figure 4.21: **VP potentiation of mEPSC amplitudes was blocked by Pep2m-AVKI.** Pep2m-AVKI blocks the VP potentiation of mEPSC amplitude (B.) **Raster plot of mEPSC events.** Control mEPSCs (**Black**) VP stimulated mEPSCs with Pep2m-AVKI (**Red**) and VP potentiated mEPSCs (**Blue**).

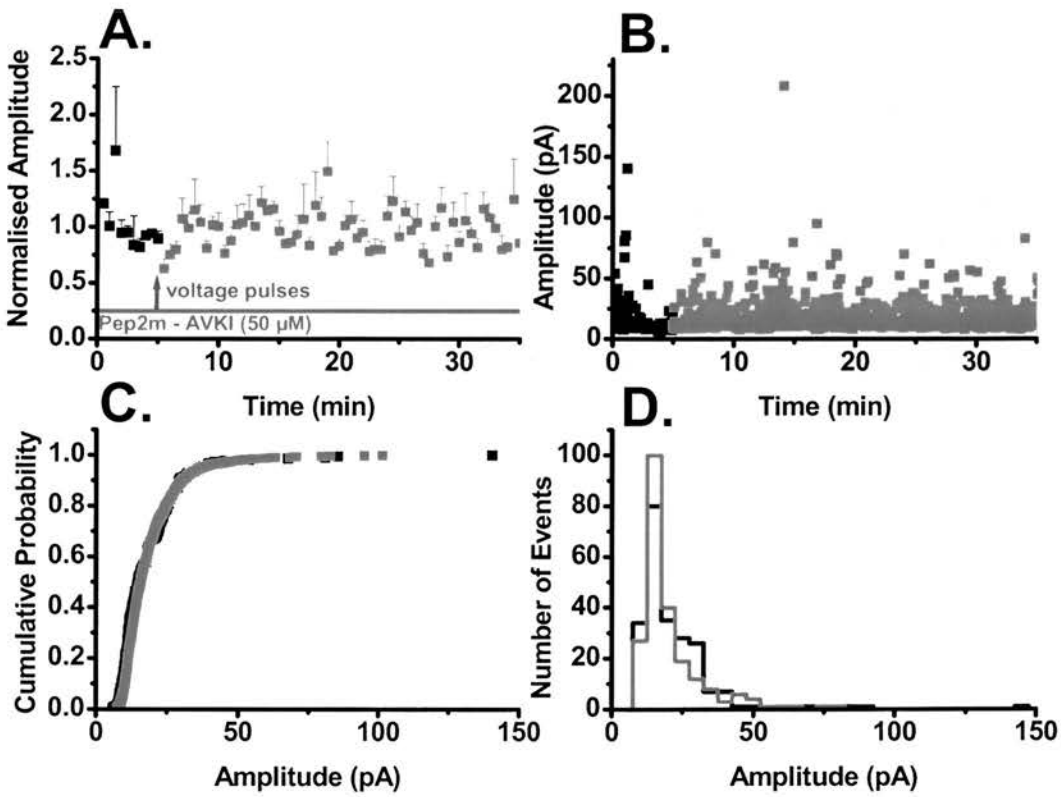

Figure 4.22: **VP potentiation of mEPSC amplitudes was blocked by Pep2m-AVKI (con't).** (A.) A single cell amplitude time course showing blockade of VP potentiation by the pipette inclusion of Pep2m-AVKI. (B.) Corresponding scatter plot of mEPSC amplitudes, showing no increase in event distribution. (C.) Cumulative probability plots for both control and VP stimulated Pep2m-AVKI treated mEPSCs overlap, indicating no increases in mEPSC amplitudes following stimulation. (D.) Amplitude histograms for control and Pep2m-AVKI mEPSC over the same time period (5 min) show no significant change in event distribution.

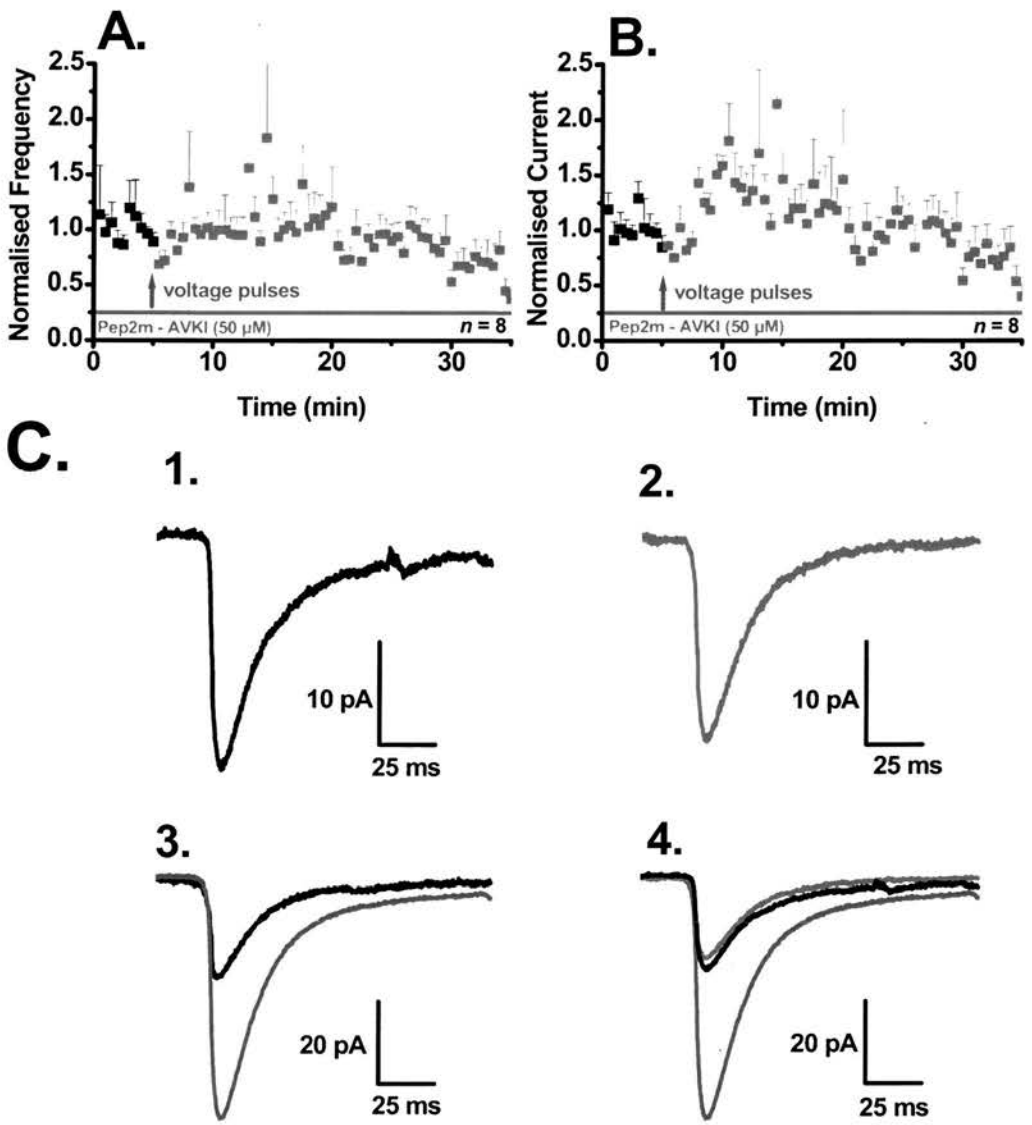

Figure 4.23: **Further characterization of Pep2m-AVKI block of VP potentiation.** Pipette inclusion of Pep2m-AVKI blocked the VP potentiation of mEPSC frequency (A.) and allowed for a small transient potentiation of mEPSC currents (B.) **mEPSC overlays for Pep2m** (C.) Analysis of 100 mEPSCs from the control period (1.) and the Pep2m- AVKI treated period (2.) show no significant change in rise or decay times when overlaid (4.) mEPSCs from interleaved control recording have significantly larger amplitudes following VP stimulation (3.).

4.10: Importance of GluR1 AMPA receptor

CA1 pyramidal cells typically have two types of AMPA receptors, protein complexes made up from hetro-dimers of either GluR1/GluR2 receptors or GluR2/ GluR3 receptors. So far, the investigation of the receptor requirements for VP potentiation of mEPSC amplitudes has shown a dependency upon the GluR2 receptor. The purpose of this series of experiments is to classify the effects of GluR1 inhibition on non VP stimulated mEPSCs. To facilitate this study Pep1-TGL (Ser-Ser-Gly-Met-Pro-Leu-Gly-Ala-Thr-Gly-Leu) was applied via the patch pipette restricting its application to the postsynaptic cell only. Pep1-TGL is a peptide sequence targeted to the TGL motif that corresponding to the C terminus of the GluR1 subunit. TGL motif represents the binding site for the structural protein SAP 97, usually utilized for the transport of the NMDA receptor subunits.

Inclusion of this peptide (Pep1-TGL 50 μM) had no significant effect on the amplitudes of mEPSCs across the experimental time course (Figure 4.24 A: Control 21.7 ± 2.3 pA: Pep1-TGL 23.1 ± 3.1 pA. n = 3). The amplitude of all mEPSCs was shown in a typical scatter plot and indicates no major changes in distribution. The plot of the frequency mEPSCs with Pep1-TGL indicates no significant change in mEPSC frequency across the time course (Figure 4.24C: Control 0.5 ± 1.6 Hz: Pep1-TGL 0.5 ± 0.1 Hz). Furthermore inclusion of Pep1-TGL had no significant effect on total mEPSC current (Figure 4.24 D: control 0.3 ± 0.1 nA: Pep1-TGL 0.5 ± 0.2 nA)

Analysis of 100 control Pep1-TGL mEPSC indicate a mean control mEPSC with an amplitude of 21.3 ± 0.1 pA and displays rise and τ decay times of 2.0 ± 0.2 ms and 16.5 ± 1.1 ms respectively. Analysis of events from the Pep1-TGL period indicate a mean event with an amplitude of 21.9 ± 0.1 pA with a rise time and decay time constant of 2.1 ± 0.2 ms and 14.6 ± 0.9 ms respectively.

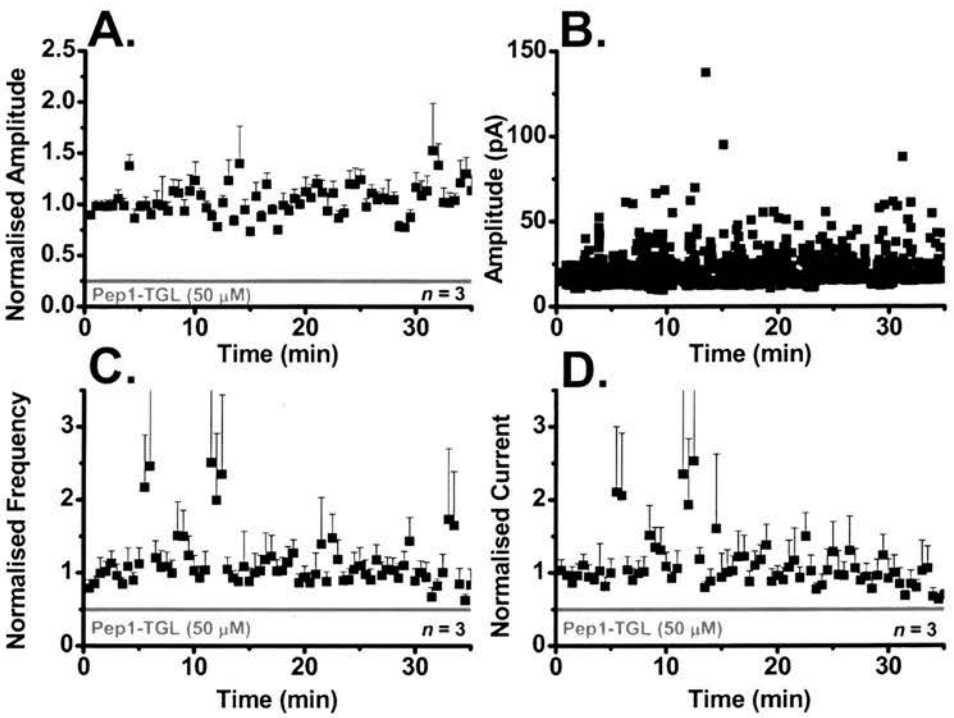

Figure 4.24: **Pep1-TGL does not affect non potentiated mEPSC amplitudes**. (A.) Control recording show no significant change in mEPSC amplitude with inclusion of Pep1-TGL (50 μM). (B.) The distribution of mEPSC amplitudes does not increase with inclusion of Pep1-TGL. Application of Pep1-TGL had no significant effect on either mEPSC frequency (C.) or total current (D.).

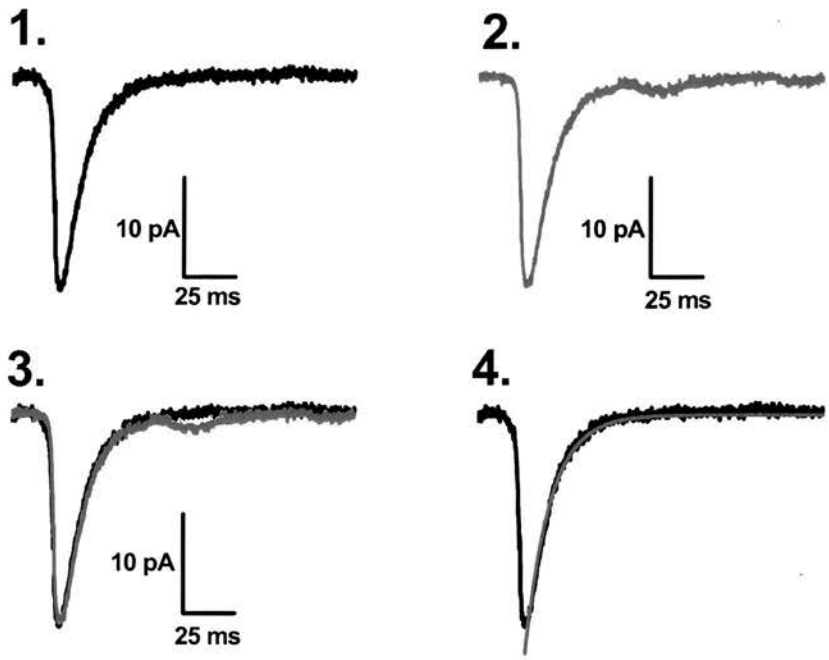

Figure 4.25: **Control experiments with Pep1-TGL.** Average of 100 mEPSCs from the control period shows mEPSCs which typically have mean amplitudes of about 20 pA (1.). Application of Pep1-TGL has no significant effect on the baseline amplitude of the mEPSC (2.). When these mean events are overlaid, there is little difference in the mean amplitude, and rise or decay phase of these mEPSCs are similar (3.). Fitting control mEPSC with a single exponential indicates the goodness of fit for the decay time constant.

4.11: Blockade of the GluR1 receptor, inhibits the VP potentiation of mEPSC amplitudes.

In the previous set of experiments, it was found that the compartmentalized application of Pep-TGL had no significant effect on the amplitudes of non VP stimulated mEPSCs. In this series of experiments, the same peptide was used to determine if the GluR1 receptor is required for the VP potentiation of mEPSC amplitudes, as the GluR1 subunits exploit trafficking pathways usually reserved for NMDA receptor subunits.

Following the application of the VP stimulus to the Pep1-TGL infused CA1 pyramidal cells there was no significant increase in the amplitudes of the mEPSCs (Figure 4.26A: Control 21.5 ± 1.6 pA: VP Pep1-TGL 22.7 ± 0.10 pA), while interleaved control VP recordings indicate a potentiation of mEPSC amplitudes (Control 22.2 ± 1.9: VP 40.5 ± 2.1pA. $n = 5$).

The cumulative probability plots (Figure 4.27C) for the mEPSC amplitudes in this experiment overlap, highlighting little effect of the VP stimulation in promoting an increase in AMPA receptor number at the synapse. This lack of potentiation was highlighted with the histogram of mEPSC amplitudes, which has a clear leftward skew, indicating a high probability of small amplitude mEPSCs, in both the Pep1-TGL control and the VP stimulated time periods.

mEPSC frequency following the VP stimulus shows a 1 minute burst period and transient not significant potentiation of mEPSC frequency (Figure 4.28 A: Control 0.6 ± 0.1 Hz: VP Pep1-TGL 0.7 ± 0.1 Hz). Inclusion of Pep1-TGL as expected further blocked the potentiation of mEPSC currents (Figure 4.28B: Control 0.4 ± 0.1 nA: VP Pep1-TGL 0.5 ± 0.1 nA), while interleaved total mEPSC currents potentiated.

Analyses of 100 mEPSCs from both of the time periods show little change in the mean amplitudes, rises and decay times of these mEPSCs. Control mean mEPSC amplitude was 20.1 ± 0.4 pA with a rise and τ decay time of 1.3 ± 0.3 ms and 13.4 ± 1.1 ms respectively, while the VP Pep1-TGL mEPSC had similar values with a mean amplitude of 19.8 ± 0.3 pA and rise and τ decay time of 1.4 ± 0.2 ms and 14.8 ± 1.2 ms respectively. Analysis of 100 mEPSC from the VP potentiated interleaved control show a potentiated mEPSC has a mean amplitude of 44.1 ± 0.8 pA with a rise time and decay time constant of 1.8 ± 0.2 ms and 14.1 ± 0.8 ms respectively.

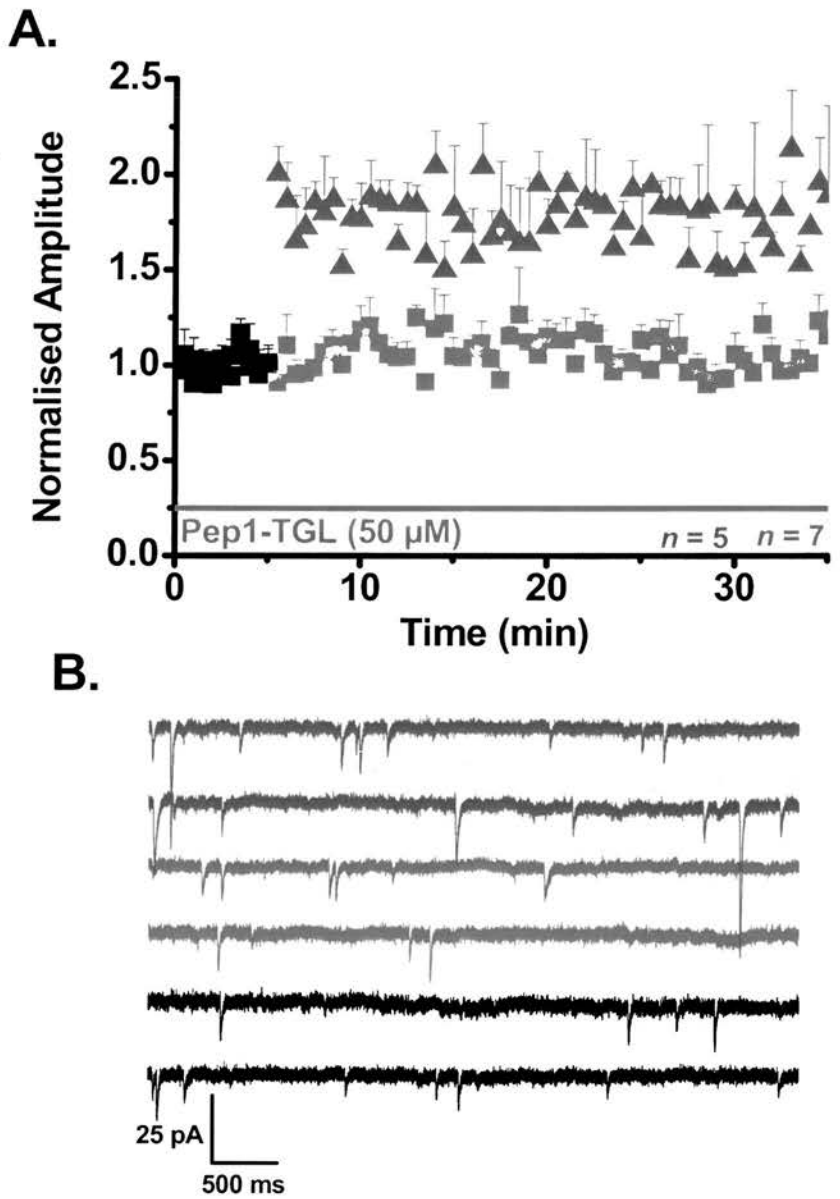

Figure 4.26: **VP potentiation of mEPSC amplitudes was blocked by Pep1-TGL.** (A.) Pep2m-AVKI blocks the VP potentiation of mEPSC amplitude (B.) **Raster plot of mEPSC events.** Control mEPSCs (**Black**) VP stimulated mEPSCs with Pep1-TGL (**Red**) show not significant difference in mEPSC amplitude, while VP potentiated mEPSC amplitudes are larger (**Blue**).

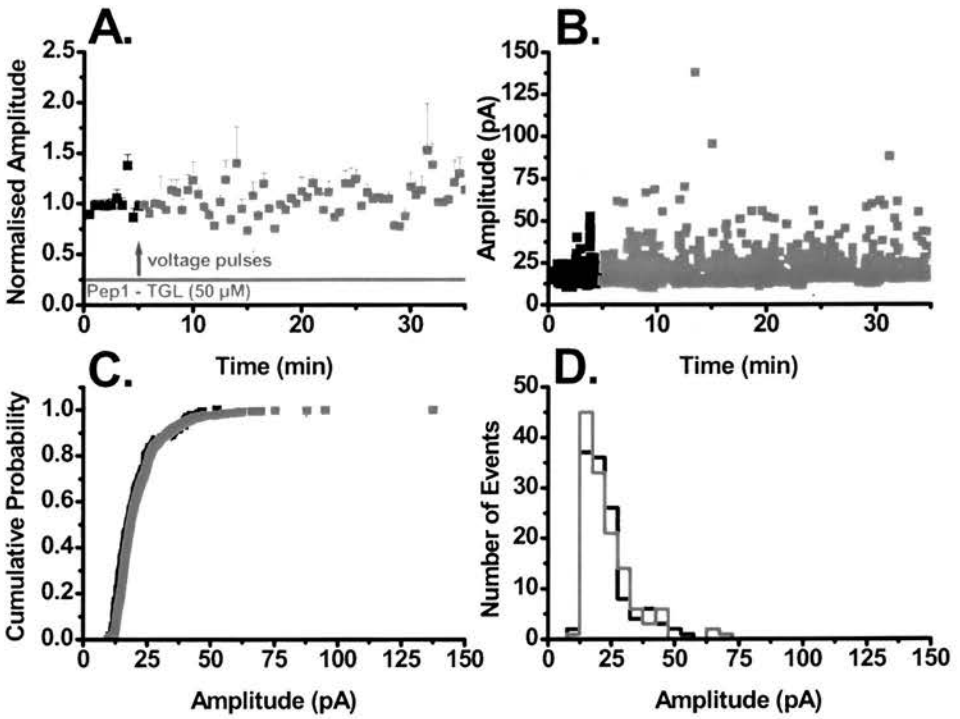

Figure 4.27: **Pep1-TGL blocks the VP potentiation of mEPSC amplitudes**. (A.) A single cell example, pipette inclusion of Pep1-TGL blocks the VP induced potentiation of mEPSC amplitudes. (B.) The distribution of mEPSC amplitudes does not increase with application of Pep1-TGL. (C.) Cumulative probability plots overlap indicating little difference between the two groups (D.) Amplitude histogram for control and Pep1-TGL (5 min following application) show no significant change in the amplitude distribution of the mEPSCs.

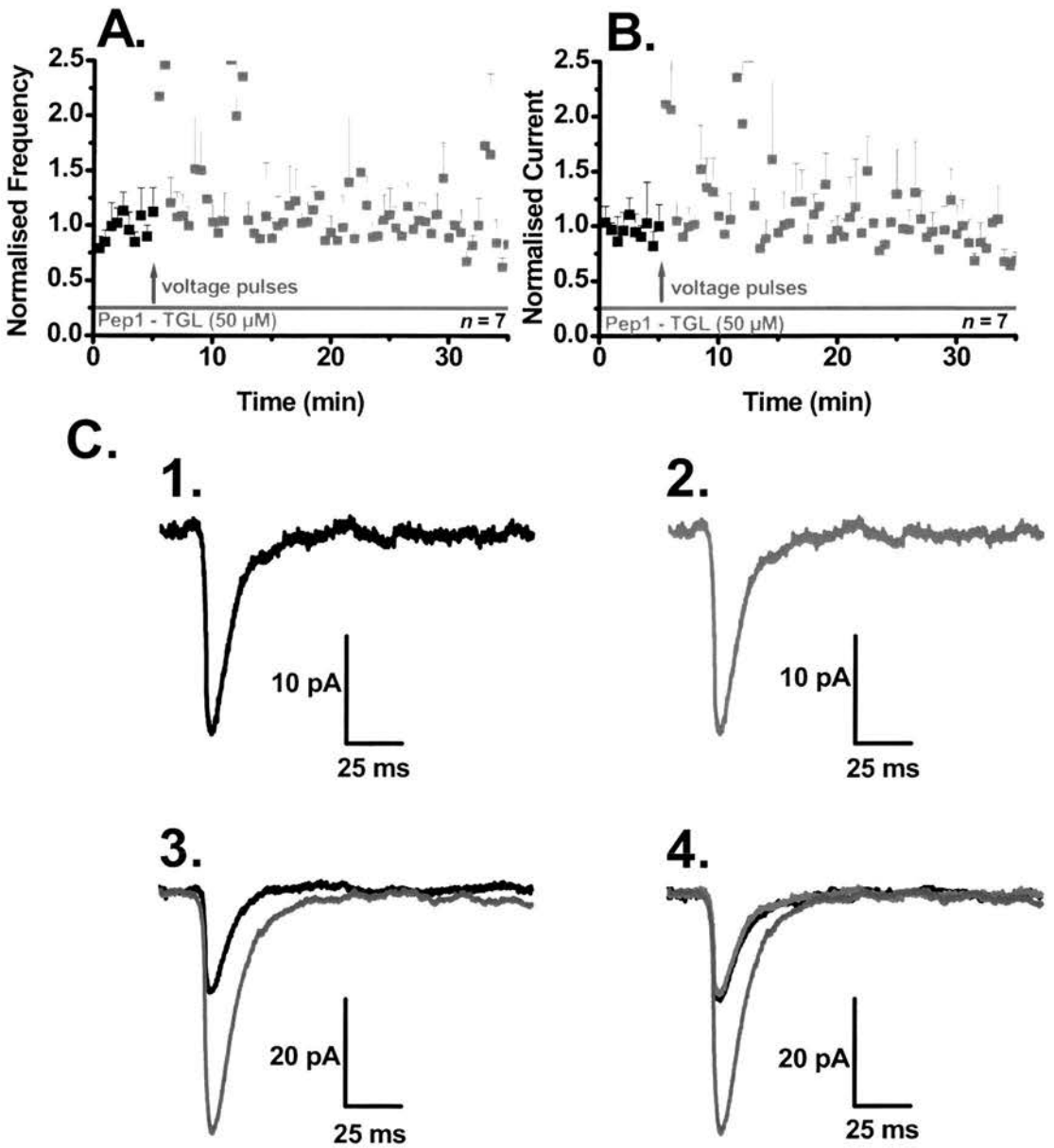

Figure 4.28: **Further characterization of Pep1-TGL block of VP potentiation.** Pipette inclusion of Pep1-TGl blocked the VP potentiation of mEPSC frequency (A.) and mEPSC currents (B.) **mEPSC overlays for Pep1-TGL** (C.) Analysis of 100 mEPSCs from the control period (1.) and the Pep1-TGl treated period (2.) show no significant change in rise or decay times when overlaid (4.) mEPSCs from interleaved control recording have significantly larger amplitudes following VP stimulation (3.).

Discussion- Voltage pulse potentiation is dependent upon post synaptic membrane fusion events

So far I have shown that the voltage pulse stimulating protocol brings about reliable sustainable potentiation of mEPSC amplitudes and that this potentiation is presumably mediated via the insertion of new AMPA receptors into activated synapses or changes in the conductance of these receptors. If this potentiation of mEPSC amplitudes is mediated by the insertion on AMPA receptors, then what are the mechanistic pathways involved in this insertion. To answer this I looked at previously identified transport pathways to determine if they impact on the voltage-pulse potentiation of mEPSC amplitudes.

4.12: Importance of NSF to voltage-pulse potentiation

NSF (N-ethylmaleimide sensitive fusion protein) is a core protein found to exist individually and as a component of two presynaptic protein complexes SNAP25 - soluble NEM attachment protein of 25 kDa and SNARE (transmembrane SNAP receptors) complex. Both of which are required for the induction of calcium dependent presynaptic vesicular docking bringing about the release of neurotransmitter (Chen et al., 1999; May et al., 2001). Surprisingly within pre- and postsynaptic terminals there is a synergy of function and the same proteins have been shown to regulate the delivery of AMPA receptors to the postsynaptic membrane (Song et al., 1998; Braithwaite et al., 2000; Braithwaite et al., 2002). More specifically it has been demonstrated that there is an association between the NSF protein and the GluR2 AMPA receptor, the subunit which confers the Ca^{2+} impermeability of the AMPA receptors (Osten et al., 1998; Osten and Ziff, 1999; Shi et al., 2001). This receptor trafficking method is not unique to AMPA receptors but is also utilised by the nicotinic α7 receptor subunit (Liu et al., 2005).

In the initial set of experiments, I included the NSF inhibitor N-ethylmaleimide (NEM 5 mM) in the internal solution compartmentalizing the application of this inhibitor to the postsynaptic cell. I appreciate that the chemical structure of this inhibitor will confer a degree of membrane permeability; leak of NEM from the postsynaptic cell would inhibit vesicle release and ultimately influence mEPSC frequency. From my experiments this aspect might be applicable as over the time course of the experiment there was significant reduction in mEPSC frequency, by nearly 1 event per second. Alternatively there exists the possibility of a reduction in postsynaptic detection, expressed by changes to the normal AMPA receptor turn over rate, as receptors would be removed but not inserted due to the block by NEM, this reduction in functional postsynaptic component creating only

whispering synapses (Voronin and Cherubini, 2004). This would also be observed as a change in frequency – this needs to be investigated further.

The primary focus of the experiments described in this Chapter is to provide insight into mechanisms which govern mEPSC amplitude changes; application of NEM, in the absence of voltage-pulses did not significantly affect the mean amplitude of the mEPSCs. This may be seen as an unusual finding when considering, the possibility that the frequency change is mediated by a loss of postsynaptic sites. The consideration that the amplitude distribution of all the mEPSCs is very tight and that the reduction in synaptic site number is most likely to occur from the least strong synapses first, which would result in the loss of small amplitude mEPSC. This loss is unlikely to make a significant enough impact on mean mEPSC amplitudes due to the normalizing process. Furthermore, there is no significant difference in the amplitude histogram of control and NEM treated mEPSCs, implying no major changes in mEPSC amplitude distribution.

Stimulating with the voltage pulse protocol induced the typical inward calcium currents induced by the depolarizing phase of the voltage-pulses protocol. These currents have previously been shown to result from the activation of L-type calcium channel. Application of NEM blocked the voltage-pulse potentiation of mEPSC amplitudes, while interleaved control recordings showed typical potentiation of mEPSC amplitudes.

The conclusion from this experiment is that NSF protein or structures containing this protein domain found in the postsynaptic compartment, regulate the insertion of AMPA receptors during voltage-pulse potentiation of mEPSC amplitudes. Interestingly the mEPSC frequency time course shows a similar reduction to that shown in the control recordings, however there is a very obvious DSI current (Wilson et al., 2001) as discussed with normal voltage-pulse recordings shown with this experiment. Moreover the voltage-pulse stimulation of NEM treated mEPSCs has no significant effect on the rise time and decay time constant of the mEPSCs.

To further develop the idea that receptor insertion mediates voltage-pulse potentiation of mEPSC amplitudes, I decided to target SNAP-25, a NSF containing adaptor protein. SNAP 25 is specifically cleaved by the application of botulinum toxin A (Botox). Furthermore this application of Botox, when included in the patch-pipette does not cross through the membrane. Indeed if this was to occur then there would be a total blockade of vesicular release at the affected synapses. The small change in mEPSC frequency does not support this idea. Pipette inclusion of Botox blocked the voltage-pulse potentiation of mEPSC amplitudes, while interleaved control data showed potentiation of mEPSC amplitude but with a different profile across the time course. Again this experiment indicates a

requirement for the NSF containing SNAP 25 in the voltage pulse potentiation of mEPSC amplitudes.

The transient potentiation of mEPSC frequency shown with the voltage-pulse stimulus is similarly blocked by the application of Botox, the reduction in mEPSC frequency is similar to the reduction shown with NEM although the control frequency is lower. This finding does not aid the explanation, as to the site of mEPSC frequency change, or even if that explanation is realistic. As I am assuming that the rate of release is almost constant, therefore I feel that this reduction in event frequency is mediated by a balance between both pre (reducing vesicle release) and postsynaptic mechanisms (reduction in the number of active synapse).

4.13: Peptide inhibition of voltage-pulse potentiation

To this point I have used, one selective and one broad spectrum inhibitor of membrane fusion events to determine the relationship between the NSF protein and insertion of AMPA receptors into active synapses. To develop this idea further, I selected the same site of inhibition but used the complementary target. This was achieved by using selective peptides targeted to the NSF binding site on the intracellular C terminal of the GluR2 receptor. This experiment has many advantages over the standard NEM experiment, as these peptides are specific for only one site i.e. the actual receptor which is being inserted, and is reported to have no significant effect on the NSF and SNAP 25 protein structures. Due to the fact that they are composed of ten amino acids they do not display membrane permeability which is a potential issue with the NSF experiments. In a set of control experiments Pep2m a peptide sequence target to the GluR2 NSF binding site had no significant effect on the mEPSC amplitude time course. Evidence from other groups using the traditional presynaptic stimulus for EPSC recording reported that application of this peptide resulted in a reduction in control amplitudes of the EPSCs (Nishimune et al., 1998; Song et al., 1998; Osten and Ziff, 1999; Song and Huganir, 2002). The possible explanation for this difference could be referenced to the synaptic silencing generated by the applied stimulus required for the generation of the EPSC (Xiao et al., 2004).

Again a reduction in mEPSC frequency was shown with the inclusion of this peptide, but as discussed before this result is a source of further study as the source for this change is undeterminable at this time with this experimental setup.

The potentiation of mEPSC amplitudes by application of voltage pulses was blocked by the pipette inclusion of Pep2m, confirming the NEM results and further indicating that it is the interaction between the NSF peptide and GluR2 AMPA receptor subunit which

mediate this potentiation. The experimental versatility of the peptides was next utilised as a simple single amino acid substitution at position 8 where an asparagine ($R\text{-}CH_2CONH_2$) residue is replaced by a serine ($R\text{-}CH_2OH$) residue renders a functionally inactive peptide (Pep4c). Application of Pep4c does one of two things it proves that application of this inactive form does not inhibit the voltage-pulse potentiation of mEPSC amplitudes; in fact application of this peptide consistently generated some of the largest mEPSCs recorded in the study. The second, that the block of potentiation produced by Pep2m is simply not due to a non-specific effect, brought about by the postsynaptic compartmentalized application of this peptide. Furthermore the rundown in event amplitude shown with EPSC recording was not evident with the mEPSC amplitudes following the voltage-pulse stimulus, strengthening the possibility that this rundown is dependent upon repetitive stimulation (Prof John Isaac supports this experimental premise- personal communication Neuroscience San Diego 2004) As with typical voltage-pulse recordings the application of Pep4c does not block the potentiation of mEPSC frequency or total current produced by these pyramidal cells

4.14: Other AMPA receptor delivery mechanisms

NSF dependent delivery mechanisms for AMPA receptor insertion into active synapses is not the only transport mechanism for these receptors. AMPA receptors can be trafficked by three PDZ domain containing proteins, which are structurally unique. Single PDZ containing structural protein, PICK1 (protein interacting with C kinase 1) and the larger multi PDZ containing proteins GRIP1 (Glutamate receptor interacting protein 1) and ABP (AMPA receptor binding protein) form protein complexes which assemble into scaffolding networks with which AMPA receptors associate in order to facilitate activity dependent receptor insertion.

AMPA receptors have also been found to hijack the traditional NMDA receptor delivery pathway requiring postsynaptic density protein PSD 95, via a secondary attachment protein Stargazin (Chen et al., 2000; Choi et al., 2002; Schnell et al., 2002; Vandenberghe et al., 2005)

In this series of experiments I applied a derivative of Pep2m, again via the pipette solution compartmentalising its application to the postsynaptic cell. This derivative Pep2m-AVKI is specifically targetted to the PICK1 binding site on the C-terminus of the GluR2 AMPA receptor subunit, while not affecting the interactions of the AMPA receptor with either GRIP or ABP. Inclusion of this peptide in the non-potentiated mEPSC recordings had no significant effect on the non-potentiated mEPSC and mEPSC frequency and current

displayed the typical pattern of reduction across the time course of the experiment apart from a period of burst activity the trend is the same.

Application of the voltage pulse, in the presence of Pep2m-AVKI did not give the usual degree of potentiation of mEPSC amplitudes although a small, but significant, potentiation of mEPSC amplitudes of around 20 % was observed for a 10 minute period following stimulation. It is tempting to suggest that this resulted through the interaction of the GluR2-GluR3 receptor with ABP (Srivastava et al., 1998; Wyszynski et al., 1999; Osten et al., 2000). Furthermore interleaved control recordings highlighted that typical potentiation of mEPSC amplitude was in fact possible. Therefore this small potentiation of mEPSC amplitude may be mediated by the actions of GRIP1/ABP, while generation of full voltage-pulse potentiation may require a functional interaction between the GluR2 AMPA receptor subunit and PICK 1.

The application of this peptide blocks the transient frequency potentiation of mEPSC amplitude, but does not fully mask the potentiation of the total current which shows a small increase (30 %) across the time course as the amplitude potentiation. This change is vastly smaller than the current change shown with voltage-pulse potentiation which is approximately a 2.5 fold increase following the voltage-pulse stimulus.

4.15: AMPA receptor subunit composition

In mature hippocampal pyramidal cells, the subunit composition of AMPA receptors are considered to be heterodimers of either GluR1-GluR2 subunits or GluR2-GluR3 subunits (Wenthold et al., 1996). GluR4 subunits are expressed early in development and are replaced by the adult repertoire of subunits by the seventh post natal day (Zhu et al., 2000).

LTP studies have indicated that complexes of GluR1-GluR2 subunits are rapidly inserted following synaptic stimulation, with these later being replaced with complexes of GluR2-GluR3 (Shi et al., 2001; Lee et al., 2003).

In a final series of experiment I used a peptide (Pep1-TGL) that interacted with a motif found only on the short C terminus of GluR1 receptors. This TGL motif has been shown to be the site of interaction of the GluR1 subunit with PDZ domains of SAP97 and PSD95 (Leonard et al., 1998; Lisman and Zhabotinsky, 2001; Lim et al., 2002; Rumbaugh et al., 2003), NARP (O'Brien et al., 1998; O'Brien et al., 1999; O'Brien et al., 2002), protein 4.1 (Ruberti and Dotti, 2000; Shen et al., 2000), stargazin (Lim et al., 2002; Schnell et al., 2002) and PICK1 (Hirbec et al., 2002). Application of this peptide blocks only the trafficking of GluR1- GluR2 subunits, and had no significant effect on the non potentiated mEPSC currents. Following voltage-pulse stimulation the typical potentiation of mEPSC amplitudes

shown in the interleaved control experiments was blocked by Pep1-TGL. These results further demonstrated that the initial potentiation of mEPSC amplitude is unlikely to be mediated by the insertion of GluR2-GluR3 subunits and that the later replacement synaptic GluR1-GluR2 subunits by GluR2- GluR3 is dependent upon the insertion of the GluR1-GluR2, as there were no late stage changes in mEPSC amplitudes indicative of an increase in AMPA receptor number.

This concludes the characterisation of the requirement of post synaptic membrane fusion events to facilitate the insertion of different AMPA receptor subunits, to bring about the potentiation of mEPSCs in CA1 pyramidal neurones in organotypic slice cultures.
In the next Results Chapter I will describe a series of experiments that test directly the kinase regulation of voltage pulse potentiation, in particular the requirement for a poorly described kinase (PI-3 kinase) which is essential for the development of voltage pulse potentiation.

Chapter Five:

Kinase regulation of voltage-pulse potentiation

Kinase regulation of VP potentiation

The kinase regulation underlying the regulation of voltage pulse potentiation was initially addressed by (Wyllie and Nicoll, 1994), who found both a role for CaMKII (Lisman et al., 2002; Poncer et al., 2002) in initiating the potentiation of mEPSC amplitudes, and with further experimentation revealed a sustainable form of VP potentiation would be achieved by blockade of postsynaptic phosphatases. The differing expression of VP potentiation of mEPSC amplitudes shown in this study, in combination with other studies showing a requirement for PI-3 kinase in mediating glycine induced LTP of synaptic transmission, facilitated investigation of the possible requirement of PI-3 kinase for L-type calcium channel mediated VP potentiation of mEPSC amplitudes.

The function of phosphoinositide 3 kinases (PI-3 Kinase) are not well described in terms of LTP based synaptic plasticity or memory experiments, but is known to be an important signaling molecule in pathways required for LTP including NMDA receptor dependent activation of MAP kinase and Atk/PKB (Perkinton et al., 2002) as well as the upstream regulation of CREB (Du and Montminy, 1998). A role for AMPA receptors regulating CREB has been shown through the PI-3 kinase activation of MAP kinase (Perkinton et al., 1999).

In other systems PI-3 kinase has been shown to play pivotal roles in translating a variety of extracellular stimuli (growth factors and hormones) into a wide range of cellular processes. This kinase is further known to be important in cancer development through regulation of the tumor suppressor PTEN (Cantley and Neel, 1999; Leevers et al., 1999; Leslie and Downes, 2002).

Signal transduction requires the metabolism of inositol phospholipids, and two clear pathways compete for this substrate. The first is the well characterized phospholipase C (PLC) pathway. Hydrolysis of phosphatidylinositiol(4,5) bisphosphate (PtdIns(4,5)P_2) via this pathway produces two products inositol (1,4,5) triphosphate (Ins (1,4,5)P_3) which regulates intracellular release of Ca^{2+} from stores, and diacylglycerol (DAG) which signals PKC. The second metabolic pathway via the phosphoinositide 3-kinases (PI-3 kinase), produces different end products via the phosphorylation of 3'-OH position of the inositol ring of inositol phospholipids and produces phosphatidylinositiol (3) phosphate (PtdIns(3)P), phosphatidylinositiol (3,4) bisphosphate (PtdIns (3,4)P_2) and phosphatidylinositiol (3,4,5) triphosphate (PtdIns(3,4,5)P_3)(Cantrell, 2001).

Inhibition of this reaction is achieved by the broad spectrum PI-3 kinase inhibitor, wortmannin. Wortmannin is a highly cell permeable antifungal antibiotic isolated from penicillium fumiculosum (Wymann et al., 1996; Walker et al., 2000).

5.1: Characterization of wortmannin's effect on non VP stimulated mEPSCs.

In this series of experiments, the effect of PI-3 kinase inhibition on the non VP stimulated mEPSC was characterised. Wortmannin has no significant effect on the amplitudes of non-potentiated mEPSC over the experimental time course (Figure 5.1: control 22.6 ± 0.1 pA: wortmannin 22.4 ± 1.5 pA. $n = 4$). In combination with this a scatter plot of all mEPSC amplitudes from the control period does not indicate an increase in the spread of mEPSC amplitude, when all events are plotted as in a cumulative probability plot there is no apparent difference in the amplitude probabilities between the two groups as both plots overlap. When the amplitude of the mEPSCs from the control period and the first five minutes following application of wortmannin are compared there is no significant difference between the two groups, both groups show a leftward skewed distribution, indicative of small amplitude events. Raster plot of events, indicate no major differences of mEPSC amplitudes between the control and the wortmannin treated events (See Figure 5.2 C). The frequency of mEPSCs did change with the application of wortmannin the frequency of mEPSCs significantly reduces from the control value of 1.4 ± 0.4 Hz to the treated value of 1.3 ± 0.2 Hz and to 0.5 ± 0.2 Hz by the 20-25 minute time period. This reduction in mEPSC frequency is difficult to attribute to the actions of wortmannin as similar frequency reduction is shown in control recordings. This reduction in the frequency of the mEPSCs as expected is paralleled with a reduction in the total mEPSC current. This mEPSC current produced by these pyramidal cells have a control value of 1.5 ± 0.1 nA which is stable across the wortmannin treated period 1.5 ± 0.3 nA, but reduces to 0.6 ± 0.2 nA by the 20-25 minute time period.

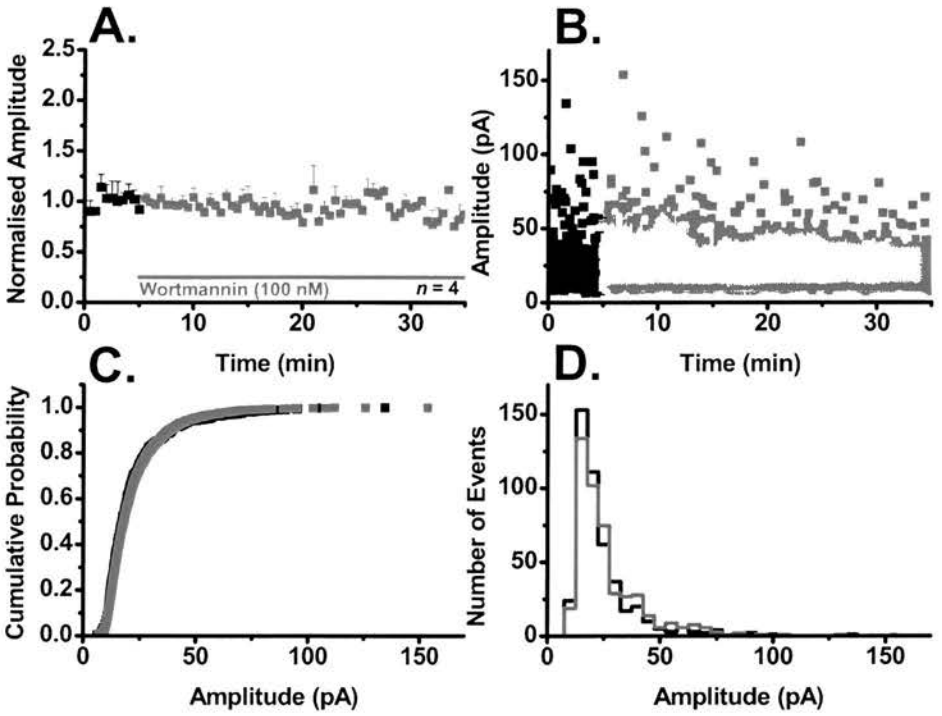

Figure 5.1: **Characterization of wortmannin on non potentiated mEPSCs.** (A.) Application of 100 nM Wortmannin had no significant effect on non potentiated mEPSCs. (B.) The distribution of mEPSC amplitudes does not change significantly with application of wortmannin. (C.) Cumulative probability plots for each data group overlap, indicating no significant differences in mEPSC amplitudes. (D.) Amplitude histogram distributions do not change following the application of wortmannin.

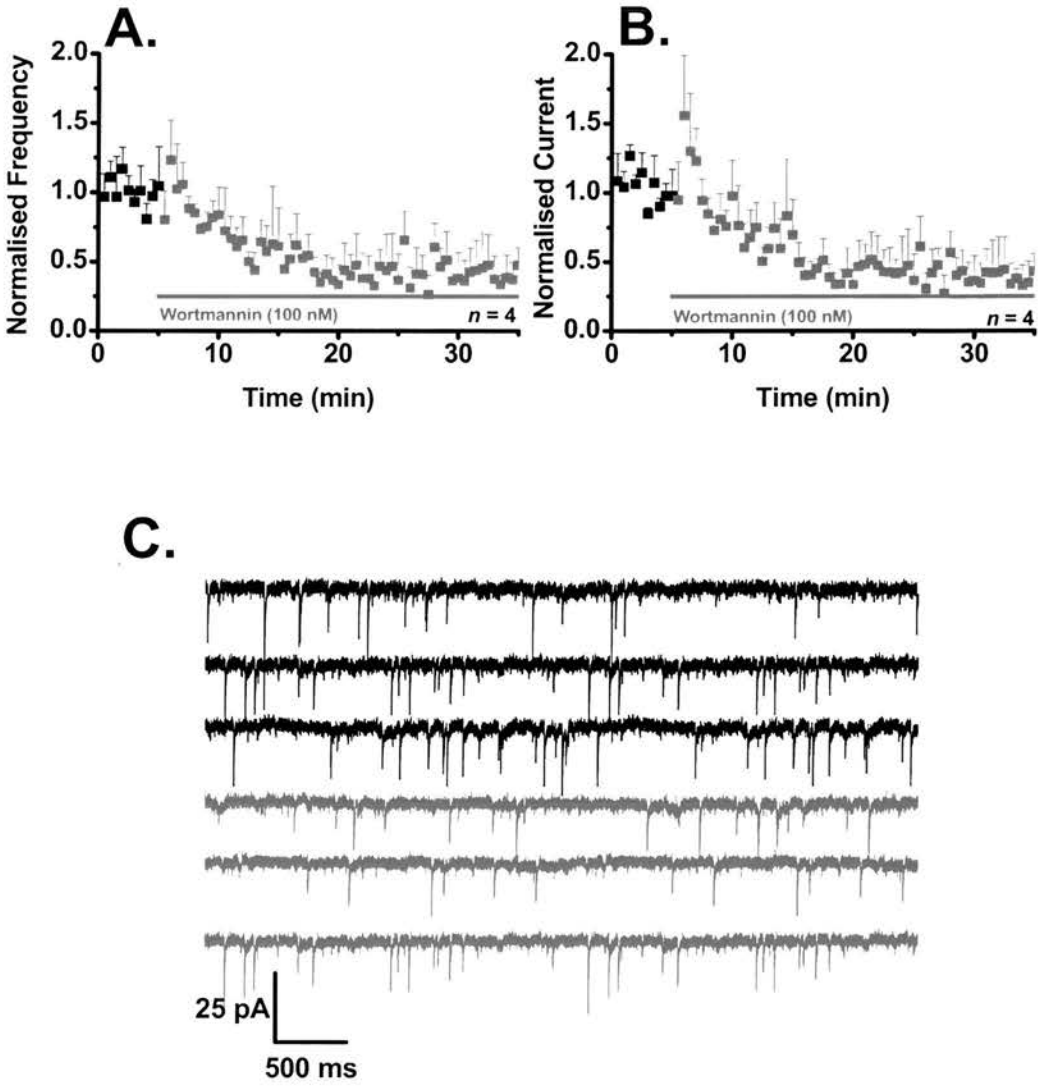

Figure 5.2: **Characterization of wortmannin on non potentiated mEPSCs (con't).** (A.) Application of wortmannin reduces mEPSC frequency across the time of the experiment ($p > 0.05$). (B.) mEPSC total current shows a parallel reduction in mEPSC current is also significant ($p < 0.01$). (C.) mEPSC raster plot, showing both control and wortmannin treated mEPSCs, which have similar amplitudes and frequencies.

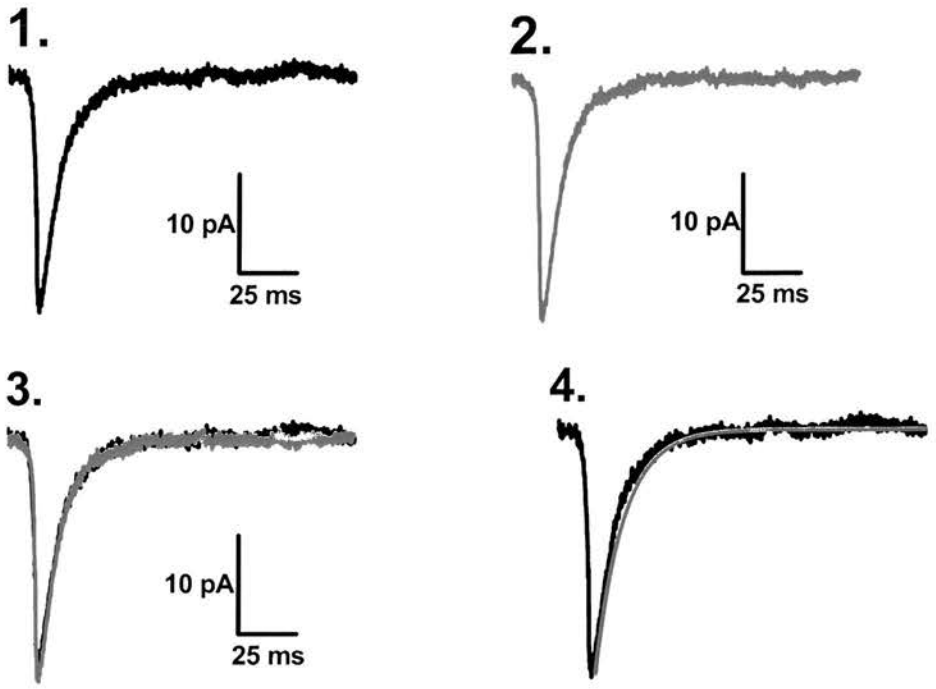

Figure 5.3: **Control wortmannin mEPSC overlays.** Analysis of 100 mEPSCs from the control period show a mean event of 20 pA (1.) which is consistent with control mEPSC mean amplitudes from other recordings. Application of wortmannin (2.) has no significant effect on the mean amplitude of these mEPSC, and showed little difference in the rise and decay times of these events when overlaid (3.). Fitting the decay time exponential to the control mEPSC indicates the goodness of fit for these events (4.).

5.2: Blockade of PI-3 kinase inhibits the potentiation of mEPSC amplitudes.

In the previous experimental series, wortmannin failed to have any significant effect on the amplitudes of the non VP stimulated mEPSCs, indicating that functional AMPA receptors found in the membrane do not require PI-3 kinase for normal function. In the next series of experiments, the objective was to characterise the induction phase of VP potentiation, that is PI-3 kinase activity required for the induction of VP potentiation of mEPSC amplitudes?

In this series of experiments bath application of wortmannin (100 nM) blocked the induction of VP potentiation of mEPSC amplitudes (Figure 5.4A: control 23.8 ± 2.1 pA: VP Wortmannin 23.8 ± 3.8 pA. n = 8). In a series of interleaved control data, the VP stimulus induced a significant increase in the amplitudes of the mEPSCs (control 21.83 ± 2.4 pA: VP 43.5 ± 5.0 pA. n = 6). Typical mEPSCs from each experimental period are shown in figure 5.5B, mEPSCs from the interleaved controls, show significantly larger amplitudes.

A single cell representation displays this lack of potentiation following the VPs; again a scatter plot does not highlight any significant spread of mEPSC amplitudes. Cumulative probability plot for both control and VP stimulated wortmannin treated mEPSCs overlap, indicating a blockade of the VP potentiation of mEPSC amplitudes. Furthermore the leftward distribution of this trace indicates a high probability of small amplitude events. Analysis of the distribution of an amplitude histogram of mEPSCs from both time periods shows no significant differences in the distribution of these histograms, as both traces show a typical leftward skewed distribution.

Application of wortmannin blocked the transient frequency potentiation shown with VP stimulation, as the frequency of mEPSCs reduces across the time course of the experiment (Figure 5.6A: control 1.9 ± 0.4 Hz: VP Wortmannin 1.7 ± 0.3 Hz). The frequency of the interleaved control mEPSCs showed no significant potentiation and reduced across the time course (control 1.2 ± 0.2 Hz: VP 0.9 ± 0.2 Hz: 20-25 minute 0.6 ± 0.1 Hz). Although the magnitude of the VP frequency decrease appears to be significantly greater it is not the case, as this represents a 46 % decrease across the time course, where as the VP wortmannin treated mEPSCs show a 40.6 % decrease across the same time course. Application of wortmannin inhibited any potentiation of mEPSC currents following the VP stimulus (control 1.4 ± 0.4 nA: VP wortmannin 1.4 ± 0.3 nA).

Analysis of one hundred mEPSCs from each time period (figure 5.6C) indicates little or no significant difference in mean amplitudes (control 17.8 ± 0.1 pA: VP Wortmannin 17.9 ± 0.1 pA). The 10-90% rise times for the mean mEPSC are similar for control mEPSCs and the wortmannin treated VP stimulated mEPSCs (control 1.0 ± 0.2 ms: VP Wortmannin 1.3 ± 0.1 ms). Similarly decay time constant show little difference between the two groups (control 9.6 ± 0.9 ms: VP Wortmannin 10.1 ± 1.2 ms).

Analysis of 100 mEPSCs from the peak of the mEPSC potentiation from the interleaved control data show a mean mEPSC with significantly increased amplitude (51.2 ± 0.6 pA), however the rise time and decay time constant are not significantly different for these events (Rise 1.3 ± 0.1 ms : τ decay 9.8 ± 0.7 ms).

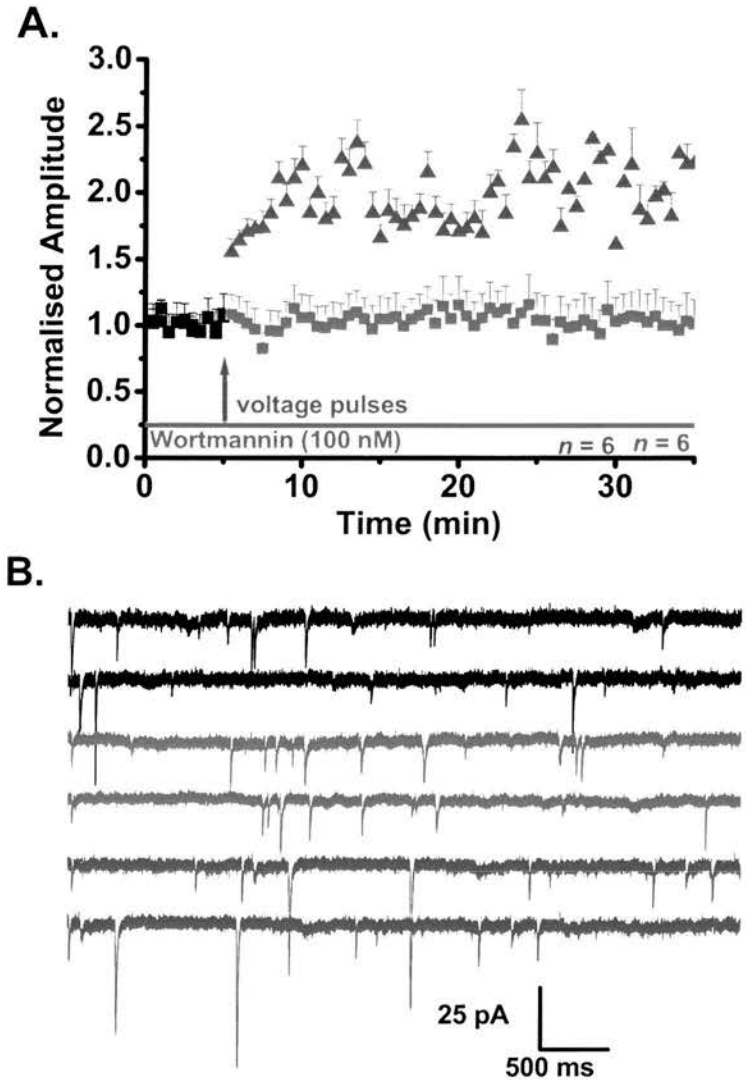

Figure 5.4: **Wortmannin blocks VP potentiation of mEPSC amplitudes.** (A.) bath application of wortmannin (100 nM) blocks the induction of VP potentiation, while interleaved control recordings show typical potentiation of mEPSC amplitudes. (B.) Raster plot of mEPSCs, control and VP stimulated wortmannin treated mEPSCs show similar amplitudes, while interleaved control mEPSC form the potentiated period have much larger amplitudes.

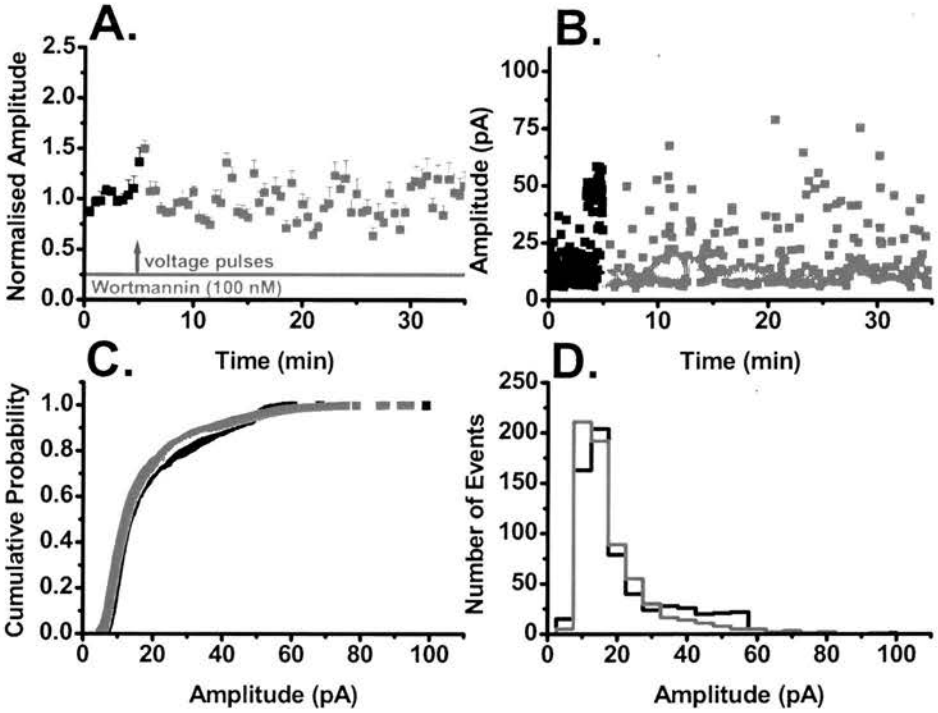

Figure 5.5: **Wortmannin blocks VP potentiation of mEPSC amplitudes (con't).** (A.) Application of Wortmannin (100 nM) blocked the VP potentiation of mEPSC amplitudes. (B.) The distribution of mEPSC amplitudes does not change significantly with application of wortmannin. (C.) Cumulative probability plots for each data group overlap, indicating no significant differences in mEPSC amplitudes. (D.) Amplitude histogram distributions do not change following VP stimulation when wortmannin is applied.

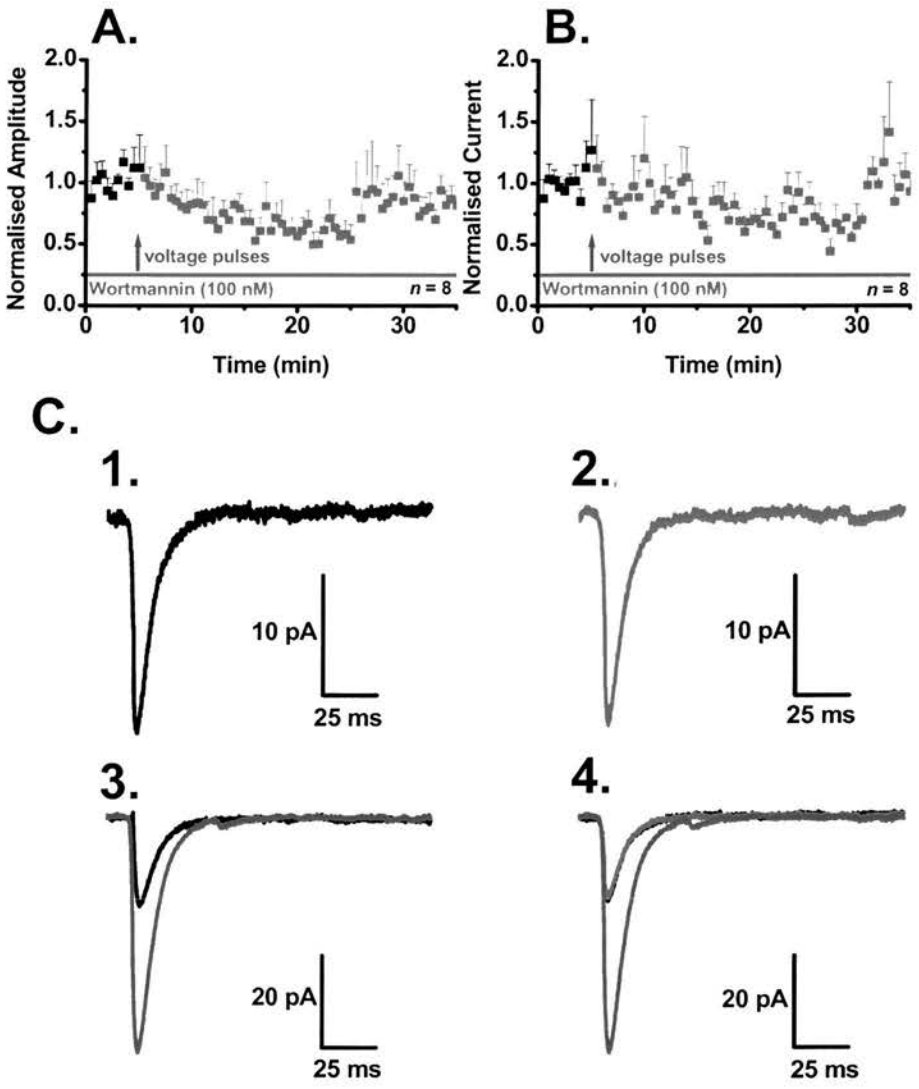

Figure 5.6: **Further characterization of inhibition of VP potentiation by wortmannin.** Application of wortmannin blocks both the potentiation of mEPSC frequency (A.) and current (B.) across the time course. **Control mEPSC overlays.** Analysis of 100 mEPSCs from the control period show a mean event of 20 pA (1.) which is consistent with control mEPSC mean amplitudes from other recordings. Application of wortmannin (2.) blocks the VP potentiation of mEPSC amplitudes. Interleaved control VP recording show typical potentiation of mEPSC amplitudes (3.) when overlaid both control and wortmannin treated cells showed little difference in the amplitude, rise, and decay times of these events (4.).

5.3: Confirming PI-3 kinase inhibition of VP potentiation

Due to the variety of actions that PI-3 kinase is been associated with, it was important to check the specificity of this blockade of the induction of VP potentiation of mEPSC amplitudes, by wortmannin. To achieve this we used a synthetic inhibitor (2-(4-Morpholinyl)-8-phenyl-1(4H)-benzopyran-4-one hydrochloride) LY 294002-hydrochloride (5 μM), to complement the wortmannin study.

In a series of control experiments, application of LY 294002 (5 μM) via the recording solution had no significant effect on the control mEPSC amplitudes (See Figure 5.7A: Control 23.1 ± 1.1 pA: VP LY 294002, 21.6 ± 2.6 pA. $n = 3$). Again scatter plots of mEPSC amplitudes show no difference in the amplitude distribution following application LY 294002. The cumulative probability plot for both control and LY 294002 treated mEPSCs overlap, indicating little significant difference between the control and treated mEPSC. Furthermore, the leftward distribution of this trace indicates a high probability of small amplitude events, the 50 % probability of 18.7 pA with an 80 % probability for the control mEPSCs of 28.7 pA and for the VP stimulated mEPSCs with 26.8 pA. Analysis of the distribution of an amplitude histogram of mEPSCs from both time periods shows no significant differences in the distribution of these histograms, as both traces show a typical leftward skewed distribution (Figure 5.7 C,D).

The frequency of mEPSCs appears to be relatively stable throughout the control period, but increases following the application of LY 294002, however this apparent potentiation is not significant and the result of a burst of activity (Figure 5.8A: Control 1.4 ± 0.1 Hz: VP LY 294002, 1.6 ± 0.3 Hz).

Total mEPSC current parallels this frequency change, appearing stable (no significant change) across the time course except for a burst of activity following application of LY 294002 (See Figure 5.23: Control 1.7 ± 0.5 nA: VP LY 294002, 2.2 ± 0.4 nA). Raster plot indicates typical mEPSCs from both periods indicate that there are no major differences between the two groups of mEPSCs (Figure 5.8 C).

Analysis of one hundred mEPSCs from each time period indicates little or no significant difference in mean amplitudes (Figure 5.10: Control 20.9 ± 0.2 pA: LY 294002, 20.5 ± 0.5 pA). The 10-90% rise times for the mean mEPSC are similar for control mEPSCs and the LY 294002 treated VP stimulated mEPSCs (Control 2.0 ± 0.3 ms: LY 294002, 2.1 ± 0.3 ms). Similarly, decay time constant shows little difference between the two groups (14.5 ± 1.4 ms: LY 294002, 14.5 ± 2.0 ms).

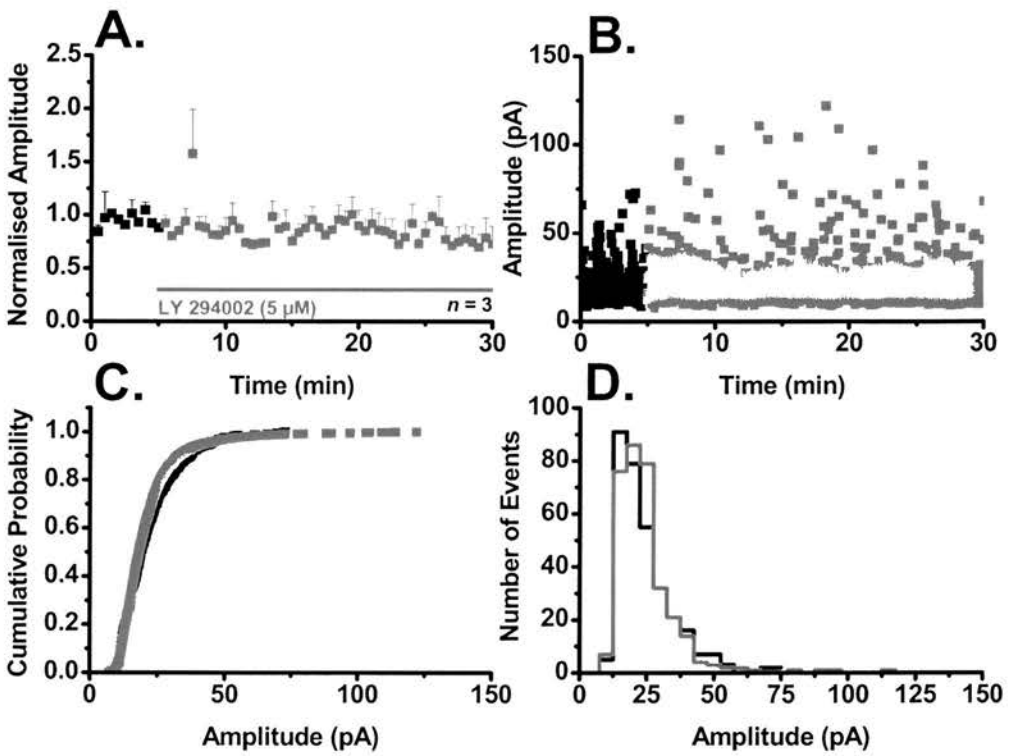

Figure 5.7: **Characterization of LY 284002 affects on non potentiated mEPSCs**. (A.) Application of LY 294002 (5 µM) had no significant affect on the mean amplitude of control mEPSCs. (B.) There were no significant increases in the distribution of mEPSC amplitudes following application of LY 294002. Although one 200 pA mEPSC does occur at 20 minutes, but was excluded from figure (C.) Cumulative probability plots overlap, indicating no differences with amplitude probability between the two groups. (D.) Amplitude histograms show no significant change in distribution following application of LY 294002.

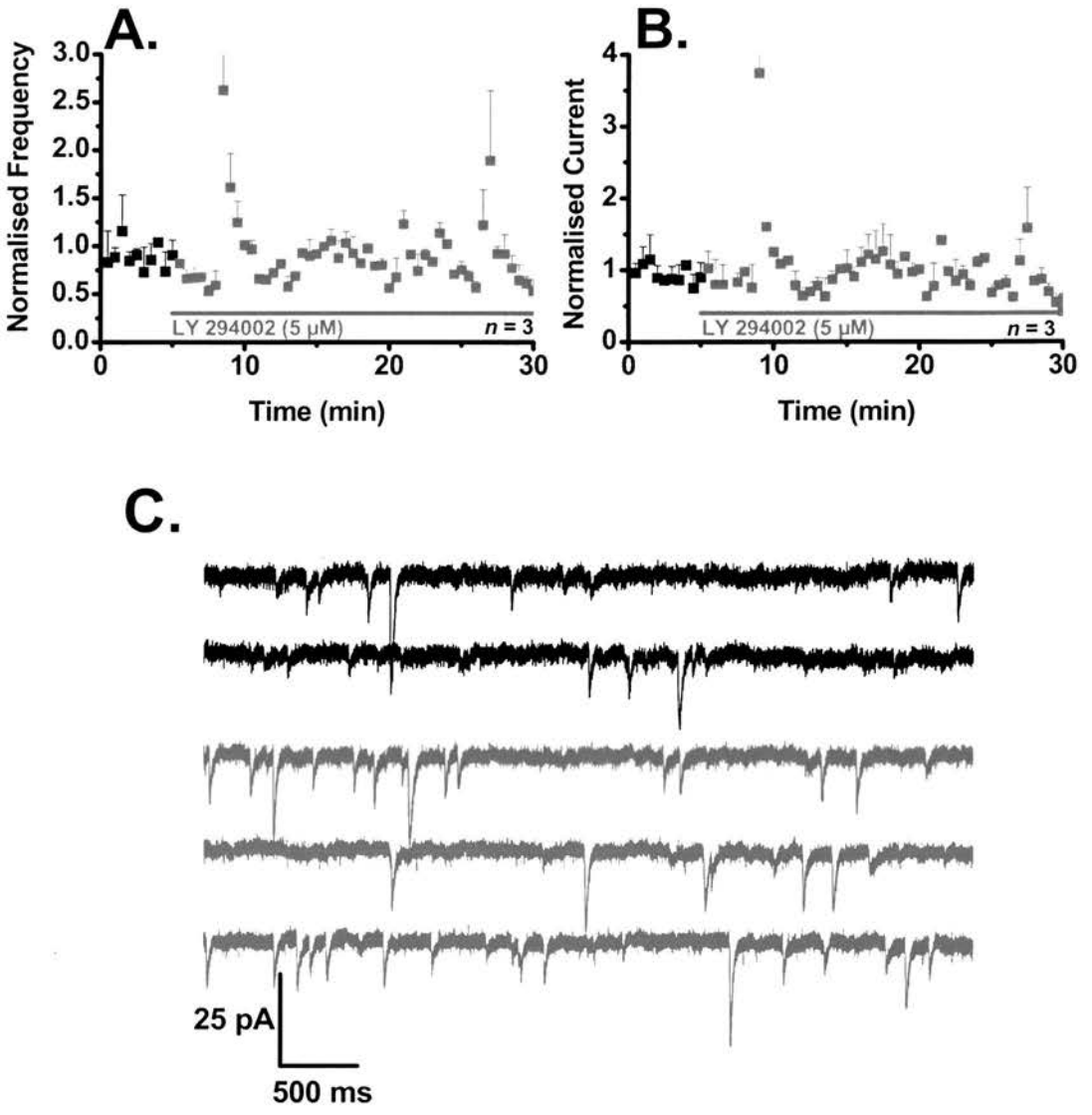

Figure 5.8: **Characterization of LY 284002 affects on non potentiated mEPSCs (con't).** Application of wortmannin blocks both the potentiation of mEPSC frequency (A.) and current (B.) across the time course. (C.) Raster plot of representative mEPSCs from both control (**black**) and LY 294002 (**red**) treated time periods.

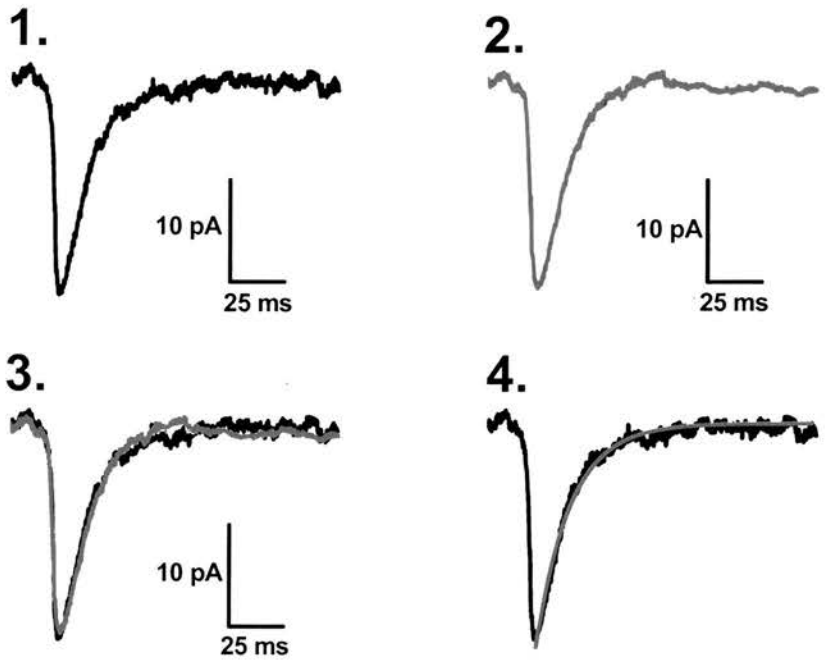

Figure 5.9: **Control LY 294002 mEPSC overlays.** Analysis of 100 mEPSCs from the control period show a mean event of 20 pA (1.) which is consistent with control mEPSC mean amplitudes from other recordings. Application of LY 294002 has no significant effect on the mean mEPSC amplitude (2.). When control and LY 294002 treated mEPSCs are overlaid, there are no apparent differences in amplitude, rise or decay times between the two groups.

5.4: Blockade of VP potentiation of mEPSC amplitudes by LY 294002

In the previous experimental series, the application of LY 294002 like wortmannin failed to have any significant effect on the amplitudes of the non VP stimulated mEPSCs. Indicating that functional AMPA receptors found in the membrane may not require PI-3 kinase for normal

function, in this next series of experiment, the objective was to determine if LY 294002 induced a similar blockade of the induction of VP potentiation of mEPSC amplitudes.

In this series of experiments bath application of LY 294002 (5 μM) blocked the induction of VP potentiation of mEPSC amplitudes (Figure 5.10A: control 20.6 ± 2.8 pA: VP LY 294002, 22.4 ± 2.9 pA. n = 6), while interleaved control recordings show typical VP potentiation. Figure 5.11B highlights the differences in the amplitudes of the mEPSCs between the LY 294002 treated mEPSCs and the VP potentiated events.

Single cell experiments highlight the finding that application of LY 294002 inhibits the VP potentiation of mEPSC amplitudes further showing no significant increase in the scatter of mEPSC amplitudes. Cumulative probability plot for both control and VP stimulated LY 294002 treated mEPSCs overlap. Indicating a blockade of the VP potentiation of mEPSC amplitudes by LY 294002, furthermore the leftward distribution of this trace indicates a high probability of small amplitude events, the 50 % probability of 17.2 pA with an 80 % probability for the control mEPSCs of 27.2pA and for the VP stimulated mEPSCs with LY 294002 24.79 pA. Analysis of the distribution of an amplitude histogram of mEPSCs from both time periods shows no significant differences in the distribution of these histograms, as both traces show a typical leftward skewed distribution (See Figure 5.11 C.D).

Application of LY 294002, shows the similar reduction in mEPSC frequency shown with application of wortmannin, again this reduction cannot be assigned to a function of the inhibitor used as a similar reduction in event frequency is shown with control recordings. However interleaved control recordings showed the transient frequency potentiation shown with VP stimulation (Figure 5.12A: control 1.2 ± 0.5 Hz: VP 1.7 ± 0.2 Hz:).

The current generated by the mEPSCs from the interleaved control data, show the robust potentiation of the mEPSC currents shown with VP potentiation (control: 0.8 ± 0.4 nA: VP 2.3 ± 0.3 nA). Application of wortmannin inhibited the potentiation of mEPSC currents following the VP stimulus (control 1.2 ± 0.4 nA: VP LY 294002, 1.1 ± 0.3 nA).

Analysis of one hundred mEPSCs from each time period indicates no significant difference in mean amplitude, rise or decay times. Although 100 mEPSCs from the peak of the mEPSC potentiation from the interleaved control data show a mean mEPSC with significantly increased amplitude, however the rise times and decay time constants are not significantly different when compared to the LY294002 treated events.

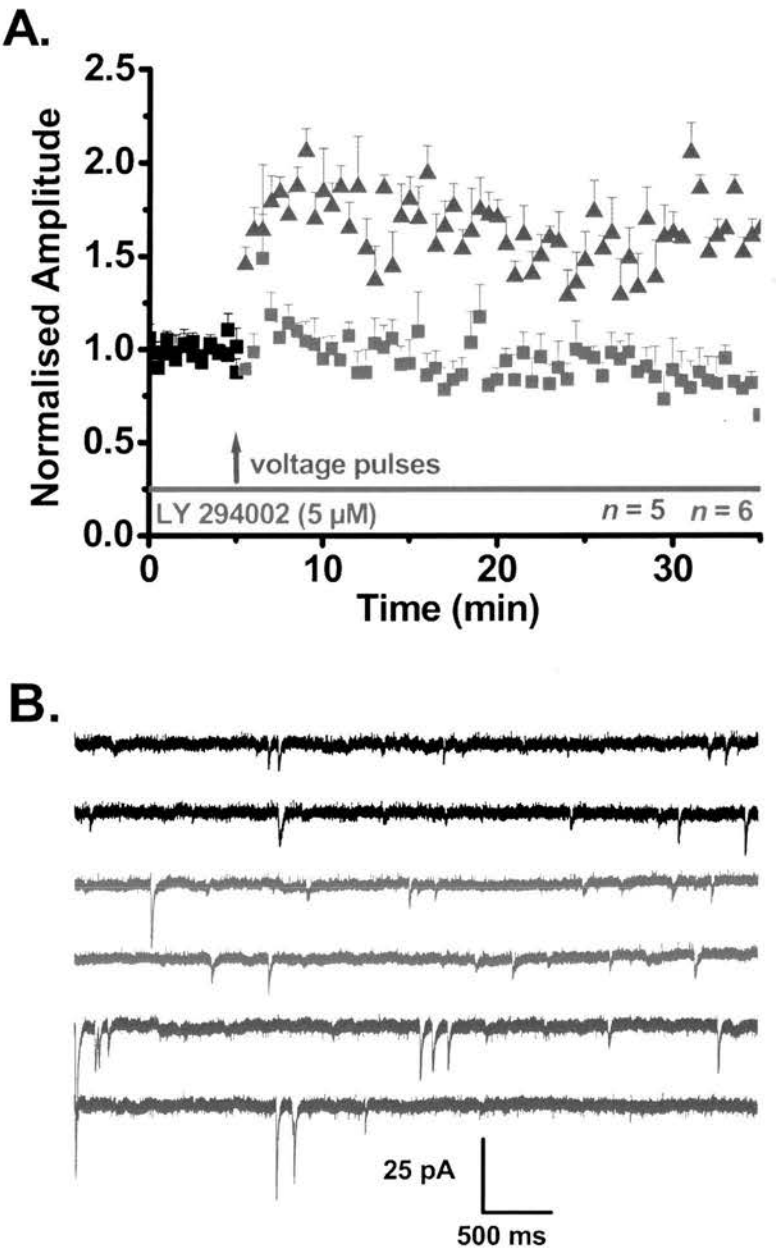

Figure 5.10: **LY 294002 blocks the VP potentiation of mEPSC amplitudes.** (A.) Application of LY 294002 (5 μM) blocks the VP potentiation of mEPSC amplitudes, while interleaved control data show typical amplitude potentiation. (B.) Raster plot of mEPSC from control (**black**), LY 294002 (**Red**) and interleaved control time periods (**blue**).

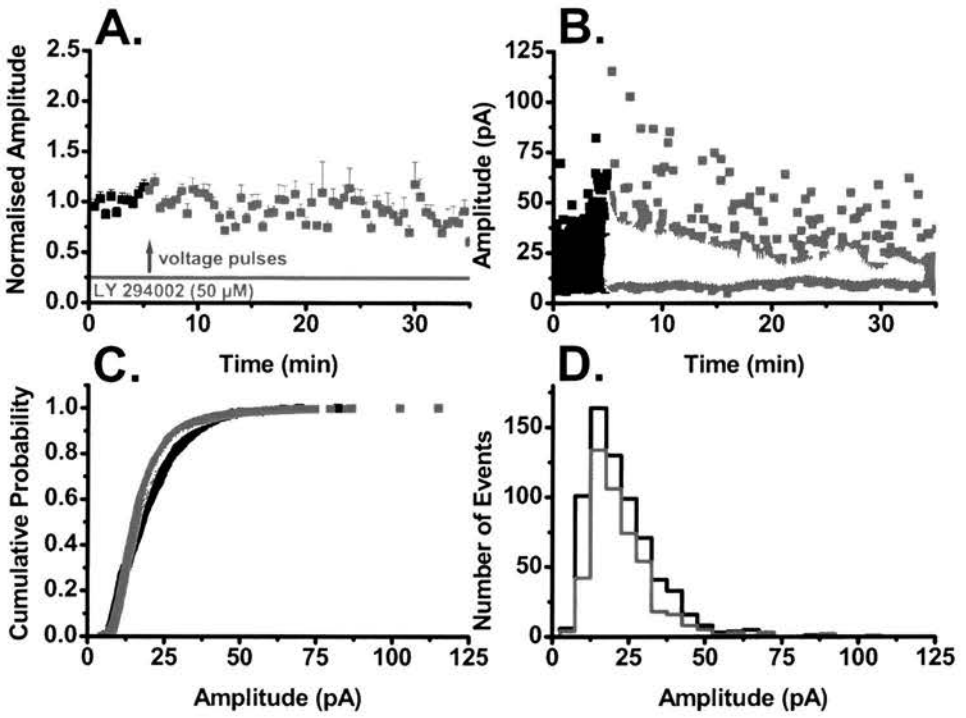

Figure 5.11: **Application of LY 284002 blocks the VP potentiated of mEPSC amplitudes**. (A.) single cell amplitude time course, application of LY 294002 (5 μM) blocks the induction of VP potentiation of mEPSC amplitudes. (B.) There were no significant increases in the distribution of mEPSC amplitudes following VP stimulation with LY 294002 (5 μM). (C.) Cumulative probability plots overlap, indicating no differences with amplitude probability between the two groups. (D.) Amplitude histograms show no significant change in distribution following application of LY 294002.

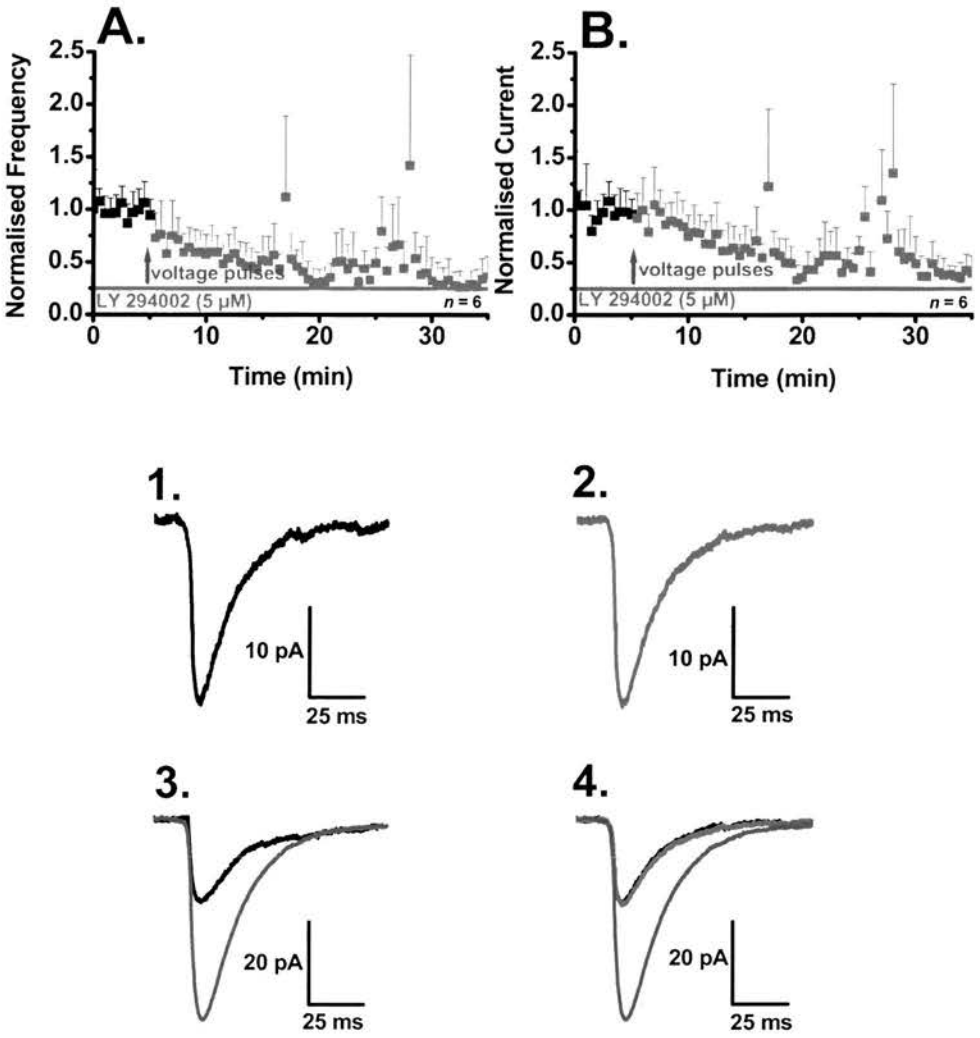

Figure 5.12: **Further characterization of inhibition of VP potentiation by LY 294002.** Application of LY 294002 blocks both the potentiation of mEPSC frequency (A.) and current (B.) across the time course. **Control mEPSC overlays.** Analysis of 100 mEPSCs from the control period show a mean event of 20 pA (1.) which is consistent with control mEPSC mean amplitudes from other recordings. Application of LY 294002 (2.) blocks the VP potentiation of mEPSC amplitudes. Interleaved control VP recording show typical potentiation of mEPSC amplitudes (3.) When overlaid both control and wortmannin treated cells showed little difference in the amplitude, rise, and decay times of these events (4.).

5.5: LY 303511

In the previous set of experiments, the application of LY 294002 blocked the induction of VP potentiation, while interleaved control recordings showed the mEPSC amplitude potentiation associated with the VP stimulus.

To detail the selectivity of LY29402 ($C_{19}H_{18}N_2O_2$) the inactive analogue LY 303511 ($C_{19}H_{17}NO_3$) was used. This analogue is inactive due to a substitution in the morpholine ring when compared to LY 294002.

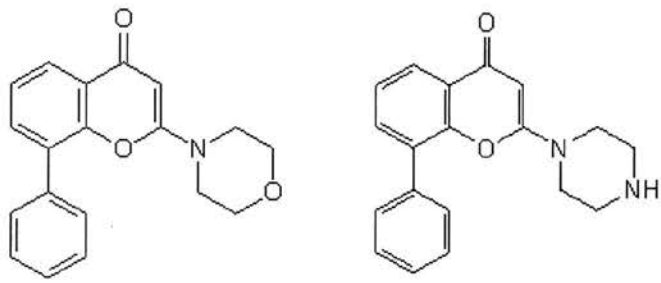

LY 294002 LY 303511

The application of this inactive analogue allows for the typical VP potentiation of mEPSC amplitudes (Figure 5.13A: control 22.7 ± 4.1 pA: VP LY 303511, 40.5 ± 2.6 pA. $n = 5$). Following VP stimulation there is an increase in the distribution of the mEPSC amplitudes. This potentiation is confirmed by the cumulative probability plot as this indicates two completely separate groups, with the potentiated mEPSCs being of significantly larger amplitudes. Analysis of the amplitudes of mEPSCs for the 5 minute period following VP stimulation, showed a rightward shift in the amplitude distribution, when compared to control events.

The frequency of mEPSC show the transient potentiation previously demonstrated with VP potentiation (Figure 5.14A: control 1.5 ± 0.1 Hz: VP LY 303511, 1.7 ± 0.1 Hz. $n = 5$). The mEPSC currents show potentiation after the VP stimulus with the bath applied inactive LY 303511 (Figure 5.14B: control 1.2 ± 0.6 Hz: VP LY 303511, 2.5 ± 0.2 Hz. $n = 5$). Analysis of one hundred mEPSCs from each time period, show a control mEPSC with mean amplitude of 20.2 ± 0.2 pA, this event has a rise time of 1.2 ± 0.2 ms and a decay time constant of 9.0 ± 1.2 ms.

Following the VP stimulus with LY 303511, there is a significant potentiation of the mean mEPSC amplitude, 53.3 ± 0.3 pA, with a small shift in rise and decay time constant, 1.3 ± 0.1 ms and 11.1 ± 0.7 ms respectively. These experiments rendered some of the largest mEPSCs recorded;

analysis of 100 of the largest mEPSCs shows an event with mean amplitude of 171.3 pA with a mean rise time and decay time constant of 1.9 ± 0.1 ms and 15.7 ± 1.1 ms respectively.

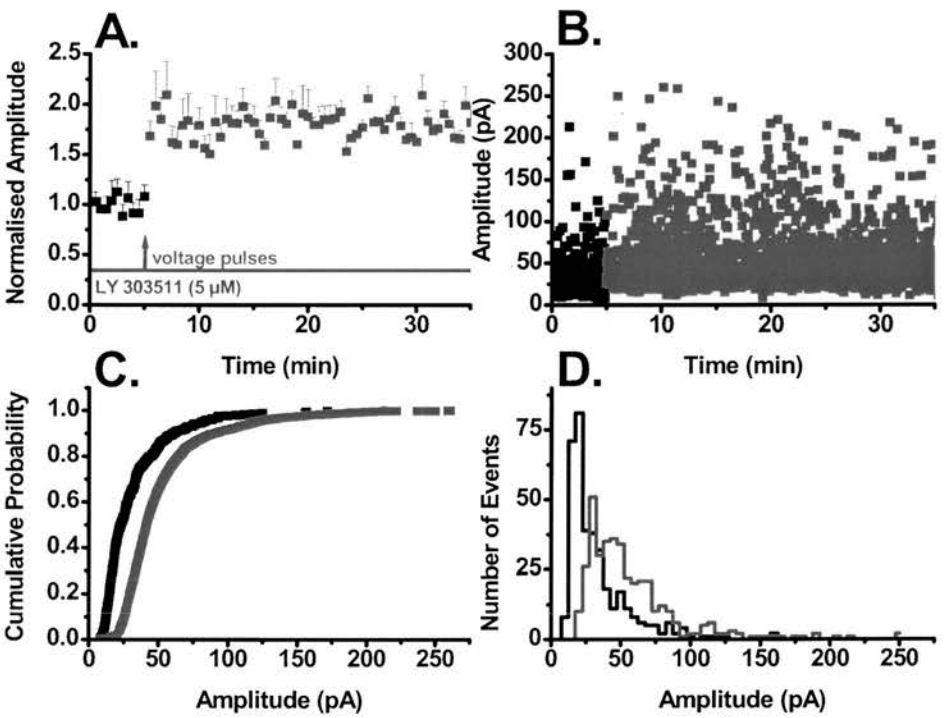

Figure 5.13: **An inactive isoform of LY 294002 allows for the VP potentiation of mEPSC amplitudes.** (A.) Application of LY 303511 (5 µM) does not inhibit the VP potentiation of mEPSC amplitudes. (B.) The distribution of the amplitude scatter plot increases following VP stimulation with LY 303511 (5 µM). (C.) Cumulative probability plots show clear separation between the two groups, indicating a higher amplitude probability for the VP potentiated mEPSCs. (D.) Amplitude histograms show clear rightward shift with VP potentiation with LY 303511 (5 µM).

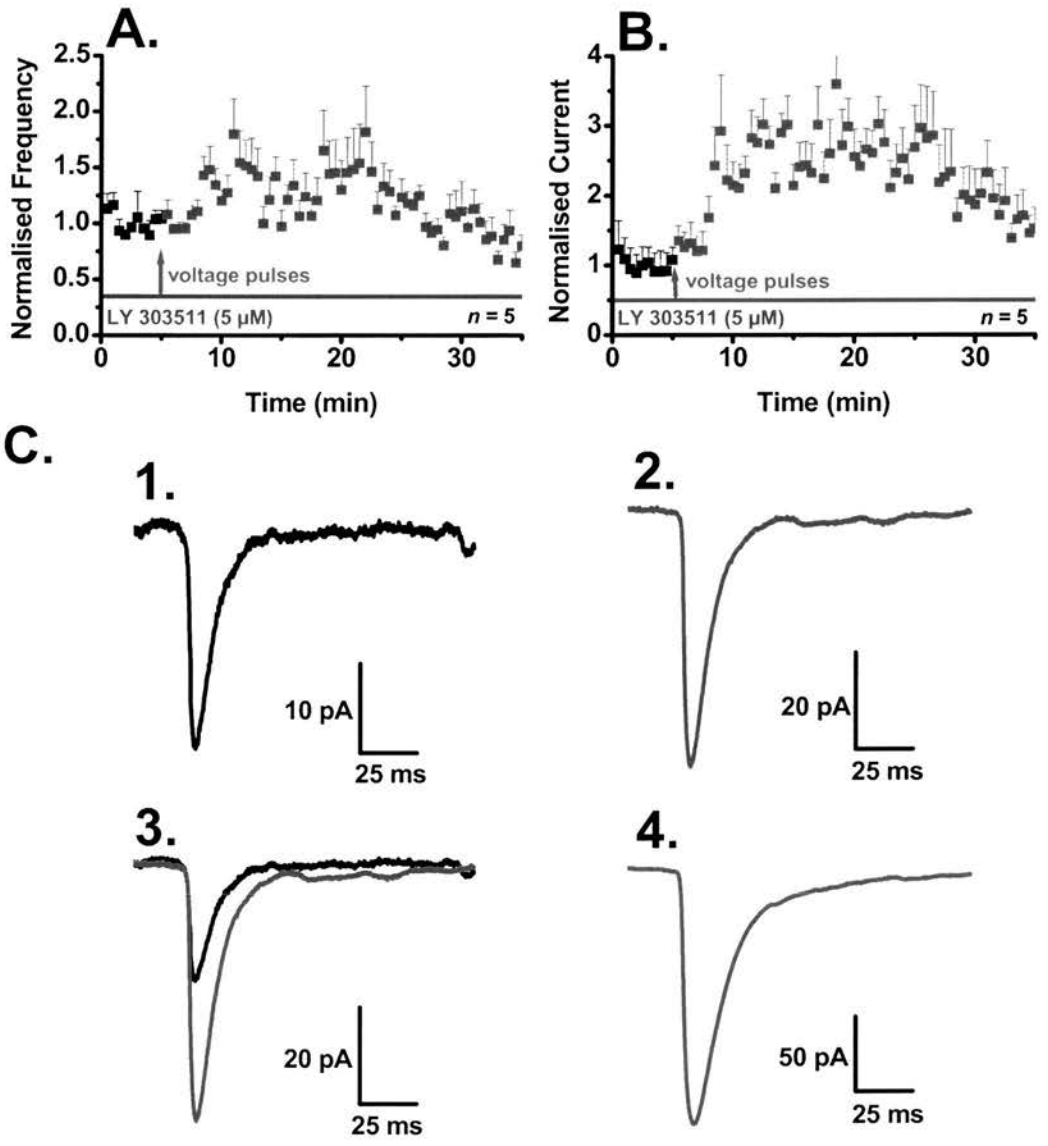

Figure 5.14: **Further characterisation of VP potentiation with LY 303511.** (A.) Application of LY 303511 does not inhibit the significant potentiation of both mEPSC frequency (A.) and current (B.). **mEPSC overlays for LY 303511.** Analysis of 100 mEPSCs from the control period shows a mean event of 20 pA (1.) Application of LY 303511 (2.) does not block the VP potentiation of mEPSC amplitudes (3.). Mean mEPSC from 100 of the largest mEPSCs from the single cell recording.

5.6: Maintenance of the VP potentiation of mEPSC amplitudes is dependent upon PI-3 kinase.

Sanna et al., (2002) described a requirement for PI-3 kinase in the expression of LTP, but not for the induction of LTP. In the pervious set of experiment, the role of PI-3 kinase in establishing the induction of VP potentiation of mEPSC amplitudes was well characterised. Extrapolating upon this difference, I wanted to know if the sustained potentiation of mEPSC amplitudes shown with VP potentiation was dependent upon active PI-3 kinase, and will show reversibility of potentiation with application of wortmannin.

In this series of experiment a VP stimulus was given, and then 5 minutes post stimulus wortmannin (100 nM) was per-fused via a gravity feed at a perfusion rate of 4.5 ml/min into a 2 ml bath. Following the VP stimulus there was a significant potentiation of mEPSC amplitude, this potentiation was reversed by the application of wortmannin and returns to around the control amplitude in approximately 10 – 12 minutes (Figure 5.15: control 20.1 ± 1.0 pA: VP 38.7 ± 2.5 pA: wortmannin 19.5 ± 2.7 pA. n = 8). Events from each time period highlight show little difference between the control and the VP stimulated wortmannin treated events from the 20-25 minute time period, while the VP stimulated event have much larger amplitudes (Figure 5.15B).

A typical single cell experiment highlights the finding that application of wortmannin reverses the significant VP potentiation of mEPSC amplitude (Figure 5.16: control 18.4 ± 0.7 pA: VP 36.9 ± 1.7 pA: wortmannin 27.5 ± 2.9 pA). The cumulative probability plots for this experiment are interesting as the control and VP mEPSCs do not overlap, and the plots show the typical rightward shift shown with VP potentiation. This indicates a shift in the amplitude probability for these events 50 % 12.0 pA and 26.1 pA respectively and 26.1 pA and 41.6 pA for the 80 % probability for the control and VP potentiated mEPSCs.

However the application of wortmannin reversed the amplitude potentiation of the mEPSCs, this is highlighted by 50 % and 80 % probabilities of 21.5 pA and 33.12 pA which fall between the control and VP amplitude probability. Analysis of the distribution of an amplitude histogram of mEPSCs show a significant rightward shift for the VP stimulated mEPSC (control mEPSCs have left ward skewed distribution). The distributions of mEPSCs from the VP stimulated wortmannin treated mEPSCs have features of both the leftward skewed and the rightward distributions, indicative of a change from the VP potentiated mEPSC trace (Figure 5.16 C.D).

The frequency of mEPSCs reduces across the time course of the experiment. VP stimulus induced no significant frequency potentiation, comparison of frequencies from control and VP stimulated periods were not significantly different (Figure 5.18 A: control 12.5 ± 0.1 Hz: VP 1.2 ± 0.1 Hz: wortmannin 0.8 ± 0.2 Hz).

The total current, showed a 22 % increase following the VP stimulus, but application of wortmannin blocked this potentiation and caused a significant reduction by the 20-25 minute time period (Figure: 5.17 B: control 0.8 ± 0.1 nA: VP 1.0 ± 0.1 nA: wortmannin 0.6 ± 0.2 nA).

Analysis of one hundred mEPSCs from each time period (Figure 5.18) indicates a significant difference in mean amplitudes, following the VP stimulus, however this potentiation is reversed with application of wortmannin (control 22.4 ± 0.2 pA: VP 57.1 ± 1.1 pA: wortmannin 28.5 ± 0.2 pA). The 10-90 % rise times for the mean mEPSC from all three time periods are similar (control 1.5 ± 0.1 ms: VP 1.6 ± 0.1 ms: wortmannin 1.2 ± 0.2 ms). Similarly decay time constant show little difference between the three groups (control 10.0 ± 0.7 ms: VP 11.2 ± 0.3 ms: wortmannin 10.0 ± 1.1 ms).

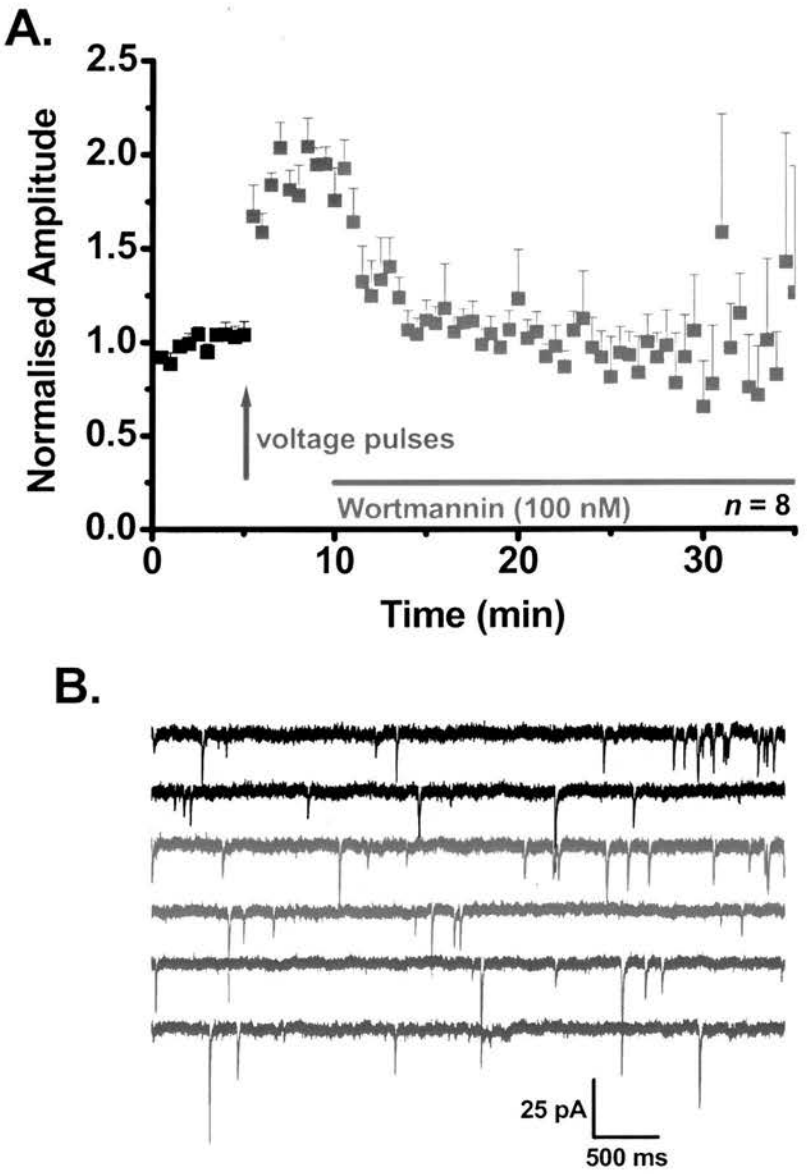

Figure 5.15: **Reversal of the VP potentiation of mEPSC amplitudes by wortmannin.** (A.) Following the VP stimulus the resulting mEPSC amplitude potentiation was inhibited by the application of wortmannin. (B.) Raster plots representitive mEPSC from control (**black**) VP potentiated (**blue**) and wortmannin treated (**red**) periods.

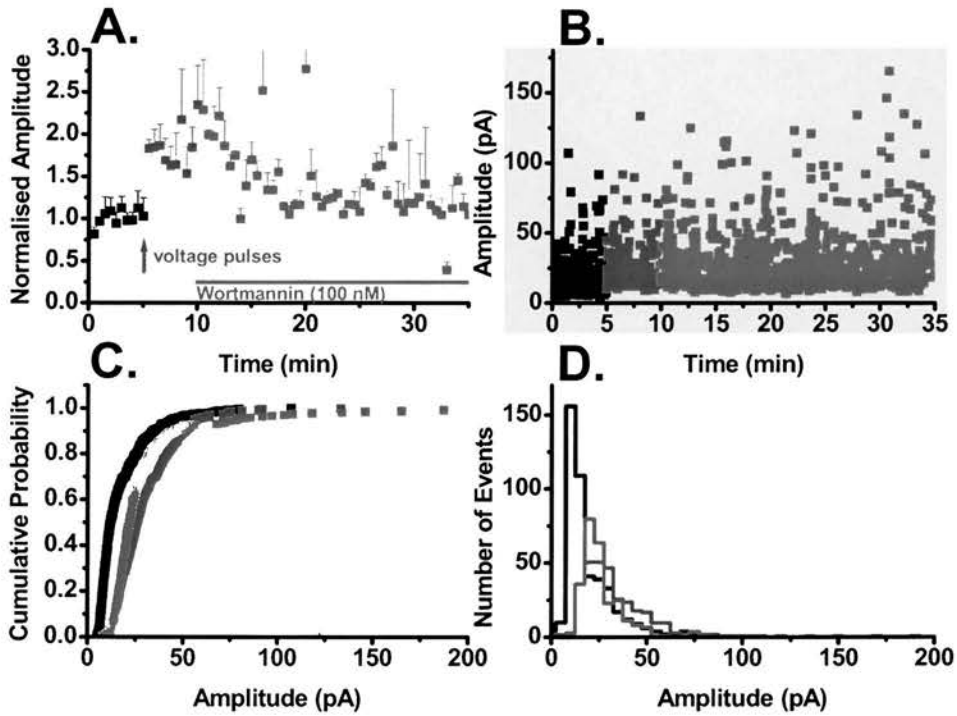

Figure 5.16: **Characterization of the reversal of VP amplitude potentiation by wortmannin. (A.)** A single cell representation of the reversal of VP potentiation by wortmannin. (B.) Scatter plot of all mEPSC amplitudes from single cell example. (C.) Cumulative probability plot shows clear separation between the control and potentiated event s indicative of a potentiation of mEPSC amplitudes, while wortmannin treated mEPSCs fall between the control and potentiated plots indicative of a reducing trend in mEPSC amplitude. (D.) Amplitude index mirrors the cumulative probability plot, potentiated mEPSCs show a clear rightward shift, indicating a higher probability of large amplitude events, while the wortmannin treated events regress towards the leftward skewed distribution of the control mEPSCs.

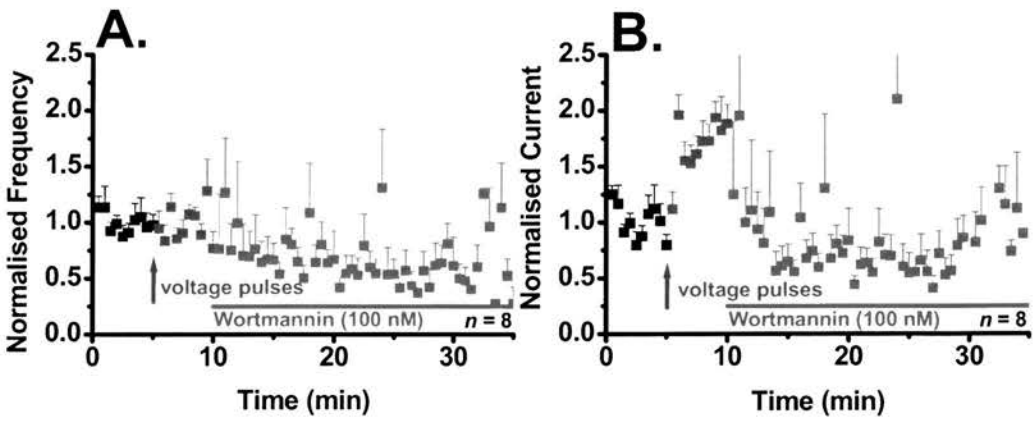

Figure 5.17: **Further characterization of wortmannin on VP potentiation.** (A.) following the VP stimulus there was no mEPSC frequency potentiation, with application of wortmannin the frequency reduced across the time course to approximately half of the control frequency. (B.) The VP potentiation of mEPSC currents was reduced with application of wortmannin.

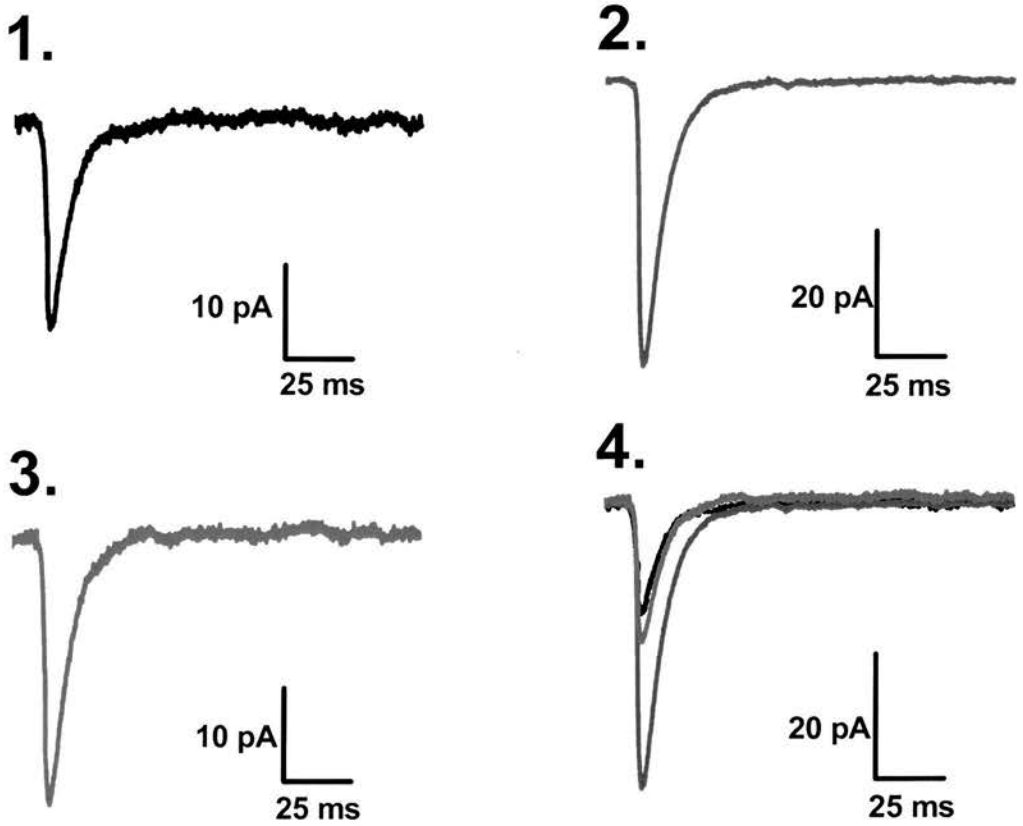

Figure 5.18: **Analysis of 100 mEPSCs from each time period.** Control period mEPSCs show a mean event of with an amplitude of approximately 20 pA (1.) Consistent with control mEPSC mean amplitudes from other recordings. (2.) Application of the VP stimulus induces a significant potentiation of mEPSC amplitudes. (3.) Analysis of 100 wortmannin treated mEPSCs show a reduction in mean mEPSC amplitude. (4.) When all mean traces are overlaid a clear potentiation of the VP stimulated mEPSCs is shown, with control and wortmannin treated mEPSCs having similar amplitudes.

5.7: Ensuring that the maintenance of VP potentiation of mEPSC amplitude is PI-3 kinase dependent.

In the previous set of experiments a significant potentiation of mEPSC amplitudes was reversed by inhibition of PI-3 kinase. This result suggests a role of this kinase in the cycling of AMPA into active synapses of the dendritic spine. To validate the role of PI-3 kinase the experiment was repeated but LY 294002 (5 μM) was applied instead of wortmannin.

Following the VP stimulus there was a significant potentiation of mEPSC amplitude, this potentiation was later reversed by the application of LY 294002, returning to around the control amplitude in approximately 15 minutes (Figure 5.19 A: Control 18.0 ± 1.1 pA: VP 33.3 ± 1.6 pA: VP LY 294002, 19.5 ± 2.7 pA. $n = 7$). Control and the VP stimulated LY 294002 treated mEPSCs show little difference in mEPSC amplitudes, while the VP stimulated mEPSCs have much larger amplitudes (Figure 5.19 B).

A typical single cell experiments highlight the finding that application of LY 294002 reverses the significant VP potentiation of mEPSC amplitude (Figure 5.20 A: Control 19.7 ± 0.6 pA: VP 39.8 ± 1.7 pA: VP LY 294002, 18.9 ± 2.2 pA). The cumulative probability plots for this experiment are interesting as the control and VP mEPSCs do not overlap. The VP potentiated mEPSCs show the typical rightward shift in the plot, indicating a shift in the amplitude probability for these events 50 % 15.5 pA and 23.7 pA respectively and 24.7 pA and 38.2 pA for the 80 % probability for the control and VP potentiated mEPSCs. However the application of LY 294002 reversed the amplitude potentiation of the mEPSCs, this is highlighted by 50 % and 80 % probabilities of 16.4 pA and 26.0 pA which fall between the control and VP amplitude probability. Analysis of the distribution of an amplitude histogram of mEPSCs show a significant rightward shift for the VP stimulated mEPSC (control mEPSCs have left ward skewed distribution). The distributions of mEPSCs from the VP stimulated LY 294002 treated mEPSCs have features of both the leftward skewed and the rightward distributions, indicative of a change from the VP potentiated mEPSC trace (See Figure 5.20 C.D).

The frequency of mEPSCs though the time course of this experiment is shows a transient potentiation following the application of PI-3 kinase, but reduces across the time course of the experiment. The VP stimulus from did not bring about a significant mEPSC frequency potentiation, comparison of frequencies from control and VP stimulated periods were not significantly different (Figure 5.21 A: Control 1.1 ± 0.1 Hz: VP 0.8 ± 0.1 Hz: VP LY 294002, 0.9 ± 0.2 Hz). The total current, was shown to increase following the VP stimulus, but application of wortmannin blocked this potentiation and caused a significant reduction by the 20-25 minute time period (Figure : 5.21

B: Control 0.5 ± 0.1 nA: VP 0.7 ± 0.2 nA: VP LY 294002, 0.5 ± 0.1 nA). Analysis of one hundred mEPSCs from each time period indicates a significant difference in mean amplitudes (Figure 5.22: Control 20.6 ± 0.5 pA: VP 44.8 ± 0.4 pA: VP LY 294002, 24.1 ± 0.7 pA). The 10-90 % rise times for the mean mEPSC from all three time periods are similar (Control 1.6 ± 0.3 ms: VP 2.1 ± 0.3 ms: VP LY 294002, 1.8 ± 0.4 ms). Similarly decay time constants show a small increase between control and VP potentiated events, but there is no significant difference between the control and the VP stimulated LY 294002 treated mEPSC groups (control 20.7 ± 1.5 ms: VP 29.0 ± 1.5 ms: VP LY 294002 22.0 ± 1.5 ms).

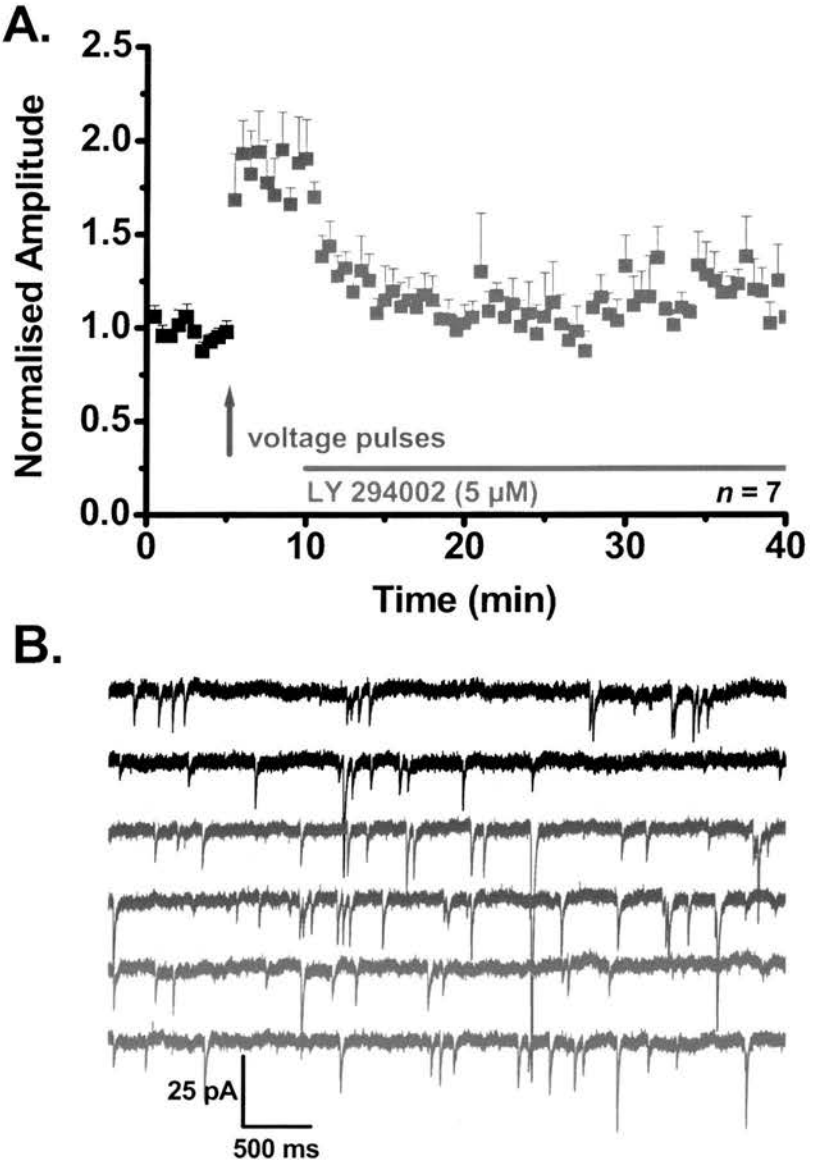

Figure 5.19: **Maintenance of VP mEPSC amplitude potentiation is PI-3 kinase dependent.** The potentiation of mEPSC amplitudes was reversed by the application of LY 294002. Figure (B.) Raster plots for inhibition of the maintenance of VP potentiation. Control mEPSCs (**Black**), VP potentiated (**Blue**) LY 294002 treated mEPSC (**Red**).

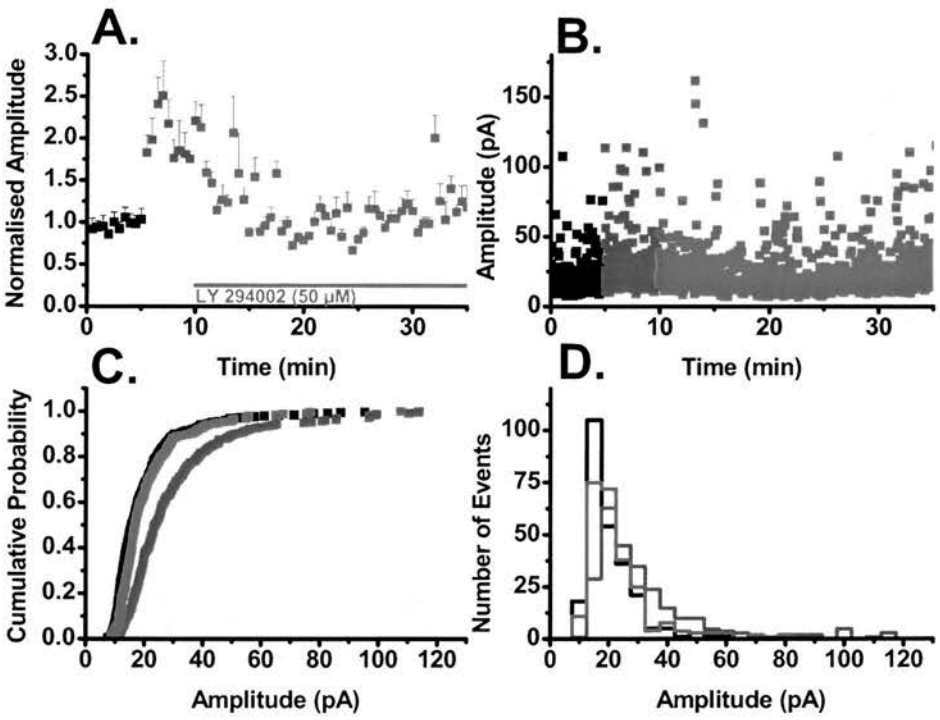

Figure 5.20: **Characterization of the reversal of VP potentiation by LY 294002.** (A.) A single cell representation of the reversal of VP potentiation by LY 294002. (B.) Scatter plot of all mEPSC amplitudes from single cell example. (C.) Cumulative probability plot shows clear separation between the control and potentiated event s indicative of a potentiation of mEPSC amplitudes, while LY 294002 treated mEPSCs fall between the control and potentiated plots indicative of a reducing trend in mEPSC amplitude. (D.) Amplitude index mirrors the cumulative probability plot, potentiated mEPSCs show a clear rightward shift, indicating a higher probability of large amplitude events, while the LY 294002 treated events regress towards the leftward skewed distribution of the control mEPSCs.

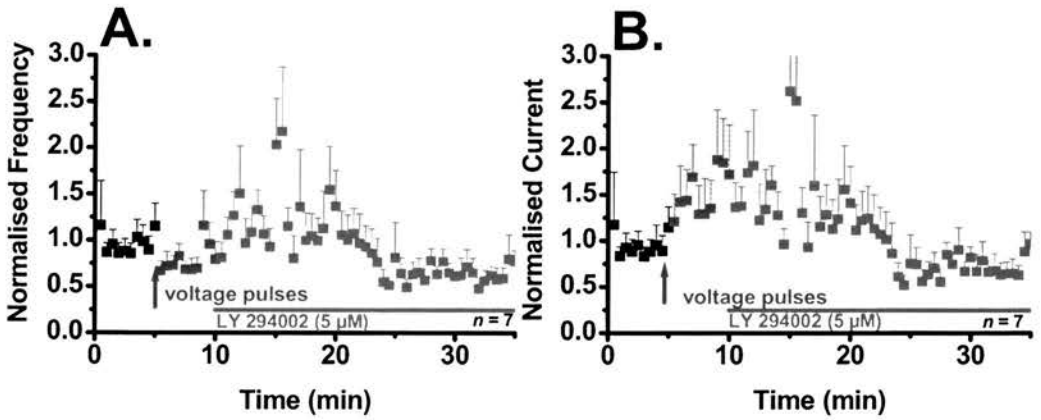

Figure 5.21: **Further characterization of LY 294002 inhibition of VP potentiation.**
(A) Application of the voltage pulses did not induce a potentiation of mEPSC frequency; however, a transient potentiation of mEPSC frequency was shown following application of LY 294002. (B.) Following the VP stimulus there was a potentiation of mEPSC currents, this potentiation was reversed by the application of LY 294002.

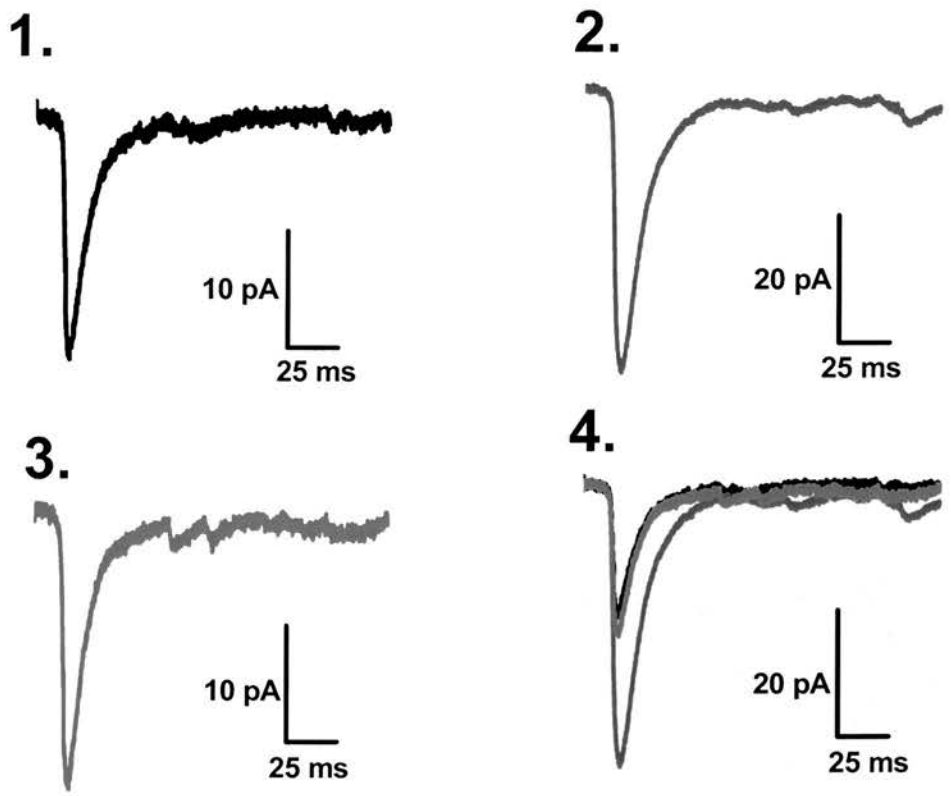

Figure 5.22: **mEPSCs overlays from LY 294002 inhibition of VP potentiation.** Control period mEPSCs show a mean event of with an amplitude of approximately 20 pA (1.) Consistent with control mEPSC mean amplitudes from other recordings. (2.) Application of the VP stimulus induces a significant potentiation of mEPSC amplitudes. (3.) Analysis of 100 LY 294002 treated mEPSCs shows a reduction in mean mEPSC amplitude. (4.) When all mean traces are overlaid a clear potentiation of the VP stimulated mEPSCs is shown, with control and LY 294002 treated mEPSCs having similar amplitudes.

5.8: Background to PI-3 kinase

In this series of experiments I aimed to characterize the effects of PI-3 kinase in the voltage pulse potentiation of mEPSC amplitude, which I have demonstrated has a requirement for postsynaptic membrane fusion events. Specifically the previous Chapter showed there to be interactions between the GluR2 subunit and NSF and PICK1 proteins, and with the GluR1 through the TGL binding motif to the possible effectors of this trafficking pathway stargazin and the NMDA receptor transport proteins SAP97 and PSD95.

Scientific interest in PI-3 kinase signaling originates from a loss of PTEN a tumour suppressor gene from dividing cancer cells. The PTEN tumour suppressor protein is a phosphoinositide 3-phosphatase that, by metabolising phosphatidylinositol 3,4,5-trisphosphate (PtdIns(3,4,5)P(3)), acts in direct antagonism to growth factor stimulated PI 3-kinases (Leslie and Downes, 2002).

Within neuronal cells PI-3 kinase function requires the same substrate for action as phospholipase C namely phosphatidylinositol (4,5) bisphosphate (PtdIns $(4,5)P_2$). Metabolism via the PLC pathway generates two second messengers, IP3 and DAG. IP3 acts on ryanodine receptors to release calcium from internal stores and generate the calcium induced calcium release (CICR) current, while DAG activates protein kinase C. From earlier experiments (see Chapter 3.17) I have determined that intracellular release of the store calcium is critical for the development of voltage-pulse potentiation.

Metabolism via the PI-3 kinase pathway produces three second messengers PtdIns(3)P, PtdIns$(3,4)P_2$, PtdIns$(3,4,5)P_3$ each of these second messenger proteins have diverse cellular functions, mediated via PKA/AKT (Cantley and Neel, 1999; Cantrell, 2001) and Rac/Rho GTPases (Liliental et al., 2000).

Due to the functional crossover with PLC, and the knowledge that PLC products mediate cellular trafficking mechanisms, the role of phosphoinositide 3 kinase (PI-3 kinases) in excitatory synaptic transmission was highlighted when PI-3 kinase was shown to be required in the glycine induced LTP of mEPSC currents in cultured hippocampal neurones (Sanna et al., 2002., 2002; Man et al., 2003). PI-3 kinase again overlaps with the PLC signaling pathway to bring about the activation PKC. PI-3 kinase interaction with PKB signaling pathway will activate PKC via a feed back loop which exists through PDK1 which activates PKC (Chou et al., 1998) (for review see (Chou et al., 1998; Vanhaesebroeck and Alessi, 2000; Cantrell, 2001).

In summary, the kinase regulation of cellular processes is a vast highly complex inter-regulating system. PI-3 kinase has been shown to be important in the regulation of LTP in pyramidal cells although the mechanism has never been fully described.

5.9: PI-3 kinase is required for the induction of voltage pulse potentiation

Man et al (2003) reported a requirement for PI-3 kinase with glycine dependent induction of LTP, my aim was to characterise the importance of PI-3 kinase for voltage-pulse potentiation of mEPSC amplitudes. Application of wortmannin (Powis et al., 1994) a specific PI-3 kinase inhibitor had no significant effect on the amplitude of non – potentiated mEPSCs, indicating that AMPA receptors in active synapses are stable or that the basal turnover rate is very low that the inhibition of AMPA receptor insertion by wortmannin is not represented by a change in mEPSC amplitudes. Wortmannin further blocks the induction of voltage-pulse potentiation of mEPSC amplitudes.

A further complication exists as PI-3 kinase has been found to regulate the function of the L-type Ca^{2+} channels (Steinberg, 2001) which could account for the blockade on the induction of mEPSC amplitude potentiation. Furthermore PI-3 kinase has been shown to regulate presynaptic P/Q and N type Ca^{2+} channels (Wu et al., 2002) which may account for the reduction in mEPSC frequency shown with application of wortmannin.

In these experiments this implied blockade of the L-type Ca^{2+} channels is not significant, due to the observation of recurrent inward currents induced by the depolarising phase of the voltage step. Generation of these currents was previously found to be dependent upon active L-type Ca^{2+} channels. Therefore if the currents are occurring then the receptors must be functional, and supplying the postsynaptic cell with calcium.

This experimental finding was then verified using a synthetic PI-3 kinase inhibitor LY 294002 (Vlahos et al., 1994; Perkinton et al., 2002). Here again the application of this PI-3 kinase inhibitor had no significant effect on non potentiated mEPSCs amplitudes, but blocked the induction of the potentiation of mEPSC amplitudes, while interleaved control recordings showed typical potentiation of mEPSC amplitudes. These experiments confirmed the importance of PI-3 kinase for the induction of voltage-pulse potentiation of mEPSC amplitudes.

The function of LY 294002 was further checked with and an inactive analogue LY 303511, with application of this analogue did not inhibit the sustainable voltage-pulse potentiation of mEPSC amplitudes.

5.10: Maintaining voltage pulse potentiation

The maintenance phase of voltage-pulse potentiation became the next target to determine if PI-3 kinase is required for this stable potentiation of mEPSC amplitudes. Sanna et al., 2002 showed a requirement of PI-3 kinase, for the expression but not for the induction or the maintenance of both NMDA receptor and VDCC-dependent LTP in the hippocampal CA1 region. Expression was defined as the recovery of induced LTP following wash out of these inhibitors.

Our findings in the first instance contradict those of Sanna et al., 2002 in that PI-3 kinase is required for the induction of voltage-pulse potentiation. This is probably due, to the vast diversity of regulatory functions of this kinase. Figure 1.5 indicates some of the diversity of regulation which PI-3 kinase displays. It has been linked with other major kinases (AKT/PKB and PKC) which have previously been identified as regulators of traditional NMDA receptor dependent LTP (See Figure 1.5) An interesting observation as PI-3 kinase has also been shown to also regulate NMDA receptor function (Perkinton et al., 2002; Crossthwaite et al., 2004).

In the next set of experiments a significant potentiation of mEPSC amplitude was first generated. Then, wortmannin was applied five minutes after the stimulus; this application reversed the potentiation, but did not ablate all mEPSC events. I did not check the reversibility of the blockade of voltage-pulse potentiation as did Sanna et al., 2002, due to two factors, the experimental set up of using whole-cell patched pyramidal cells precludes experiments which require a long time course due to dialysis of the cell with the internal solution. The second reason that the chemistry of wortmannin suggests that it cannot be washed out as Sanna et al. (2002) indicated. Wortmannin binds at Lys-883, resulting in a covalent complex which irreversibly inhibits PI-3 kinase (Wymann et al., 1996; Walker et al., 2000).

The blockade of the maintenance of voltage-pulse potentiation, was further checked with LY 294002 application of this synthetic PI-3 kinase inhibitor again reversed the voltage-pulse potentiation of mEPSC amplitudes. But took a longer time period to reverse the potentiation back towards control mEPSC amplitude, thereby confirming the requirement of PI-3 kinase in the maintenance of the voltage-pulse potentiation of mEPSC amplitudes.

Summary of all experimental findings

1. Voltage-pulse potentiation

The experimental results indicate that the voltage-pulse stimulation protocol provides an excellent mechanism through which postsynaptic function that underlies the long term potentiation of synaptic function may be probed. The characterising experiments proved that initially potentiation of mEPSC amplitude was possible and that the stimulation resulted in a stable increase mEPSC amplitudes. This potentiation was later found to be dependent upon the activation of L-type voltage gated calcium channels and not NMDA receptors a functional requirement for traditional LTP. A requirement of the potentiation is release of intracellular store calcium, as the activation of only the L-type calcium channel was insufficient for the induction of voltage-pulse potentiation.

Furthermore, considering the duration of each experiment being significantly shorter than any typical LTP experiment, application of any inhibitor (except CNQX) did not completely ablate the synaptic transmission mediating mEPSCs. Suggesting that in the pyramidal cells there are synapses which display almost stable AMPA receptors through which this transmission is mediated.

2. Post synaptic membrane fusion events are required for receptor trafficking

This phenomenon of voltage-pulse potentiation was later shown to be expressed through a postsynaptic mechanism dependent upon postsynaptic membrane fusion events, involving interactions between the NSF and SNAP 25 proteins in postsynaptic membrane with the GluR2 AMPA receptor subunit. The potentiation was then compartmentalised into which hetrodimers are dependent at which point of the potentiation. In experiments where the PICK1 binding site of the GluR2 receptor subunit and the TGL binding site of the GluR1 receptor subunit were inhibited, proved a requirement for insertion of hetrodimers of these subunits to mediate the magnitude and stability of the potentiation of mEPSC amplitudes. While the GluR2- GluR3 subunit complexes only mediate a very small potentiation of mEPSC amplitudes following the voltage-pulse stimulus, with insertion of these receptors occurring through the PICK1 related peptide ABP (Srivastava et al., 1998; Srivastava and Ziff, 1999).

3. Kinase regulation of voltage-pulse potentiation

Intracellular kinase regulation of any form of potentiation is a complex inter-regulating process; I selected a poorly described PI-3 kinase, which shares the same

regulatory substrate as a very well defined protein kinase cascade the PLC activation of PKC. The results from this study support and contradict previously published data. Man et al found that PI-3 kinase was important in the induction phase of glycine induced LTP. Our data support this finding as voltage-pulse potentiation was blocked by PI-3 kinase inhibition.

However, the work of Sanna et al., (2002) suggests that PI-3 kinase is only required for the expression of LTP and not maintenance or induction. I found that PI-3 kinase was essential for regulating the induction of the potentiation of mEPSC amplitudes which is typically expressed as an increase in AMPA receptor insertion into synapses. Furthermore this kinase was essential for the maintenance of the potentiation of mEPSC amplitudes, expressed by the recycling and insertion of AMPA receptors into the synapse to maintain the potentiated response.

The voltage-pulse to study potentiation protocol represents and excellent protocol through which biochemical methods can be applied to discern the mechanisms required for receptor trafficking to activated synapses.

Further experiments

1. Imaging changes in postsynaptic AMPA receptor number

The application of confocal microscopy, could be used to verify the two main premises of this thesis, the first that the mEPSC amplitude increase shown following VP potentiation, is brought about by the insertion of new AMPA receptors into nascent and active synapses in these CA1 pyramidal cells

The second premise of the voltage pulse potentiation paradigm holds that the transient potentiation of mEPSC frequency is made possible through a post synaptic mechanism, mainly the unsilencing of previous silent synapses. To address this concept with voltage-pulse potentiation I would use optical indicators of AMPA receptors, namely using con-focal imaging to view the movement green fluorescent protein (GFP) tagged AMPA receptors following application of the VP stimulus.

Developing this experiment further I would use a pHluorin-GluR2 receptor (Miesenbock et al., 1998; Perestenko et al., 2003).This AMPA receptor has a pH sensitive form of the traditional GFP attached. This protein pHluorin, changes it fluorescence intensity with movement from the more acidic cytosol to the less acidic synaptic site, through this intensity change we could look at receptor turnover following VP stimulation. Also it could provide an answer to site of the reduction in frequency shown in control recordings and with

the application of NEM. Whether this is due to rundown of vesicle release from the presynaptic terminal or due to a postsynaptic mechanism, by which AMPA receptors in the least stable synapses are removed, bringing about a physiological silence at these synapses induced by the application of the toxin is not clear. This postsynaptic phenomenon would mediate a reduction in the detection probability and hence a post synaptic frequency change.

2. Knock out animals

Other key experiments would involve the use of knock out mice; my interests would involve investigation of the receptor subunits involved in the voltage-pulse potentiation of mEPSC amplitude in the stargazing mouse. Through interactions with the stargazin protein, GluR1 receptor subunits join transport mechanisms usually reserved for NMDA receptor subunits.

Other experiments would involve the characterisation of voltage pulse potentiation in knockouts of both GluR1 and GluR2 AMPA receptor subunits. Further, investigation of protein kinase regulation of voltage pulse potentiation are needed, one important task is to try to identify if there are any kinases utilised in voltage-pulse potentiation which are not activated in traditional NMDA receptor LTP.

The potential for investigation with the voltage pulse stimulating protocol is immense, this experimental set up could easily be applied to investigation of the cellular actions of AMPAkines, potentiators of the function of AMPA receptors currently developed as a cure for Alzheimer's disease and Schizophrenia (Tsai and Coyle, 2002).

Bibliography

Bibliography

Abe K, Chisaka O, Van Roy F, Takeichi M (2004) Stability of dendritic spines and synaptic contacts is controlled by alpha N-catenin. Nat Neurosci 7:357-363.

Abraham WC, Bear MF (1996) Metaplasticity: the plasticity of synaptic plasticity. Trends Neurosci 19:126-130.

Alford S, Frenguelli BG, Schofield JG, Collingridge GL (1993) Characterization of Ca2+ signals induced in hippocampal CA1 neurones by the synaptic activation of NMDA receptors. J Physiol 469:693-716.

Amaral DG, Ishizuka N, Claiborne B (1990) Neurons, numbers and the hippocampal network. Prog Brain Res 83:1-11.

Amaral SG, D G, MP W (1995) Hippocampal formation. In: Paxinos G (ed) The Rat Nervous System: 433-495.

Ameri A (1999) The effects of cannabinoids on the brain. Prog Neurobiol 58:315-348.

Andersen P (1990) Synaptic integration in hippocampal CA1 pyramids. Prog Brain Res 83:215-222.

Andrasfalvy BK, Magee JC (2001) Distance-dependent increase in AMPA receptor number in the dendrites of adult hippocampal CA1 pyramidal neurons. J Neurosci 21:9151-9159.

Andrasfalvy BK, Magee JC (2004) Changes in AMPA receptor currents following LTP induction on rat CA1 pyramidal neurones. J Physiol 559:543-554.

Andrasfalvy BK, Smith MA, Borchardt T, Sprengel R, Magee JC (2003) Impaired regulation of synaptic strength in hippocampal neurons from GluR1-deficient mice. J Physiol 552:35-45.

Anwyl R (1999) Metabotropic glutamate receptors: electrophysiological properties and role in plasticity. Brain Res Brain Res Rev 29:83-120.

Banke TG, Bowie D, Lee H, Huganir RL, Schousboe A, Traynelis SF (2000) Control of GluR1 AMPA receptor function by cAMP-dependent protein kinase. J Neurosci 20:89-102.

Barria A, Malinow R (2002) Subunit-specific NMDA receptor trafficking to synapses. Neuron 35:345-353.

Barry MF, Ziff EB (2002) Receptor trafficking and the plasticity of excitatory synapses. Curr Opin Neurobiol 12:279-286.

Baskys A, Malenka RC (1991) Agonists at metabotropic glutamate receptors presynaptically inhibit EPSCs in neonatal rat hippocampus. J Physiol 444:687-701.

Bayer KU, De Koninck P, Leonard AS, Hell JW, Schulman H (2001) Interaction with the NMDA receptor locks CaMKII in an active conformation. Nature 411:801-805.

Bear M (2003) Bidirectional plasticity: from theroy to reality. 358.

Bekkers JM, Stevens CF (1995) Quantal analysis of EPSCs recorded from small numbers of synapses in hippocampal cultures. J Neurophysiol 73:1145-1156.

Benke TA, Luthi A, Isaac JT, Collingridge GL (1998) Modulation of AMPA receptor unitary conductance by synaptic activity. Nature 393:793-797.

Benke TA, Luthi A, Palmer MJ, Wikstrom MA, Anderson WW, Isaac JT, Collingridge GL (2001) Mathematical modelling of non-stationary

fluctuation analysis for studying channel properties of synaptic AMPA receptors. J Physiol 537:407-420.
Bergles DE, Jahr CE (1997) Synaptic activation of glutamate transporters in hippocampal astrocytes. Neuron 19:1297-1308.
Berridge MJ (1993) Inositol trisphosphate and calcium signalling. Nature 361:315-325.
Berridge MJ (1997) Elementary and global aspects of calcium signalling. J Exp Biol 200:315-319.
Berridge MJ (1998) Neuronal calcium signaling. Neuron 21:13-26.
Berridge MJ, Irvine RF (1984) Inositol trisphosphate, a novel second messenger in cellular signal transduction. Nature 312:315-321.
Birnbaumer L, Campbell KP, Catterall WA, Harpold MM, Hofmann F, Horne WA, Mori Y, Schwartz A, Snutch TP, Tanabe T, et al. (1994) The naming of voltage-gated calcium channels. Neuron 13:505-506.
Blakely RD, Sung U (2000) SNARE-ing neurotransmitter transporters. Nat Neurosci 3:969-971.
Bleakman D, Lodge D (1998) Neuropharmacology of AMPA and kainate receptors. Neuropharmacology 37:1187-1204.
Bliss TV, Lomo T (1973) Long-lasting potentiation of synaptic transmission in the dentate area of the anaesthetized rabbit following stimulation of the perforant path. J Physiol 232:331-356.
Bliss TV, Collingridge GL, Morris RG (2003) Introduction. Long-term potentiation and structure of the issue. Philos Trans R Soc Lond B Biol Sci 358:607-611.
Blitz DM, Foster KA, Regehr WG (2004) Short-term synaptic plasticity: a comparison of two synapses. Nat Rev Neurosci 5:630-640.
Bondeva T, Pirola L, Bulgarelli-Leva G, Rubio I, Wetzker R, Wymann MP (1998) Bifurcation of lipid and protein kinase signals of PI3Kgamma to the protein kinases PKB and MAPK. Science 282:293-296.
Borgdorff AJ, Choquet D (2002) Regulation of AMPA receptor lateral movements. Nature 417:649-653.
Boss BD, Turlejski K, Stanfield BB, Cowan WM (1987) On the numbers of neurons in fields CA1 and CA3 of the hippocampus of Sprague-Dawley and Wistar rats. Brain Res 406:280-287.
Bowie D, Lange GD (2002) Functional Stoichiometry of Glutamate Receptor Desensitization. J Neurosci 22:3392-3403.
Braithwaite SP, Meyer G, Henley JM (2000) Interactions between AMPA receptors and intracellular proteins. Neuropharmacology 39:919-930.
Braithwaite SP, Xia H, Malenka RC (2002) Differential roles for NSF and GRIP/ABP in AMPA receptor cycling. Proc Natl Acad Sci U S A 99:7096-7101.
Breakwell NA, Rowan MJ, Anwyl R (1996) Metabotropic glutamate receptor dependent EPSP and EPSP-spike potentiation in area CA1 of the submerged rat hippocampal slice. J Neurophysiol 76:3126-3135.
Breakwell NA, Rowan MJ, Anwyl R (1998) (+)-MCPG Blocks Induction of LTP in CA1 of Rat Hippocampus via Agonist Action at an mGluR Group II Receptor. J Neurophysiol 79:1270-1276.

Broad LM, Armstrong DL, Putney JW, Jr. (1999) Role of the inositol 1,4,5-trisphosphate receptor in Ca(2+) feedback inhibition of calcium release-activated calcium current (I(crac)). J Biol Chem 274:32881-32888.

Brown SS (1999) Cooperation between microtubule- and actin-based motor proteins. Annu Rev Cell Dev Biol 15:63-80.

Budde T, Meuth S, Pape HC (2002) Calcium-dependent inactivation of neuronal calcium channels. Nat Rev Neurosci 3:873-883.

Burnashev N, Zhou Z, Neher E, Sakmann B (1995) Fractional calcium currents through recombinant GluR channels of the NMDA, AMPA and kainate receptor subtypes. J Physiol (Lond) 485:403-418.

Cantley LC, Neel BG (1999) New insights into tumor suppression: PTEN suppresses tumor formation by restraining the phosphoinositide 3-kinase/AKT pathway. Proc Natl Acad Sci U S A 96:4240-4245.

Cantrell DA (2001) Phosphoinositide 3-kinase signalling pathways. J Cell Sci 114:1439-1445.

Carroll RC, Beattie EC, von Zastrow M, Malenka RC (2001) Role of AMPA receptor endocytosis in synaptic plasticity. Nat Rev Neurosci 2:315-324.

Chazot PL, Coleman SK, Cik M, Stephenson FA (1994) Molecular characterization of N-methyl-D-aspartate receptors expressed in mammalian cells yields evidence for the coexistence of three subunit types within a discrete receptor molecule. J Biol Chem 269:24403-24409.

Chen L, Chetkovich DM, Petralia RS, Sweeney NT, Kawasaki Y, Wenthold RJ, Bredt DS, Nicoll RA (2000) Stargazin regulates synaptic targeting of AMPA receptors by two distinct mechanisms. Nature 408:936-943.

Chen YA, Scheller RH (2001) SNARE-mediated membrane fusion. Nat Rev Mol Cell Biol 2:98-106.

Chen YA, Scales SJ, Patel SM, Doung YC, Scheller RH (1999) SNARE complex formation is triggered by Ca2+ and drives membrane fusion. Cell 97:165-174.

Chen YH, Li MH, Zhang Y, He LL, Yamada Y, Fitzmaurice A, Shen Y, Zhang H, Tong L, Yang J (2004) Structural basis of the alpha(1)-beta subunit interaction of voltage-gated Ca(2+) channels. Nature 429:675-680.

Chetkovich DM, Chen L, Stocker TJ, Nicoll RA, Bredt DS (2002a) Phosphorylation of the postsynaptic density-95 (PSD-95)/discs large/zona occludens-1 binding site of stargazin regulates binding to PSD-95 and synaptic targeting of AMPA receptors. J Neurosci 22:5791-5796.

Chetkovich DM, Bunn RC, Kuo SH, Kawasaki Y, Kohwi M, Bredt DS (2002b) Postsynaptic targeting of alternative postsynaptic density-95 isoforms by distinct mechanisms. J Neurosci 22:6415-6425.

Choi J, Ko J, Park E, Lee JR, Yoon J, Lim S, Kim E (2002) Phosphorylation of stargazin by protein kinase A regulates its interaction with PSD-95. J Biol Chem 277:12359-12363.

Choi S, Klingauf J, Tsien RW (2000) Postfusional regulation of cleft glutamate concentration during LTP at 'silent synapses'. Nat Neurosci 3:330-336.

Choquet D, Triller A (2003) The role of receptor diffusion in the organization of the postsynaptic membrane. Nat Rev Neurosci 4:251-265.

Chou MM, Hou W, Johnson J, Graham LK, Lee MH, Chen CS, Newton AC, Schaffhausen BS, Toker A (1998) Regulation of protein kinase C zeta by PI 3-kinase and PDK-1. Curr Biol 8:1069-1077.

Chung HJ, Xia J, Scannevin RH, Zhang X, Huganir RL (2000) Phosphorylation of the AMPA receptor subunit GluR2 differentially regulates its interaction with PDZ domain-containing proteins. J Neurosci 20:7258-7267.

Clements JD, Feltz A, Sahara Y, Westbrook GL (1998) Activation kinetics of AMPA receptor channels reveal the number of functional agonist binding sites. J Neurosci 18:119-127.

Colledge M, Scott JD (1999) AKAPs: from structure to function. Trends Cell Biol 9:216-221.

Colledge M, Dean RA, Scott GK, Langeberg LK, Huganir RL, Scott JD (2000) Targeting of PKA to glutamate receptors through a MAGUK-AKAP complex. Neuron 27:107-119.

Collingridge GL, Singer W (1990) Excitatory amino acid receptors and synaptic plasticity. Trends Pharmacol Sci 11:290-296.

Collingridge GL, Kehl SJ, McLennan H (1983) Excitatory amino acids in synaptic transmission in the Schaffer collateral-commissural pathway of the rat hippocampus. J Physiol 334:33-46.

Collingridge GL, Isaac JT, Wang YT (2004) Receptor trafficking and synaptic plasticity. Nat Rev Neurosci 5:952-962.

Conn PJ, Pin J-P (1997) PHARMACOLOGY AND FUNCTIONS OF METABOTROPIC GLUTAMATE RECEPTORS. Annu Rev Pharmacol Toxicol 37:205-237.

Corkin S (2002) What's new with the amnesic patient H.M.? Nat Rev Neurosci 3:153-160.

Cossart R, Epsztein J, Tyzio R, Becq H, Hirsch J, Ben-Ari Y, Crepel V (2002) Quantal release of glutamate generates pure kainate and mixed AMPA/kainate EPSCs in hippocampal neurons. Neuron 35:147-159.

Cousin MA, Malladi CS, Tan TC, Raymond CR, Smillie KJ, Robinson PJ (2003) Synapsin I-associated phosphatidylinositol 3-kinase mediates synaptic vesicle delivery to the readily releasable pool. J Biol Chem.

Crossthwaite AJ, Valli H, Williams RJ (2004) Inhibiting Src family tyrosine kinase activity blocks glutamate signalling to ERK1/2 and Akt/PKB but not JNK in cultured striatal neurones. J Neurochem 88:1127-1139.

Cull-Candy S, Brickley S, Farrant M (2001) NMDA receptor subunits: diversity, development and disease. Curr Opin Neurobiol 11:327-335.

Dahia PL (2000) PTEN, a unique tumor suppressor gene. Endocr Relat Cancer 7:115-129.

Datta K, Bellacosa A, Chan TO, Tsichlis PN (1996) Akt is a direct target of the phosphatidylinositol 3-kinase. Activation by growth factors, v-src and v-Ha-ras, in Sf9 and mammalian cells. J Biol Chem 271:30835-30839.

Davidson GA, Varhol RJ (1995) Kinetics of thapsigargin-Ca(2+)-ATPase (sarcoplasmic reticulum) interaction reveals a two-step binding mechanism and picomolar inhibition. J Biol Chem 270:11731-11734.

Davies CH, Collingridge GL (1996) Regulation of EPSPs by the synaptic activation of GABAB autoreceptors in rat hippocampus. J Physiol 496 (Pt 2):451-470.

Daw MI, Chittajallu R, Bortolotto ZA, Dev KK, Duprat F, Henley JM, Collingridge GL, Isaac JT (2000) PDZ proteins interacting with C-terminal GluR2/3 are involved in a PKC-dependent regulation of AMPA receptors at hippocampal synapses. Neuron 28:873-886.

De Paola V, Arber S, Caroni P (2003) AMPA receptors regulate dynamic equilibrium of presynaptic terminals in mature hippocampal networks. Nat Neurosci 6:491-500.

De Simoni A, Griesinger CB, Edwards FA (2003) Development of rat CA1 neurones in acute versus organotypic slices: role of experience in synaptic morphology and activity. J Physiol 550:135-147.

DeBello WM, O'Connor V, Dresbach T, Whiteheart SW, Wang SS, Schweizer FE, Betz H, Rothman JE, Augustine GJ (1995) SNAP-mediated protein-protein interactions essential for neurotransmitter release. Nature 373:626-630.

Desmond NL, Scott CA, Jane JA, Jr., Levy WB (1994) Ultrastructural identification of entorhinal cortical synapses in CA1 stratum lacunosum-moleculare of the rat. Hippocampus 4:594-600.

Dev KK, Nakanishi S, Henley JM (2004) The PDZ Domain of PICK1 Differentially Accepts Protein Kinase C-{alpha} and GluR2 as Interacting Ligands. J Biol Chem 279:41393-41397.

DiGregorio DA, Nusser Z, Silver RA (2002) Spillover of glutamate onto synaptic AMPA receptors enhances fast transmission at a cerebellar synapse. Neuron 35:521-533.

Dingledine R, Borges K, Bowie D, Traynelis SF (1999) The glutamate receptor ion channels. Pharmacol Rev 51:7-61.

Ditlevsen DK, Kohler LB, Pedersen MV, Risell M, Kolkova K, Meyer M, Berezin V, Bock E (2003) The role of phosphatidylinositol 3-kinase in neural cell adhesion molecule-mediated neuronal differentiation and survival. J Neurochem 84:546-556.

Dong H, Zhang P, Song I, Petralia RS, Liao D, Huganir RL (1999) Characterization of the glutamate receptor-interacting proteins GRIP1 and GRIP2. J Neurosci 19:6930-6941.

Du K, Montminy M (1998) CREB is a regulatory target for the protein kinase Akt/PKB. J Biol Chem 273:32377-32379.

Edwards FA (1995) Anatomy and electrophysiology of fast central synapses lead to a structural model for long-term potentiation. Physiol Rev 75:759-787.

Ehlers MD (2000) Reinsertion or degradation of AMPA receptors determined by activity-dependent endocytic sorting. Neuron 28:511-525.

Ehlers MD, Mammen AL, Lau LF, Huganir RL (1996) Synaptic targeting of glutamate receptors. Curr Opin Cell Biol 8:484-489.

Ehrlich I, Malinow R (2004) Postsynaptic density 95 controls AMPA receptor incorporation during long-term potentiation and experience-driven synaptic plasticity. J Neurosci 24:916-927.

Emptage N, Bliss TV, Fine A (1999) Single synaptic events evoke NMDA receptor-mediated release of calcium from internal stores in hippocampal dendritic spines. Neuron 22:115-124.

Engelman HS, MacDermott AB (2004) Presynaptic ionotropic receptors and control of transmitter release. Nat Rev Neurosci 5:135-145.

Engert F, Bonhoeffer T (1999) Dendritic spine changes associated with hippocampal long-term synaptic plasticity. Nature 399:66-70.
Esteban JA (2003) AMPA receptor trafficking: a road map for synaptic plasticity. Mol Interv 3:375-385.
Esteban JA, Shi SH, Wilson C, Nuriya M, Huganir RL, Malinow R (2003) PKA phosphorylation of AMPA receptor subunits controls synaptic trafficking underlying plasticity. Nat Neurosci 6:136-143.
Fagni L, Chavis P, Ango F, Bockaert J (2000) Complex interactions between mGluRs, intracellular Ca2+ stores and ion channels in neurons. Trends Neurosci 23:80-88.
Fasshauer D, Margittai M (2004) A transient N-terminal interaction of SNAP-25 and syntaxin nucleates SNARE assembly. J Biol Chem 279:7613-7621.
Fatt P, Katz B (1952) Spontaneous subthreshold activity at motor nerve endings. J Physiol 117:109-128.
Feng W, Shi Y, Li M, Zhang M (2003) Tandem PDZ repeats in glutamate receptor-interacting proteins have a novel mode of PDZ domain-mediated target binding. Nat Struct Biol 10:972-978.
Finley MF, Patel SM, Madison DV, Scheller RH (2002) The core membrane fusion complex governs the probability of synaptic vesicle fusion but not transmitter release kinetics. J Neurosci 22:1266-1272.
Fitzjohn SM, Collingridge GL (2004) Endocannabinoids; losing inhibition to increase learning capacity? Neuron 43:762-764.
Fitzjohn SM, Pickard L, Duckworth JK, Molnar E, Henley JM, Collingridge GL, Noel J (2001) An electrophysiological characterisation of long-term potentiation in cultured dissociated hippocampal neurones. Neuropharmacology 41:693-699.
Fitzsimonds RM, Poo MM (1998) Retrograde signaling in the development and modification of synapses. Physiol Rev 78:143-170.
Franciosi S (2001) AMPA receptors: potential implications in development and disease. Cell Mol Life Sci 58:921-930.
Fujii S, Matsumoto M, Igarashi K, Kato H, Mikoshiba K (2000) Synaptic plasticity in hippocampal CA1 neurons of mice lacking type 1 inositol-1,4,5-trisphosphate receptors. Learn Mem 7:312-320.
Gahwiler BH, Capogna M, Debanne D, McKinney RA, Thompson SM (1997) Organotypic slice cultures: a technique has come of age. Trends Neurosci 20:471-477.
Gallo V, Haydar T (2003) GABA: exciting again in its own right. J Physiol 550:665.
Gallo V, Upson LM, Hayes WP, Vyklicky L, Jr., Winters CA, Buonanno A (1992) Molecular cloning and development analysis of a new glutamate receptor subunit isoform in cerebellum. J Neurosci 12:1010-1023.
Ganeshina O, Berry RW, Petralia RS, Nicholson DA, Geinisman Y (2004) Synapses with a segmented, completely partitioned postsynaptic density express more AMPA receptors than other axospinous synaptic junctions. Neuroscience 125:615-623.
Garner CC, Nash J, Huganir RL (2000) PDZ domains in synapse assembly and signalling. Trends Cell Biol 10:274-280.

Gasparini S, Saviane C, Voronin LL, Cherubini E (2000) Silent synapses in the developing hippocampus: lack of functional AMPA receptors or low probability of glutamate release? Proc Natl Acad Sci U S A 97:9741-9746.

Gerst JE (2003) SNARE regulators: matchmakers and matchbreakers. Biochim Biophys Acta 1641:99-110.

Goda Y, Davis GW (2003) Mechanisms of synapse assembly and disassembly. Neuron 40:243-264.

Gomperts SN, Carroll R, Malenka RC, Nicoll RA (2000) Distinct roles for ionotropic and metabotropic glutamate receptors in the maturation of excitatory synapses. J Neurosci 20:2229-2237.

Gomperts SN, Rao A, Craig AM, Malenka RC, Nicoll RA (1998) Postsynaptically silent synapses in single neuron cultures. Neuron 21:1443-1451.

Gotte M, von Mollard GF (1998) A new beat for the SNARE drum. Trends Cell Biol 8:215-218.

Gouaux E (2003) Structure and Function of AMPA Receptors. J Physiol (Lond):jphysiol.2003.054320.

Greger IH, Khatri L, Kong X, Ziff EB (2003) AMPA receptor tetramerization is mediated by q/r editing. Neuron 40:763-774.

Groc L, Gustafsson B, Hanse E (2002) Spontaneous unitary synaptic activity in CA1 pyramidal neurons during early postnatal development: constant contribution of AMPA and NMDA receptors. J Neurosci 22:5552-5562.

Gustafsson B, Wigstrom H (1990) Long-term potentiation in the hippocampal CA1 region: its induction and early temporal development. Prog Brain Res 83:223-232.

Hajos N, Katona I, Naiem SS, MacKie K, Ledent C, Mody I, Freund TF (2000) Cannabinoids inhibit hippocampal GABAergic transmission and network oscillations. Eur J Neurosci 12:3239-3249.

Harris EW, Cotman CW (1986) Long-term potentiation of guinea pig mossy fiber responses is not blocked by N-methyl D-aspartate antagonists. Neurosci Lett 70:132-137.

Harris KD, Csicsvari J, Hirase H, Dragoi G, Buzsaki G (2003) Organization of cell assemblies in the hippocampus. Nature 424:552-556.

Harvey J, Collingridge GL (1992) Thapsigargin blocks the induction of long-term potentiation in rat hippocampal slices. Neurosci Lett 139:197-200.

Hayashi Y, Shi SH, Esteban JA, Piccini A, Poncer JC, Malinow R (2000) Driving AMPA receptors into synapses by LTP and CaMKII: requirement for GluR1 and PDZ domain interaction. Science 287:2262-2267.

Heynen AJ, Quinlan EM, Bae DC, Bear MF (2000) Bidirectional, activity-dependent regulation of glutamate receptors in the adult hippocampus in vivo. Neuron 28:527-536.

Higuchi M, Maas S, Single FN, Hartner J, Rozov A, Burnashev N, Feldmeyer D, Sprengel R, Seeburg PH (2000) Point mutation in an AMPA receptor gene rescues lethality in mice deficient in the RNA-editing enzyme ADAR2. Nature 406:78-81.

Hirbec H, Perestenko O, Nishimune A, Meyer G, Nakanishi S, Henley JM, Dev KK (2002) The PDZ proteins PICK1, GRIP, and syntenin bind multiple glutamate receptor subtypes. Analysis of PDZ binding motifs. J Biol Chem 277:15221-15224.

Hirbec H, Francis JC, Lauri SE, Braithwaite SP, Coussen F, Mulle C, Dev KK, Couthino V, Meyer G, Isaac JT, Collingridge GL, Henley JM (2003) Rapid and Differential Regulation of AMPA and Kainate Receptors at Hippocampal Mossy Fibre Synapses by PICK1 and GRIP. Neuron 37:625-638.

Hoffman AF, Lupica CR (2000) Mechanisms of cannabinoid inhibition of GABA(A) synaptic transmission in the hippocampus. J Neurosci 20:2470-2479.

Hollmann M, Heinemann S (1994) Cloned glutamate receptors. Annu Rev Neurosci 17:31-108.

Hong RM, Mori H, Fukui T, Moriyama Y, Futai M, Yamamoto A, Tashiro Y, Tagaya M (1994) Association of N-ethylmaleimide-sensitive factor with synaptic vesicles. FEBS Lett 350:253-257.

Hou L, Klann E (2004) Activation of the phosphoinositide 3-kinase-Akt-mammalian target of rapamycin signaling pathway is required for metabotropic glutamate receptor-dependent long-term depression. J Neurosci 24:6352-6361.

Hou Q, Gao X, Zhang X, Kong L, Wang X, Bian W, Tu Y, Jin M, Zhao G, Li B, Jing N, Yu L (2004) SNAP-25 in hippocampal CA1 region is involved in memory consolidation. Eur J Neurosci 20:1593-1603.

Huettner JE (2003) Kainate receptors and synaptic transmission. Prog Neurobiol 70:387-407.

Hume RI, Dingledine R, Heinemann SF (1991) Identification of a site in glutamate receptor subunits that controls calcium permeability. Science 253:1028-1031.

Hunter T (1995) Protein kinases and phosphatases: the yin and yang of protein phosphorylation and signaling. Cell 80:225-236.

Im YJ, Park SH, Rho SH, Lee JH, Kang GB, Sheng M, Kim E, Eom SH (2003) Crystal structure of GRIP1 PDZ6-peptide complex reveals the structural basis for class II PDZ target recognition and PDZ domain-mediated multimerization. J Biol Chem 278:8501-8507.

Isaac JT (2003) Postsynaptic silent synapses: evidence and mechanisms. Neuropharmacology 45:450-460.

Isaac JT, Luthi A, Palmer MJ, Anderson WW, Benke TA, Collingridge GL (1998) An investigation of the expression mechanism of LTP of AMPA receptor-mediated synaptic transmission at hippocampal CA1 synapses using failures analysis and dendritic recordings. Neuropharmacology 37:1399-1410.

Ishikawa T, Sahara Y, Takahashi T (2002) A single packet of transmitter does not saturate postsynaptic glutamate receptors. Neuron 34:613-621.

Jia Z, Agopyan N, Miu P, Xiong Z, Henderson J, Gerlai R, Taverna FA, Velumian A, MacDonald J, Carlen P, Abramow-Newerly W, Roder J (1996) Enhanced LTP in mice deficient in the AMPA receptor GluR2. Neuron 17:945-956.

Jonas P, Monyer H (1999) Ionotropic glutamate receptors in the CNS. Handbook of Experimental Pharmacology 141.

Kapur A, Yeckel MF, Gray R, Johnston D (1998) L-Type calcium channels are required for one form of hippocampal mossy fiber LTP. J Neurophysiol 79:2181-2190.

Kauer JA, Malenka RC, Nicoll RA (1988a) NMDA application potentiates synaptic transmission in the hippocampus. Nature 334:250-252.

Kauer JA, Malenka RC, Nicoll RA (1988b) A persistent postsynaptic modification mediates long-term potentiation in the hippocampus. Neuron 1:911-917.

Kemp JA, McKernan RM (2002) NMDA receptor pathways as drug targets. Nat Neurosci 5 Suppl:1039-1042.

Kim CH, Chung HJ, Lee HK, Huganir RL (2001) Interaction of the AMPA receptor subunit GluR2/3 with PDZ domains regulates hippocampal long-term depression. Proc Natl Acad Sci U S A 98:11725-11730.

Kim E, Sheng M (2004) PDZ domain proteins of synapses. Nat Rev Neurosci 5:771-781.

Kohler M, Kornau HC, Seeburg PH (1994) The organization of the gene for the functionally dominant alpha-amino-3-hydroxy-5-methylisoxazole-4-propionic acid receptor subunit GluR-B. J Biol Chem 269:17367-17370.

Korkotian E, Segal M (1997) Calcium-containing organelles display unique reactivity to chemical stimulation in cultured hippocampal neurons. J Neurosci 17:1670-1682.

Krupp JJ, Vissel B, Thomas CG, Heinemann SF, Westbrook GL (1999) Interactions of calmodulin and alpha-actinin with the NR1 subunit modulate Ca2+-dependent inactivation of NMDA receptors. J Neurosci 19:1165-1178.

Kullmann DM (1994) Amplitude fluctuations of dual-component EPSCs in hippocampal pyramidal cells: implications for long-term potentiation. Neuron 12:1111-1120.

Kullmann DM (2003) Silent synapses: what are they telling us about long-term potentiation? Philos Trans R Soc Lond B Biol Sci 358:727-733.

Kullmann DM, Nicoll RA (1992) Long-term potentiation is associated with increases in quantal content and quantal amplitude. Nature 357:240-244.

Kullmann DM, Siegelbaum SA (1995) The site of expression of NMDA receptor-dependent LTP: new fuel for an old fire. Neuron 15:997-1002.

Kullmann DM, Asztely F (1998) Extrasynaptic glutamate spillover in the hippocampus: evidence and implications. Trends Neurosci 21:8-14.

Kullmann DM, Erdemli G, Asztely F (1996) LTP of AMPA and NMDA receptor-mediated signals: evidence for presynaptic expression and extrasynaptic glutamate spill-over. Neuron 17:461-474.

Kullmann DM, Perkel DJ, Manabe T, Nicoll RA (1992) Ca2+ entry via postsynaptic voltage-sensitive Ca2+ channels can transiently potentiate excitatory synaptic transmission in the hippocampus. Neuron 9:1175-1183.

Kumar A, Foster TC (2004) Enhanced long-term potentiation during aging is masked by processes involving intracellular calcium stores. J Neurophysiol 91:2437-2444.

Laube B, Kuhse J, Betz H (1998) Evidence for a tetrameric structure of recombinant NMDA receptors. J Neurosci 18:2954-2961.

Lauri SE, Bortolotto ZA, Nistico R, Bleakman D, Ornstein PL, Lodge D, Isaac JT, Collingridge GL (2003) A role for Ca2+ stores in kainate receptor-dependent synaptic facilitation and LTP at mossy fiber synapses in the hippocampus. Neuron 39:327-341.

Lee HK, Barbarosie M, Kameyama K, Bear MF, Huganir RL (2000) Regulation of distinct AMPA receptor phosphorylation sites during bidirectional synaptic plasticity. Nature 405:955-959.

Lee HK, Takamiya K, Han JS, Man H, Kim CH, Rumbaugh G, Yu S, Ding L, He C, Petralia RS, Wenthold RJ, Gallagher M, Huganir RL (2003) Phosphorylation

of the AMPA receptor GluR1 subunit is required for synaptic plasticity and retention of spatial memory. Cell 112:631-643.
Lee SH, Simonetta A, Sheng M (2004) Subunit rules governing the sorting of internalized AMPA receptors in hippocampal neurons. Neuron 43:221-236.
Leevers SJ, Vanhaesebroeck B, Waterfield MD (1999) Signalling through phosphoinositide 3-kinases: the lipids take centre stage. Curr Opin Cell Biol 11:219-225.
Lehre KP, Danbolt NC (1998) The number of glutamate transporter subtype molecules at glutamatergic synapses: chemical and stereological quantification in young adult rat brain. J Neurosci 18:8751-8757.
Leonard AS, Davare MA, Horne MC, Garner CC, Hell JW (1998) SAP97 is associated with the alpha-amino-3-hydroxy-5-methylisoxazole-4-propionic acid receptor GluR1 subunit. J Biol Chem 273:19518-19524.
Lerma J (2003) Roles and rules of kainate receptors in synaptic transmission. Nat Rev Neurosci 4:481-495.
Leslie NR, Downes CP (2002) PTEN: The down side of PI 3-kinase signalling. Cell Signal 14:285-295.
Levy LM, Warr O, Attwell D (1998) Stoichiometry of the glial glutamate transporter GLT-1 expressed inducibly in a Chinese hamster ovary cell line selected for low endogenous Na+-dependent glutamate uptake. J Neurosci 18:9620-9628.
Li J, Yen C, Liaw D, Podsypanina K, Bose S, Wang SI, Puc J, Miliaresis C, Rodgers L, McCombie R, Bigner SH, Giovanella BC, Ittmann M, Tycko B, Hibshoosh H, Wigler MH, Parsons R (1997) PTEN, a putative protein tyrosine phosphatase gene mutated in human brain, breast, and prostate cancer. Science 275:1943-1947.
Li P, Kerchner GA, Sala C, Wei F, Huettner JE, Sheng M, Zhuo M (1999) AMPA receptor-PDZ interactions in facilitation of spinal sensory synapses. Nat Neurosci 2:972-977.
Li WC, Soffe SR, Roberts A (2004) Glutamate and acetylcholine corelease at developing synapses. Proc Natl Acad Sci U S A 101:15488-15493.
Liliental J, Moon SY, Lesche R, Mamillapalli R, Li D, Zheng Y, Sun H, Wu H (2000) Genetic deletion of the Pten tumor suppressor gene promotes cell motility by activation of Rac1 and Cdc42 GTPases. Curr Biol 10:401-404.
Lim IA, Hall DD, Hell JW (2002) Selectivity and promiscuity of the first and second PDZ domains of PSD-95 and synapse-associated protein 102. J Biol Chem 277:21697-21711.
Lim IA, Merrill MA, Chen Y, Hell JW (2003) Disruption of the NMDA receptor-PSD-95 interaction in hippocampal neurons with no obvious physiological short-term effect. Neuropharmacology 45:738-754.
Lin B, Brucher FA, Colgin LL, Lynch G (2002) Long-term potentiation alters the modulator pharmacology of AMPA-type glutamate receptors. J Neurophysiol 87:2790-2800.
Lin Y, Skeberdis VA, Francesconi A, Bennett MV, Zukin RS (2004) Postsynaptic density protein-95 regulates NMDA channel gating and surface expression. J Neurosci 24:10138-10148.
Lipscombe D, Helton TD, Xu W (2004) L-type calcium channels: the low down. J Neurophysiol 92:2633-2641.

Lisman J, Schulman H, Cline H (2002) The molecular basis of CaMKII function in synaptic and behavioural memory. Nat Rev Neurosci 3:175-190.

Lisman JE, Zhabotinsky AM (2001) A model of synaptic memory: a CaMKII/PP1 switch that potentiates transmission by organizing an AMPA receptor anchoring assembly. Neuron 31:191-201.

Lissin DV, Carroll RC, Nicoll RA, Malenka RC, von Zastrow M (1999) Rapid, activation-induced redistribution of ionotropic glutamate receptors in cultured hippocampal neurons. J Neurosci 19:1263-1272.

Lissin DV, Gomperts SN, Carroll RC, Christine CW, Kalman D, Kitamura M, Hardy S, Nicoll RA, Malenka RC, von Zastrow M (1998) Activity differentially regulates the surface expression of synaptic AMPA and NMDA glutamate receptors. Proc Natl Acad Sci U S A 95:7097-7102.

Littleton JT, Barnard RJ, Titus SA, Slind J, Chapman ER, Ganetzky B (2001) SNARE-complex disassembly by NSF follows synaptic-vesicle fusion. Proc Natl Acad Sci U S A 98:12233-12238.

Liu SQ, Cull-Candy SG (2000) Synaptic activity at calcium-permeable AMPA receptors induces a switch in receptor subtype. Nature 405:454-458.

Liu Z, Tearle AW, Nai Q, Berg DK (2005) Rapid activity-driven SNARE-dependent trafficking of nicotinic receptors on somatic spines. J Neurosci 25:1159-1168.

Lledo PM, Zhang X, Sudhof TC, Malenka RC, Nicoll RA (1998) Postsynaptic membrane fusion and long-term potentiation. Science 279:399-403.

Lomeli H, Mosbacher J, Melcher T, Hoger T, Geiger JR, Kuner T, Monyer H, Higuchi M, Bach A, Seeburg PH (1994) Control of kinetic properties of AMPA receptor channels by nuclear RNA editing. Science 266:1709-1713.

Lømo T (1966) frequency potentiation of excitatory synaptic activity in the area of the hippocampal formation. Acta Physiol Scand 68:128.

Lovinger DM (1991) Trans-1-aminocyclopentane-1,3-dicarboxylic acid (t-ACPD) decreases synaptic excitation in rat striatal slices through a presynaptic action. Neurosci Lett 129:17-21.

Luscher C, Frerking M (2001) Restless AMPA receptors: implications for synaptic transmission and plasticity. Trends Neurosci 24:665-670.

Luscher C, Xia H, Beattie EC, Carroll RC, von Zastrow M, Malenka RC, Nicoll RA (1999) Role of AMPA receptor cycling in synaptic transmission and plasticity. Neuron 24:649-658.

Luthi A, Schwyzer L, Mateos JM, Gahwiler BH, McKinney RA (2001) NMDA receptor activation limits the number of synaptic connections during hippocampal development. Nat Neurosci 4:1102-1107.

Luthi A, Chittajallu R, Duprat F, Palmer MJ, Benke TA, Kidd FL, Henley JM, Isaac JT, Collingridge GL (1999) Hippocampal LTD expression involves a pool of AMPARs regulated by the NSF-GluR2 interaction. Neuron 24:389-399.

Lynch MA (2004) Long-term potentiation and memory. Physiol Rev 84:87-136.

Ma AD, Metjian A, Bagrodia S, Taylor S, Abrams CS (1998) Cytoskeletal reorganization by G protein-coupled receptors is dependent on phosphoinositide 3-kinase gamma, a Rac guanosine exchange factor, and Rac. Mol Cell Biol 18:4744-4751.

MacDermott AB, Role LW, Siegelbaum SA (1999) Presynaptic ionotropic receptors and the control of transmitter release. Annu Rev Neurosci 22:443-485.

Machaca K (2003) Ca2+-calmodulin-dependent protein kinase II potentiates store-operated Ca2+ current. J Biol Chem 278:33730-33737.
Magee JC, Cook EP (2000) Somatic EPSP amplitude is independent of synapse location in hippocampal pyramidal neurons. Nat Neurosci 3:895-903.
Mainen ZF, Malinow R, Svoboda K (1999) Synaptic calcium transients in single spines indicate that NMDA receptors are not saturated. Nature 399:151-155.
Malenka RC (2003a) Opinion: The long-term potential of LTP. Nat Rev Neurosci 4:923-926.
Malenka RC (2003b) Synaptic plasticity and AMPA receptor trafficking. Ann N Y Acad Sci 1003:1-11.
Malenka RC, Nicoll RA (1997) Silent synapses speak up. Neuron 19:473-476.
Malenka RC, Nicoll RA (1999) Long-term potentiation--a decade of progress? Science 285:1870-1874.
Malenka RC, Bear MF (2004) LTP and LTD; An Embarrassment of Riches. Neuron 44:5-21.
Malenka RC, Kauer JA, Zucker RS, Nicoll RA (1988) Postsynaptic calcium is sufficient for potentiation of hippocampal synaptic transmission. Science 242:81-84.
Malinow R, Malenka RC (2002) AMPA receptor trafficking and synaptic plasticity. Annu Rev Neurosci 25:103-126.
Malinow R, Mainen ZF, Hayashi Y (2000) LTP mechanisms: from silence to four-lane traffic. Curr Opin Neurobiol 10:352-357.
Mammen AL, Huganir RL, O'Brien RJ (1997) Redistribution and stabilization of cell surface glutamate receptors during synapse formation. J Neurosci 17:7351-7358.
Man HY, Ju W, Ahmadian G, Wang YT (2000) Intracellular trafficking of AMPA receptors in synaptic plasticity. Cell Mol Life Sci 57:1526-1534.
Man HY, Wang Q, Lu WY, Ju W, Ahmadian G, Liu L, D'Souza S, Wong TP, Taghibiglou C, Lu J, Becker LE, Pei L, Liu F, Wymann MP, MacDonald JF, Wang YT (2003) Activation of PI3-kinase is required for AMPA receptor insertion during LTP of mEPSCs in cultured hippocampal neurons. Neuron 38:611-624.
Manabe T, Renner P, Nicoll RA (1992) Postsynaptic contribution to long-term potentiation revealed by the analysis of miniature synaptic currents. Nature 355:50-55.
Marchal C, Mulle C (2004) Postnatal maturation of mossy fibre excitatory transmission in mouse CA3 pyramidal cells: a potential role for kainate receptors. J Physiol 561:27-37.
Martin SJ, Morris RG (2002) New life in an old idea: the synaptic plasticity and memory hypothesis revisited. Hippocampus 12:609-636.
Martin SJ, Grimwood PD, Morris RG (2000) Synaptic plasticity and memory: an evaluation of the hypothesis. Annu Rev Neurosci 23:649-711.
Matias CM, Dionisio JC, Arif M, Quinta-Ferreira ME (2003) Effect of D-2 amino-5-phosphonopentanoate and nifedipine on postsynaptic calcium changes associated with long-term potentiation in hippocampal CA1 area. Brain Res 976:90-99.

Matsuda K, Fletcher M, Kamiya Y, Yuzaki M (2003) Specific Assembly with the NMDA Receptor 3B Subunit Controls Surface Expression and Calcium Permeability of NMDA Receptors. J Neurosci 23:10064-10073.

Mattson MP, LaFerla FM, Chan SL, Leissring MA, Shepel PN, Geiger JD (2000) Calcium signaling in the ER: its role in neuronal plasticity and neurodegenerative disorders. Trends Neurosci 23:222-229.

May AP, Whiteheart SW, Weis WI (2001) Unraveling the mechanism of the vesicle transport ATPase NSF, the N-ethylmaleimide-sensitive factor. J Biol Chem 276:21991-21994.

McKinney RA, Luthi A, Bandtlow CE, Gahwiler BH, Thompson SM (1999a) Selective glutamate receptor antagonists can induce or prevent axonal sprouting in rat hippocampal slice cultures. Proc Natl Acad Sci U S A 96:11631-11636.

McKinney RA, Capogna M, Durr R, Gahwiler BH, Thompson SM (1999b) Miniature synaptic events maintain dendritic spines via AMPA receptor activation. Nat Neurosci 2:44-49.

Meldrum BS (1998) The glutamate synapse as a therapeutical target: perspectives for the future. Prog Brain Res 116:441-458.

Meldrum BS (2000) Glutamate as a neurotransmitter in the brain: review of physiology and pathology. J Nutr 130:1007S-1015S.

Meunier FA, Lisk G, Sesardic D, Dolly JO (2003) Dynamics of motor nerve terminal remodeling unveiled using SNARE-cleaving botulinum toxins: the extent and duration are dictated by the sites of SNAP-25 truncation. Mol Cell Neurosci 22:454-466.

Miesenbock G, De Angelis DA, Rothman JE (1998) Visualizing secretion and synaptic transmission with pH-sensitive green fluorescent proteins. Nature 394:192-195.

Misner DL, Sullivan JM (1999) Mechanism of Cannabinoid Effects on Long-Term Potentiation and Depression in Hippocampal CA1 Neurons. J Neurosci 19:6795-6805.

Misra C, Brickley SG, Wyllie DJ, Cull-Candy SG (2000) Slow deactivation kinetics of NMDA receptors containing NR1 and NR2D subunits in rat cerebellar Purkinje cells. J Physiol 525 Pt 2:299-305.

Monyer H, Burnashev N, Laurie DJ, Sakmann B, Seeburg PH (1994) Developmental and regional expression in the rat brain and functional properties of four NMDA receptors. Neuron 12:529-540.

Morgan JR (2003) Sniffing calcium from the outside: an extracellular calcium sensor for synaptic vesicle recycling. J Physiol 551:2.

Morgan SL, Teyler TJ (1999) VDCCs and NMDARs underlie two forms of LTP in CA1 hippocampus in vivo. J Neurophysiol 82:736-740.

Mosher HS (1986) The chemistry of tetrodotoxin. Ann N Y Acad Sci 479:32-43.

Nagase T, Ito KI, Kato K, Kaneko K, Kohda K, Matsumoto M, Hoshino A, Inoue T, Fujii S, Kato H, Mikoshiba K (2003) Long-term potentiation and long-term depression in hippocampal CA1 neurons of mice lacking the IP(3) type 1 receptor. Neuroscience 117:821-830.

Nakagawa T, Cheng Y, Ramm E, Sheng M, Walz T (2005) Structure and different conformational states of native AMPA receptor complexes. Nature 433:545-549.

Nicoll RA, Malenka RC (1995) Contrasting properties of two forms of long-term potentiation in the hippocampus. Nature 377:115-118.
Nicoll RA, Malenka RC (1999) Expression mechanisms underlying NMDA receptor-dependent long-term potentiation. Ann N Y Acad Sci 868:515-525.
Nicoll RA, Kauer JA, Malenka RC (1988) The current excitement in long-term potentiation. Neuron 1:97-103.
Nicoll RA, Frerking M, Schmitz D (2000) AMPA receptors jump the synaptic cleft. Nat Neurosci 3:527-529.
Niikura Y, Abe K, Misawa M (2004) Involvement of L-type Ca2+ channels in the induction of long-term potentiation in the basolateral amygdala-dentate gyrus pathway of anesthetized rats. Brain Res 1017:218-221.
Nishimune A, Isaac JT, Molnar E, Noel J, Nash SR, Tagaya M, Collingridge GL, Nakanishi S, Henley JM (1998) NSF binding to GluR2 regulates synaptic transmission. Neuron 21:87-97.
Nishiyama M, Hong K, Mikoshiba K, Poo MM, Kato K (2000) Calcium stores regulate the polarity and input specificity of synaptic modification. Nature 408:584-588.
Nó RLd (1934) Studies on the structure of the cerebral cortex.II. Continuation of the study of the ammonic system. J Psychol Neurol 46:113-177.
Noel J, Ralph GS, Pickard L, Williams J, Molnar E, Uney JB, Collingridge GL, Henley JM (1999) Surface expression of AMPA receptors in hippocampal neurons is regulated by an NSF-dependent mechanism. Neuron 23:365-376.
Nusser Z (1999) A new approach to estimate the number, density and variability of receptors at central synapses. Eur J Neurosci 11:745-752.
Nusser Z (2000) AMPA and NMDA receptors: similarities and differences in their synaptic distribution. Curr Opin Neurobiol 10:337-341.
Nusser Z, Lujan R, Laube G, Roberts JD, Molnar E, Somogyi P (1998) Cell type and pathway dependence of synaptic AMPA receptor number and variability in the hippocampus. Neuron 21:545-559.
Obrenovitch TP, Urenjak J (1997) Altered glutamatergic transmission in neurological disorders: from high extracellular glutamate to excessive synaptic efficacy. Prog Neurobiol 51:39-87.
O'Brien R, Xu D, Mi R, Tang X, Hopf C, Worley P (2002) Synaptically targeted narp plays an essential role in the aggregation of AMPA receptors at excitatory synapses in cultured spinal neurons. J Neurosci 22:4487-4498.
O'Brien RJ, Kamboj S, Ehlers MD, Rosen KR, Fischbach GD, Huganir RL (1998) Activity-dependent modulation of synaptic AMPA receptor accumulation. Neuron 21:1067-1078.
O'Brien RJ, Xu D, Petralia RS, Steward O, Huganir RL, Worley P (1999) Synaptic clustering of AMPA receptors by the extracellular immediate-early gene product Narp. Neuron 23:309-323.
Oliet SH, Malenka RC, Nicoll RA (1997) Two distinct forms of long-term depression coexist in CA1 hippocampal pyramidal cells. Neuron 18:969-982.
Osten P, Ziff EB (1999) AMPA receptor forms a biochemically functional complex with NSF and alpha- and beta-SNAPs. Ann N Y Acad Sci 868:558-560.
Osten P, Khatri L, Perez JL, Kohr G, Giese G, Daly C, Schulz TW, Wensky A, Lee LM, Ziff EB (2000) Mutagenesis reveals a role for ABP/GRIP binding to

GluR2 in synaptic surface accumulation of the AMPA receptor. Neuron 27:313-325.

Osten P, Srivastava S, Inman GJ, Vilim FS, Khatri L, Lee LM, States BA, Einheber S, Milner TA, Hanson PI, Ziff EB (1998) The AMPA receptor GluR2 C terminus can mediate a reversible, ATP-dependent interaction with NSF and alpha- and beta-SNAPs. Neuron 21:99-110.

Pacelli GJ, Kelso SR (1991) Trans-ACPD reduces multiple components of synaptic transmission in the rat hippocampus. Neurosci Lett 132:267-269.

Palmer MJ, Isaac JT, Collingridge GL (2004) Multiple, developmentally regulated expression mechanisms of long-term potentiation at CA1 synapses. J Neurosci 24:4903-4911.

Pare D, Llinas R (1995) Intracellular study of direct entorhinal inputs to field CA1 in the isolated guinea pig brain in vitro. Hippocampus 5:115-119.

Pare D, Lebel E, Lang EJ (1997) Differential impact of miniature synaptic potentials on the soma and dendrites of pyramidal neurons in vivo. J Neurophysiol 78:1735-1739.

Park M, Penick EC, Edwards JG, Kauer JA, Ehlers MD (2004) Recycling endosomes supply AMPA receptors for LTP. Science 305:1972-1975.

Partin KM, Fleck MW, Mayer ML (1996) AMPA receptor flip/flop mutants affecting deactivation, desensitization, and modulation by cyclothiazide, aniracetam, and thiocyanate. J Neurosci 16:6634-6647.

Partridge LD, Valenzuela CF (1999) Ca2+ store-dependent potentiation of Ca2+-activated non-selective cation channels in rat hippocampal neurones in vitro. J Physiol 521 Pt 3:617-627.

Paschen W, Doutheil J, Gissel C, Treiman M (1996) Depletion of neuronal endoplasmic reticulum calcium stores by thapsigargin: effect on protein synthesis. J Neurochem 67:1735-1743.

Passafaro M, Nakagawa T, Sala C, Sheng M (2003) Induction of dendritic spines by an extracellular domain of AMPA receptor subunit GluR2. Nature 424:677-681.

Pasternack A, Coleman SK, Jouppila A, Mottershead DG, Lindfors M, Pasternack M, Keinanen K (2002) Alpha-amino-3-hydroxy-5-methyl-4-isoxazolepropionic acid (AMPA) receptor channels lacking the N-terminal domain. J Biol Chem 277:49662-49667.

Patel S, Latterich M (1998) The AAA team: related ATPases with diverse functions. Trends Cell Biol 8:65-71.

Perestenko P, Ashby MC, Henley JM (2003) Real-time imaging of alpha-amino-3-hydroxy-5-methyl-4-isoxazolepropionic acid receptor (AMPA receptor) movements in neurons. Biochem Soc Trans 31:880-884.

Perez JL, Khatri L, Chang C, Srivastava S, Osten P, Ziff EB (2001) PICK1 targets activated protein kinase Calpha to AMPA receptor clusters in spines of hippocampal neurons and reduces surface levels of the AMPA-type glutamate receptor subunit 2. J Neurosci 21:5417-5428.

Perez-Otano I, Ehlers MD (2004) Learning from NMDA receptor trafficking: clues to the development and maturation of glutamatergic synapses. Neurosignals 13:175-189.

Perez-Otano I, Schulteis CT, Contractor A, Lipton SA, Trimmer JS, Sucher NJ, Heinemann SF (2001) Assembly with the NR1 subunit is required for surface expression of NR3A-containing NMDA receptors. J Neurosci 21:1228-1237.

Perkinton MS, Sihra TS, Williams RJ (1999) Ca(2+)-permeable AMPA receptors induce phosphorylation of cAMP response element-binding protein through a phosphatidylinositol 3-kinase-dependent stimulation of the mitogen-activated protein kinase signaling cascade in neurons. J Neurosci 19:5861-5874.

Perkinton MS, Ip JK, Wood GL, Crossthwaite AJ, Williams RJ (2002) Phosphatidylinositol 3-kinase is a central mediator of NMDA receptor signalling to MAP kinase (Erk1/2), Akt/PKB and CREB in striatal neurones. J Neurochem 80:239-254.

Petralia RS, Esteban JA, Wang YX, Partridge JG, Zhao HM, Wenthold RJ, Malinow R (1999) Selective acquisition of AMPA receptors over postnatal development suggests a molecular basis for silent synapses. Nat Neurosci 2:31-36.

Pickard L, Noel J, Henley JM, Collingridge GL, Molnar E (2000) Developmental changes in synaptic AMPA and NMDA receptor distribution and AMPA receptor subunit composition in living hippocampal neurons. J Neurosci 20:7922-7931.

Piomelli D, Beltramo M, Giuffrida A, Stella N (1998) Endogenous cannabinoid signaling. Neurobiol Dis 5:462-473.

Polsky A, Mel BW, Schiller J (2004) Computational subunits in thin dendrites of pyramidal cells. Nat Neurosci 7:621-627.

Poncer JC, Malinow R (2001) Postsynaptic conversion of silent synapses during LTP affects synaptic gain and transmission dynamics. Nat Neurosci 4:989-996.

Poncer JC, Esteban JA, Malinow R (2002) Multiple mechanisms for the potentiation of AMPA receptor-mediated transmission by alpha-Ca2+/calmodulin-dependent protein kinase II. J Neurosci 22:4406-4411.

Powis G, Bonjouklian R, Berggren MM, Gallegos A, Abraham R, Ashendel C, Zalkow L, Matter WF, Dodge J, Grindey G, et al. (1994) Wortmannin, a potent and selective inhibitor of phosphatidylinositol-3-kinase. Cancer Res 54:2419-2423.

Rameh LE, Cantley LC (1999) The role of phosphoinositide 3-kinase lipid products in cell function. J Biol Chem 274:8347-8350.

Reyes A (2001) Influence of dendritic conductances on the input-output properties of neurons. Annu Rev Neurosci 24:653-675.

Reyes M, Stanton PK (1996) Induction of hippocampal long-term depression requires release of Ca2+ from separate presynaptic and postsynaptic intracellular stores. J Neurosci 16:5951-5960.

Robbe D, Alonso G, Duchamp F, Bockaert J, Manzoni OJ (2001) Localization and Mechanisms of Action of Cannabinoid Receptors at the Glutamatergic Synapses of the Mouse Nucleus Accumbens. J Neurosci 21:109-116.

Robert A, Howe JR (2003) How AMPA receptor desensitization depends on receptor occupancy. J Neurosci 23:847-858.

Rodgers EE, Theibert AB (2002) Functions of PI 3-kinase in development of the nervous system. Int J Dev Neurosci 20:187-197.

Romorini S, Piccoli G, Jiang M, Grossano P, Tonna N, Passafaro M, Zhang M, Sala C (2004) A functional role of postsynaptic density-95-guanylate kinase-

associated protein complex in regulating Shank assembly and stability to synapses. J Neurosci 24:9391-9404.
Rong R, Ahn JY, Huang H, Nagata E, Kalman D, Kapp JA, Tu J, Worley PF, Snyder SH, Ye K (2003) PI3 kinase enhancer-Homer complex couples mGluRI to PI3 kinase, preventing neuronal apoptosis. Nat Neurosci 6:1153-1161.
Rosenmund C, Stern-Bach Y, Stevens CF (1998) The tetrameric structure of a glutamate receptor channel. Science 280:1596-1599.
Ruberti F, Dotti CG (2000) Involvement of the proximal C terminus of the AMPA receptor subunit GluR1 in dendritic sorting. J Neurosci 20:RC78.
Rumbaugh G, Sia GM, Garner CC, Huganir RL (2003) Synapse-associated protein-97 isoform-specific regulation of surface AMPA receptors and synaptic function in cultured neurons. J Neurosci 23:4567-4576.
Sanna PP, Cammalleri M, Berton F, Simpson C, Lutjens R, Bloom FE, Francesconi W (2002) Phosphatidylinositol 3-kinase is required for the expression but not for the induction or the maintenance of long-term potentiation in the hippocampal CA1 region. J Neurosci 22:3359-3365.
Schnell E, Sizemore M, Karimzadegan S, Chen L, Bredt DS, Nicoll RA (2002) Direct interactions between PSD-95 and stargazin control synaptic AMPA receptor number. Proc Natl Acad Sci U S A 99:13902-13907.
Schweizer FE, Dresbach T, DeBello WM, O'Connor V, Augustine GJ, Betz H (1998) Regulation of neurotransmitter release kinetics by NSF. Science 279:1203-1206.
Seal RP, Amara SG (1999) Excitatory amino acid transporters: a family in flux. Annu Rev Pharmacol Toxicol 39:431-456.
Seress L, Pokorny J (1981) Structure of the granular layer of the rat dentate gyrus. A light microscopic and Golgi study. J Anat 133:181-195.
Shen L, Liang F, Walensky LD, Huganir RL (2000) Regulation of AMPA receptor GluR1 subunit surface expression by a 4. 1N-linked actin cytoskeletal association. J Neurosci 20:7932-7940.
Sheng M (2001) Molecular organization of the postsynaptic specialization. Proc Natl Acad Sci U S A 98:7058-7061.
Sheng M, Lee SH (2001) AMPA receptor trafficking and the control of synaptic transmission. Cell 105:825-828.
Sheng M, Kim MJ (2002) Postsynaptic signaling and plasticity mechanisms. Science 298:776-780.
Sheng M, Hyoung Lee S (2003) AMPA receptor trafficking and synaptic plasticity: major unanswered questions. Neurosci Res 46:127-134.
Shi S, Hayashi Y, Esteban JA, Malinow R (2001) Subunit-specific rules governing AMPA receptor trafficking to synapses in hippocampal pyramidal neurons. Cell 105:331-343.
Shulman RG, Hyder F, Rothman DL (2002) Biophysical basis of brain activity: implications for neuroimaging. Q Rev Biophys 35:287-325.
Simpson PB, Challiss RA, Nahorski SR (1995) Neuronal Ca2+ stores: activation and function. Trends Neurosci 18:299-306.
Smith MA, Ellis-Davies GC, Magee JC (2003) Mechanism of the distance-dependent scaling of Schaffer collateral synapses in rat CA1 pyramidal neurons. J Physiol 548:245-258.

Smith TC, Howe JR (2000) Concentration-dependent substate behavior of native AMPA receptors. Nat Neurosci 3:992-997.
Smith TC, Wang LY, Howe JR (2000) Heterogeneous conductance levels of native AMPA receptors. J Neurosci 20:2073-2085.
Soderling TR, Derkach VA (2000) Postsynaptic protein phosphorylation and LTP. Trends Neurosci 23:75-80.
Sommer B, Kohler M, Sprengel R, Seeburg PH (1991) RNA editing in brain controls a determinant of ion flow in glutamate-gated channels. Cell 67:11-19.
Sommer B, Keinanen K, Verdoorn TA, Wisden W, Burnashev N, Herb A, Kohler M, Takagi T, Sakmann B, Seeburg PH (1990) Flip and flop: a cell-specific functional switch in glutamate-operated channels of the CNS. Science 249:1580-1585.
Song I, Huganir RL (2002) Regulation of AMPA receptors during synaptic plasticity. Trends Neurosci 25:578-588.
Song I, Kamboj S, Xia J, Dong H, Liao D, Huganir RL (1998) Interaction of the N-ethylmaleimide-sensitive factor with AMPA receptors. Neuron 21:393-400.
Sourdet V, Debanne D (1999) The role of dendritic filtering in associative long-term synaptic plasticity. Learn Mem 6:422-447.
Srivastava S, Ziff EB (1999) ABP: a novel AMPA receptor binding protein. Ann N Y Acad Sci 868:561-564.
Srivastava S, Osten P, Vilim FS, Khatri L, Inman G, States B, Daly C, DeSouza S, Abagyan R, Valtschanoff JG, Weinberg RJ, Ziff EB (1998) Novel anchorage of GluR2/3 to the postsynaptic density by the AMPA receptor-binding protein ABP. Neuron 21:581-591.
Standley S, Tocco G, Tourigny MF, Massicotte G, Thompson RF, Baudry M (1995) Developmental changes in alpha-amino-3-hydroxy-5-methyl-4-isoxazole propionate receptor properties and expression in the rat hippocampal formation. Neuroscience 67:881-892.
Steck PA, Pershouse MA, Jasser SA, Yung WK, Lin H, Ligon AH, Langford LA, Baumgard ML, Hattier T, Davis T, Frye C, Hu R, Swedlund B, Teng DH, Tavtigian SV (1997) Identification of a candidate tumour suppressor gene, MMAC1, at chromosome 10q23.3 that is mutated in multiple advanced cancers. Nat Genet 15:356-362.
Steinberg SF (2001) PI3King the L-type calcium channel activation mechanism. Circ Res 89:641-644.
Stern P, Behe P, Schoepfer R, Colquhoun D (1992) Single-channel conductances of NMDA receptors expressed from cloned cDNAs: comparison with native receptors. Proc Biol Sci 250:271-277.
Stoppini L, Buchs PA, Muller D (1991) A simple method for organotypic cultures of nervous tissue. J Neurosci Methods 37:173-182.
Sucher NJ, Awobuluyi M, Choi YB, Lipton SA (1996) NMDA receptors: from genes to channels. Trends Pharmacol Sci 17:348-355.
Sullivan JM (2000) Cellular and Molecular Mechanisms Underlying Learning and Memory Impairments Produced by Cannabinoids. Learn Mem 7:132-139.
Sutton MA, Wall NR, Aakalu GN, Schuman EM (2004) Regulation of dendritic protein synthesis by miniature synaptic events. Science 304:1979-1983.
Takumi Y, Matsubara A, Rinvik E, Ottersen OP (1999a) The arrangement of glutamate receptors in excitatory synapses. Ann N Y Acad Sci 868:474-482.

Takumi Y, Ramirez-Leon V, Laake P, Rinvik E, Ottersen OP (1999b) Different modes of expression of AMPA and NMDA receptors in hippocampal synapses. Nat Neurosci 2:618-624.

Terashima A, Cotton L, Dev KK, Meyer G, Zaman S, Duprat F, Henley JM, Collingridge GL, Isaac JT (2004) Regulation of synaptic strength and AMPA receptor subunit composition by PICK1. J Neurosci 24:5381-5390.

Tovar KR, Westbrook GL (2002) Mobile NMDA receptors at hippocampal synapses. Neuron 34:255-264.

Treiman M, Caspersen C, Christensen SB (1998) A tool coming of age: thapsigargin as an inhibitor of sarco-endoplasmic reticulum Ca(2+)-ATPases. Trends Pharmacol Sci 19:131-135.

Tsai G, Coyle JT (2002) Glutamatergic mechanisms in schizophrenia. Annu Rev Pharmacol Toxicol 42:165-179.

Turrigiano GG (2000) AMPA receptors unbound: membrane cycling and synaptic plasticity. Neuron 26:5-8.

Turrigiano GG (2002) A recipe for ridding synapses of the ubiquitous AMPA receptor. Trends Neurosci 25:597-598.

Tyler WJ, Pozzo-Miller LD (2001) BDNF enhances quantal neurotransmitter release and increases the number of docked vesicles at the active zones of hippocampal excitatory synapses. J Neurosci 21:4249-4258.

Ulrich D, Luscher HR (1993) Miniature excitatory synaptic currents corrected for dendritic cable properties reveal quantal size and variance. J Neurophysiol 69:1769-1773.

Van Damme P, Callewaert G, Eggermont J, Robberecht W, Van Den Bosch L (2003) Chloride influx aggravates Ca2+-dependent AMPA receptor-mediated motoneuron death. J Neurosci 23:4942-4950.

Vandenberghe W, Nicoll RA, Bredt DS (2005) Stargazin is an AMPA receptor auxiliary subunit. Proc Natl Acad Sci U S A 102:485-490.

Vanhaesebroeck B, Alessi DR (2000) The PI3K-PDK1 connection: more than just a road to PKB. Biochem J 346 Pt 3:561-576.

Vanhaesebroeck B, Leevers SJ, Panayotou G, Waterfield MD (1997) Phosphoinositide 3-kinases: a conserved family of signal transducers. Trends Biochem Sci 22:267-272.

Vanhaesebroeck B, Higashi K, Raven C, Welham M, Anderson S, Brennan P, Ward SG, Waterfield MD (1999) Autophosphorylation of p110delta phosphoinositide 3-kinase: a new paradigm for the regulation of lipid kinases in vitro and in vivo. Embo J 18:1292-1302.

Vlahos CJ, Matter WF, Hui KY, Brown RF (1994) A specific inhibitor of phosphatidylinositol 3-kinase, 2-(4-morpholinyl)-8-phenyl-4H-1-benzopyran-4-one (LY294002). J Biol Chem 269:5241-5248.

Voronin LL, Cherubini E (2003) "Presynaptic silence" may be golden. Neuropharmacology 45:439-449.

Voronin LL, Cherubini E (2004) 'Deaf, mute and whispering' silent synapses: their role in synaptic plasticity. J Physiol 557:3-12.

Walker EH, Perisic O, Ried C, Stephens L, Williams RL (1999) Structural insights into phosphoinositide 3-kinase catalysis and signalling. Nature 402:313-320.

Walker EH, Pacold ME, Perisic O, Stephens L, Hawkins PT, Wymann MP, Williams RL (2000) Structural determinants of phosphoinositide 3-kinase inhibition by

wortmannin, LY294002, quercetin, myricetin, and staurosporine. Mol Cell 6:909-919.

Walsh MJ, Kuruc N (1992) The postsynaptic density: constituent and associated proteins characterized by electrophoresis, immunoblotting, and peptide sequencing. J Neurochem 59:667-678.

Wang Q, Liu L, Pei L, Ju W, Ahmadian G, Lu J, Wang Y, Liu F, Wang YT (2003) Control of synaptic strength, a novel function of Akt. Neuron 38:915-928.

Wang S, Jia Z, Roder J, Murphy TH (2002) AMPA receptor-mediated miniature synaptic calcium transients in GluR2 null mice. J Neurophysiol 88:29-40.

Wang Y, Ju W, Liu L, Fam S, D'Souza S, Taghibiglou C, Salter M, Wang YT (2004) {alpha}-Amino-3-hydroxy-5-methylisoxazole-4-propionic Acid Subtype Glutamate Receptor (AMPAR) Endocytosis Is Essential for N-Methyl-D-aspartate-induced Neuronal Apoptosis. J Biol Chem 279:41267-41270.

Ward SG, Finan P, Welham MJ (2003) PI3K comes of age. Nat Immunol 4:2.

Watanabe J, Beck C, Kuner T, Premkumar LS, Wollmuth LP (2002) DRPEER: a motif in the extracellular vestibule conferring high Ca2+ flux rates in NMDA receptor channels. J Neurosci 22:10209-10216.

Wenthold RJ, Petralia RS, Blahos J, II, Niedzielski AS (1996) Evidence for multiple AMPA receptor complexes in hippocampal CA1/CA2 neurons. J Neurosci 16:1982-1989.

Wilson RI, Kunos G, Nicoll RA (2001) Presynaptic specificity of endocannabinoid signaling in the hippocampus. Neuron 31:453-462.

Woodside BL, Borroni AM, Hammonds MD, Teyler TJ (2004) NMDA receptors and voltage-dependent calcium channels mediate different aspects of acquisition and retention of a spatial memory task. Neurobiol Learn Mem 81:105-114.

Wu G-Y, Malinow R, Cline HT (1996) Maturation of a Central Glutamatergic Synapse. Science 274:972-976.

Wu L, Bauer CS, Zhen XG, Xie C, Yang J (2002) Dual regulation of voltage-gated calcium channels by PtdIns(4,5)P2. Nature 419:947-952.

Wu X, Zhu D, Jiang X, Okagaki P, Mearow K, Zhu G, McCall S, Banaudha K, Lipsky RH, Marini AM (2004) AMPA protects cultured neurons against glutamate excitotoxicity through a phosphatidylinositol 3-kinase-dependent activation in extracellular signal-regulated kinase to upregulate BDNF gene expression. J Neurochem 90:807-818.

Wyllie DJ, Nicoll RA (1994) A role for protein kinases and phosphatases in the Ca(2+)-induced enhancement of hippocampal AMPA receptor-mediated synaptic responses. Neuron 13:635-643.

Wyllie DJ, Manabe T, Nicoll RA (1994) A rise in postsynaptic Ca2+ potentiates miniature excitatory postsynaptic currents and AMPA responses in hippocampal neurons. Neuron 12:127-138.

Wyllie DJ, Behe P, Nassar M, Schoepfer R, Colquhoun D (1996) Single-channel currents from recombinant NMDA NR1a/NR2D receptors expressed in Xenopus oocytes. Proc Biol Sci 263:1079-1086.

Wymann MP, Bulgarelli-Leva G, Zvelebil MJ, Pirola L, Vanhaesebroeck B, Waterfield MD, Panayotou G (1996) Wortmannin inactivates phosphoinositide 3-kinase by covalent modification of Lys-802, a residue involved in the phosphate transfer reaction. Mol Cell Biol 16:1722-1733.

Wyszynski M, Valtschanoff JG, Naisbitt S, Dunah AW, Kim E, Standaert DG, Weinberg R, Sheng M (1999) Association of AMPA receptors with a subset of glutamate receptor-interacting protein in vivo. J Neurosci 19:6528-6537.

Wyszynski M, Kim E, Dunah AW, Passafaro M, Valtschanoff JG, Serra-Pages C, Streuli M, Weinberg RJ, Sheng M (2002) Interaction between GRIP and Liprin-alpha/SYD2 Is Required for AMPA Receptor Targeting. Neuron 34:39-52.

Xiao MY, Wasling P, Hanse E, Gustafsson B (2004) Creation of AMPA-silent synapses in the neonatal hippocampus. Nat Neurosci 7:236-243.

Yang S-N, Tang Y-G, Zucker RS (1999) Selective Induction of LTP and LTD by Postsynaptic [Ca2+]i Elevation. J Neurophysiol 81:781-787.

Yasuda R, Sabatini BL, Svoboda K (2003) Plasticity of calcium channels in dendritic spines. Nat Neurosci 6:948-955.

Yeckel MF, Berger TW (1995) Monosynaptic excitation of hippocampal CA1 pyramidal cells by afferents from the entorhinal cortex. Hippocampus 5:108-114.

Yu RC, Jahn R, Brunger AT (1999) NSF N-terminal domain crystal structure: models of NSF function. Mol Cell 4:97-107.

Zhu JJ, Malinow R (2002) Acute versus chronic NMDA receptor blockade and synaptic AMPA receptor delivery. Nat Neurosci 5:513-514.

Zhu JJ, Esteban JA, Hayashi Y, Malinow R (2000) Postnatal synaptic potentiation: delivery of GluR4-containing AMPA receptors by spontaneous activity. Nat Neurosci 3:1098-1106.

Zhu JJ, Qin Y, Zhao M, Van Aelst L, Malinow R (2002) Ras and Rap control AMPA receptor trafficking during synaptic plasticity. Cell 110:443-455.

Ziff EB (1997) Enlightening the postsynaptic density. Neuron 19:1163-1174.

Ziv NE, Garner CC (2004) Cellular and molecular mechanisms of presynaptic assembly. Nat Rev Neurosci 5:385-399.

Zucchi R, Ronca-Testoni S (1997) The sarcoplasmic reticulum Ca2+ channel/ryanodine receptor: modulation by endogenous effectors, drugs and disease states. Pharmacol Rev 49:1-51.